

CHEMICAL INHIBITORS OF PHOSPHATIDYLINOSITOL TRANSFER PROTEINS
ENABLE HIGHLY SELECTIVE INTERFERENCE WITH SPECIFIC PATHWAYS OF
PHOSPHOINOSITIDE SIGNALING IN CELLS

Aaron Hugh Nile

A dissertation submitted to the faculty of the University of North Carolina at Chapel Hill in partial fulfillment of the requirements for the degree of Doctor of Philosophy in the Department of Cell and Developmental Biology in the School of Medicine.

Chapel Hill
2014

Approved by:

Vytas Bankaitis

Kerry Bloom

Ben Major

Bob Duronio

Garry Johnson

© 2014
Aaron Hugh Nile
ALL RIGHTS RESERVED

ABSTRACT

Aaron Hugh Nile: Chemical Inhibitors of Phosphatidylinositol Transfer Proteins Enable Highly Selective Interference With Specific Pathways of Phosphoinositide Signaling in Cells
(Under the direction of Vytas Bankaitis)

Phosphatidylinositol phosphates (PIP) are phosphorylated derivatives of phosphatidylinositol (PtdIns) that signal to and regulate diverse cellular functions including membrane trafficking, cytokinesis, cell cycle regulation and DNA repair. PIP-signaling is regulated by a variety of proteins through degradation, phosphorylation and dephosphorylation. Members of the Sec14-like phosphatidylinositol transfer protein superfamily (Sec14-PITPs) have at least two functions which include lipid-binding platforms and/or ‘nanoreactors’ that direct PtdIns-OH kinase activity to generate discrete PIP-pools. In Chapter 1, I outline the current literature on the Sec14-superfamily and the structurally unrelated START-like PITPs with special emphasis on mammalian PITPs, and how their disruption results in a number of inherited mammalian diseases.

Neither Sec14-like or START-like PITPs have been targeted for chemical intervention using small molecule inhibitors (SMIs). The development of PITP-directed SMIs provide applications not only as tool compounds, but also as therapeutic agents that inhibit a number of pathogenic organisms and potentially as activators of defective PITPs. As proof-of-concept, I developed the first PITP-directed SMIs that specifically inhibit the prototype Sec14-like PITP from *Saccharomyces cerevisiae*. In yeast, Sec14 connects the production of phosphatidylinositol

4-phosphate (PtdIns(4)P) and phosphatidylcholine (PtdCho) metabolism with trafficking through the *trans*-Golgi/endosomal network. In Chapter 2, I describe the development of the Sec14-directed SMI, 4-chloro-3-nitrophenyl(4-(2-methoxyphenyl) piperazin-1-yl)methanones or NPPM. These SMIs specifically and directly inhibit Sec14 through its hydrophobic cavity, likely by a halogen-bonding mechanism. Based on my work in Chapter 2, I developed a routine for the rapid validation of novel P1TP-directed SMIs from a variety of organisms that will streamline future SMI-identification. Together, these data deliver proof-of-concept that P1TP-directed SMIs offer new and generally applicable avenue for intervening with phosphoinositide signaling pathways with selectivities superior to those afforded by contemporary lipid kinase-directed strategies. Finally, the study of PIPs has been advanced through the development of multiple methodologies that both detect and modify PIPs *in vivo*. In Chapter 3, I discuss current methods used to monitor and manipulate PIP-signaling pathways with special emphasis on SMIs that target PIP-modifying enzymes.

To my parents.

ACKNOWLEDGEMENTS

I would like to thank my family for supporting all of my endeavors: Hugh Nile, Dody Nile, Amber Nile, Alexis Nile, Brett Hartmann and Mars Hartmann.

To my childhood friends: Billy Springer, Bo Brown, Shane Thomas, Kory Manley, Katelynn Pfeil, Erin Pfeil-McCullough, Brad McCullough, Eric Miller, Lora Brown, Ashley Moore and Brian Birkmire.

My colleagues and friends from current and past institutions: Robert Sons, Brent Hehl, Kelly Watson, Liz Lessey-Morillon, Deepak Jha, Maria Aleman, Dileep Varma, Anita Nair-Varma, Alison Totura, Cheryl Miller, Crystal Neeley, the Recover Room, the Cellar, Tangi Smallwood, Marty Newman, Ashley Clark, Chris Noel, Sarah Nicolson, Rob Davis, Nooshin Lotfi, Bob Fellner, Erin Kirk, Jason Brunton, Stephen Busan, Sandi Wong, Damon Shattuck, Nick Spidale, Matt Geden, Doug Cyr, Pat Brenwald, Con Beckers, Scott Hammond, Aysha Osmani, Stephen Osmani, Jian-Qiu Wu and all of the office staff in the Department of Cell and Developmental Biology.

I would like to thank members of the Bankaitis Lab, in particular: Carl Mousley, Aby Grabon, Ramiro Diz, Mark McDermott, Danish Kahn, Peihua Yuan, Jihui Ren, Ashutosh Tripathi and James Alb.

To Vytas for giving me the freedom and opportunities I needed to succeed.

PREFACE

This Ph.D. thesis was initiated in the Department of Cell Biology at UNC-Chapel Hill and was completed in the Department of Cell and Molecular Medicine at Texas A&M.

Chapter 1's figures and text were modified with permission from an article published in *Clinical Lipidology* (2010) entitled "Mammalian diseases of phosphatidylinositol transfer proteins and their homologs" (Nile, Bankaitis et al. 2010). This article was co-first authored with Aby Grabon.

Chapter 2 is an extended version of work published in *Nature Chemical Biology* (2014) entitled "PITPs as Targets for Selectively Interfering With Phosphoinositide Signaling in Cells" (Nile, Tripathi et al. 2014).

Chapter three was written for this thesis, and is tentatively titled "Identification and Application of Novel Approaches for Selectively Interfering With Phosphoinositide Signaling in Cells Through PITPs" which is being solicited as a review article.

TABLE OF CONTENTS

LIST OF TABLES.....	xviii
LIST OF FIGURES.....	xviii
LIST OF ABBREVIATIONS AND SYMBOLS.....	xxii
CHAPTER 1: MAMMALIAN DISEASES OF PHOSPHATIDYLINOSITOL TRANSFER PROTEINS AND THEIR HOMOLOGUES.....	1
Overview.....	1
Introduction.....	1
Operational definitions for the PITPs.....	4
Sec14-like and START-like PITPs.....	4
The slippery faces of lipid transfer activities.....	6
Sec14-Like PITPs as molecules.....	9
Sec14 and integration of PtdCho metabolic signals.....	9
The anatomy of phospholipid exchange by Sec14-like PITPs.....	10
The core engineering of a Sec14 nanoreactor.....	12
Primed PtdIns-presentation models versus lipid transfer models.....	14

A PITP-centric strategy for linking lipid metabolism to phosphoinositide signaling.....	17
Mammalian Sec14-domain protein disorders.....	19
Stand-alone Sec14-like proteins and disease.....	21
α -tocopherol transfer protein and vitamin E status.....	21
Caytaxin and cerebellar ataxia.....	23
Cellular retinaldehyde binding protein and the vertebrate visual cycle.....	25
Multi-domain Sec14-like proteins and disease.....	28
Rho guanine nucleotide exchange proteins with Sec14 domains.....	29
DBL.....	29
Kalirin /Duo.....	30
TRIO.....	31
DBS.....	32
RhoGAPS.....	33
CDC42GAP/p50RhoGAP.....	33
Neurofibromin RasGAPs.....	34
Sec14-like protein tyrosine phosphatase.....	35

Type 1 START-like PITPs as molecules.....	38
Cellular functions.....	42
Vertebrate models for type 1 PITP-associated disease.....	43
PITP α and neurological disease.....	44
Anatomy of neurodegenerative disease in PITP α -deficient mice.....	46
Cell non-autonomous mechanisms for PITP α -dependent neuroprotection.....	49
PITP α and cell autonomous signaling.....	49
PITP α -insufficiencies and chylomicron retention disease.....	53
<i>pitpa</i> ^{0/0} mice and hepatic steatosis.....	58
PITP α --a link between Ins nutrition and lipoprotein metabolism?.....	59
PITP α and the pancreas.....	60
Zebrafish type 1 PITPs.....	61
PITPs and fungal pathogens.....	63
Conclusions and future perspectives.....	64
Materials and methods.....	67
Sequence alignment.....	67
Molecular graphics.....	68

CHAPTER 2: CHEMICAL INHIBITORS OF PHOSPHATIDYLINOSITOL TRANSFER PROTEINS ENABLE HIGHLY SELECTIVE INTERFERENCE WITH SPECIFIC PATHWAYS OF PHOSPHOINOSITIDE SIGNALING IN CELLS	69
Overview	69
Introduction	70
Results: NPPM-like SMIs	72
Identification of candidate Sec14-directed SMIs	72
Expansion of the candidate Sec14-directed SMI set	79
Yeast sensitivity to NPPM is a function of Sec14 expression levels	84
NPPMs directly and selectively inhibit Sec14 <i>in vitro</i>	86
NPPM structure activity relationships	88
Sec14 inhibition and chemical nature of the NPPM halide	94
NPPM docking pose within the Sec14 phospholipid-binding pocket	95
NPPM-resistant Sec14 proteins	101
NPPMs and <i>sec14-1^{ts}</i> at non-permissive temperature induce a G2 cell-cycle arrest	104
Sec14 is the sole essential NPPM target in cells	106
NPPMs induce phospholipase D activity in vegetative yeast	108

NPPM intoxication and genetic ablation of Sec14 activity evoke similar phenotypes.....	111
NPPMs discriminate between chemically distinct phosphoinositide pools.....	124
NPPMs discriminate between local PtdIns(4)P signaling pathways.....	134
Discussion of NPPM-like Sec14-directed inhibitors.....	138
Results: alternative Sec14-directed SMIs.....	147
The natural product himbacine is an active Sec14-inhibitor.....	151
Sec14 inhibitors show inhibitory activity against pathogenic yeast in the <i>Candida</i> genus.....	154
Discussion: alternative Sec14-directed inhibitors.....	160
Materials and methods.....	162
Molecular graphics and chemical drawing.....	162
Yeast strains, media and reagents.....	162
Small molecule inhibitors.....	162
Chemogenomic screening.....	163
Docking simulations.....	163
GOLD docking.....	164
Hydrophobic scoring.....	164
Glide docking.....	165

PLIF.....	166
Hierarchical cluster analysis.....	166
FACS sorting.....	167
Protein purification.....	167
Rat liver microsomes.....	168
PtdIns-transfer assays.....	168
Statistical analyses.....	169
Growth rate analyses.....	169
[³ H]-serine labeling of yeast cells.....	170
Choline release assay.....	171
Homology modeling of Sec14 closed conformation.....	172
Site-directed mutagenesis.....	172
Transmission electron microscopy.....	172
Metabolic labeling and immunoprecipitation.....	173
Phosphoinositide analyses.....	174
Fluorescence imaging.....	175
Simulation of charge distribution on activated aryl halides.....	176

Invertase secretion assays.....	177
Sequence alignment.....	178
NPPM chemogenomic interactions.....	178
CHAPTER 3: MEASURING AND MODULATING PHOSPHOINOSITIDE SIGNALING IN CELLS.....	180
Overview.....	180
Introduction.....	181
Methods to monitor phosphatidylinositol phosphate status.....	184
Direct measurement of phosphatidylinositol phosphates.....	184
Mass spectrometry.....	186
Isomer-specific PIP antibodies.....	187
PtdIns phosphate binding domains.....	188
PH domains.....	191
PX domains.....	192
GLUE domains.....	193
Tubby domains.....	194
BATS domains.....	196
PROPPINs.....	196

SYLF domains.....	197
EHD domains	197
FERM domains.....	199
BAR domains.....	200
FYVE domains.....	201
PIP biosensors and FRET.....	203
Coincidence detection.....	204
Modulation of cellular phosphatidylinositol phosphates.....	205
Addition of exogenous phosphatidylinositol phosphates.....	205
Genetic modulation of PIP modifying enzymes.....	207
Chemical- and light-induced enzyme targeting.....	209
Pharmacological intervention of phosphoinositide signaling.....	210
Small molecule inhibitor validation in <i>S.cerevisiae</i>	211
Inhibitors of PIP signaling pathways.....	212
Akt/PKB inhibitors.....	213
PtdIns-3-kinases inhibitors.....	213
PTEN PtdIns 3-phosphatase inhibitors.....	217

Chemical modulators of SHIP phosphatase.....	220
Screening for synaptojanin inhibitors.....	224
Inhibitors of PtdIns-4-kinases.....	226
Inhibitors of phospholipase C.....	232
Inhibitors of inositol monophosphatase (IMPase).....	236
Conclusions and future directions.....	239
Utilizing counter-ligand and pocket geometry to identify isomer-specific PITP inhibitors.....	239
Identification of SMIs directed against PITPs.....	242
SMIs against ‘bypass Sec14’ proteins and phospholipase D	242
Closing remarks.....	244
FUNDING SOURCES.....	251
REFERENCES.....	252

LIST OF TABLES

Table 1. Other selected Sec14-like proteins	36
Table 2. Chapter one summary	66
Table 3. SMI 741 inhibits dimorphic transitions in <i>Candida albicans</i>	159
Table 4. Chapter two summary	178
Table 5. List of PtdIns phosphate binding domains.....	189
Table 6. Yeast strains	245
Table 7. Protein expression plasmids.....	247
Table 8. Yeast expression plasmids	249

LIST OF FIGURES

Figure 1. Transfer vs. nanoreactor models for PITP function.....	8
Figure 2. The Sec14-fold.	12
Figure 3. Differential phospholipid binding strategies by Sec14-like PITPs.	14
Figure 4. The PtdIns-binding bar code in Sec14-like proteins.	18
Figure 5. Domain arrangements of Sec14-like proteins	20
Figure 6. PITP α Structures.....	41
Figure 7. Intestinal and hepatic steatosis in PITP α -deficient mice.....	57
Figure 8. Identification of 4130-1278 and 4130-1276 as candidate Sec14-directed SMIs.	73
Figure 9. Chemogenomic interaction-profiles of 4130-1276 and 4130-1278.	78
Figure 10. <i>In vivo</i> SAR analyses.....	82
Figure 11. NPPMs specifically inactivate Sec14.....	85
Figure 12. <i>In vitro</i> SAR analyses.....	92
Figure 13. NPPM SAR relationships.....	93
Figure 14. Homology model of a closed Sec14 conformer.	98
Figure 15. <i>In silico</i> docking solutions for 6748-481 binding by Sec14.....	99
Figure 16. Interaction fingerprints of representative 6748-481 docking poses.	100
Figure 17. Sec14 mutants resistant to NPPM inhibition.....	102
Figure 18. Sec14 ^{S173C} is resistant to inhibition by NPPMs.....	103
Figure 19. Active-NPPMs phenocopy <i>sec14-1^{ts}</i> cell cycle arrest.....	105
Figure 20. Sec14 is the sole essential cellular target of bioactive NPPMs.	107
Figure 21. NPPM intoxication stimulates phospholipase D activity in vegetative yeast.	110
Figure 22. NPPMs induce accumulation of TGN/endosomal compartments.	113

Figure 23. ‘Bypass Sec14’ are resistant to NPPM-induced accumulation of defective TGN/endosomal compartments.	114
Figure 24. <i>SEC14</i> ^{S173C} cells are resistant to NPPM-induced accumulation of defective TGN/endosomal compartments.	115
Figure 25. NPPMs induce defects in bulk endocytosis.	116
Figure 26. Endocytic recycling of GFP-Snc1 is retarded in NPPM-intoxicated cells.....	117
Figure 27. Sec14-active NPPMs block invertase secretion.	118
Figure 28. ‘Bypass Sec14’ mutations correct NPPM-induced trafficking defects.	119
Figure 29. Sec14 ^{S173C} yeast secrete invertase in the face of Sec14-active NPPMs.	120
Figure 30. Sec14-active NPPMs induce CPY trafficking defects.	121
Figure 31. NPPM induced CPY trafficking defects are poorly reversible.	122
Figure 32. NPPM-induced CPY trafficking block is dose-and time-dependent.....	123
Figure 33. ‘Bypass Sec14’ mutations and Sec14 ^{S173C} expression alleviate NPPM-induced CPY trafficking defects.....	124
Figure 34. Sec14-active NPPMs target specific phosphoinositide classes.	128
Figure 35. GFP-2xPH ^{PLCδ1} plasma membrane association is unperturbed by challenge with Sec14-active NPPMs.	129
Figure 36. PtdIns(4)P biosensors.	131
Figure 37. GFP-2xPH ^{Osh2} localization to membranes is unperturbed in <i>kes1Δ</i> ‘bypass Sec14’ mutants by challenge with Sec14-active NPPMs.	133
Figure 38. NPPMs discriminate between Sec14- and Sfh4-mediated PtdIns(4)P signaling.	136
Figure 39. The Sec14 PtdIns and PtdCho binding barcodes.....	140
Figure 40. Aromatic nucleophilic substitution of NPPMs.....	145
Figure 41. Mechanism for NPPM-mediated inhibition of Sec14.	146
Figure 42. Hierarchical analysis of SAR reveals 12 structural clusters.....	148
Figure 43. Inhibition of Sec14-mediated PtdIns transfer activity.....	149

Figure 44. Resistance of Sec14 inhibitors to genetic ‘bypass Sec14’ mutants.....	151
Figure 45. The structure of himbacine.....	152
Figure 46. Himbacine inhibits Sec14-mediated PtdIns transfer activity <i>in vitro</i>	153
Figure 47. Mutations in the PtdCho binding site of Sec14 confer Himbacine-resistance.	154
Figure 48. Chemical structure of SMI 741	156
Figure 49. Inhibition of <i>Saccharomyces cerevisiae</i> Sec14 <i>in vitro</i> by SMI 741	157
Figure 50. SMI 741 inhibits dimorphic transitions in <i>Candida albicans</i>	158
Figure 51. Structure of phosphoinositides	182
Figure 52. PIP diversity in yeast and mammals.....	183
Figure 53. Sfh1 has an elongated hydrophobic cavity.....	241

LIST OF ABBREVIATIONS AND SYMBOLS

°	Degree
Δ	Deletion
2μ	Episomal plasmid
3AC	3-α-aminocholestane
11- <i>cis</i> -ROL	11- <i>cis</i> -retinol
Å	Angstrom (10 ⁻¹⁰ meter)
aa	Amino acid
ADP	Adenosine diphosphate
all- <i>trans</i> -RAL	All- <i>trans</i> -retinaldehyde
APCI	Atmospheric pressure chemical ionization
ATA	Aurintricarboxylic acid
ATP	Adenosine triphosphate
α-TOH	α-tocopherol
αTTP	α-tocopherol binding protein
AVED	Ataxia with vitamin E deficiency
BiPh(2,3',4,5',6)P ₅	Biphenyl-derived polyphosphate, biphenyl 2,3',4,5',6-pentakisphosphate
BSA	Bovine serum albumin

CEN	Centromeric plasmid
CHX	Cycloheximide
CID	Chemically induced dimerization
$C_{\log P}$	Calculated partition coefficient for n-octanol/water
CPDA	<i>N</i> -[4-(4-chlorobenzyloxy) pyridin-2-yl]-2-(2,6-difluorophenyl)-acetamide
cpm	Counts/minute
CRD	Chylomicron retention disease
DHR-1	Dock homology region 1
DIC	Differential interference contrast
DMSO	Dimethyl sulfoxide
<i>dt</i>	Dystonic rat
<i>db</i>	Diabetes
dl	Decaliter
EDTA	Ethylenediaminetetraacetic acid
EHD	Eps15 homology domain
ENTH	Epsin NH ₂ -terminal homology
ER	Endoplasmic reticulum

ESI	Electrospray ionization
ET-18-OCH ₃	Edelfosine
Etn	Ethanolamine
FAB	Fast atom bombardment
FERM	4.1/ezrin/radixin/moesin
FM4-64	<i>N</i> -[3-Triethylammoniumpropyl]-4- [<i>p</i> -diethylaminophenylhexatrienyl] pyridinium dibromide
FYVE	Fab 1, YOTB, Vac 1, and EEA1
G6Pase	Glucose-6-phosphatase
GAPs	GTPase activating proteins
GEFs	Guanine nucleotide exchange proteins
GFP	Green fluorescent protein
GLUE	GRAM-Like Ubiquitin-binding in EAP45
GO	Gene ontology
Gro	Glycerol
[³ H]	Tritium
HINT	Hydrophobic INTeractions
HIV	Human immunodeficiency virus

HPLC	High-performance liquid chromatography
hr	Hour
IC ₅₀	Half maximal inhibitory concentration
IMPase	Inositol monophosphatase
Ins	Soluble inositol
Ins-phosphates	Phosphorylated forms of D- <i>myo</i> -inositol
IPs	Inositol polyphosphates
<i>ji</i>	Jittery mouse
<i>ji</i> ^{hes}	Hesitant mouse
<i>ji</i> ^{swd}	Sidewinder mouse
kanga	Kanga mouse
kDa	Kilodalton
<i>KES1</i>	KrE11-1 suppressor
LBDD	Ligand-based drug design
LC-MS	Liquid chromatography mass spectrophotometry
LD	Lipid droplets
LOF	Loss of function

<i>LSB6</i>	Las Seventeen binding protein 1
M	Molar
m	10^{-3}
m	Meter
MALDI	Matrix-assisted laser desorption/ionization
mg	Milligram
min	Minute
mm	Millimolar
MP	Methylenephosphonate
mRFP	Monomeric red fluorescent protein
ms	Metabolically-stabilized
MS	Mass spectrometry
<i>MSS4</i>	Multicopy suppressor of Stt4 mutation
mol%	Molar %
MW	Molecular weight
NaCl	Sodium chloride
NaN ₃	Sodium azide
n	10^{-9}

nM	Nanomolar
nm	Nanometer
NMR	Nuclear magnetic resonance
NPPM	nitrophenyl(4-(2-methoxyphenyl) piperazin-1-yl)methanones
OD	Optical density
p	10^{-12}
p	Protein
PAGE	Polyacrylamide gel electrophoresis
PC	Personal computer
PDB	Protein databank file
PH	Pleckstrin homology
PT	Phosphorothioate
<i>PIK1</i>	Phosphatidylinositol kinase 1
PIP	Phosphatidylinositol phosphate
PITP	Phosphatidylinositol transfer proteins
PLD	Phospholipase D
PLC	Phospholipase C

PLIF	Protein-ligand interaction fingerprint
PMSF	Phenylmethanesulfonyl fluoride
PSD1	PtdSer decarboxylase 1
PSD2	PtdSer decarboxylase 2
PtdCho	Phosphatidylcholine
PtdEtn	Phosphatidylethanolamine
PtdIns	Phosphatidylinositol
PtdIns(3)P	PtdIns(3)phosphate
PtdIns(4)P	PtdIns(4)phosphate
PtdIns(5)P	PtdIns(5)phosphate
PtdIns(3,4)P ₂	PtdIns(3,4)bisphosphate
PtdIns(3,5)P ₂	PtdIns(3,5)bisphosphate
PtdIns(4,5)P ₂	PtdIns(4,5)bisphosphate
PtdIns(3,4,5)P ₃	PtdIns(3,4,5)trisphosphate
PtdOH	Phosphatidic acid
PtdSer	Phosphatidylserine
PTPases	Protein tyrosine phosphatases

pV	Peroxovanadium
PX	Phox homology
Qdots	Quantum dots
RNA	Ribonucleic acid
RNAi	RNA interference
Rpm	Rotations/minute
SAHN	Sequential agglomerative hierarchical nonoverlapping
s.d	Standard deviation
SDS	Sodium doadecyl sulfide
Sec14	Secretory protein 14
s.e.m	Standard error mean
Sfh1	Sec14 homology protein 1
Sfh2	Sec14 homology protein 2
Sfh3	Sec14 homology protein 3
Sfh4	Sec14 homology protein 4
Sfh5	Sec14 homology protein 5
SGA	Synthetic genetic array

siRNA	Small interfering RNA
SM	Sphingomyelin
SMI	Small molecule inhibitor
<i>STT4</i>	Staurosporine and temperature sensitive
TCA	Trichloroacetic acid
TG	Triglycerides
TOF	Time of flight
TGN	<i>Trans</i> -Golgi network
TOR	Target of rapamycin
TS	Temperature sensitive
UV	Ultra violet light
μ	10 ⁻⁶
μCi	Microcuri
μl	Microliter
μM	Micro molar
<i>vb</i>	Vibrator mouse
WASP	Wiskott-Aldrich Syndrome protein

<i>wobbly</i>	Wobbly mouse
WT	Wild-type
wt	Weight
YPD	Yeast peptone dextrose
VO-OHpic	Vandyl complexed to hydroxypicolinic acid
vol	Volume
<i>VPS34</i>	Vacuolar protein sorting 3

CHAPTER 1: MAMMALIAN DISEASES OF PHOSPHATIDYLINOSITOL TRANSFER PROTEINS AND THEIR HOMOLOGUES¹

Overview

Inositol and phosphoinositide signaling pathways represent major regulatory systems in eukaryotes. The physiological importance of these pathways is amply demonstrated by the variety of diseases that involve derangements in individual steps in inositide and phosphoinositide production and degradation. These diseases include numerous cancers, lipodystrophies and neurological syndromes. Phosphatidylinositol transfer proteins (PITPs) are emerging as fascinating regulators of phosphoinositide metabolism. Recent advances identify PITPs (and PITP-like proteins) as outstanding candidates for coincidence-detecting units which spatially and temporally coordinate the activities of diverse aspects of the cellular lipid metabolome with phosphoinositide signaling. These insights are providing new ideas regarding mechanisms of inherited mammalian diseases associated with derangements in the activities of PITPs and PITP-like proteins.

Introduction

The involvement of phosphorylated forms of *D-myo*-inositol (Ins-phosphates) and phosphatidylinositol (phosphoinositides) in eukaryotic signal transduction is well documented (Michell 2008). Indeed, the breadth of inositide and phosphatidylinositol

¹ This chapter is an extended version of an article published in the journal of Clinical Lipidology. The original citation is as follows: Nile, A. H., V. A. Bankaitis, V.A., Grabon, A. (2010). "Mammalian diseases of phosphatidylinositol transfer proteins and their homologs," *Clinical lipidology* 5(6): 867-897.

(PtdIns)-based signaling has inspired some to anoint Ins as evolution's favorite molecule (Irvine 2005). This is not an idle proclamation given the diversity of phosphorylated products that can be generated from Ins-containing compounds. For example, yeast generate five phosphoinositides (PtdIns[3]P, PtdIns[4]P, PtdIns[5]P, PtdIns[4,5]P₂, and PtdIns[3,5]P₂) while higher eukaryotes produce seven (the five listed for yeast plus PtdIns[3,4]P₂ and PtdIns[3,4,5]P₃). The case for Ins-phosphates is more impressive. As each position of the 6-member Ins ring can be phosphorylated (and in at least several cases pyro-phosphorylated), the cabal of possible soluble Ins-phosphate species is immense (63 + Ins for monophosphates and 728 + Ins if one imposes a limit of only two phosphates per Ins-OH). These statistics identify the versatility of Ins as a six-bit chip where specific signaling information is encoded by a unique combination of positionally-specific phosphorylations on the Ins ring. The Ins-phosphate chemical code is subsequently interpreted by proteins which have the appropriate Ins-phosphate binding specificities.

Use of Ins as a signaling scaffold, either in the form a soluble Ins-phosphate or a membrane-incorporated phosphoinositide, requires a fine coordination between biosynthetic activities (PtdIns-kinases) and degradative processes (catalyzed by phospholipases and phosphoinositide phosphatases). Comprehensive reviews focusing on the metabolism of Ins-phosphates and phosphoinositides treat these issues in detail, and the reader is referred to them (Fruman, Meyers et al. 1998; Martin 1998; Di Paolo and De Camilli 2006; Strahl and Thorner 2007). In this regard, the physiological importance of Ins and PtdIns metabolism is obvious. Defects in the enzymes that directly catalyze specific biosynthetic or degradative reactions in Ins-phosphate or phosphoinositide metabolic pathways result in a variety of inherited human diseases (Majerus and York 2009; Liu and Bankaitis 2010). The landscape

assumes even greater complexity when issues of spatial/temporal control of phosphoinositide production and degradation (i.e. issues critical to biological regulation of Ins-phosphate and phosphoinositide signaling) are considered. In this review, we will limit discussion to the production arm of phosphoinositide signaling.

Present discussions of the roles for phosphoinositides in cell regulation focus on: **(i)** the function of these lipids as metabolic reservoirs for second messengers (e.g. diacylglycerol and soluble Ins-phosphates), and **(ii)** their involvement in the formation of membrane binding platforms for specific proteins (Balla 2005; McLaughlin and Murray 2005; Lemmon 2008). Regarding the latter context, the ability of a mammalian cell to produce 7 chemically distinct phosphoinositides allows for creation of a diverse set of binding platforms. The chemical heterogeneity of phosphoinositides is in turn interpreted by protein binding motifs such as PH-domains, FYVE-domains, PX-domains, and even basic patches on protein surfaces that execute phosphoinositide binding by purely electrostatic mechanisms (see **Chapter 3**; Balla 2005; McLaughlin and Murray 2005; Lemmon 2008).

Discussions of phosphoinositide signaling are dominated by product-centric models that fail to capture important dynamics that accompany production of these lipids. These discussions also do not adequately describe the consequences these mechanisms have with regard to functional diversification of phosphoinositide signaling. The principle message to be delivered in this review is that we do not yet understand important aspects for how lipid signaling is regulated in eukaryotic cells, nor do we understand how the larger lipid metabolome is integrated with phosphoinositide signaling. An emerging concept that bears on this theme is a specific phosphoinositide generated by a specific lipid kinase can nonetheless have multiple biological outcomes in a single cell eukaryote (Routt, Ryan et al.

2005; Schaaf, Ortlund et al. 2008; Bankaitis, Mousley et al. 2010). Thus, biological outcome is not solely determined by the chemical nature of the phosphoinositide, nor is it determined by the PtdIns kinase that produced it. Rather, biological outcome tracks with non-enzymatic proteins that stimulate PtdIns kinase activities. These accessory proteins are the PtdIns/phosphatidylcholine (PtdCho)-transfer proteins (PITPs), and the data suggest PITPs ‘instruct’ physiological outcomes for PtdIns kinase activities (Routt, Ryan et al. 2005; Schaaf, Ortlund et al. 2008; Bankaitis, Mousley et al. 2010). PITP-like protein domains hold similar potential for providing such instructive functions, and these domains are found in intriguing contexts. The importance of PITPs and PITP-domain proteins in eukaryotic cell biology and physiology is amply demonstrated by the mammalian diseases associated with derangements in the function of such proteins. Herein, we review the PITPs and mammalian diseases of PITP-like protein dysfunction.

Operational definitions for the PITPs

Sec14-like and START-like PITPs

All eukaryotes express PITPs. The so-called ‘classical’ PITPs (a purely historical definition), which are best studied, mobilize PtdIns and PtdCho transfer between membranes *in vitro*. These PITPs bind PtdIns and PtdCho in a mutually exclusive manner. PtdIns is the preferred binding substrate, and the rate of PtdIns-transfer is some 20-fold greater than that for PtdCho (Wirtz 1991). This results from the greater affinity of PITP for PtdIns relative to PtdCho. Presently, PITPs are most often interpreted to function as lipid carriers that supply PtdIns synthesized in endoplasmic reticulum membranes to membranes that are low in PtdIns (*e.g.* the plasma membrane) yet execute an active phosphoinositide cycle (Cockcroft and

Carvou 2007). The ‘non-classical’ PITPs are so designated because these retain the ability to bind/transfer PtdIns, but do not conserve PtdCho-binding/transfer activity (Li, Routt et al. 2000; Routt, Ryan et al. 2005; Phillips, Vincent et al. 2006). The non-classical PITPs which, ironically, almost certainly outnumber the classical versions, provide interesting cases for how the diversity in lipid binding by PITPs and PITP-like proteins translates to the awesome diversity in biological outcome for phosphoinositide signaling (see below).

PITPs are highly conserved. The conservation of PITPs breaks down into two distinct branches based on their structural folds: (i) the Sec14-like PITPs, and (ii) the START-like (StAR-related lipid transfer) PITPs. To date, all START-like PITPs studied are classical PITPs, while Sec14-like proteins include both classical and non-classical varieties. As described in detail below, the Sec14 and START folds are unrelated although these do share some general properties. Whether Sec14-like and START-like PITPs evolutionarily converge on common functional mechanisms, or whether their shared transfer activities are purely coincidental, remains to be determined.

Fungi, plants, metazoans, and apicomplexan parasites are rich in Sec14-like proteins, and these constitute an ancient and uniquely eukaryotic protein superfamily. The founding member of this PITP class is yeast Sec14 (Bankaitis, Malehorn et al. 1989; Bankaitis, Aitken et al. 1990; Phillips, Vincent et al. 2006). As detailed below, the Sec14 superfamily counts amongst its >1500 members the mammalian retinaldehyde binding proteins, domains of Rho-GEF proteins, the neurofibromin Ras-GAPs, and plant phosphoinositide binding proteins. Even simple eukaryotes such as yeast express multiple Sec14-like proteins (*S. cerevisiae* expresses 6), while *D. melanogaster*, *C. elegans*, mice, humans, and plants (*A. thaliana*) each express greater than 20 Sec14-domain proteins.

By contrast, the START-like PITP family is a rather sparse one, is structurally unrelated to the Sec14-like proteins (Yoder, Thomas et al. 2001; Phillips, Vincent et al. 2006), and is further subdivided into Type 1 and Type 2 PITPs. The soluble START-like PITPs (Type 1 PITPs) are ~ 35 kD MW and are homologous to each other. The Type II proteins are larger constructions with a domain homologous to the entire Type 1 START-like PITP sequence appended to the N-termini of large membrane-associated modules. The START-like PITP family is not expanded to a large degree from flies (two Type 1 PITPs and one Type 2 PITP) to humans (three Type 1 PITPs and two Type 2 PITPs; 17). The Type 2 PITPs exhibit complex modular arrangements, but the PITP domain is the essential component of at least one of these proteins--the ca. 900 amino acid *Drosophila* Type 2 PITP RdgB. This protein is required for the fly photoresponse – a high capacity phosphoinositide signaling system. Yet, the 280 residue PITP domain of RdgB (comprises only ca. 25% of the total RdgB protein sequence) is both necessary and sufficient for rescue of the retinal degeneration associated with RdgB inactivation, and for restoration of a seemingly wild-type photoresponse in flies lacking the full-length protein (Milligan, Alb et al. 1997). This review focuses on Type 1 PITPs because these are better represented in models for mammalian disease.

The slippery faces of lipid transfer activities

Because PITPs are not enzymes, translation of PITP-associated lipid exchange activities to biochemical or biological mechanisms is difficult. While discussions of biological mechanisms for PITP function remain anchored to the historical concept that PITPs are bona fide carrier proteins that deliver lipid from one intracellular membrane

system to another (**Figure 1a**), such arguments are inherently circular. That is, PITPs are defined on the basis of an operational transfer assay of uncertain functional significance, and the transfer activity is subsequently featured as the central cellular activity executed by the PITP. Arguments that directly translate PITP *in vitro* transfer activities to facilitated mobilization of lipid between intracellular membranes *in vivo* are wrapped in important biological assumptions. One central assumption made in such transfer models is that lipid synthesis is restricted to a few intracellular compartments. As our understanding of cellular lipid biosynthetic capabilities grows, this assumption is coming under increasing fire.

The general acceptance of lipid transfer mechanisms notwithstanding, there is little direct evidence to support simple transfer models for any individual PITP. This evidentiary gap reflects the difficulties in experimentally testing transfer models in physiologically relevant settings. Are there other perspectives from which to view the PITP/lipid transfer problem? Insights culled from studies on PITPs, particularly PITPs of the Sec14-superfamily; do indeed suggest new and detailed mechanistic possibilities. The available evidence is most consistent with Sec14, and other Sec14-like proteins, functioning as ‘primed’ lipid biosensors that couple binding of lipids other than PtdIns (sensor function) to a PtdIns-presentation activity (**Figure 1b**). The PtdIns-presentation function potentiates PtdIns-kinase activity by making PtdIns a better substrate for the enzyme. Thus, Sec14-like PITPs are engaged in the action of small machines, or nanoreactors, where metabolic and signaling reactions are integrated, and the products generated in a spatially and temporally appropriate manner. We define a minimal nanoreactor as a functional interaction between a phospholipid-bound PITP and a PtdIns kinase. ‘Nanoreactor’ models do not describe PITPs as *trans*-organellar lipid carriers, and offer new perspectives on how to interpret functions of

PITP-like modules in multi-domain proteins. The Sec14 paradigm provides new ideas from which to view mechanisms of PITP function, and recent evidence suggests these new concepts might extend to Type 1 PITPs.

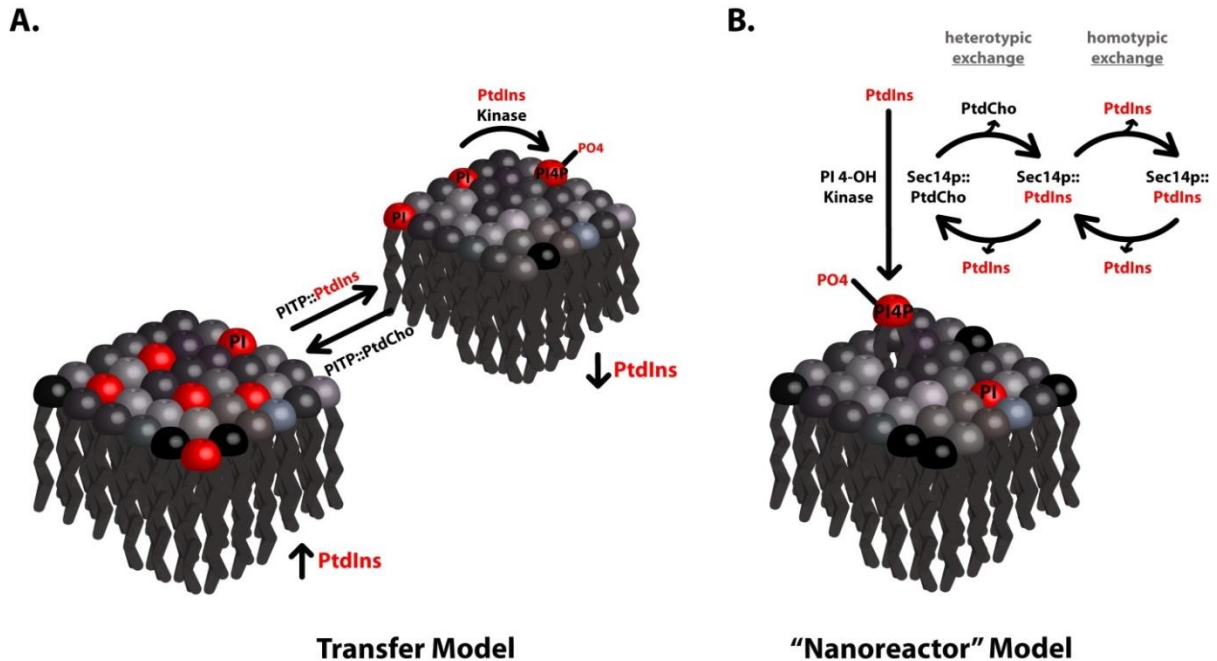


Figure 1. Transfer vs. nanoreactor models for PITP function

(a) Lipid transfer models invoke a vectorial carrier function for PITPs where PtdIns is transported from membranes of high PtdIns concentration (ER) to relatively PtdIns-poor membranes of the distal compartments of the secretory pathway which house PtdIns-4OH kinase activity (TGN/endosomes or plasma membrane). These models describe productive transfer as involving one heterotypic exchange reaction per donor and acceptor membrane (*i.e.* two such exchanges per cycle). (b) The ‘nanoreactor’ model predicts that PITPs stimulates PtdIns 4-OH kinase activity by executing multiple rounds of phospholipid-exchange at a single membrane site. Only heterotypic exchange reactions generate PtdIns configurations suitable for effective PtdIns-presentation.

Sec14-like PITPs as molecules

Sec14 and integration of PtdCho metabolic signals

Sec14, the major yeast PITP, is required for membrane trafficking through the *trans*-Golgi network/endosomal system where it acts in a retrograde endosome to TGN trafficking capacity, and is essential for yeast cell viability (Phillips, Vincent et al. 2006; Mousley, Tyeryar et al. 2008; Bankaitis, Mousley et al. 2010). ‘Bypass Sec14’ mutations that permit yeast viability in the absence of the normally essential Sec14 provide unique avenues for diagnosing how Sec14 translates its PtdIns/PtdCho-transfer activities to biological function (Cleves, Novick et al. 1989; Cleves, McGee et al. 1991; Cleves, McGee et al. 1991; Fang, Kearns et al. 1996; Rivas, Kearns et al. 1999; Li, Rivas et al. 2002). The ‘bypass Sec14’ mutants reveal a remarkably intimate coupling between the cellular requirement for Sec14 function and activity of the CDP-choline pathway for PtdCho biosynthesis. That is, inactivation of the CDP-choline pathway obviates the cellular Sec14 requirement (Cleves, McGee et al. 1991; Cleves, McGee et al. 1991). These studies also show that yeast mutants deranged for phospholipid biosynthesis, such that PtdIns is the major membrane phospholipid (~40 mol%—as compared to 20 mol% for wild-type yeast and 5 mol% for mammalian cells), still require Sec14 for cell viability. A PtdIns surfeit of this magnitude should present a condition where PITP-driven PtdIns-supply requirements are no longer necessary—yet, the Sec14 requirement for cell viability and TGN/endosomal function stands. These various data are difficult to reconcile with PtdIns- and PtdCho-transfer models for Sec14 (Cleves, McGee et al. 1991; Cleves, McGee et al. 1991). Rather, ‘bypass Sec14’ mutants identify Sec14 as an essential integrator required for proper coordination of a specific arm of PtdCho-metabolism with phosphoinositide synthesis. This integration is

essential for membrane trafficking through the TGN/endosomal system (Cleves, McGee et al. 1991; Cleves, McGee et al. 1991; Fang, Kearns et al. 1996; Rivas, Kearns et al. 1999; Li, Rivas et al. 2002; Phillips, Vincent et al. 2006; Schaaf, Ortlund et al. 2008; Bankaitis, Mousley et al. 2010).

The anatomy of phospholipid exchange by Sec14-like PITPs

All ideas regarding mechanisms of PITP function assign an important role for the phospholipid-exchange activities of these proteins. These remarkable activities are sustained by thermal energy alone and require no additional co-factors. What are the mechanics of the phospholipid exchange reaction from the perspective of the PITP and from the perspective of phospholipid ligand? Crystallographic studies show the Sec14-domain (smart00516) to be a ca. 280 amino acid two-lobed globular structure that encases a large hydrophobic cavity which defines the phospholipid-binding pocket (Sha, Phillips et al. 1998; Phillips, Sha et al. 1999; Schaaf, Ortlund et al. 2008). Electron paramagnetic resonance measurements report that the hydrophobicity parameters of the pocket are such that this cavity, from the perspective of the phospholipid binding substrate, offers an environment that is similar to that provided by a membrane leaflet. Thus, incorporation of a phospholipid from a membrane into the Sec14 interior, and vice versa, is primarily driven by partitioning of a phospholipid between two chemically equivalent environments (Smirnova, Chadwick et al. 2007). How the phospholipid is brought to the point where such a partitioning choice is available remains unclear.

Access to the binding pocket is gated by a helical substructure whose configuration is flipped open in apo-Sec14 conformers that occur when Sec14 is docked onto membrane surfaces (**Figure 2a**; Sha, Phillips et al. 1998; Ryan, Temple et al. 2007; Schaaf, Ortlund et al. 2008). The helical gate is closed in holo-Sec14 conformers (**Figure 2b**), and these represent solution configurations for Sec14::PtdIns and Sec14::PtdCho complexes. The transitions between the ‘open’ and ‘closed’ conformers that accompany phospholipid binding and release on membrane surfaces are dominated by an 18Å displacement of the helical gate (**Figure 2**). Helical gate dynamics are controlled by a compact ‘gating module’ that regulates an extensive H-bond network through which conformational information is transduced to the helical gate upon membrane binding (Ryan, Temple et al. 2007).

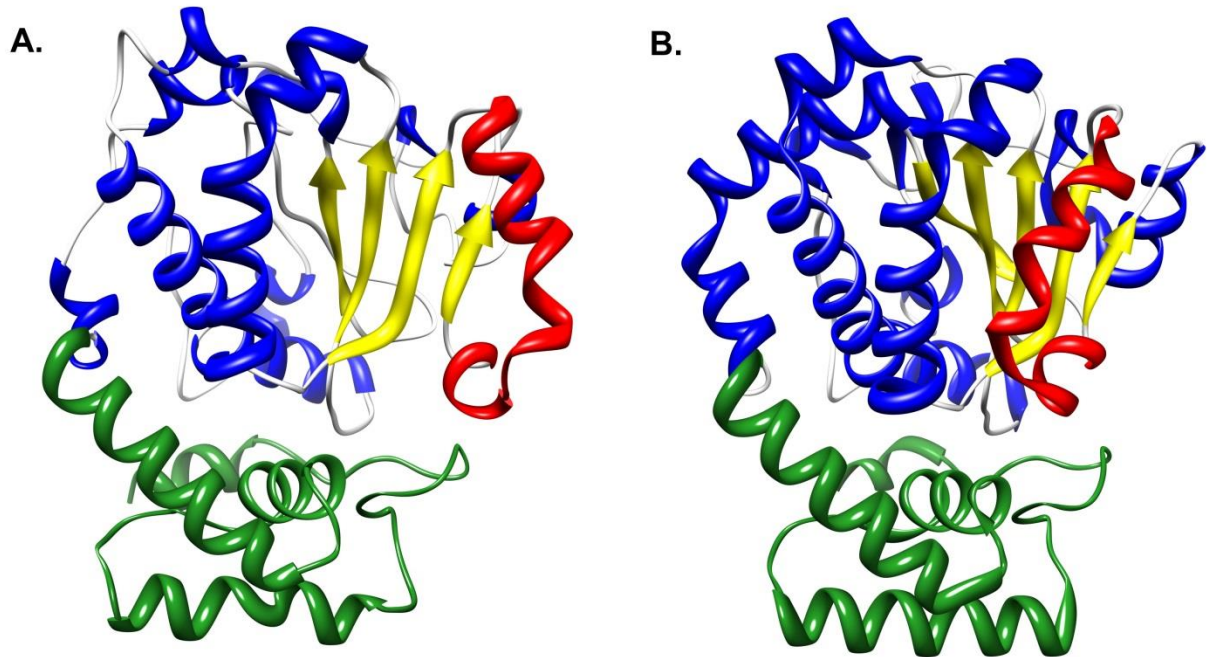


Figure 2. The Sec14-fold.

Crystal structure of two *Saccharomyces cerevisiae* Sec14-like PITPs. (a) The major yeast PITP, Sec14 is shown in its open conformation (pdb 1AUA—two bound detergent molecules are excluded). (b) The close Sec14 homolog Sfh1 in its closed conformation (pdb 3B7Z—the bound phospholipid was omitted). The β -strands comprising the floor of the phospholipid binding pocket are in yellow, while the α -helices that form the walls of the pocket are in blue. Access to the hydrophobic pocket is mediated by conformational transitions of the A10/T4 ‘helical gate’ shown in red. The four N-terminal α -helices (α 1- α 4) comprise the N-terminal lobe (or ‘tripod motif’; green).

The core engineering of a Sec14 nanoreactor

How does Sec14 use its PtdIns- and PtdCho-transfer activities to integrate PtdCho metabolism with phosphoinositide synthesis? The solution to this problem is encoded in the way Sec14 binds its phospholipid ligands. The most remarkable feature of Sec14 (and Sfh1) is the striking difference in the binding poses of PtdIns and PtdCho upon incorporation into the hydrophobic pocket (**Figure 3**). While the acyl chain regions of each phospholipid

occupy overlapping physical space, the respective headgroups are stabilized by distant regions of the hydrophobic pocket. This curious and unexpected engineering for how Sec14 binds distinct phospholipid headgroups is of functional significance as heterotypic phospholipid exchange capability must be housed within individual protein molecules in order for Sec14 to potentiate PtdIns 4-OH kinase activities *in vivo* (Schaaf, Ortlund et al. 2008; Bankaitis, Mousley et al. 2010). In principle, Sec14 employs a coincidence-detection strategy that integrates PtdCho metabolic information with the action of PtdIns 4-OH kinases—*i.e.* Sec14 employs its heterotypic PtdIns-/PtdCho-exchange activities to sense (bind) local PtdCho and so prime a ‘PtdIns-presentation’ unit, or ‘nanoreactor’, that stimulates PtdIns 4-OH kinases. The necessity for such a complex program stems from the biological inadequacy of PtdIns 4-OH kinases as interfacial enzymes when confronted with PtdIns substrates incorporated into genuine membrane bilayers (Schaaf, Ortlund et al. 2008; Bankaitis, Mousley et al. 2010).

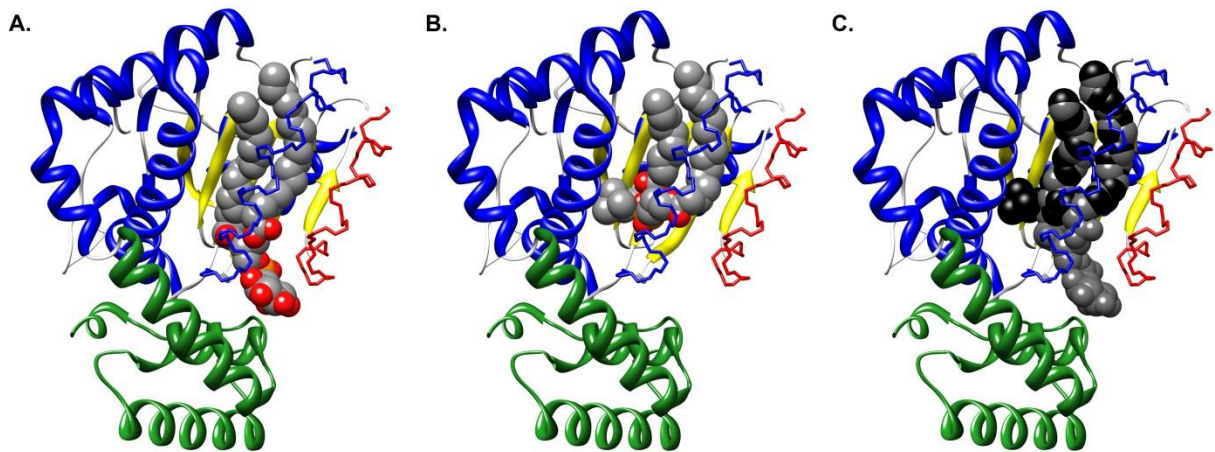


Figure 3. Differential phospholipid binding strategies by Sec14-like PITPs.

Structure of Sfh1 bound to: (a) PtdIns (pdb 3B7Z); (b) PtdCho (pdb 3B7Z). (c) A description of the configurations of both PtdIns (gray) and PtdCho (black) in the Sfh1/Sec14-fold. The data are from crystals composed of approximately equal numbers of unit cells of Sfh1 bound to PtdIns and Sfh1 bound to PtdCho (pdb 3B7Z). The A10/T4 ‘helical gate’ that mediates lipid entry is in red, surrounding α -helices are in blue, the ‘tripod motif’ is in green and β -strands that compose the floor of the hydrophobic pocket are in yellow. The polar headgroups of PtdIns and PtdCho bind at distinct sites within the hydrophobic pocket, while the acyl chain space within the hydrophobic pocket overlaps for these phospholipids.

Primed PtdIns-presentation models versus lipid transfer models

The concept that Sec14 employs heterotypic exchange in a concerted phospholipid sensing/presentation cycle portrays the associated *in vitro* PtdIns-/PtdCho-transfer activities in a very different light than do lipid transfer models. An attractive aspect of presentation/nanoreactor models is these frame specific and experimentally testable hypotheses. Several are presented here for discussion. While the questions are framed in the context of Sec14, each of these ideas generates questions that generally pertain to functional interpretations of PITPs and other lipid transfer proteins.

Presentation models do not demand physical transfer of lipids from one intracellular destination to the other—it is the cycle that is the key. How many average exchange cycles does Sec14 complete during its membrane dwell time? Presentation models embrace the possibility that many such cycles are executed per membrane association window, while transfer models describe a scenario where there is one exchange cycle per transfer event.

Is physical disengagement of Sec14 from membranes required for execution of biological function? The simplest transfer models demand this be the case, although membrane ‘contact site’ models leave open the possibility that a membrane-bound Sec14 could still retain biological function. Space limitations prohibit detailed discussions of ‘contact-site’ models but the concept is reviewed elsewhere (Wu and Voelker 2002; Holthuis and Levine 2005), and readers are referred to these for further information. Presentation models easily accommodate scenarios where Sec14 (or other LTP domains) are biologically functional as membrane-bound multi-domain molecules.

Is a complete cycle of exchange obligatory for function, or are abortive exchanges productive? Transfer models demand completion of a pick-up and delivery cycle. Not so for presentation models. The ‘presentation’ concept describes a trapping of PtdIns molecules in a transitory state, one where the PtdIns is neither fully membrane- nor protein-incorporated, and is therefore particularly vulnerable to modification by PtdIns 4-OH kinases. Such a mechanism posits that an invading PtdIns molecule is prevented from fully incorporating into the Sec14 hydrophobic pocket by a leaving PtdCho. Such a frustrated PtdIns molecule can be marked by a PtdIns 4-OH kinase without the PtdIns ever having fully incorporated itself into the Sec14 hydrophobic pocket. Interestingly, PtdCho enters/exits the hydrophobic pocket much more slowly than does PtdIns. This raises the possibility that multiple rounds

of abortive PtdIns incorporation may occur per single PtdCho egress event—thereby providing a physical picture of priming. A formal corollary to this hypothesis is that an appropriate covalent adduct of PtdCho, or any other suitable steric obstacle, within the Sec14 hydrophobic pocket might still be compatible with the capability of Sec14 to stimulate PtdIns 4-OH kinase activity— even though this arrangement is physically incompatible with lipid exchange.

What trajectories do lipid molecules follow during entry/exit from the Sec14 hydrophobic pocket? Do PtdIns and PtdCho share similar trajectories (*e.g.* same entry and exit portals), or do these trace different paths? Reductionist questions of this sort are not particularly important for understanding inter-organelle lipid transfer mechanisms. However, solutions to these questions are central to an understanding of how presentation/nanoreactor mechanisms work because heterotypic phospholipid trajectories define the operative anatomy of the presentation process.

Finally, how are Sec14 ‘sensing’ territories defined? This question relates to how spatial regulation of phosphoinositide synthesis is controlled. We define a sensing territory as that area on a given membrane where the PITP is executing biologically productive heterotypic phospholipid exchange reactions (*i.e.* result in enhanced phosphoinositide synthesis). For membrane-tethered versions of Sec14-like PITPs (see below), the spatial restriction of the tethering (by accessory membrane-binding domains, membrane-binding via protein-protein or protein-lipid interactions intrinsic to the Sec14 domain), determines the sensing territory. The cytosolic Sec14, however, potentiates the activities of distinct PtdIns 4-OH kinases that reside in distinct intracellular compartments within the same cell. How is this accomplished for such a nomadic PITP? Transient interactions of Sec14 with a guiding

platform (protein or lipid) might contribute at some level. The PtdIns 4-OH kinase itself is an obvious candidate for such a landmark. However, the ability of the structurally unrelated vertebrate Type 1 PITPs to act as functional Sec14 surrogates in yeast argues against privileged Sec14/PtdIns 4-OH kinase interactions (Skinner, Alb et al. 1993; Tanaka and Hosaka 1994; Ile, Kassen et al. 2010). As discussed in detail elsewhere (Bankaitis, Mousley et al. 2010), more stochastic arrangements can still be biologically productive (*i.e.* result in enhanced synthesis of phosphoinositide).

A PITP-centric strategy for linking lipid metabolism to phosphoinositide signaling

The Sec14-fold is an evolutionarily ancient and versatile one conserved from single cell eukaryotes to man. Its expansion throughout the eukaryotic kingdom reflects an impressive diversification of the unit to bind a wide variety of lipids and lipophilic molecules. Primary sequence comparisons identify well-conserved crystal structure-based PtdIns-binding signatures in many of these proteins; however, PtdCho-binding signatures are not extensively conserved (Schaaf, Ortlund et al. 2008; Bankaitis, Mousley et al. 2010). These binding signatures, or bar codes, represent translation of 3-dimensional structural information into a 2-dimensional primary sequence read-out. The PtdIns-binding bar code is depicted in **Figure 4**. It is an attractive proposition that Sec14 superfamily proteins couple metabolism of a diverse set of lipids/lipophilic molecules (*i.e.* of Sec14-protein ligands) with phosphoinositide synthesis – thereby coordinating disparate arms of the lipid metabolome with common phosphoinositide signaling pathways. These models might generally apply to PITPs and PITP-domain proteins. We highlight these new perspectives in this review.

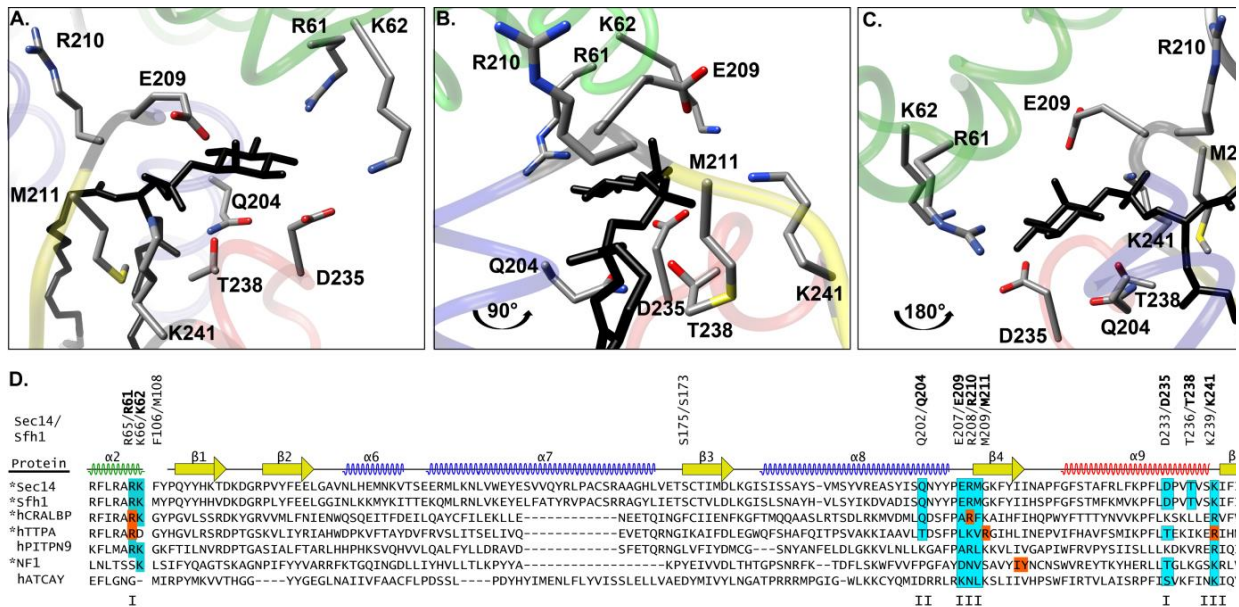


Figure 4. The PtdIns-binding bar code in Sec14-like proteins.

(a) Crystal structure of Sfh1 bound to PtdIns (black; 3B7N) highlighting residues within the PtdIns binding bar code. The tripod-motif is in green, the floor of the hydrophobic pocket is in yellow, and the α -helices are in blue with the exception of the helical gate, which is in red. (b) Orientation of the Sfh1 molecule is rotated by 90° counterclockwise parallel to the floor. (c) Orientation of the Sfh1 molecule is rotated by 180° counterclockwise parallel to the floor. (d) ClustalX2 alignments of selected Sec14-superfamily members (identified at right; proteins whose crystal structures have been solved are indicated with an (*) were superimposed onto the Sfh1 crystal structure using secondary structural elements as guide (diagrammed at top). Residues critical for PtdIns headgroup and backbone coordination are boxed and shaded in cyan – I, coordinate the Ins-headgroup; II, coordinate the glycerol backbone; III, coordinate the phosphate moiety through which the Ins headgroup is esterified to the glycerol backbone. Positions of missense substitution within the PtdIns-binding bar code of the corresponding Sec14-like protein that cause disease are highlighted by orange boxes.

Mammalian Sec14-domain protein disorders

Mammals employ the versatile Sec14 fold in diverse ways – in some cases as stand-alone domains or, more frequently, as modules that contribute to more complex arrangements in multi-domain proteins. Due to the sheer scope of the Sec14 superfamily, only a limited sampling of proteins can be summarized here. We primarily restrict attention to those Sec14-like proteins whose dysfunction is related to inherited mammalian disease (**Figure 5**).

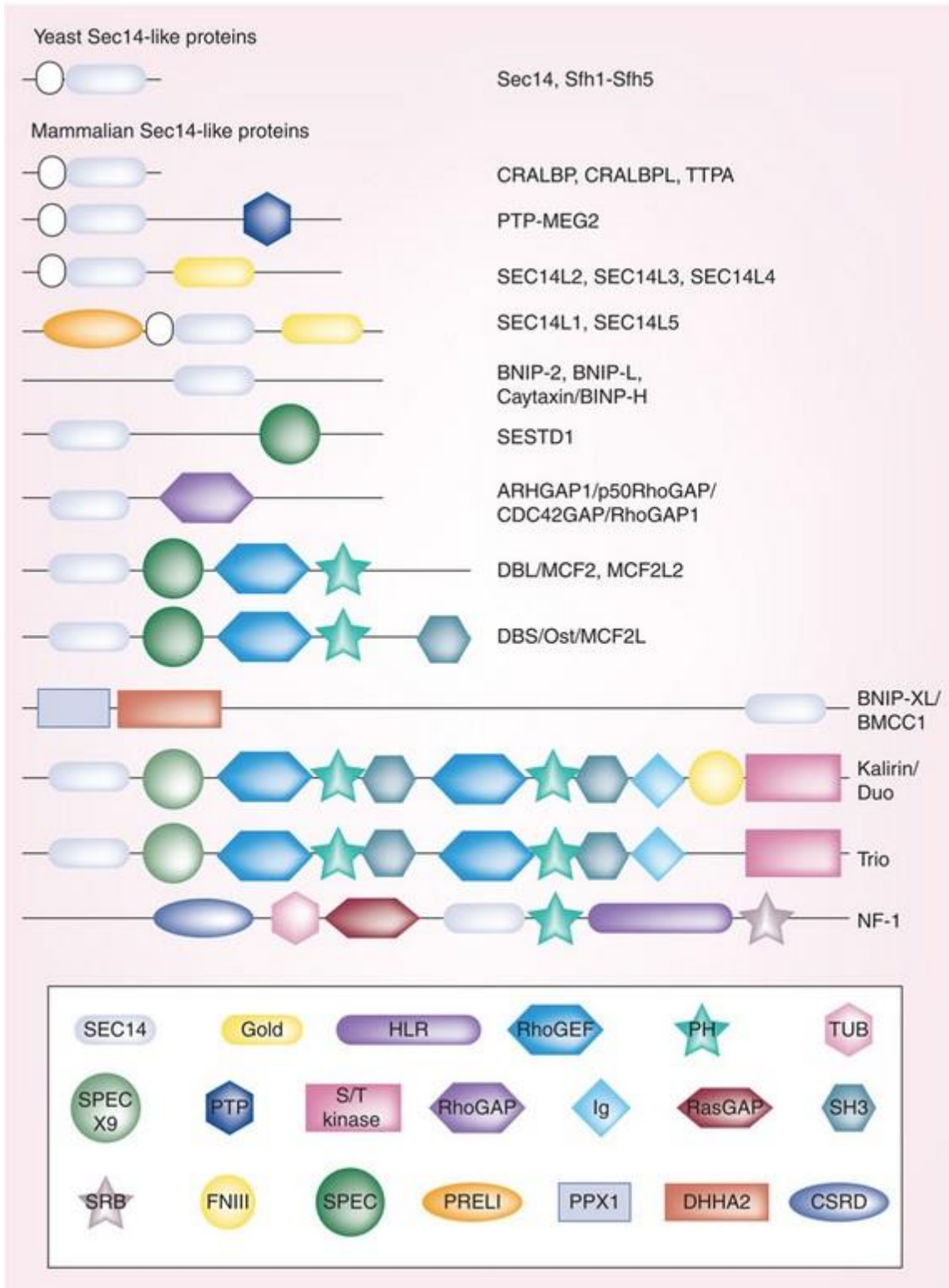


Figure 5. Domain arrangements of Sec14-like proteins

Representative Sec14-like proteins are schematized and ordered by general complexity. Domains of interest are identified.

Stand-alone Sec14-like proteins and disease

The stand-alone Sec14-like proteins regulate a variety of cellular events including the visual cycle, vitamin E homeostasis, apoptosis, and membrane trafficking. Individual derangements in these stand-alone Sec14-like proteins primarily manifest themselves as neurological disorders. Some outstanding examples are summarized below. In some cases, the identities of the ligands which occupy the hydrophobic pocket are known. For others, no ligand that incorporates into the protein interior is known. Yet, many Sec14-like proteins exhibit a recognizable structurally defined PtdIns-binding bar code (Schaaf, Ortlund et al. 2008). Whether these proteins do indeed bind PtdIns, and whether these are capable of channeling PtdIns to phosphoinositide synthesis, raises interesting questions for study.

α -tocopherol transfer protein and vitamin E status

Ataxia with vitamin E deficiency (AVED) is an autosomal recessive, progressive neurodegenerative disorder caused by deficiencies in the Sec14-like α -tocopherol binding protein (α TTP; Mariotti, Gellera et al. 2004). This human disease is hallmarked by low vitamin E levels, and manifests itself through hyporeflexia, ataxia, muscle weakness, dementia, visual field contraction and even complete blindness, and cardiac arrhythmias (Aparicio, Belanger-Quintana et al. 2001). Treatment for AVED involves high doses of orally administered vitamin E (1200 to 1500 mg/day) which restores vitamin E to normal circulating levels of 0.5-2.0 mg/dl. Indeed, if administered prior to extensive progression of disease, either post-symptomatic or pre-symptomatic delivery of vitamin E can effectively reverse, or entirely prevent, AVED (Doria-Lamba, De Grandis et al. 2006). Mice engineered for α TTP deficiency similarly exhibit low levels of circulating vitamin E, and present late-

onset neurological deficits (Terasawa, Ladha et al. 2000; Yokota, Igarashi et al. 2001; Leonard, Terasawa et al. 2002).

At least 25 mutations have been described in the 278-amino acid, α TTP structural gene (*TTPA*). These fall into two clinical categories: those resulting in severe AVED with early onset and, and those characterized by milder AVED with late onset (Di Donato, Bianchi et al. 2010). Several mutations in conserved residues (*e.g.* R₅₉W, E₁₄₁K, and R₂₂₁W) compromise α -TOH binding/transfer and result in severe AVED (Morley, Panagabko et al. 2004). By contrast, the R₁₉₂H, H₁₀₁Q, and A₁₂₀T missense substitutions involve partially conserved residues, do not strongly compromise α -TOH binding /transfer, and result in mild AVED (Qian, Atkinson et al. 2006; Morley, Cecchini et al. 2008).

It is generally accepted that α TTP is the master regulator of plasma vitamin E levels. In comparative studies, α TTP preferentially binds and transfers α -tocopherol (α -TOH) between membranes *in vitro* relative to other tocopherols (Akihiro, Makoto et al. 1997; Panagabko, Morley et al. 2003; Zhang, Frahm et al. 2009). It is thought that α TTP employs such a transfer activity to channel α -TOH to a secretory, rather than a degradatory, fate (Traber 2007; Clarke, Burnett et al. 2008). Some models suggest that α TTP does so by mediating direct transport of α -TOH from endosomes to the plasma membrane for incorporation into very low density lipoproteins in an ABCA1 transporter-dependent hepatic secretory pathway (Horiguchi, Arita et al. 2003; Qian, Morley et al. 2005). Consistent with this view, α TTP expression enhances α -TOH secretion in cultured hepatocytes (Arita, Nomura et al. 1997; Qian, Atkinson et al. 2006).

The Sec14 nanoreactor concept suggests an alternative model— α TTP may link heterotypic α -TOH/PtdIns binding/exchange to generation of a phosphoinositide pool dedicated to biogenesis of α -TOH-rich exocytic vesicles. This model predicts that compromise of the PtdIns-binding bar code in α TTP will inactivate the protein. In this regard, the R₂₂₁W missense substitution, which results in severe AVED, directly alters the PtdIns-binding bar code. This position corresponds to Sec14 residue K₂₃₉. This residue helps coordinate binding of the phosphate moiety through which the Ins headgroup is esterified to the glycerol backbone. Substitutions at this position specifically compromise PtdIns binding by Sec14 (Phillips, Sha et al. 1999; Schaaf, Ortlund et al. 2008). Similarly, the R₁₉₂H AVED-associated missense substitution in α TTP corresponds to Sec14 amino acid G₂₁₀ – a residue positioned adjacent to core elements of the PtdIns-binding bar code.

Caytaxin and cerebellar ataxia

Cayman-type cerebellar ataxia is a rare autosomal recessive disorder whose incidence is limited to an isolated population on the Grand Cayman Island resulting from defects in the brain-specific, Sec14-like presynaptic protein termed caytaxin. Clinical manifestations include cerebellar hypoplasia, psychomotor retardation, hypotonia from birth, prominent non-progressive cerebellar dysfunctions that manifest through intention tremors, dysarthric speech, and a wide-base ataxic gait. This disease is distinguished from other ataxias by the presence of nystagmus and the lack of retinal defects (Nystuen, Benke et al. 1996; Bomar, Benke et al. 2003). Although lipid ligand(s) for caytaxin are not known, structural modeling suggests PtdIns lipids are tenable candidates (Bomar, Benke et al. 2003; Xiao, Gong et al. 2007)—a concept fortified by a recognizable structural bar code for PtdIns-binding (Schaaf,

Ortlund et al. 2008). Analyses of Cayman-type ataxic individuals reveal two polymorphisms. One disrupts an exon-intron boundary leading to truncation of much of the protein, and an S₃₀₁R missense mutation (Bomar, Benke et al. 2003). Our analyses project S₃₀₁ to fall into the helical gate region of the caytaxin Sec14-fold, suggesting gate dynamics that regulate transitions between open and closed caytaxin conformers might be compromised. An interesting question for future address is whether compromise of the putative caytaxin PtdIns-binding bar code inactivates the protein.

Much of what is known about caytaxin is derived from the study of rodent models. Caytaxin derangements result in a spectrum of motor malfunctions/dystonia in the jittery (*ji*), hesitant (*ji^{hes}*), sidewinder (*ji^{swd}*) and *wobbly* mice [<http://mutagenetix.scripps.edu/home.cfm>], and the well-characterized dystonic (*dt*) rat (Xiao and LeDoux 2005). A battery of electrophysiological and biochemical studies define the olivocerebellar pathway, particularly in the response of Purkinje cells to climbing fiber projections, as the point of functional abnormality in the *dt* rat (LeDoux and Lorden 2002). The *dt* rat cerebellar cortex exhibits altered transcript levels for signaling pathway components that regulate cell-surface signaling, calcium homeostasis, extracellular matrix, and PtdIns signaling (Xiao, Gong et al. 2007). Upregulation of caytaxin in human prefrontal cortex is also associated with altered calcium homeostasis and immune system imbalances in schizophrenia (Martins-de-Souza, Gattaz et al. 2009). Interestingly, while *dt* rats normally die by postnatal day 40, cerebellectomy rescues both ataxia and viability, suggesting that aberrant cerebellar signaling lies at the root of the observed dysfunctions (LeDoux, Lorden et al. 1993; LeDoux, Lorden et al. 1995; Raike, Jinnah et al. 2005).

Caytaxin physically interacts with number of proteins—including the E3 ubiquitin ligase CHIP (Grelle, Kostka et al. 2006), and peptidyl-prolyl isomerase during neuronal differentiation (Buschdorf, Chew et al. 2008). These associations suggest caytaxin function may be regulated by its binding to these proteins. Furthermore, the caytaxin Sec14-domain binds the kidney-type glutaminase – an enzyme which converts glutamine to the abundant neurotransmitter glutamate. Caytaxin over-expression results in the translocation of the enzyme from the cell body to neurite terminals, and reduces steady state glutamate levels by inhibiting glutaminase. On this basis, it is speculated that caytaxin deficiency-associated glutamate elevation underlies the clinical manifestations of cayman-type cerebellar ataxia (Grelle, Kostka et al. 2006). Moreover, overexpression of either caytaxin (or its Sec14-domain alone) result in the elongation of processes in MCF-7 cells, as is the case with overexpression of the caytaxin homologue BNIP-2 (Hayakawa, Itoh et al. 2007; Aoyama, Hata et al. 2009). Finally, caytaxin also scaffolds kinesin light chain 1 in cultured hippocampal cells, thereby facilitating transport of vesicle cargo (Aoyama, Hata et al. 2009).

Cellular retinaldehyde binding protein and the vertebrate visual cycle

In vertebrates, light absorption by opsin results in photoisomerization of 11-*cis*-retinaldehyde (11-*cis*-RAL) to all-*trans*-retinaldehyde (all-*trans*-RAL). Thus, 11-*cis*-RAL regeneration is essential for a sustained vertebrate visual cycle. Detailed description of the vertebrate visual cycle is beyond the scope of this review; and the reader is referred to detailed reviews on the subject (Thompson and Gal 2003; Travis, Golczak et al. 2007). An important component of 11-*cis*-RAL regeneration is the Sec14-like cellular retinal-binding protein (CRALBP1). Multiple pathologies are associated with CRALBP1 dysfunction

including: retinitis pigmentosa, fundus albipunctatus, Newfoundland rod/cone dystrophy, and Bothnia dystrophy. It is suggested that all of these disorders are manifestations of retinitis punctata albescens (a flecked retinal dystrophy characterized by early onset night blindness, uniform white-yellow spots across the fundus and the progression of macula and retina atrophy resulting in legal blindness) which is also a manifestation of CRALBP1 insufficiencies (Thompson and Gal 2003; Saari and Crabb 2005). Moreover, mice deficient in CRALBP1 manifest large reductions in rates of rhodopsin regeneration, 11-*cis*-RAL production, and dark adaptation after illumination. Unlike the case in humans, photoreceptor degeneration is not observed (Saari, Nawrot et al. 2001).

CRALBP1 is a soluble protein, primarily expressed in retinal pigment epithelium cells (RPE) and in Müller cells, but not in their adjacent photoreceptors (Thompson and Gal 2003). In RPE cells, CRALBP1 directly bind the 11-*cis*-retinol (11-*cis*-ROL) formed after the isomerization of all-*trans*-retinyl ester, or from activated 11-*cis*-retinyl esters used as a storage mechanism (Stecher, Gelb et al. 1999). CRALBP1 functions primarily to: (i) regulate esterification of 11-*cis*-ROL (Stecher, Gelb et al. 1999), and (ii) act as a carrier molecule to assist in the oxidation of 11-*cis*-ROL to 11-*cis*-RAL in the vertebrate visual cycle (Saari, Bredberg et al. 1994). CRALBP1 associates with 11-*cis*-retinoldehydrogenase (RDH5) in a ternary complex that involves interaction with ezrin, actin and the PDZ domain of EPB-50. In this fashion, CRALBP1 is hypothesized to metabolically channel 11-*cis*-ROL to RDH5 for oxidation (Nawrot, West et al. 2004). CRALBP1 binds acidic phospholipids, and this binding promotes release of bound 11-*cis*-retinal (Saari, Nawrot et al. 2009). It is not yet clear whether 11-*cis*-retinal release is mediated by competition for an overlapping binding site within the CRALBP1 hydrophobic pocket (*i.e.* in effect a Sec14-like heterotypic

lipid exchange reaction), or whether acidic phospholipid interactions with the protein surface evoke conformational changes that eject 11-*cis*-retinal.

Several naturally-occurring mutations in CRALBP1 compromise retinoid binding (R₁₅₁Q, M₂₂₆K), or enhance its binding (e.g. R₂₃₄W; Maw, Kennedy et al. 1997; Golovleva, Bhattacharya et al. 2003). In this regard, the autosomal recessive, Bothnia dystrophy presents an interesting case. Pathologies include night blindness in early childhood, and progressive macular/peripheral retinal degeneration (Burstedt, Sandgren et al. 1999; Golovleva, Köhn et al. 2010). Bothnia dystrophy occurs in 1:3500 births worldwide with increased incidence in northern Sweden, primarily as a result of inheritance of the R₂₃₄W and M₂₂₆K variants (Golovleva, Köhn et al. 2010). The crystal structures of 11-*cis*-RAL-bound CRALBP1 and the R₂₃₄W mutant were recently solved (He, Lobsiger et al. 2009). These studies reveal that R₂₃₄W further stabilizes bound 11-*cis*-RAL by increasing packing interactions within the binding cavity. Additionally, R₂₃₄ resides in a conserved basic cleft of CRALBP1. R₂₃₄ corresponds to Sec14 residue R₂₀₈ which helps coordinate PtdIns binding by Sec14 and is a component of the Sec14 structural bar code for PtdIns binding (Phillips, Sha et al. 1999; Schaaf, Ortlund et al. 2008).

Although discussions of CRALBP1 are dominated by its involvement in the vertebrate visual cycle, elevated CRALBP1 levels are associated with altered calcium homeostasis and immune system imbalances in schizophrenia (Martins-de-Souza, Gattaz et al. 2009). CRALBP1 may also represent a human autoimmune uveitis autoantigen (Deeg, Raith et al. 2007), and its status may affect ethanol preference in mice (Treadwell, Pagniello et al. 2004).

Multi-domain Sec14-like proteins and disease

The Sec14 superfamily is too large to cover in one review. The distant members of the superfamily, the BNiP proteins which primarily function in apoptosis, are reviewed elsewhere (Zhang, Cheung et al. 2003; Curwin and McMaster 2008), and will not be emphasized here. Rather, we focus on a set of examples relevant to human disease.

Small GTPases of the Rho/Rac/Cdc42 families regulate a number of cellular activities such as migration, cytoskeleton dynamics, cell cycle progression, gene expression, cell adhesion, and others (García-Mata and Burridge 2007). These do so by functioning in binary switch mode between GTP- (active) and GDP-bound (inactive) states. Modular proteins with Sec14-domains include a number of regulators of small GTPase signaling; *i.e.* guanine nucleotide exchange proteins (GEFs) and GTPase activating proteins (GAPs). Sec14-like domains are also associated with other enzymatic activities such as protein kinases and protein-tyrosine phosphatases. In these multi-domain protein contexts, Sec14 domains are posited to function as nanoreactors that stimulate ‘on demand’ phosphoinositide synthesis in the immediate vicinity of the particular catalytic domain of the protein—thereby effecting an efficient regulation of protein enzymatic activity (Bankaitis, Mousley et al. 2010). The spectrum of diseases caused by derangements in Sec14-like proteins include various cancers, neurological disorders, developmental, and trafficking defects. Some outstanding examples are summarized below and the relevant Sec14-domains often present recognizable PtdIns-binding bar codes.

Rho guanine nucleotide exchange proteins with Sec14 domains

The Dbl family of RhoGEFs is defined by a ca. 200-residue Dbl homology (DH) domain positioned adjacent to a C-terminal ca. 100-residue plekstrin homology (PH) domain. Of the approximately 70 Dbl-family RhoGEFs, four (Dbl, Dbs/Ost, Duo/Kalirin and Trio) exhibit Sec14-domains (Rossman, Der et al. 2005; García-Mata and Burridge 2007; Curwin and McMaster 2008). All four RhoGEFs are expressed as multiple spliceoforms, not all of which harbor a Sec14-domain, thereby offering mechanisms for differentially regulating the functional properties and subcellular localization of individual isoforms (Johnson, Penzes et al. 2000; Ueda, Kataoka et al. 2004; Kostenko, Mahon et al. 2005; Portales-Casamar, Briançon-Marjollet et al. 2006).

DBL

Dbl, the founding member of the Dbl family of RhoGEFs, is represented by least four splice variants—three of which contain a Sec14-domain. This domain regulates Dbl localization and GEF activities (Komai, Mukae-Sakairi et al. 2003), and binds [PtdIns(3)P, PtdIns(4)P and PtdIns(5)P] *in vitro* (Ueda, Kataoka et al. 2004). Oncogenic forms of Dbl exist that exclude the N-terminal 496 residues of the protein, thereby truncating the Sec14-domain and several spectrin repeats (Vanni, Mancini et al. 2002; Rossman, Der et al. 2005). These oncogenic forms of Dbl influence cell migration, cell polarity and vascularization of epithelial tissue in murine lens (Fardin, Ognibene et al. 2009). Dbl null mice are rather normal phenotypically, although these do present measurable defects in dendrite elongation (Hirsch, Pozzato et al. 2002).

Kalirin /Duo

Kalirin/Duo is a neuronal RhoGEF represented by at least eleven forms, six of which contain a Sec14-domain (Kalirin-SOLO, 4, 7, 8, 9, and 12) (McPherson, Eipper et al. 2002; Rabiner, Mains et al. 2005; Schiller, Ferraro et al. 2008). Full-length kalirin (Kalirin-12) is a complex protein that exhibits a Sec14-like domain, nine spectrin-like repeats, two DH, two PH, two SH3, one Ig, one FnIII, and one Ser/Thr protein kinase-like domain (**Figure 5**) (Penzes, Johnson et al. 2001). The isolated Kalirin Sec14-domain is reported to bind phosphoinositides based on crude lipid blot assays (Schiller, Ferraro et al. 2008). Kalirin nullizygous mice show cognitive and working memory deficiencies associated with reduced neuronal spine densities and abnormal spine morphologies (Cahill, Xie et al. 2009). These neuronal morphology defects are also manifested in ex vivo culture (Xie, Cahill et al. 2010). Additionally, Kalirin is implicated as a genetic risk factor for ischemic stroke (Krug, Manso et al. 2010), coronary artery disease (Wang, Hauser et al. 2007), Alzheimer's disease (Youn, Ji et al. 2007), and schizophrenia (Cahill, Xie et al. 2009; Hayashi-Takagi, Takaki et al. 2010).

The predominant Kalirin, Kalirin-7, is an important regulator of dendritic spine development and functional plasticity (Penzes and Jones 2008; Saneyoshi, Fortin et al. 2010). NMDA receptor activation in pyramidal neurons induces a CaMkII-dependent phosphorylation of Kalirin-7 on its Sec14-domain. This phosphorylation stimulates Kalirin-7 GEF activity, and elicits enlargement of neuronal spines via enhanced activation of Rac1 (Xie, Srivastava et al. 2007). Moreover, the Kalirin-7 Sec14-domain may also interact with G β subunits of heterotrimeric G-proteins (Nishida, Kaziro et al. 1999). Although it is clear that the Sec14-domain is important for Kalirin-7 function, the mechanisms for how the

Sec14-domain interfaces with other Kalirin-7 domains is not understood. As the Sec14-domain is implicated as a negative regulators of other Dbl family members (Kostenko, Mahon et al. 2005), and phosphorylation of the Sec14-domain promotes GEF activity, a negative regulatory role is a distinct possibility (Xie, Srivastava et al. 2007). Whether lipid binding is involved in such a circuit remains to be determined. Moreover, variants produced from an alternative translation start site truncate the Sec14 domain and the first four spectrin repeats (Δ -Kalirin-7) exhibit distinct properties with regard to regulation of endocytosis, solubility, oligomerization state, cytoskeleton binding and subcellular localization (Schiller, Ferraro et al. 2008).

TRIO

Trio contains a Sec14-domain and 8-9 spectrin repeats linked to two DH-domains, two PH-domains, two SH3-modules, one Ig-domain, and one serine/threonine kinase catalytic domain (**Figure 5**; Rossman, Der et al. 2005; Briançon-Marjollet, Ghogha et al. 2008). Trio is represented by at least six isoforms, five of which contain a Sec14-domain (Portales-Casamar, Briançon-Marjollet et al. 2006). Trio nullizygous mice fail in embryonic development with deranged organization of neural tissues and defects in fetal skeletal muscle (O'Brien, Seipel et al. 2000). Recent studies implicate Trio in netrin-1/DCC-dependent axon guidance through its ability to activate Rac1 (Briançon-Marjollet, Ghogha et al. 2008), and its expression is associated with invasive tumor growth and rapid tumor cell proliferation in bladder cancer (Zheng, Simon et al. 2004). Moreover, genome association studies also link Trio expression to esophageal squamous cell carcinoma (Chattopadhyay, Singh et al. 2010). The short Solo/Trio8 isoform (contains the Sec14-domain), which is primarily expressed in

Purkinje cells, localizes to endosomes where it activates Rho GTPases and promotes neurite elongation in developing Purkinje cells. The Sec14-domain is suggested to contribute to endosomal localization of this isoform (Sun, Nishikawa et al. 2006). Human Trio also potentiates the nerve growth factor pathway for RhoG- and Rac1-dependent neurite outgrowth in PC12 cells. The Sec14-domain is dispensable for the neurite promoting activity of Trio, however (Estrach, Schmidt et al. 2002).

DBS

The Dbs/Ost RhoGEF is a proto-oncogene that modulates cell motility in human derived breast epithelial cells via activation of Cdc42 and Rac1 (Liu, Adams et al. 2009). The protein consists of an N-terminal Sec14 domain, two spectrin repeats, DH domain, PH domain and an SH3 domain (**Figure 5**; Kostenko, Mahon et al. 2005). The purified Dbs Sec14-domain binds a variety of phosphoinositides in crude lipid-blot assays (Kostenko, Mahon et al. 2005), and the Sec14-domain is responsible for directing Dbs subcellular localization so that it can interact with its primary substrate Cdc42 (Ueda, Kataoka et al. 2004). Sec14-domain activities are not simple as this module also inhibits Dbs transforming activity by interacting with the PH domain and regulating subcellular localization (Kostenko, Mahon et al. 2005). Whether this Sec14/PH-domain interaction is regulated by lipid binding remains to be determined.

RhoGAPS

The RhoGAP family is populous – counting in excess of 70 members. Of those, p50RhoGAP/Cdc42GAP and BPGAP1 are similar proteins that exhibit N-terminal Sec14-domains appended to RhoGAP domains by proline-rich linker domains (**Figure 5**; Tcherkezian and Lamarche-vane 2007).

CDC42GAP/p50RhoGAP

Mice deficient for Cdc42GAP exhibit multiple premature aging defects including reduction in body mass, loss of subdermal adipose, muscular atrophy, osteoporosis and delayed wound healing (Wang, Yang et al. 2007), and present enhanced rates of JNK-mediated basal apoptosis (Wang, Yang et al. 2005). As may be expected, Cdc42GAP-deficient murine embryonic fibroblasts display elevated Cdc42 activity, and these cells are prone to spontaneous formation of filipodia with defects in directional migration (Yang, Wang et al. 2006). Cdc42GAP derangements are implicated in human disorders such as Waldenstrom Macroglobulinemia (Hatjiharissi, Ngo et al. 2007) and human chronic myeloid leukemia (Jin, Liu et al. 2009). CDC42GAP is also suggested to be a counter-regulator of tubule formation, forecasting a role in angiogenesis (Engelse, Laurens et al. 2008).

The Sec14-like domain is responsible for localization of Cdc42GAP to endosomes as evidenced by the fact that missense substitutions in the presumptive Sec14-like lipid binding pocket result in Cdc42GAP mislocalization. In that regard, Cdc42GAP interacts with the Rab11 GTPase, suggesting a link between Rab and Rho GTPases and endosome dynamics (Sirokmány, Szidonya et al. 2006). Cdc42GAP exists in an autoinhibited state that is

controlled in part by intermolecular interactions between amino acids 1-48 and 169-197 which reside in the Sec14-like domain. Interaction with the prenyl group of small GTPases promotes the release of autoinhibition (Moskwa, Paclet et al. 2005).

Neurofibromin RasGAPs

Neurofibromin NF-1 encodes for a 2818 residue RasGAP that is homologous to the yeast RasGAPs, Ira1 and Ira2 (Cichowski and Jacks 2001; D'Angelo, Welte et al. 2006). Defects in NF-1 result in the progressive, autosomal dominant disorder, neurofibromatosis type 1 affecting 1:3500 individuals world-wide. The disease manifests through multiple brown skin macules (café-au-lait spots), intertriginous freckling, iris hamartoma (Lisch nodules), and learning disabilities. NF1 patients are also at a higher risk for optical gliomas and neurofibromas (Friedman 1999; Ferner, Huson et al. 2007). NF-1 primarily regulates p21-Ras-GTP levels, thereby modulating downstream cascades including Ras/MAPK and Akt/mTOR pathways. Loss of NF-1 activity deregulates of these pro-proliferative pathways and inhibits apoptosis (Gottfried, Viskochil et al. 2010).

NF-1 has three discrete domains: the RasGAP catalytic module (Xu, O'Connell et al. 1990), the Sec14-like domain (Aravind, Neuwald et al. 1999), and a PH-domain (D'Angelo, Welte et al. 2006). Several other domains have recently been defined largely on the basis of bioinformatic analyses (**Figure 5**; Bonneau, Lenherr et al. 2009). A number of missense substitutions elicit NF1 loss-of-function phenotypes without destabilizing the protein (Upadhyaya, Maynard et al. 1995; Fahsold, Hoffmeyer et al. 2000). Several of these map to the Sec14-domain, thereby demonstrating the functional importance of this domain for NF-1

biological activity. A series of these disease-associated mutations affect residues that either comprise, or flank, the hinge domain of Sec14-like proteins. These substitutions likely interfere with conformational transitions of the helix which gates the hydrophobic pocket (Welti, Fraterman et al. 2007). Additionally, a tandem repeat mutation identified in a neurofibromatosis patient with Noonan's disease duplicates a linker region between the NF1 Sec14- and PH-domains—indicating inter-domain communications between the Sec14-, PH-, and RasGAP-domains are required for proper NF1 activity (D'Angelo, Welti et al. 2006).

Sec14-like protein tyrosine phosphatase

A Sec14-module is incorporated into the 68kDa, cytoplasmic, protein-tyrosine phosphatase MEG2/PTPN9 (Huynh, Wang et al. 2003; Alonso, Sasin et al. 2004; Saito, Tautz et al. 2007). *In vitro* experiments suggest PTP-MEG2 binds PtdIns(3,5)P₂, PtdIns(4,5)P₂, PtdIns(3,4,5)P₃ and phosphatidylserine (Zhao, Fu et al. 2003). Thus, interaction of the Sec14-domain with lipids may control both MEG2 localization and phosphatase activity. Murine MEG2 is highly expressed in the brain, liver, kidneys, and testes. Mice deficient for MEG2 exhibit embryonic lethality with a penetrance of >90% with hemorrhage, neural tube defects, decreased size, immunodeficiency, and abnormal bone development. It is suggested that many of these dysfunctions result from defects in secretory processes (Wang, Yang et al. 2005). MEG2 targets to the cytoplasmic face of secretory vesicles in a Sec14-domain-dependent manner where it promotes vesicle fusion by dephosphorylating (and activating) the N-ethylmaleimide-sensitive factor essential for resolving cis SNARE-pins (Huynh, Bottini et al. 2004). While missense substitutions projected to compromise PtdIns binding do not prevent MEG2 association with vesicles,

these substitutions do inactivate the protein for stimulating vesicular fusion (Huynh, Wang et al. 2003; Saito, Williams et al. 2007). The available data suggest the MEG2 Sec14-domain executes functions in addition to membrane targeting.

Table 1. Other selected Sec14-like proteins			
Gene	Protein	Description	References
BNIP-2	BNIP-2	Pro-apoptotic and promotes Cdc42 mediated cell elongation through its Sec14-like domain.	(Boyd, Malstrom et al. 1994; Zhang, Cheung et al. 2003; Zhou, Guy et al. 2005; Sall, Zhang et al. 2010)
BNIP1	BNIP1/ BNIP2	Pro-apoptotic, increases cell migration and may play a role in metastasis.	(Qin, Hu et al. 2003; Zhang, Cheung et al. 2003; Xie, Qin et al. 2007)
BMCC1/ BNIP-XL	BMCC1/ BNIP-XL	Pro-apoptotic protein highly expressed in the human nervous system. Interacts with RhoA via Sec14 domain, and is a favorable signature in neuroblastomas.	(Zhang, Cheung et al. 2003; Machida, Fujita et al. 2005; Valencia, Cotten et al. 2007; Soh and Low 2008; Clarke, Zhao et al. 2009)
BPGAP1	BPGAP1	Promotes pseudopodia formation, Erk signaling.	(Shang, Zhou et al. 2003; Johnstone, Castellví-Bel et

		Elevated levels associated with colorectal cancer and invasive cervical cancer.	al. 2004; Lua and Low 2004; Lua and Low 2005; Song, Lee et al. 2008)
CRALBPL/ RLBP1L1	Clavesin1	Regulates late endosome/lysosome morphology in neurons and is upregulated in hepatocellular carcinoma.	(Kong, Ye et al. 2006; Zhao, Xu et al. 2008; Katoh, Ritter et al. 2009)
	Clavesin2	Regulates late endosome/lysosome morphology in neurons.	(Katoh, Ritter et al. 2009)
Sec14L1	SEC14L1	Regulates cholinergic transporters and synaptic vesicle formation.	(Ribeiro, Ferreira et al. 2007; Saito, Tautz et al. 2007)
Sec14L5	SEC14L5	Unknown	(Saito, Tautz et al. 2007)
Sec14L2	SEC14L2/ TAP1/SPF	Role cholesterol synthesis during fasting. In humans a potential link to breast carcinogenesis and prostate cancer.	(Ni, Wen et al. 2005; Shibata, Jishage et al. 2006; Saito, Tautz et al. 2007; Wen, Li et al. 2007; Johnykutty, Tang et al. 2009; Wang, Ni et al. 2009)
Sec14L3	SEC14L3/	Potential link with drug	(Kempná, Zingg et al.

	TAP2/p45	induced lung adenocarcinoma in mice.	2003; Saito, Tautz et al. 2007; Bortner, Das et al. 2009)
Sec14L4	SEC14L4/TAP3	Unknown	(Saito, Tautz et al. 2007)
SESTD1	Solo/ HIPLP	Elevated levels in the thalamus and brain with potential functions in cone guidance and smooth muscle contraction. It was shown to be embryonic lethal in mice and the Sec14 domain is involved in Rho activation.	(Bezzarides, Ramsey et al. 2004; Mische, Bieberstein et al. 2010; Yang and Cheyette 2013)
MOSPD2	MSPD2	Unknown function in humans but it localized with zebrafish maternal expression in eggs	(Hong, Levin et al. 2010)

Type 1 START-like PITPs as molecules

As is the case for Sec14-like PITPs, the origins of START-like PITPs are rooted deep in eukaryotic evolution. Database searches identify candidate Type 1 PITP-like proteins in protists with highly streamlined genomes (*e.g. Giardia, Enterocytozoon, Encephalitozoon*). Because we highlight PITPs in the context of mammalian disease in this review, we focus primarily on what we know about the mammalian versions of these proteins. There are three

mammalian START-like Type 1 PITPs (PITP α , RdgB β , PITP β). Essentially nothing is known about RdgB β and we will ignore it for the remainder of this review. Rather, we focus on the homologous PITP α and PITP β both of which are classical PITPs. These proteins are encoded by distinct genes, yet share 77% identity at the primary sequence level. PITP β is expressed as two splice variants (termed canonical and alternative on a historical basis) which differ only in the extreme C-terminal primary sequence of the protein (Tanaka and Hosaka 1994; Morgan, Allen-baume et al. 2006; Phillips, Ile et al. 2006). Zebrafish (*Danio rerio*) also express a mammalian-like cohort of Type 1 PITPs with the addition of a unique PITP β -like version designated PITP γ . The Type 1 PITP roster extends to interesting details of Type 1 PITP diversity— *i.e.* zebrafish execute precisely the same exon-skipping splicing event as do mammals in generating the canonical and alternative PITP β splice variants (Ile, Kassen et al. 2010).

Crystal structures for both PITP α and PITP β are available, and multiple structural models for PITP α have been solved (**Figure 6**). These include high resolution structures for PtdCho-bound and phospholipid-free forms (Yoder, Thomas et al. 2001; Schouten, Agianian et al. 2002), and a lower resolution structure for the PtdIns-bound form (Tilley, Skippen et al. 2004). As indicated above, Type 1 PITPs are structurally unrelated to Sec14-like PITPs and are characterized by a START structural fold that forms a single large lipid-binding cavity. Unlike the case for Sec14-like PITPs, PtdIns and PtdCho assume very similar poses within the Type 1 PITP lipid binding cavity (**Figure 6**). The Type 1 PITP strategy for phospholipid binding suggests these proteins may not operate in a Sec14-like nanoreactor/PtdIns-presentation mode. However, genetic data identify residues Ser25 and Pro78 as being specifically required for PtdIns-binding/transfer by PITP α (Yoder, Thomas et al. 2001)—

even though neither residue uniquely contacts PtdIns, or influences other residues that do so, in the holo-PITP α structure. The existence of such enigmatic ligand-specific binding/transfer mutants suggests that PtdCho and PtdIns trajectories during lipid exchange are different in Type 1 PITPs, but ultimately converge on similar poses in the closed conformer. Indeed, Type 1 PITPs rescue both cell viability and phosphoinositide production in yeast devoid of Sec14. Because yeast membranes are rich in PtdIns (20mol%), these data indicate Type 1 PITPs can function in a Sec14-like nanoreactor/PtdIns-presentation mode (Skinner, Alb et al. 1993; Tanaka and Hosaka 1994). Whether these do so in the PtdIns-poor mammalian cell (PtdIns represents 5mol% of bulk phospholipid) is difficult to demonstrate, yet, structural studies suggest that the apo-PITP α conformer displays an open channel which provides access to the headgroup binding region. This channel provides a path via which a lipid kinase could potentially access a PITP-bound PtdIns headgroup (Schouten, Agianian et al. 2002). Such a mechanism requires productive PITP-PtdIns kinase interactions to occur during the interfacial lipid exchange reaction. This concept is consistent with nanoreactor/PtdIns-presentation modes of action.

The structural studies also suggest how Type 1 PITPs interact with membrane surfaces. Type 1 PITPs present a loop with adjacent Trp residues (Trp₂₀₃ and Trp₂₀₄ in PITP α) and it is reported that compromise of this Trp-Trp motif inactivates the PITP -- presumably by compromising PITP interaction with membranes (Tilley, Skippen et al. 2004). This is a controversial issue as other studies, while demonstrating a requirement for this motif in the more stable association of PITP β with Golgi membranes *in vivo*, nonetheless demonstrate the motif is neither important for the types of transient membrane interactions

that accompany lipid exchange reactions nor is it important for biological function in a vertebrate context (Phillips, Ile et al. 2006).

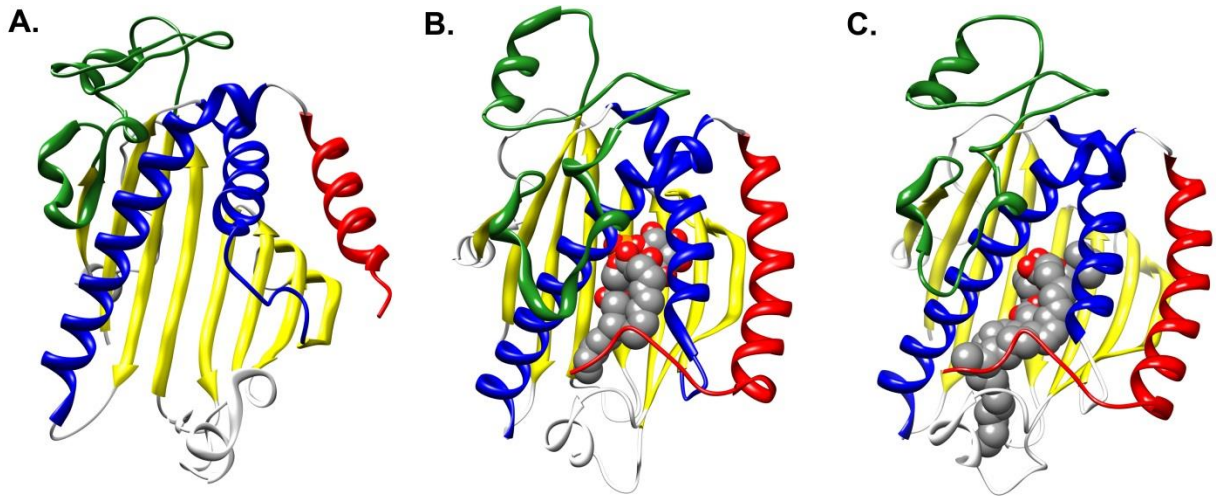


Figure 6. PITP α Structures.

(a) PITP α apo-structure depicting an open conformation (pdb 1KCM); (b) PtdIns-bound form (pdb 1UW5); (c) PtdCho-bound form (pdb 1T27). The eight β -strands (yellow) of PITP α comprise the hydrophobic cavity floor and two α -helices generate the cavity walls (blue). Additional components of PITP α include a regulatory loop (green), a COOH-terminal region (red) and a lipid exchange loop (gray).

Cellular functions

The similarity between PITP α and PITP β notwithstanding, the proteins exhibit important differences including: (i) PITP α localizes to the cytosol/nucleus while PITP β targets to the *trans*-Golgi complex, (ii) PITP β is able to bind/transfer the ceramide-based PL sphingomyelin (SM), in addition to the glycerol-PLs PtdIns and PtdCho, while PITP α only binds/transfers PtdIns and PtdCho. From a functional perspective, PITP β appears to execute important housekeeping function(s) in the face of robust PITP α expression (Alb, Phillips et al. 2002), while PITP α is not essential for cell viability. As discussed in detail below, PITP α nullizygosity results in neonatal lethality—even though normal levels of PITP β are expressed in the nullizygotes.

Remarkably little is known about the cellular functions of Type 1 PITPs. Data from permeabilized cell systems report PITP α stimulates Ca²⁺-activated secretory granule exocytosis (Hay and Martin 1995), secretory vesicle and immature granule budding from hepatocyte and neuroendocrine *trans*-Golgi network (TGN; Ohashi, Jan de Vries et al. 1995), and plasma membrane receptor/G-protein-coupled phosphoinositide hydrolysis by phospholipase C (PLC) (Thomas, Cunningham et al. 1993). PITP α requirements for agonist-stimulated phosphoinositide synthesis are recorded whether signaling occurs via receptor or non-receptor tyrosine kinases, or through PLC β or PLC γ 1 (Kauffmann-Zeh, Thomas et al. 1995; Xie, Ding et al. 2005). Using a more physiological system, silencing experiments suggest a cellular role for mammalian PITP β in regulating nuclear envelope morphology and retrograde membrane trafficking from *cis*-Golgi membranes to the endoplasmic reticulum (Carvou, Holic et al. 2010). Below, we review functional studies of vertebrate Type 1 PITPs

with murine models as primary focus. Both the congruence and the dissonance between cellular studies and animal studies of Type 1 PITPs are discussed.

Vertebrate models for type 1 PITP-associated disease

Precisely how Type 1 PITP biochemical properties translate to biological activity of the individual proteins remains to be determined. The RdgB β remains uncharacterized, and only recently have insights in vertebrate PITP β function been forthcoming (Carvou, Holic et al. 2010; Ile, Kassen et al. 2010). However, it is clear that PITP α , at least, is essential for the viability of vertebrate organisms—including mammals. Our understanding of the physiological consequences that accompany impaired PITP α functionality derive from analyses of a series of mouse lines with graded reductions in PITP α activity. Hypomorphic lines include the *vibrator* homozygous mice (*vb/vb*) and *vb/null* heterozygous mice (Weimar, Lane et al. 1982; Hamilton, Smith et al. 1997; Alb, Phillips et al. 2007), which express 20% and 10% of wild-type levels of wild-type PITP α , respectively. The *vb* allele is the result of a serendipitous insertion of an IAP retro-transposon into an intronic region of the *pitpa* structural gene--thereby reducing the efficiency with which the cognate pre-mRNA is processed (Weimar, Lane et al. 1982; Hamilton, Smith et al. 1997).

There are presently two categories of what are operationally considered to represent *pitpa* null alleles. One is an engineered deletion which eliminates two exons encoding essential functional elements of the protein. The second is an insertion of a recombinant retro-transposon which harbors splice-trap activity and interrupts PITP α mRNA translation without deleting any portion of the structural gene. Mice homozygous for either the deletion

allele or the splice-trap insertion fail to produce detectable amounts of PITP α protein and exhibit indistinguishable phenotypes (Alb, Cortese et al. 2003). Most of the detailed characterizations executed to date involve mice homozygous for the deletion allele.

PITP α and neurological disease

PITP α is produced in most (if not all) cells, but it is particularly highly expressed in brain and cerebellum. In the adult rat, PITP α is produced most robustly in cerebellar Purkinje neurons and granule cells (Nyquist and Helmkamp 1989; Imai, Tanaka et al. 1997; Utsunomiya, Owada et al. 1997). Consistent with these expression data, murine model systems report an important role for PITP α in maintaining integrity of the spinocerebellar system. PITP α null (*pitpa*^{0/0}) and hypomorphic mice exhibit striking neurological defects--the severities of which are proportional to the level of PITP α expressed (Weimar, Lane et al. 1982; Alb, Cortese et al. 2003; Alb, Phillips et al. 2007).

The *vb* mouse line takes its name from the rapid whole-body tremor observed in *vb/vb* homozygotes that reflects a progressive, and ultimately fatal, neurodegenerative disease. Genetic modifiers strongly affect the lifespan of *vb/vb* homozygotes. In the inbred C57/B6 background, these hypomorphs live for 31-35 days after birth while, in outbred or even other inbred backgrounds, lifespans of up to six months are recorded (Weimar, Lane et al. 1982). One such genetic modifier operates at the level of improving 'read-through' of the IAP element that defines the *vb* insertion mutation, and elevating both the levels of mature PITP α mRNA and wild-type protein produced. The net result is that lifespan is increased (Floyd, Gold et al. 2003).

By contrast, *pitpa*^{0/0} mice are born at the expected Mendelian frequencies but usually expire within several days of birth. In rare instances, the *pitpa*^{0/0} homozygotes can persist for 10-13 days after birth. The inability of the nullizygotes to thrive is hallmarked by obvious tremor and impaired motor capacity (Alb, Cortese et al. 2003). Unlike the case of *vb/vb* mice, the abbreviated lifespan of *pitpa*^{0/0} homozygotes is independent of genetic background, and is accompanied by two additional signature pathologies – hypoglycemia and intestinal chylomicron retention disease (CRD; Alb, Cortese et al. 2003; Alb, Phillips et al. 2007). These syndromes are addressed in subsequent sections and, as discussed below, contribute to the rate of onset of neurological disease in PITP α -deficient animals.

The neurodegenerative disease course of the *vb* mouse is classified into three phases. Phase I describes the “true vibrator” phenotype defined by fine, high-frequency postural tremors that become apparent ca. 15 days after the birth of *pitpa*^{vb/vb} homozygotes. Phase I postural tremors are reminiscent of the enhanced physiological tremors encountered in clinical settings (Weimar, Lane et al. 1982; Elble 1996). While the etiology of enhanced physiological tremors in humans is not known, such tremors often present as a symptom of hyperthyroidism or metabolic dysfunction such as hypoglycemia and liver disease. In that regard, *pitpa*^{0/0} mice also display hepatic steatosis and severe hypoglycemia (see below; Alb, Cortese et al. 2003).

PITP α null mice do not present Phase I phenotypes. Rather, Phase II symptoms are detected from the outset, indicating neuronal damage even at the earliest stages of postnatal life (Weimar, Lane et al. 1982; Alb, Cortese et al. 2003; Alb, Phillips et al. 2007). Phase II is marked by ataxia and action tremors. The coarse intention tremor is superimposed on the animal’s voluntary movements. These neurological symptoms are distinct, and not simply

progressive, from Phase I symptoms. Furthermore, Phase II presents with clear anatomical signs of degeneration. Neurons in the lumbar and cervical spinal cord and in the cerebellum are vacuolated, apoptotic, and display distended ER (see below). In genetic backgrounds where *vb* mice are reasonably long-lived (5-6 months), the disease progresses to a severe cerebellar atrophy (Weimar, Lane et al. 1982). For these reasons, Phase II defines the “degenerative” phase. In the inbred C57/B6 background, Phase II persists until hours before the animal perishes. The basic presentation of Phase II disease resembles the symptoms associated with clinical cases of stroke, inherited neurodegenerative disorders, and multiple sclerosis (Gauthier and Sniderman 1983; Schwab and McGeer 2008; Trapp and Nave 2008).

The terminal stages of PITP α -insufficiency define Phase III disease characterized by loss of consciousness, decreased motor tone and fasciculations, and a progressive ascending motor paralysis that ultimately leads to asphyxiation. For C57/B6 animals, Phase III signals imminent death (within hours) and appears ca. postnatal day 31-33 in the case of *vb/vb* homozygotes.

Anatomy of neurodegenerative disease in PITP α -deficient mice

PITP α null mice exhibit robust inflammation and demyelination in the spinal cord (Alb, Cortese et al. 2003). There are clear reductions in white matter in the cervical, thoracic and lumbar spinal cord, and damaged neurons are observed at the white and grey matter interface. Inflammation is evident over the entire length of the spinal cord, but is most striking in the ventral horn, i.e. where motor neuron cell bodies are located. Many of the neuronal cell bodies in the ventral horn present the vacuolation and low cytoplasmic content

typical of aponecrosis – a form of cell death associated with critically low cellular energy charge. Indeed, measurements of ATP/ADP ratios indicate *pitpa*^{0/0} cerebellum and liver present significant reductions in energy charge while brain does not. Consistent with the widespread aponecrosis occurring in those regions, mast cells and macrophages infiltrate into the perivascular matrix and vessels, as well as the perivascular tissue, indicating breach of blood-brain barrier integrity. Extensive defects in myelination are obvious in both white and gray matter regions of dorsal spinal columns, and are accompanied by axonal swelling and neuropil degeneration. Another striking property of *pitpa*^{0/0} brain is the reactive gliosis evident throughout the cerebellum -- the organ is inundated with activated microglia. Again, vacuolations of smooth ER are prevalent in cerebellar neurons of *pitpa*^{0/0} mice (Alb, Cortese et al. 2003). The fulminating spinocerebellar inflammatory disease indicates regulated exocytic pathways associated with the activities of inflammatory cells (*e.g.* mast cells) is not strongly compromised in the null animals, in contrast to data from permeabilized cells suggesting PITP α is required for such regulated exocytic events (Hay and Martin 1995; Alb, Cortese et al. 2003). These data are consistent with the report that *pitpa*^{0/0} ES cells differentiated *ex vivo* produce mast cells capable fully of executing the agonist-stimulated compound exocytosis that is a distinguishing property of these inflammatory cells (Alb, Phillips et al. 2002). Synaptic performance is also unperturbed in *pitpa*^{0/0} neurons under multiple testing regimes (Alb, Cortese et al. 2003). This is a surprising result given that the synaptic vesicle cycle is a high capacity phosphoinositide-utilizing system (Di Paolo and De Camilli 2006).

It is difficult to interpret whether the spinocerebellar degeneration observed in *pitpa*^{0/0} mice is a primary phenotype or a secondary consequence of the glucose homeostatic

and CRD defects that define major phenotypes of the null condition. The substantially postnatal development of the cerebellum dictates a robust proliferative program for cerebellar neurons. Engagement of such a vigorous cell growth program, in the face of severe hypoglycemic circumstances, must soon come to a critical point where proliferation can no longer be sustained in an inadequate physiological environment. Such a catastrophic developmental failure is expected to result in manifest necrosis and induction of a fulminating inflammatory response. These predictions are fulfilled by the cerebellar inflammatory disease of PITP α -deficient mice. With regard to the spinal cord, affected motor neurons are extraordinarily large cells, and it is likely these are especially sensitive to environmental insult. That the spinocerebellar degeneration is, at least in part, caused by a hostile physiological environment is further indicated by demonstrations that *pitpa*^{0/0} cerebellar granule cells, and dorsal root ganglia from spinal cord, are not intrinsically fragile when cultured *ex vivo*. Moreover, titration experiments indicate these *pitpa*^{0/0} neurons are not overly sensitive to reduced trophic factor availability relative to wild-type neurons (Alb, Cortese et al. 2003).

To determine the degree of interdependence among the phenotypes observed in *pitpa*^{0/0} animals, Alb et al. generated an allelic series of mice in which levels of wild-type PITP α protein are graded across a broad functional range. These studies establish that the threshold levels of PITP α activity sufficient to relieve CRD and hypoglycemia remain inadequate for sparing spinocerebellar degeneration; although onset of neurodegenerative disease is significantly delayed in the absence of hypoglycemia and CRD (Alb, Phillips et al. 2007). The collective data indicate that spinocerebellar disease is an intrinsic pathology of PITP α -deficient mice.

Cell non-autonomous mechanisms for PITP α -dependent neuroprotection

The neurodegenerative pathologies associated with PITP α insufficiencies suggest a pro-survival/anti-apoptotic role for PITP α at the cellular level. Such an activity can be formally executed in a cell-non-autonomous manner, i.e., where PITP α function is not required in neurons but must be present in non-neuronal support cells that nourish neurons. Alternatively, PITP α could exert its functions in a cell-autonomous manner where protein activity is required in the neurons themselves. The available information suggests both mechanisms may be relevant. With regard to cell non-autonomous mechanisms of PITP α action, cells over-expressing PITP α are reported to secrete an as yet uncharacterized trophic factor that promotes neuronal survival *ex vivo* (Bunte, Schenning et al. 2006). Presumably, genetic ablation of PITP α function interferes with production of this factor, thereby contributing to neuronal fragility in PITP α -deficient animals. A chemical identification of such PITP α -regulated trophic factors would constitute an important advance in our understanding of how PITP α helps confer neuroprotection to the spinocerebellar system. A cell non-autonomous mechanism of this nature forecasts that targeted ablation of PITP α function in neuronal support cells, such as glia and/or oligodendrocytes, will recapitulate at least some features of the spinocerebellar inflammatory disease recorded for *pitpa*^{0/0} mice.

PITP α and cell autonomous signaling

PITP α is identified as an essential component in promoting signaling of plasma membrane-localized receptor tyrosine kinases that register extracellular signals and transmit

the information to downstream effector pathways. Two such circuits feature prominently in discussions of intracellular mechanisms for PITP α function. First, PITP α was purified as a cytosolic factor required for EGFR signaling in a system where the ligand-dependent EGFR stimulation of phospholipase C γ (PLC γ) was reconstituted in permeabilized cells (Kauffmann-Zeh, Thomas et al. 1995). In this system, PITP α is posited to deliver PtdIns to the signaling plasma membrane so that a phosphoinositide pool required for forward EGFR signaling is generated by PtdIns 4-OH and PtdIns(4)P 5-OH kinases. Secondly, and in an analogous mechanism, PITP α is reported to be obligatorily required for signaling via the netrin receptor DCC (Xie, Ding et al. 2005). Netrins are secreted guidance cues that promote axon elongation and direct pathfinding during neuronal development, and are essential for the proper formation of major commissures in the brain and spinal chord (Serafini, Colamarino et al. 1996; Fazeli, Dickinson et al. 1997). In both studies, the major conclusion is that PITP α binds activated receptor and, in this fashion, brings PtdIns from the ER to the site of receptor/ligand engagement. This supply activity is then posited to stimulate local production of phosphoinositide and, in turn, downstream signaling (Kauffmann-Zeh, Thomas et al. 1995; Xie, Ding et al. 2005). In a related scenario, PITP α is reported as fueling a PtdIns(3)-OH kinase signaling pathway required for elongation of cortical neurons on specific extracellular matrices *ex vivo* (Cosker, Shadan et al. 2008).

The parallel logic proposed for how PITP α promotes EGFR and DCC signaling via cell autonomous mechanisms is attractive because it makes strong predictions regarding how null cells should behave in a physiological context. From the perspective of neuronal development, loss of an amplifying factor such as PITP α should impair spinal chord and brain structures whose development is netrin/DCC-dependent. Some properties of the

pitpa^{0/0} mouse are superficially consistent with such a model (Alb, Cortese et al. 2003; Alb, Phillips et al. 2007). It is a tenable hypothesis that comprehensive defects in axon guidance would lead to extensive neuronal cell death by apoptosis and, in the case of a hypoglycemic animal, aponecrosis—as is seen in *pitpa*^{0/0} mice. However, there are discrepancies between the central predictions of the proposed model for functional coupling of PITP α to DCC and *in vivo* experimental results. Significant defects in netrin signaling result in obvious structural abnormalities of the brain—including deranged development of the anterior and hippocampal commissures, and the corpus callosum (Serafini, Colamarino et al. 1996). Yet, *pitpa*^{0/0} brain does not present such obvious derangements and, moreover, the *pitpa*^{0/0} cortex is not significantly smaller than its wild-type counterpart (Alb, Phillips et al. 2007). The idea that PITP α obligatorily promotes DCC signaling is also inconsistent with the properties of the *kanga* mouse, a mutant animal with a spontaneous and clean deletion of the essential PITP α -binding domain in the DCC cytosolic tail (Finger, Bronson et al. 2002; Xie, Ding et al. 2005). While this mouse exhibits an abnormal gait, and *kanga* brain recapitulates the structural defects observed in netrin-deficient brain, the mouse nonetheless survives to adulthood and is fertile (Finger, Bronson et al. 2002). By contrast, DCC null mice present embryonic lethal phenotypes (Fazeli, Dickinson et al. 1997). The *kanga* and *pitpa*^{0/0} phenotypes are not consistent with strong compromise of DCC function in the absence of interaction with PITP α .

The EGFR-PITP α forward signaling paradigm formulated from permeabilized cell studies also fails to translate cleanly to authentic physiological contexts. As an active EGFR signaling network initiates a transcriptional response that promotes cellular survival and proliferation (Jones and Kazlauskas 2001), loss of a factor that increases the gain on forward-

signaling (*i.e.* PITP α) should compromise cell vigor and proliferative capacity. Yet, *pitpa*^{0/0} murine embryonic stem cells retain their tumorigenicity when introduced into nude mice. This is not an outcome obviously consistent with overt growth factor signaling defects. Moreover, PITP α hypomorphic animals do not present obvious *waved* phenotypes that result from defective hair follicle development in mice with even partial defects in EGFR signaling (Weimar, Lane et al. 1982; Luetkeke, Phillips et al. 1994; Alb, Phillips et al. 2007). The corresponding null phenotypes differ as well. EGFR nullizyosity generally results in embryonic lethality. In some genetic backgrounds, the knockout mice are born alive, but expire within the first postnatal week, and exhibit multiple symptoms of delayed epithelial development. Those ‘escapers’ show defective eyelid development, deranged terminal differentiation of the epidermis and hair follicles, and loss of structural integrity of intestine--as evidenced by shortening of the organ, reduced numbers of villi, and hemorrhage. Moreover, EGFR deficiency leads to respiratory failure as a consequence of structurally immature alveoli (Miettinen, Berger et al. 1995; Sibilias and Wagner 1995). No such defects are reported for *pitpa*^{0/0} mice.

In summary, the *in vivo* data are not consistent with simple models invoking obligatory roles for PITP α in forward DCC or EGFR signaling. It remains formally possible that a PITP α involvement in promoting DCC or EGFR signaling is subtle, or that this requirement exhibits an unexpected, and as yet unidentified, tissue-specificity. The idea that significant compensatory mechanisms are engaged in the face of chronic PITP α deficiency also cannot yet be dismissed. However, the counter view that PITP α does not promote forward EGFR or DCC signaling must be considered as well. These issues frame a set of important questions for future analysis.

PITP α -insufficiencies and chylomicron retention disease

A major phenotype associated with *pitpa*^{0/0} homozygosity is failure of such neonates to thrive—*i.e.* mutant animals achieve only one-half to one-third the mass of *PITP α* ^{+/+} and *PITP α* ^{0/+} heterozygous littermates within the first postnatal week. The phenotype is manifested even though the null animals nurse reasonably effectively—as evidenced by direct observation of the act and analysis of stomach contents, and by the fact that *pitpa*^{0/0} nullizygotes are not dehydrated. Whole-body chemical analyses demonstrate the reduced body mass is substantially accounted for by a pathologically low body fat content, a deficiency confirmed by the virtual absence of axillary and inguinal fat pads in nullizygotes (Alb, Cortese et al. 2003). These homeostatic pathologies stem from inefficient processing of dietary fat by the nullizygous animals, and available data report that the homeostatic deficiencies are manifestations of functional derangements in *pitpa*^{0/0} intestine and liver.

Two lines of evidence indicate that *pitpa*^{0/0} neonates cannot effectively absorb dietary fat across the intestinal epithelium. First, enterocytes of the *pitpa*^{0/0} duodenum stain unusually heavily with lipophilic agents (**Figure 7**), and this property disappears upon prolonged fasting. Second, electron microscopy reveals dramatic accumulations of lipid bodies in the lumen of the enterocyte endoplasmic reticulum (ER) of *pitpa*^{0/0} neonates—an accretion accompanied by dilations of smooth ER (**Figure 7**). These accumulated lipid bodies resemble maturing chylomicrons, *i.e.* the lipoprotein transport units that ferry dietary fat through the enterocyte secretory pathway for discharge into the circulation and disbursement throughout the body. Taken together, the morphological data indicate *pitpa*^{0/0} enterocytes are competent for: (i) hydrolysis of dietary triglycerides (TGs) into fatty acids

and monoacylglycerols, **(ii)** for transport of these hydrolytic products into the enterocyte ER lumen, and **(iii)** for reconstitution of these products into TGs for subsequent packaging into what we loosely term as chylomicron precursors. The point of failure is in inefficient export of chylomicron precursors from the enterocyte ER, through the secretory pathway, and into the circulation.

Consistent with this basic scenario, *pitpa*^{0/0} neonates present dramatic reductions in levels of circulating post-prandial TG and brain α -tocopherol (another lipophilic molecule whose transport across the enterocyte into the circulation requires a functional chylomicron pathway). The collective data suggest a PITP α involvement in the packaging of TG cores into functional chylomicron carriers for transport from the enterocyte ER. Defects in this process hallmark chylomicron retention disease (CRD). The threshold requirement for PITP α in chylomicron transport is low given that 80% reductions in PITP α expression are insufficient to induce CRD in mice, but >90% reductions in PITP α load do (Alb, Phillips et al. 2007). The defect is also tissue-autonomous as reconstitution of intestine-specific PITP α expression in the null animal rescues the chylomicron retention disease (Alb, Phillips et al. 2007).

PITP α involvements in ER functions are unanticipated, as all discussions of functional mechanisms focus on roles for PITP α in modulating plasma membrane signaling circuits (see above). It remains to be established whether PITP α is directly, or more indirectly, involved in chylomicron biogenesis. Indirect models would include regulation of chylomicron maturation from a remote compartment via some PITP α -dependent signaling pathway. Some concepts for how PITP α may directly interface with chylomicron trafficking from the ER are suggested by recent studies on the etiology of human CRD, such as

Anderson's disease and hyperbetalipoproteinemia. These CRD syndromes are autosomal recessive disorders characterized by fat malabsorption and pediatric failure to thrive (Charcosset, Sassolas et al. 2008). The associated human duodenal steatosis, when coupled with other aspects of human CRD symptomology, is similar to the CRD and associated phenotypes of *pitpa*^{0/0} mice. Positional cloning analyses demonstrate that one mechanism for inherited human CRD stems from autosomal recessive loss-of-function mutations in the SARA2 GTPase (Jones, Jones et al. 2003). SARA2 is the product of the *SAR1B* gene, and represents one of the two members of the Sar1-like small GTPases expressed in humans.

The Sar1-like GTPases are conserved from yeast to man and these are essential for nucleation of COPII vesicle formation at organized regions of the ER membrane surface termed ER exit sites (Miller and Barlowe 2001). The specific requirement for SARA2/Sar1b in chylomicron packaging for transport from the enterocyte ER is interesting because these lipoprotein cargos are much larger than typical COPII transport vesicles. One interpretation of the genetic data is that SARA2/Sar1b is a privileged GTPase dedicated to formation of atypical COPII vesicles designed to carry unusually large cargos. It follows that PITP α is a similarly privileged component of such a specialized COPII vesicle biogenic pathway (Alb, Cortese et al. 2003). Perhaps PITP α regulates an ER pool of PtdIns(4)P required for biogenesis of a subclass of COPII vesicles dedicated to transport of mega-cargos such as chylomicrons. This proposal is supported by the demonstration that mice expressing wild-type amounts of a PtdIns-binding-defective mutant of PITP α as sole source of the protein are indistinguishable from *pitpa*^{0/0} animals—including with regard to severity of CRD (Alb, Phillips et al. 2007). While the concept that PITP α modulates an ER pool of phosphoinositide departs from dogmatic views that phosphoinositides are localized

exclusively to intracellular compartments in the distal secretory pathway (D'Angelo, Vicinanza et al. 2008), recent findings that Sar1-mediated ER exit sites are formed by and regulated by PtdIns-4-phosphate signaling provide evidence to this idea (Blumental-Perry, Haney et al. 2006).

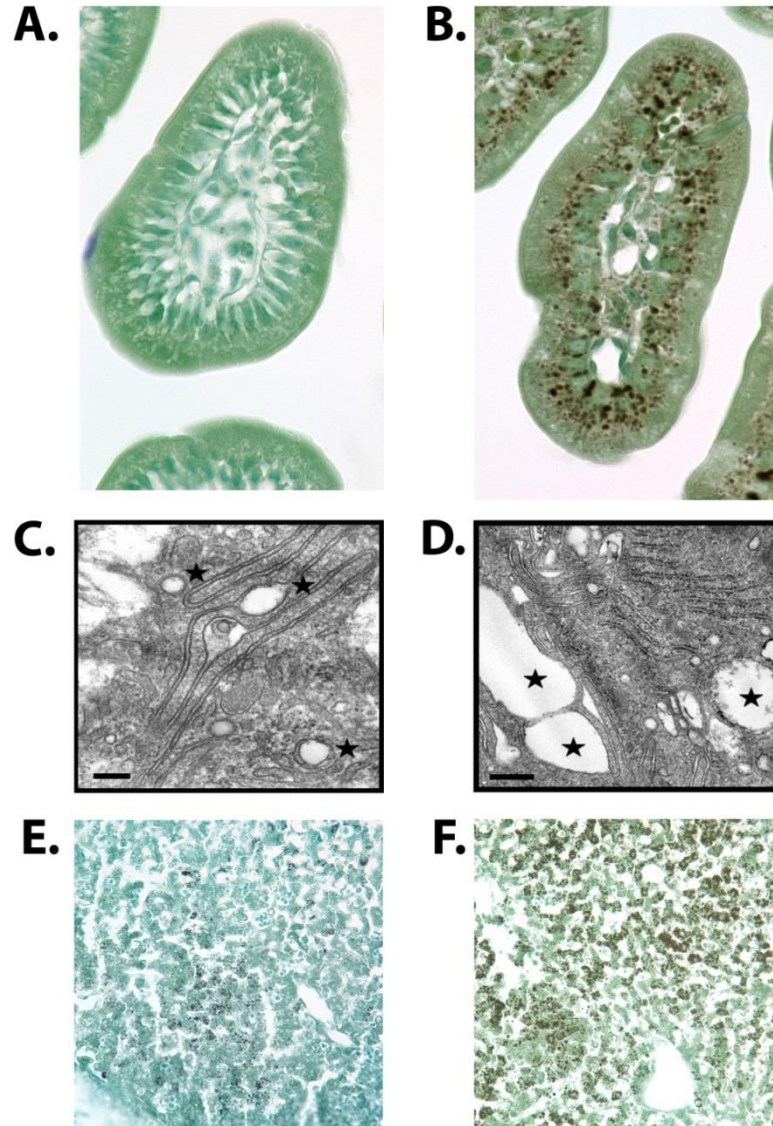


Figure 7. Intestinal and hepatic steatosis in *PITPα*-deficient mice.

Intestinal slices stained for neutral lipid content with osmium from (a) *PITPα*^{+/+} and (b) *pitpα*^{0/0} mice. Note the obvious accumulation of neutral lipid in mutant enterocytes. This accumulation is dependent on nursing and chases only slowly during periods of fast. The phenotype is also obvious in electron micrographs of the villi of duodenal enterocytes from (c) *PITPα*^{+/+} and (d) *pitpα*^{0/0} mice (scale bars are 0.2μm and 0.5μm, respectively). Lipid deposits are highlighted by (★). Liver slices stained with osmium from (e) *PITPα*^{+/+} and (f) *pitpα*^{0/0} mice are also shown.

***pitpa*^{0/0} mice and hepatic steatosis**

Intestine and liver deploy similar strategies for the processing and export of lipoprotein cargos from the ER into distal compartments of the secretory pathway and, ultimately, into the circulation. In that regard, *pitpa*^{0/0} liver also presents extensive microvesicular steatosis as evidenced by the unusually enhanced staining with osmium or the lipophilic dye Oil Red O (**Figure 7**; Alb, Cortese et al. 2003). Electron microscopic and lipidomic analyses confirm dramatic intracellular accretion of neutral lipid in the organ. In this case, however, a large fraction of the lipid accumulates in cytosolic lipid droplets (LDs) and, remarkably, in LDs that populate the nuclear matrix of *pitpa*^{0/0} hepatocytes (**Figure 7**; Alb, Cortese et al. 2003). While *vb/vb* mice do not present such dramatic symptoms of hepatic steatosis, lipidomic analyses report livers of these animals also exhibit elevated levels of neutral lipid (Monaco, Kim et al. 2004).

The intra-hepatic lipid accumulation is not the result of elevated lipid biosynthesis -- the expression of key fatty acid and lipid biosynthetic enzymes is not enhanced. Whether *pitpa*^{0/0} liver is defective in lipoprotein trafficking from the ER, as is the case in intestine, remains to be investigated. However, there is no doubt that an important aspect of lipid homeostasis is deranged in *pitpa*^{0/0} liver, and this deficiency has interesting consequences for outcomes of intestine-specific reconstitution strategies directed at alleviating CRD. Rescue of CRD by intestine-specific expression of PITP α in otherwise *pitpa*^{0/0} mice levies surprisingly modest improvements in the systemic TG and fat storage defects that characterize this animal. The basis for the inefficient translation of a functionally reconstituted intestine to more normal circulating lipoprotein levels appears to rest with enhanced accretion of lipid in the *pitpa*^{0/0} liver of such animals. We presently consider the

amplified accretion to reflect enhanced lipid flow into a dysfunctional liver that cannot adequately process circulating lipoproteins (Alb, Phillips et al. 2007). The increased import is presumably driven by a now functional intestine that efficiently secretes chylomicrons into the circulation of the otherwise *pitpa*^{0/0} mouse.

PITP α --a link between Ins nutrition and lipoprotein metabolism?

There is an old literature associating nutritional deprivation of Ins with defective lipid clearance from rodent liver and intestine. Rats fed a fatty diet accumulate triacylglycerides and cholesterol in the liver when *myo*-inositol is withheld from the diet (Hayashi, Maeda et al. 1974; Burton and Wells 1976; Burton and Wells 1977). This accumulation of neutral lipid is the result of defective mobilization of hepatic triglycerides (Hayashi, Maeda et al. 1974; Burton and Wells 1979). In the Mongolian gerbil model, *myo*-inositol starvation resulted in accumulation of lipid in the small intestine (Kroes, Hegsted et al. 1973)—a phenotype associated with qualitative changes in the fatty acid composition of enteric phospholipids (Woods and Hegsted 1979; Chu and Hegsted 1980). Notably, this condition was also marked by significantly decreased levels of circulating lipoprotein (Chu and Hegsted 1980)—a deficit which was established as the consequence of inefficient transport of lipid across the intestine (Chu and Geyer 1982).

While these observations were taken as evidence for an involvement of PtdIns metabolism with lipid transport across the intestine (Chu and Geyer 1982), no underlying mechanism for the Ins effect has yet been described. The intestinal and hepatic steatosis that characterizes *pitpa*^{0/0} mice broadly recapitulates the effects of inositol deprivation in rodents. It is now an attractive proposition that Ins deprivation and functional ablation of PITP α share

an underlying mechanism for provoking intestinal, and perhaps hepatic, steatosis. That is, that phosphoinositides play an important role in the packaging of unusual cargoes like chylomicrons, and other lipoprotein particles, for transport from the ER to late stages of the secretory pathway. This hypothesis raises the interesting possibility that PITP α sets the efficiency for lipoprotein assembly in intestine and liver, and therefore determines the capacity for lipid clearance in liver and intestine.

PITP α and the pancreas

The third signature pathology associated with *pitpa*^{0/0} mice is a severe hypoglycemia where circulating glucose levels (and insulin levels) are nearly an order of magnitude lower than those of wild-type siblings (Alb, Cortese et al. 2003; Alb, Phillips et al. 2007). One major defect appears to be in hepatic gluconeogenesis with severe deficits in both proglucagon gene expression and in circulating glucagon levels. As a result, *pitpa*^{0/0} liver inappropriately stores glycogen in the face of a catastrophic hypoglycemia (Alb, Cortese et al. 2003). As in the case of the CRD, the threshold requirement for PITP α in maintenance of proper glucose homeostasis is low. Functional PITP α reductions of 90% or greater are required for manifestation of hypoglycemia (Alb, Phillips et al. 2007).

The glucose and gluconeogenic derangements on display in *pitpa*^{0/0} neonates are accompanied by obvious structural derangements of the pancreas. While *pitpa*^{0/0} exocrine pancreas is morphologically normal, the endocrine pancreas is not. The number of recognizable islets per *pitpa*^{0/0} pancreas is strongly reduced relative to wild-type, vacuolations are evident in the islets, and the *pitpa*^{0/0} islet cells themselves are shrunken (Alb, Cortese et al. 2003). It is not yet known whether these pancreatic deficits are the result

of indirect damage inflicted by a hostile physiological environment (*e.g.* associated with CRD), or whether these are manifestations of some other intrinsic developmental problem.

Zebrafish type 1 PITPs

Zebrafish (*Danio rerio*) express a mammalian-like cohort of Type 1 PITPs with the addition of a unique PITP β -like protein designated PITP γ (Ile, Kassen et al. 2010). The conservation of Type 1 PITP roster further extends to interesting details of Type 1 PITP diversity—*i.e.* zebrafish execute precisely the same exon-skipping event as mammals do in generating the canonical and alternative PITP β splice variants. As a result, this non-mammalian model is a facile system for study of vertebrate Type 1 PITPs, and it is particularly informative with respect to the physiological functions of PITP β isoforms. Whereas functional ablation experiments have, to this point, been uninformative for the PITP γ isoform, new insights are forthcoming regarding PITP β function in this organism. Zebrafish express PITP β splice variants predominantly in the eye, and specifically to the synaptic pedicles of retinal double cone cells (Ile, Kassen et al. 2010). Morpholino-based silencing experiments demonstrate PITP β splice variant activity is required for the biogenesis and/or the maintenance of the double cone photoreceptor cell outer segments. The deficits in double cone cell outer segment biogenesis and structure are also reversible. As effectiveness of PITP β -directed morpholinos wanes with age of the morphant fish, and PITP β expression is restored, development of morphologically correct and electro-physiologically functional double cone cells is re-engaged (Ile, Kassen et al. 2010).

What functional mechanisms underlie PITP β splice variant involvement in zebrafish double cone cell outer segment biogenesis/maintenance? Cone cell outer segments are

comprised of an intricate network of membraneous discs/lamellae. These membranes are subject to a vigorous course of self-renewal that involves a high capacity membrane trafficking program (Young 1974; Ile, Kassen et al. 2010). The general localization of PITP β splice variants to the trans-Golgi network suggests a scenario where deficiencies in PITP β activity subtly compromise Golgi function in double cone cells, and evoke significant defects in biosynthetic trafficking of opsin into the outer segment. If the normally high rates of membrane turnover in these structures are maintained in the face of reduced incorporation of biosynthetic material, outer segment integrity will be compromised. In mammalian rod cells, the SARA adaptor couples PtdIns(3)P cues to syntaxin t-SNARE activity in potentiation of the vesicle fusion events involved in outer segment membrane disc formation and maintenance (Chuang, Zhao et al. 2007). One possibility is zebrafish PITP β splice variants support a similarly privileged phosphoinositide-dependent trafficking pathway in double cone cells.

The zebrafish PITP α studies are surprising in that, unlike in mice, functional ablation of PITP α results in defective gastrulation. The failure occurs at a stage where highly migratory cells of the blastoderm extend and converge to cover the yolk cell surface (Ile, Kassen et al. 2010). As in mice, PtdIns-binding is an essential functional property of PITP α activity in zebrafish development. The lack of functional redundancy between PITP α and PITP β isoforms is also clearly evident—PITP α does not compensate for PITP α deficits in zebrafish development (Ile, Kassen et al. 2010). Thus, different vertebrates employ paralogous Type 1 PITPs in substantially different ways.

PITPs and fungal pathogens

Many fungal pathogens are capable of reversibly transitioning between blastospore and hyphal growth phases, termed a dimorphic transition. Dimorphic transitions are proposed to promote pathogenic activities of fungi; however, it is likely only one of many factors (Brown and Gow 1999; Gow, Brown et al. 2002). To investigate Sec14's role in dimorphic transitions, the model system *Yarrowia lipolytica* was employed, demonstrating that Sec14p's homologue, Sec14^{YL}, is a non-essential (probably due to additional isoforms), Golgi-associated protein that modulates dimorphic transitions (Lopez, Nicaud et al. 1994). Sec14's role is thought to regulate of the delivery of cargo to the plasma membrane for mycelial growth. Interestingly, this defect can be bypassed through the addition of the neutral lipid, oleic acid (Titorenko, Ogrydziak et al. 1997) which enlarges lipid droplets and lowers the ratio of TAG to sterol esters in *Y.lipolytica* (Athenstaedt, Jolivet et al. 2006).

Candida infections or candidemia, represent a large cause of nosocomial infections in the United States, accounting for an estimated annual mortality rate between 2800 and 11,200 deaths. Of the Candida species, the majority of infectious episodes are caused by *Candida albicans* (Pfaller and Diekema 2007). *C.albicans* is a commensal, dimorphic fungus, often found in the human gastrointestinal tract. Most commonly, mucosal membranes are the sites of infection, resulting in oropharyngeal, esophageal, and vaginal candidiasis; however, more severe systemic infections occur. All individuals are susceptible to infection; however, contributing factors include wide spectrum antibiotics, corticosteroids, hormone therapy, and HIV (Calderone 2002). Interestingly, the yeast Sec14p homologue in *C.albicans*, CaSec14p, is likely an essential gene; however, its role in dimorphic transition is not clear (Monteoliva, Sanchez et al. 1996).

Additionally, multiple Sec14-like and mammalian PITP protein have been cloned from *Dictyostelium discoideum* that can bind and transfer PtdIns and PtdCho (Swigart, Insall et al. 2000). Recently, a novel Sec14-like protein was identified in *Taenia solium* or Sec14Tsol. *T.solium* is an infectious parasite found in humans and porcine that can cause cysticercosis or neurocysticercosis. Sec14Tsol binds phospholipids and is localized to the Golgi membranes of the metacestode tegument, suggesting a potential role in host interactions (Montero, Gonzalez et al. 2007; Sinha and Sharma 2009). Although antifungal agents exists for *C.albicans* (Sobel 2008) and cysticides for *T.solium* (Sinha and Sharma 2009); none probe the hydrophobic patch of Sec14, providing an attractive, and essentially virgin territory to combat these pathogens and are discussed in **Chapter 3**.

Conclusions and future perspectives

The appropriate spatial and temporal regulation of lipid metabolic flux is central to cellular homeostasis--even subtle derangements of this system lead to disease. Yet, we are far from an understanding of how diverse territories of the cellular lipid metabolome are interfaced and how lipid metabolic processes are coordinated with lipid signaling. It is becoming increasingly clear that Sec14-like PITPs, and likely PITPs in general, contribute to the integration of diverse aspects of lipid metabolism with phosphoinositide signaling. Physical pictures of how this may happen are emerging, particularly for Sec14-like proteins, and these models identify new areas for experimental inquiry. Two general areas are ripe for investigation. First, it will be interesting to discern whether the PtdIns-binding bar codes of Sec14-like proteins not annotated as PITPs (*e.g.* caytaxin, CRALBP1 and α -TTP) forecast

authentic inositol-lipid binding capabilities. If so, and it seems likely that it will be so in some cases, the activities of these proteins, and the etiologies of the associated diseases, will need to be re-interpreted. Second, the question of PtdIns-presentation function will be particularly interesting from the standpoint of Sec14- or PITP-like modules in complex multi-domain proteins. The concept that such PITP-like domains prime production of local phosphoinositide signals in response to metabolic cues, and that these phosphoinositide signals in turn modulate catalytic activities of these complex proteins, describes new conceptual frameworks for how such proteins operate. We expect that Sec14-domains in particular will garner more attention in this regard, and will become increasingly attractive targets for pharmacological intervention. The importance of being able to visualize, in living cells, when and where PITPs execute lipid exchange is also clear. Reliable conformational biosensors will be invaluable tools in those efforts, and will provide unique approaches towards faithfully imaging PITP-regulated interfaces between lipid metabolism and signaling *in vivo*.

Finally, we forecast interest in PITPs, and perhaps primarily Sec14-like PITPs, as targets for pharmaceutical intervention in the context of infectious diseases. While not discussed in this review, eukaryotic pathogens express PITP-like proteins—some of which are clearly PITPs. These proteins are sufficiently diverged from their vertebrate paralogs to suggest that identification of specific small molecule inhibitors will be feasible. It is in this arena that PITP-directed therapies, and a detailed understanding of PITP biology and biochemistry, may ultimately make the greatest impact in human health.

Table 2. Chapter one summary
PITPs and Inositol Signaling
<ul style="list-style-type: none"> • Emerging data implicate PITPs as instructors of phosphatidylinositol metabolism, a role that contributes to the functional diversification of PI signaling. • PITPs separate into two evolutionarily unrelated classes: the highly conserved Sec14-like PITPs and the metazoan PITPs. • Analysis of PITP function has been limited by the inability to describe PITPs using traditional enzyme definitions. • Structural and genetic studies on the yeast Sec14 have implicated its role as a “nanoreactor”, wherein its primary function is not simple lipid exchange between membranes, but integration of PtdCho metabolism with presentation of PtdIns to PtdIns 4-OH kinase.
Sec14-like PITPs in Human Disease
<ul style="list-style-type: none"> • Sec14-like proteins can form stand-alone proteins or be part of more complicated landscapes within multidomain proteins. • Malfunctions in Sec14-like domains result in a variety of human disorders including ataxia with vitamin E deficiency, cayman-type cerebellar ataxia, visual cycle defects, retinitis punctata albescens, and neurofibromatosis type 1. • Sec14-like proteins in general, have a conserved PtdIns binding ‘bar code’. Mutations within this region often result in protein dysfunction

and are well represented in physiologically relevant mutations.
Physiology of Mammalian Type I PITPs
<ul style="list-style-type: none">• The mammalian Type 1 PITPs are structurally unrelated to the Sec14-like PITPs, but may nonetheless function as nanoreactors.• Mice with graded reductions of PITPα expression have been used to dissect the physiological roles of PITPα. PITPα deficiency results in spinocerebellar disease, enteric and hepatic steatosis, and hypoglycemia.• PITPα is implicated in both cell autonomous and cell non-autonomous signaling mechanisms.• The roles of Type 1 PITPs are being addressed in the zebrafish model system, describing a role for PITP\square in maintaining outer segment integrity in specific cone cells.

Materials and methods

Sequence alignment

Protein sequences were acquired from the Universal Protein Resource (Consortium 2012), aggregated using UGENE (version 1.10.1; <http://ugene.unipro.ru/>)(Okonechnikov, Golosova et al. 2012), and aligned with the Clustal X2 module using the default settings (Larkin, Blackshields et al. 2007). Homologous sequences were superimposed onto structural models (PDB IDs 1AUA, 1OLM, 3B7Z, 4FMM) to highlight the PtdIns/PtdCho lipid binding barcode.

Molecular graphics

Molecular graphics and analyses were performed with the UCSF Chimera package (version 1.8; <http://www.cgl.ucsf.edu/chimera>)(Pettersen, Goddard et al. 2004).

Chimera is developed by the Resource for Biocomputing, Visualization, and Informatics at the University of California, San Francisco (supported by NIGMS P41-GM103311).

CHAPTER 2: CHEMICAL INHIBITORS OF PHOSPHATIDYLINOSITOL TRANSFER PROTEINS ENABLE HIGHLY SELECTIVE INTERFERENCE WITH SPECIFIC PATHWAYS OF PHOSPHOINOSITIDE SIGNALING IN CELLS²

Overview

Sec14-like phosphatidylinositol transfer proteins (PITPs) integrate diverse territories of intracellular lipid metabolism with stimulated phosphatidylinositol-4-phosphate production, and are discriminating portals for interrogating phosphoinositide signaling. Yet, neither Sec14-like PITPs, nor PITPs in general, have been exploited as targets for chemical inhibition for such purposes. Herein, we validate the first small molecule inhibitors (SMIs) of the yeast PITY Sec14. These SMIs are nitrophenyl(4-(2-methoxyphenyl)piperazin-1-yl)methanones (NPPMs), and are effective inhibitors *in vitro* and *in vivo*. We further establish Sec14 is the sole essential NPPM target in yeast, that NPPMs exhibit exquisite targeting specificities for Sec14 (relative to related Sec14-like PITPs), propose a mechanism for how NPPMs exert their inhibitory effects, and demonstrate NPPMs exhibit exquisite pathway selectivity in inhibiting phosphoinositide signaling in cells. These data deliver proof-of-concept that PITY-directed SMIs offer new and generally applicable avenues for intervening with phosphoinositide signaling pathways with selectivities superior to those afforded by contemporary lipid kinase-directed strategies. Additionally, we will discuss several non-NPPM Sec14-directed inhibitors, some of which are natural products or inhibit dimorphic transitions in pathogenic yeast.

² This chapter previously appeared as a shortened article in *Nature Chemical Biology*. The original citation is as follows: Nile, A. H., A. Tripathi, et al. (2014). "PITPs as targets for selectively interfering with phosphoinositide signaling in cells." *Nature Chemical Biology* **10**(1): 76-84.

Introduction

Lipid signaling modulates a wide range of cellular processes, including regulation of G-protein-coupled receptor and receptor tyrosine kinase signaling at the plasma membrane (Wymann and Schneider 2008), actin dynamics (Janmey and Lindberg 2004), transcription (Irvine 2003; Henry, Kohlwein et al. 2012), and membrane trafficking (Di Paolo and De Camilli 2006). A major pillar of eukaryotic lipid signaling involves regulated production of phosphoinositides and the soluble second messengers derived from them—*i.e.* the soluble inositol (Ins) phosphates (Strahl and Thorner 2007; Michell 2008). Phosphatidylinositol (PtdIns) is an essential phospholipid in eukaryotes that serves as metabolic precursor for both phosphoinositides and Ins-phosphates. While the chemical diversity of the Ins-phosphates is large, the phosphoinositide cabal is much simpler. Yeast produce only five phosphoinositides (PtdIns-[3]-phosphate, PtdIns-[4]-phosphate, PtdIns-[5]-phosphate, PtdIns-[4,5]-bisphosphate, and PtdIns-[3,5]-bisphosphate) while higher eukaryotes produce seven; those synthesized by yeast as well as PtdIns-[3,4]-bisphosphate and PtdIns-[3,4,5]-trisphosphate (Michell 2008). This limited phosphoinositide cohort nonetheless supports a remarkably diverse landscape of lipid signaling that modulates the actions of hundreds of proteins (Strahl and Thorner 2007). Such functional diversification emphasizes the intricacy with which phosphoinositide signaling is woven into the fabric of eukaryotic cell biology.

The acute and specific inactivation of a target enzyme is a highly desirable instrument for dissecting mechanisms of lipid signaling in cells. A major difficulty with productively achieving that goal rests with the fact that compensatory arms of lipid metabolism often buffer the desired effects of traditional (*i.e.* genetic or siRNA-based; discussed in **Chapter 3**) interventions that target lipid signaling pathways. While chemical biology offers potential

advantages in this regard, the problem continues to be a difficult one. This is especially true in the context of phosphoinositide signaling whose very diversification demands highly targeted approaches for clean analysis. Specific interventions at the level of individual lipid kinases, or compartment-specific interventions at the level of defined phosphoinositide species using sophisticated Rapalog technologies (Suh, Inoue et al. 2006; Varnai, Thyagarajan et al. 2006), remain unsatisfactorily blunt experimental instruments. Such interventions exert pleiotropic effects. These pleiotropies reflect the multitude of effector activities impaired upon inhibition of a target Ins-lipid kinase, or upon compartment-specific depletion of a specific phosphoinositide species.

PtdIns-transfer proteins (PITPs) of the Sec14 protein superfamily are key regulators of phosphoinositide signaling as evidenced by demonstrations that individual PITPs specify discrete biological outcomes of PtdIns kinase action (Schaaf, Ortlund et al. 2008; Bankaitis, Mousley et al. 2010). Deficiencies in individual Sec14-like PITPs compromise membrane trafficking through the *trans*-Golgi network (TGN) and endosomal systems (Bankaitis, Malehorn et al. 1989), decarboxylation of phosphatidylserine to phosphatidylethanolamine (Wu, Routt et al. 2000), fatty acid metabolism (Desfougères, Ferreira et al. 2008), polarized cell growth (Vincent, Chua et al. 2005) and fungal dimorphism (Lopez, Nicaud et al. 1994). Mutations in PITPs or PITP-like proteins are also root causes of mammalian neurodegenerative, pancreatic and lipoprotein biogenic diseases (Alb, Cortese et al. 2003; Nile, Bankaitis et al. 2010).

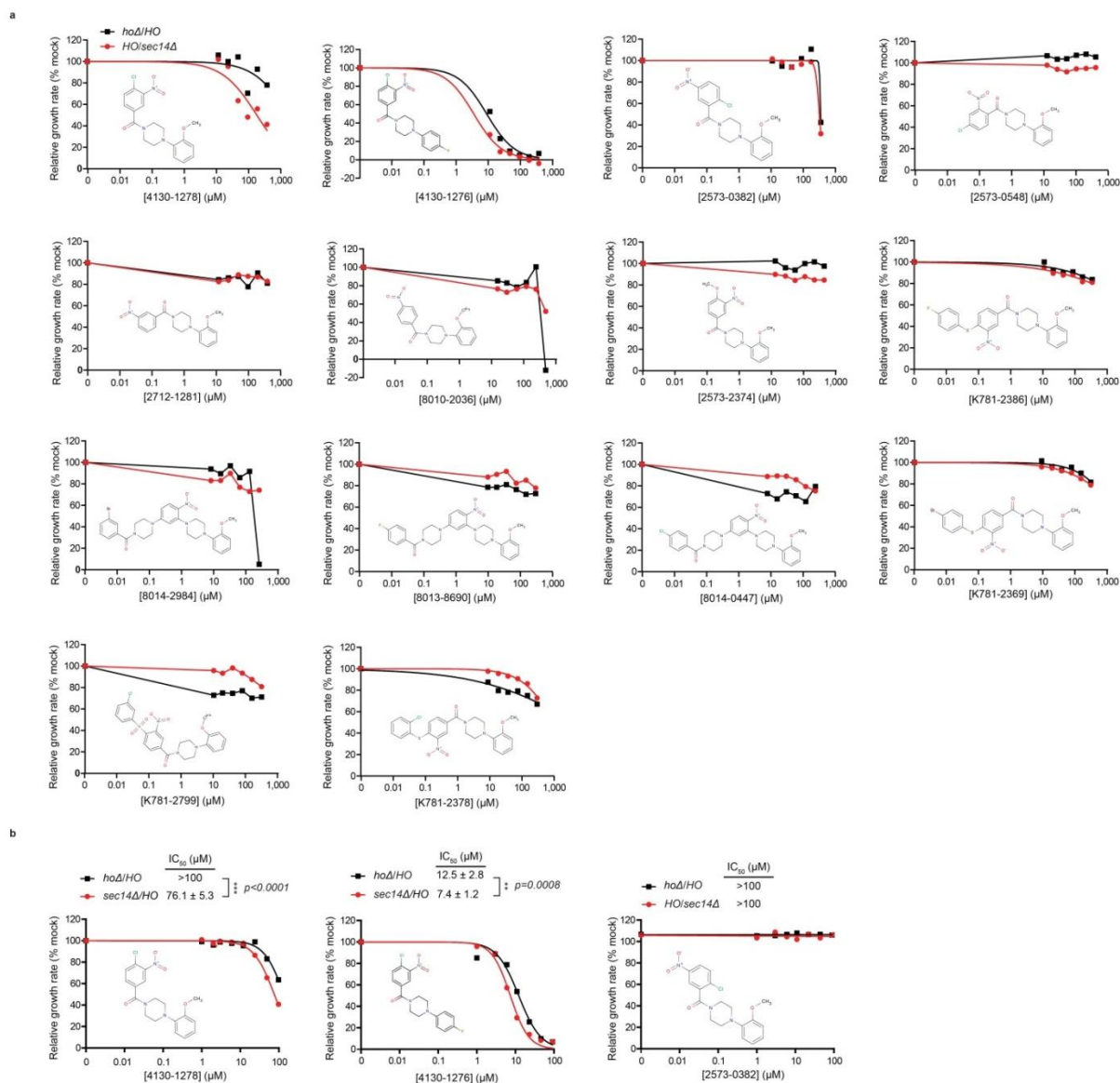
The various data indicate PITPs offer highly discriminating portals for interrogating phosphoinositide signaling, and identify PITPs as potential targets for small molecule-based inhibition of select phosphoinositide signaling pathways in cells. In this chapter, we exploit

the genetic and post-genomic tools the yeast system offers to make just that case. The power of the P1TP-directed approach resides in the exquisite specificities it affords in chemically intervening with phosphoinositide signaling. That is, it offers selectivities far superior to those delivered by strategies which target individual PtdIns-kinase isoforms or individual phosphoinositide species.

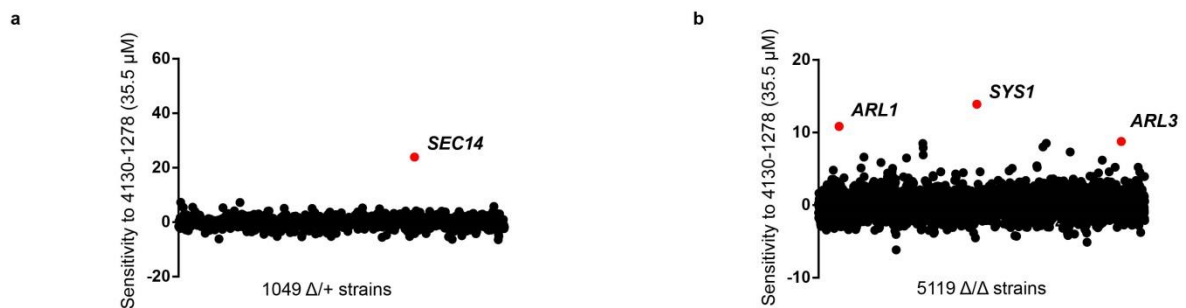
Results: NPPM-like SMIs

Identification of candidate Sec14-directed SMIs

Sec14, the major yeast P1TP, is an essential protein required for membrane trafficking through the TGN/endosomal system (Bankaitis, Malehorn et al. 1989). Chemogenomic profiling of 188 bioactive chemical inhibitors of yeast growth identified a candidate for a Sec14-directed SMI (Hoon, Smith et al. 2008). This unvalidated compound, 4130-1278 (**1**), is a 4-chloro-3-nitrophenyl(4-(2-methoxyphenyl) piperazin-1-yl)methanone (NPPM). Since 4130-1278 exhibited a mediocre potency, and only limited water solubility, we surveyed 13 other NPPM-like SMIs in a search for more promising candidate Sec14 inhibitors (see **Figure 8a**). One such derivative, 4130-1276 (**2**), exhibited superior solubility in aqueous solutions, and provoked growth arrest of a *sec14Δ/SEC14* heterozygous strain at 10-fold lower concentrations than those required for 4130-1278 to levy similar inhibitory effects (**Figure 8b**).



Chemogenomic profiling of ca. 6200 yeast deletion strains correlated gene-dosage with yeast sensitivity to 4130-1278 or 4130-1276 challenge on a genome-wide scale (**Figure 9a-f**). The profiling identified *sec14Δ/SEC14* heterozygous diploid cells as the most sensitive to 4130-1278 and 4130-1276 challenge of all homozygous Δ/Δ and heterozygous $\Delta/+$ diploids tested (non-essential and essential gene queries, respectively; **Figure 9a-f**). A limited set of other genes was also identified for which dosage reduction resulted in decreased fitness in the presence of 4130-1278 and 4130-1276 (**Figure 9c,f**). Gene functions identified in the more extensive 4130-1276 hit list included Golgi trafficking, sporulation, exocytosis, vacuolar transport, and lipid metabolism. High scoring chemogenomic interactions, include phospholipase D (PLD; *SPO14*), a strong synthetic interactor with *sec14-1^{ts}* (Xie, Fang et al. 1998; Schaaf, Ortlund et al. 2008) and the phospholipase D regulator *SRF1* (Kennedy, Kabbani et al. 2011), were independently recognized in genome-scale synthetic genetic array (SGA) analyses that employed *sec14-1^{ts}* as query allele (Mousley, Tyeryar et al. 2008; Curwin, Fair et al. 2009).



c

4130-1278 (35.5 μ M)
 Δ /+

Gene	Rank	Z-score
<i>SEC14</i>	1	23.8908
<i>CDC19</i>	2	7.26832
<i>PCF11</i>	3	7.21232
<i>SEC8</i>	4	5.78315
<i>EXO84</i>	5	5.5
<i>POP8</i>	6	5.44979
<i>YDL196W</i>	7	5.28239
<i>YKL111C</i>	8	5.25304
<i>ALG2</i>	9	5.08466
<i>ERG11</i>	10	5.02355
<i>SDO1</i>	11	4.92435
<i>SEC5</i>	12	4.16099
<i>ECM16</i>	13	4.14521
<i>PRP39</i>	14	4.12738
<i>GLC7</i>	15	4.10523
<i>PIK1</i>	16	4.04959
<i>LSM4</i>	17	4.01933

4130-1278 (35.5μM) Δ/Δ			4130-1278 (35.5μM) Δ/Δ		
Gene	Rank	Z-score	Gene	Rank	Z-score
<i>SYS1</i>	1	13.899	<i>VAM6</i>	18	5.10347
<i>ARL1</i>	2	10.8489	<i>YKR073C</i>	19	5.06826
<i>ARL3</i>	3	8.77435	<i>SPT3</i>	20	5.05281
<i>COG8</i>	4	8.50676	<i>TSC3</i>	21	4.82498
<i>COG7</i>	5	8.48062	<i>IRS4</i>	22	4.71571
<i>YML013C-A</i>	6	8.00696	<i>NKP1</i>	23	4.63974
<i>PDR1</i>	7	7.89154	<i>PTP2</i>	24	4.59421
<i>COG6</i>	8	7.31163	<i>TPC1</i>	25	4.59208
<i>ERG4</i>	9	6.91412	<i>JEM1</i>	26	4.58863
<i>SRF1</i>	10	6.60943	<i>YPR123C</i>	27	4.53827
<i>YPT31</i>	11	6.47998	<i>SSD1</i>	28	4.48337
<i>GYP1</i>	12	6.18102	<i>THP2</i>	29	4.45195
<i>SAC3</i>	13	5.86323	<i>SLG1</i>	30	4.43096
<i>SUR4</i>	14	5.41774	<i>YDR290W</i>	31	4.40208
<i>NVJ2</i>	15	5.21487	<i>ARG4</i>	32	4.29009
<i>PRO2</i>	16	5.2098	<i>MIG2</i>	33	4.05818
<i>SFH2</i>	17	5.19526	<i>SAC7</i>	34	4.03501

4130-1276 (6.7μM) Δ/Δ			4130-1276 (6.7μM) Δ/Δ		
Gene	Rank	Z-score	Gene	Rank	Z-score
SPO14	1	18.4012	SLT2	18	7.88942
SYS1	2	16.8014	COG7	19	7.76551
TSC3	3	16.4857	GYP1	20	7.75846
TRS85	4	15.3888	TPM1	21	7.74741
IRS4	5	14.7732	ERG4	22	7.72347
SSD1	6	12.6494	YGL199C	23	7.54918
NBP2	7	12.59	GIS4	24	7.07088
ARL1	8	12.0693	VIP1	25	6.94883
SRF1	9	11.5426	PTC1	26	6.77493
VPS45	10	10.7965	YHP1	27	6.62966
YPT31	11	10.0089	SFH2	28	6.59554
COG8	12	9.36347	MAL11	29	6.55088
YLR171W	13	9.22447	SWA2	30	6.52261
ARL3	14	8.617	YPR092W	31	6.43972
PDR1	15	8.46251	SAC3	32	6.41621
NVJ2	16	8.36088	EAF7	33	6.41306
APL4	17	8.14542	FYV6	34	6.37822

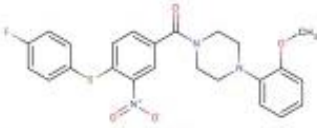
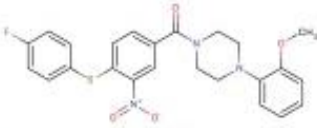
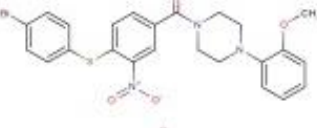
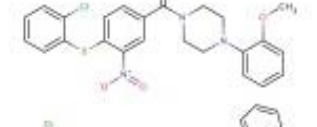
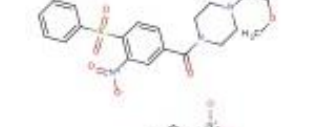
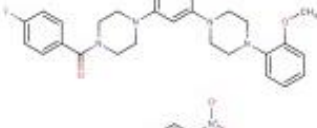
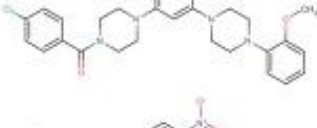
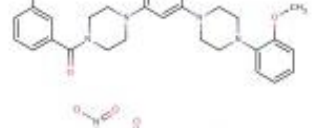

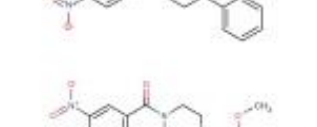
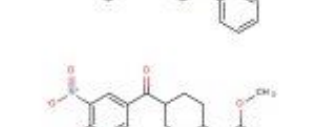

4130-1276 (6.7μM) Δ/Δ			4130-1276 (6.7μM) Δ/Δ			4130-1276 (6.7μM) Δ/Δ			4130-1276 (6.7μM) Δ/Δ		
Gene	Rank	Z-score	Gene	Rank	Z-score	Gene	Rank	Z-score	Gene	Rank	Z-score
SUR4	35	6.35295	<i>CTR9</i>	52	5.19767	<i>PEX31</i>	69	4.60402	<i>MAK10</i>	86	4.13944
BEM4	36	6.31546	<i>YDL172C</i>	53	5.153	<i>YMR102C</i>	70	4.60251	<i>YNR064C</i>	87	4.10396
<i>URA4</i>	37	6.30889	BCK1	54	5.09277	<i>YOR364W</i>	71	4.46615	<i>PMD1</i>	88	4.10291
<i>YDR290W</i>	38	6.19261	<i>WSC2</i>	55	5.05962	<i>YDR048C</i>	72	4.40403	<i>YPS7</i>	89	4.09857
<i>IMH1</i>	39	6.06085	<i>AIM18</i>	56	5.01455	<i>MCH4</i>	73	4.3891	<i>BOI1</i>	90	4.08662
<i>PEX30</i>	40	5.93686	<i>YLR169W</i>	57	5.01299	<i>HXT12</i>	74	4.34545	<i>YML013C-A</i>	91	4.068
<i>GND1</i>	41	5.84756	UBP13	58	4.98977	<i>ATG3</i>	75	4.30268	<i>SVL3</i>	92	4.05392
<i>SAC7</i>	42	5.7857	<i>NTH2</i>	59	4.94531	<i>TCO89</i>	76	4.30243	<i>CHS7</i>	93	4.00858
<i>PPM1</i>	43	5.77915	<i>YIP4</i>	60	4.90708	<i>MAC1</i>	77	4.29923	<i>APL2</i>	94	4.0032
<i>VPS51</i>	44	5.69126	<i>ARG82</i>	61	4.90349	<i>YKR073C</i>	78	4.29207			
<i>GCS1</i>	45	5.64355	<i>ACB1</i>	62	4.84194	PAR32	79	4.28377			
<i>DEP1</i>	46	5.40182	WHI3	63	4.80757	<i>PYC2</i>	80	4.26821			
<i>THP1</i>	47	5.40003	<i>LDB16</i>	64	4.77873	<i>HTA1</i>	81	4.26025			
TRS33	48	5.33775	<i>FPS1</i>	65	4.74222	SLG1	82	4.24512			
<i>APS1</i>	49	5.32573	<i>HPR1</i>	66	4.73249	ERG5	83	4.22826			
TLG2	50	5.32138	<i>VPS9</i>	67	4.70677	<i>PTR2</i>	84	4.21175			
<i>OPI1</i>	51	5.23665	<i>YPL150W</i>	68	4.64481	<i>PEP3</i>	85	4.18542			

Figure 9. Chemogenomic interaction-profiles of 4130-1276 and 4130-1278.

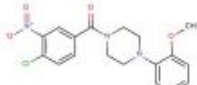
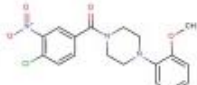
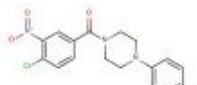
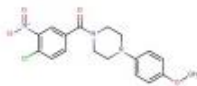
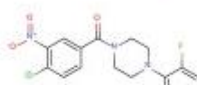
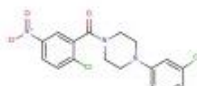
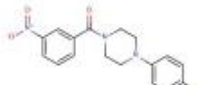
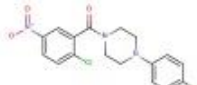
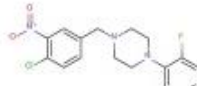
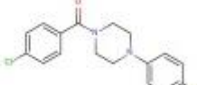
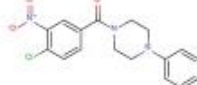
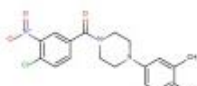
Individual sensitivities of 1050 heterozygous (a) and 4337 homozygous (b) deletion strains to 4130-1278 (35.5μM) are plotted on the y-axis. (c) Relative gene sensitivities are ranked. Genes independently identified as interactors in *sec14-1^{ts}* synthetic genetic arrays (SGAs) are highlighted in red. Individual sensitivities of 1064 heterozygous (d) and 4455 homozygous (e) deletion strains to 4130-1276 (6.7μM) are plotted on the y-axis. (f) Relative gene sensitivities are ranked. Sensitivities reflect the relative under-representation of each query strain in the pool population after culture in the presence of inhibitor compared to incubation in absence of inhibitor (see Methods). Genes so identified by statistically significant fitness defects (●) or resistance (■) are listed with corresponding P-values. Genes independently identified as interactors in *sec14-1^{ts}* synthetic genetic arrays (SGAs) are highlighted in red.

Expansion of the candidate Sec14-directed SMI set

The attractiveness of 4130-1278 and 4130-1276 as potential Sec14 inhibitors focused searches for other candidate Sec14-targeted SMIs. To this end, an expanded set of 34 compounds was assembled around the 4130-1276 scaffold. For the initial rounds of compound selection, the Chembridge chemical library was filtered using the Similarity Search (Marvin Applet tool on Hit2Lead–Cambridge database). The filter clamped structural similarity to ca. 80% of the query 4130-1276 molecule and highlighted functional groups as sites for diversification (**Figure 10a,b**). NPPMs 4130-1276, 67170-49 (**3**) and 6748-481 (**4**), were chosen as foci for further analysis because, among this group, these compounds represented the most potent inhibitors of yeast cell proliferation. The closely related analogue 5564-701 (**5**) elicited no such growth inhibitory effects and served as a convenient negative control in these studies. The structures of the five primary NPPMs of interest are presented in **Figure 11a**.

No.	Accession #		IC ₅₀ (μM)	
			hoΔ/HO	sec14Δ/HO
26	K781-2386		>200	>200
27	K781-2369		>200	>200
28	K781-2378		>200	>200
29	K781-2799		>200	>200
30	8013-8690		>200	>200
31	8014-0447		>200	>200
32	8014-2984		>200	>200
33	2573-0548		>200	>200
34	8010-2036		>200	>200
35	2712-1281		>200	>200
36	2573-2374		>200	>200

b

No.	Accession #		IC ₅₀ (μM)			
			WT	SEC14 ^Δ -28	phr1Δ	kes1Δ
1	5276-937 4130-1278		>200	ND	>200	>200
2	4130-1278		3.53±1.1	1.9±0.3	>200	>200
3	67170-49		4.03±1.9	1.14±0.3	>200	>200
4	6748-481		2.87±0.6	0.44±0.2	>200	>200
5	5564-701		>200	>200	>200	>200
6	5355-152		>200	>200	>200	>200
7	5658-722		>200	>200	>200	>200
8	5263-433		91 ± 23	8.1 ± 0.8	>200	>200
9	5357-399		27.4±3.9	6.7±1.1	>200	>200
10	5348-909		33.2±6.9	24.1±5.3	>200	183 ± 21
11	7278-196		7.70±3.0	2.26±0.5	>200	>200

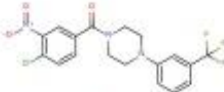
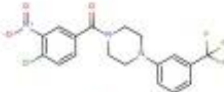
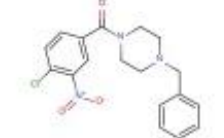
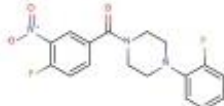
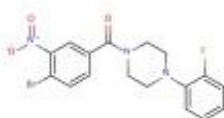
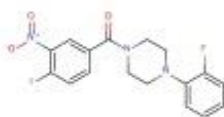
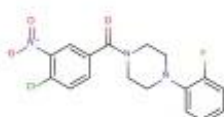
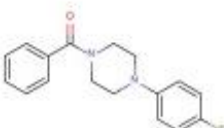
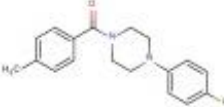
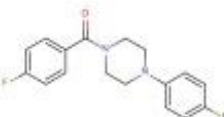
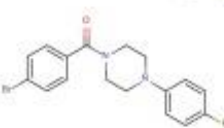
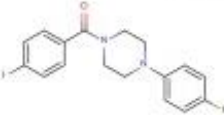
No.	Accession #		IC ₅₀ (μM)			
			WT	SEC14 ^{Δ1-10}	ck1Δ	Res1Δ
12	6628-980		104.5±33.1	17.8±4.7	>200	>200
13	5356-684		>200	>200	>200	>200
14	BBV34896-755		>>20 ^a	ND	>200	>>20 ^a
15	BBV34846-244		<<20 ^a	ND	>>20 ^a	>>20 ^a
16	Z1082689-326		<<20 ^a	ND	>>20 ^a	>>20 ^a
17	BBV34846-247		<<20 ^a	ND	>>20 ^a	>>20 ^a
18	5348-723		>200	71 ± 21	>200	>200
19	5356-628		>200	>200	>200	>200
20	5356-350		>200	110.6±9.9	>200	>200
21	5567-782		>200	>200	>200	>200
22	5353-036		6.2±2.1	2.4±0.47	>200	>200
23	7329-906		3.75±1.6	1.4±0.29	>200	>200

Figure 10. *In vivo* SAR analyses.

(a) Growth of wild-type (*hoΔ/HO*) and *sec14Δ/HO* yeast strains was monitored at $\lambda_{610\text{nm}}$ (see **Figure 8**) in the presence of the indicated SMI. IC₅₀s are displayed with the corresponding test SMI (see **Methods**). One experiment was conducted. (b) Growth inhibition of wild-type (CTY182), *SEC14*^{P-136} (CTY374), *cki1Δ* (CTY303) or *kes1Δ* (CTY159) yeast strains by the indicated SMI (see **Methods**). At least three independent experiments were conducted and the mean \pm the 95% confidence interval is displayed (see **Methods**). IC₅₀s indicated by (a) were determined by visual inspection of YPD plates or microtiter plates supplemented with the corresponding SMI.

Yeast sensitivity to NPPM is a function of Sec14 expression levels

Dose response experiments showed that haploid yeast tolerance to NPPM challenge was directly proportional to cellular Sec14 levels. NPPM 6748-481 served as representative SMI in these experiments as it is the most water soluble of the bioactive compounds, and was the most potent inhibitor of yeast growth. The half-maximal inhibitory concentration (IC_{50}) for 6748-481 was $2.9 \pm 0.6 \mu\text{M}$ for wild-type haploid cells (**Figure 11b**). When endogenous Sec14 levels were reduced approximately 7-fold (by driving *SEC14* expression from a truncated genomic *SEC14* promoter, *SEC14*^{P-136}; Salama, Cleves et al. 1990) the IC_{50} fell proportionately ($0.44 \pm 0.16 \mu\text{M}$; **Figure 11b**). The effect was specific as *SEC14*^{P-136} haploids were not sensitized to the biologically inactive 5564-701 ($IC_{50} > 200\mu\text{M}$; **Figure 11b**). Reciprocally, elevated Sec14 expression enhanced yeast resistance to the growth inhibitory properties of 6748-481 (Figure 11c).

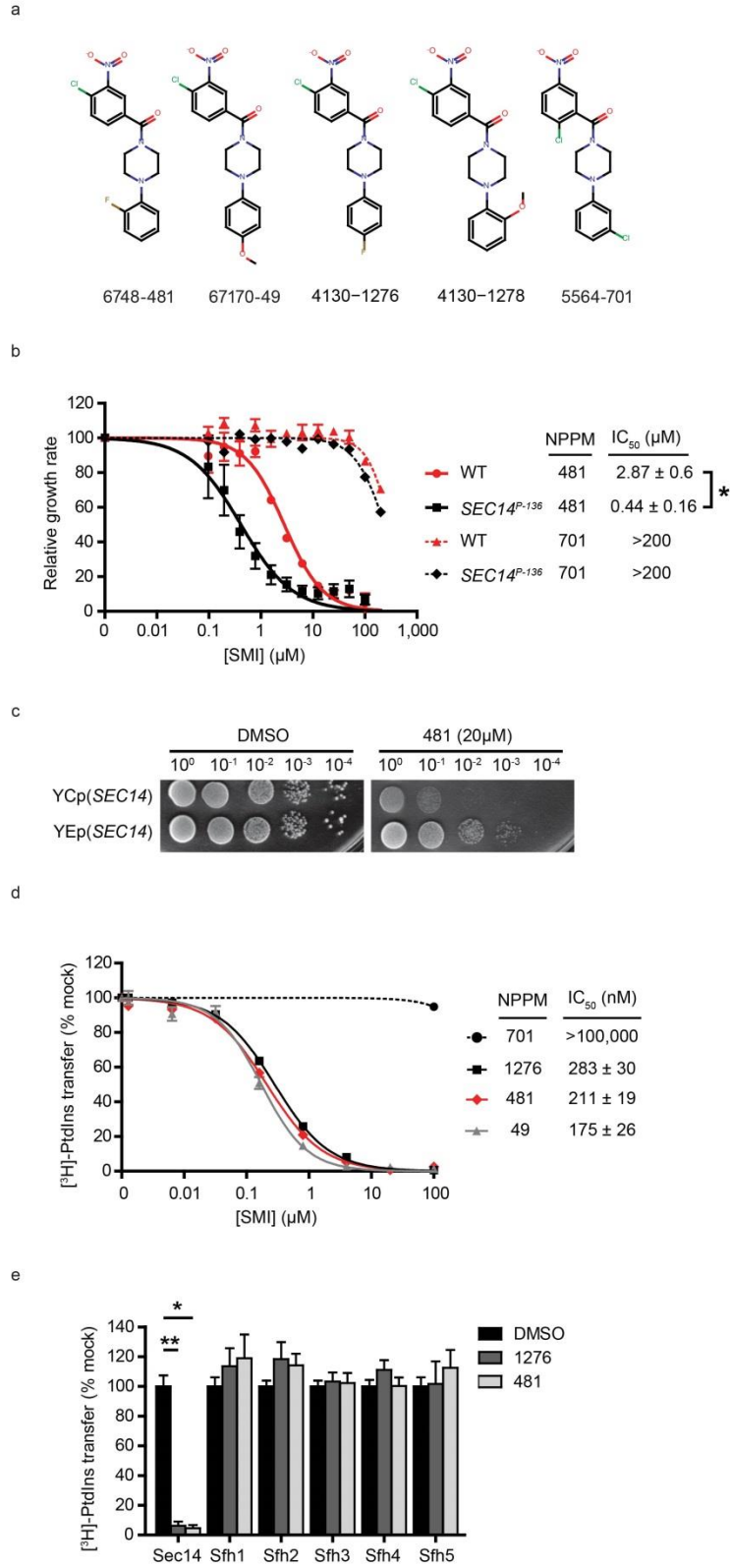


Figure 11. NPPMs specifically inactivate Sec14.

(a) Chemical structures of 6748-481, 67170-49, 4130-1276, 4130-1278 and 5564-701 are shown. (b) Growth inhibition of the wild-type (WT) control strain (CTY182; red) and *SEC14*^{P-136} (CTY374; black) strains by 6748-481 (●,■) or 5564-701 (▲,◆) was measured. Relative growth compares growth rate in presence of compound relative to the “no-drug” control (DMSO; see Methods). Data are plotted as a function of NPPM concentration (x-axis). Doubling times were measured at λ_{610nm} and values show the mean \pm s.e.m of normalized doubling times for each drug concentration from 3 independent experiments. IC₅₀s represent the 95% confidence interval from three independent experiments (P* < 0.0001; extra sum-of-squares F-test). (c) Yeast ectopically expressing either physiological levels of Sec14 [YCp(*SEC14*)], or elevated levels of Sec14 [YEp(*SEC14*)], were spotted in 10-fold dilution series onto YPD agar supplemented either with DMSO or with 6748-481 (20 μ M), as indicated, and incubated at 30°C for 48h. (d) Sec14-catalyzed transfer of [³H]-PtdIns was monitored *in vitro* using purified recombinant Sec14 in the presence of 5564-701, 4130-1276, 6748-481 or 67170-49. Relative [³H]-PtdIns transfer is a comparison of activity in presence of NPPM relative to the vehicle control (DMSO; see Methods) in assays where Sec14 protein concentration was clamped at 287nM. Values indicate the mean \pm s.e.m of triplicate determinations from 3 independent experiments. IC₅₀ values fall into the 95% confidence interval. [³H]-PtdIns input ranged from 12790-16800 cpm per assay, with background ranging from 478-751 cpm. Transfer efficiency (% of total input) ranged from 24-32%. (e) Purified recombinant Sfh proteins (10 μ g) were assayed for [³H]-PtdIns transfer in the presence and absence of indicated NPPM (40 μ M). Values are the mean \pm s.d of triplicate determinations from 3 independent experiments. P* = 1.8202E⁻¹¹ and P** = 4.31133E⁻¹² relative to mock DMSO control (two-tailed t-test with heteroscedastic variance, Microsoft Excel 2010). [³H]-PtdIns input ranged from 14441-15101 cpm per assay, with background ranging from 640-657 cpm. Transfer efficiency (% of total input) varied as a function of protein assayed: Sec14 (24-32%), Sfh1 (10-14%), Sfh2 (8-11%), Sfh3 (11-14%), Sfh4 (7-12%) and Sfh5 (3-4%).

NPPMs directly and selectively inhibit Sec14 *in vitro*

To establish whether bioactive NPPMs target Sec14 directly, the sensitivities of Sec14 activity to NPPM challenge were measured in a purified system. As Sec14 is not an enzyme, its activity is operationally defined by the energy-independent exchange of PtdIns and PtdCho monomers between liposomal membranes *in vitro* (Schaaf, Ortlund et al. 2008). In titrations where purified Sec14 was clamped at 287nM (see Methods), NPPMs 67170-49,

6748-481 and 4130-1276 displayed potent and dose-dependent inhibitions of Sec14-mediated [³H]-PtdIns transfer. The IC₅₀s ranged from 175-283nM (**Figure 11d**). At these concentrations, the Sec14:NPPM molar stoichiometries were ca. 1:1.

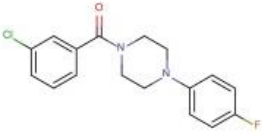
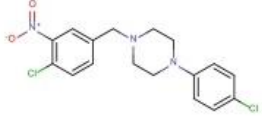
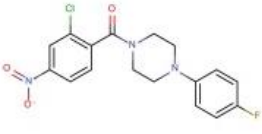
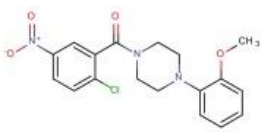
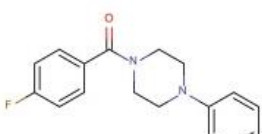
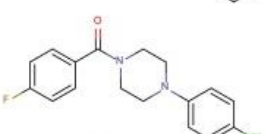
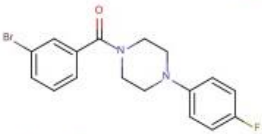
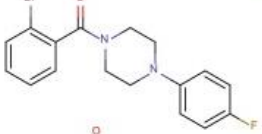
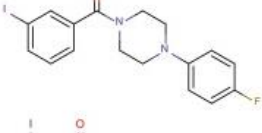
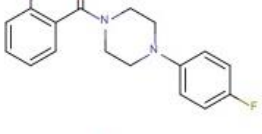
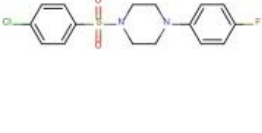
Two experiments excluded trivial possibilities that NPPMs interfere with Sec14 lipid exchange activities via non-specific membrane-active effects. First, a number of closely related, yet biologically inactive, NPPMs (*e.g.* 5564-701) failed to diminish Sec14-mediated PtdIns-transfer--even at concentrations 500-fold above the IC₅₀s measured for the active NPPMs (**Figure 11d; Figure 12**). Second, the NPPM sensitivities for [³H]-PtdIns transfer were assayed for each of the other five yeast Sec14-like PITPs (Sfh1-Sfh5; Li, Routt et al. 2000). Neither of the two Sec14-active NPPMs tested (6748-481 and 4130-1276) interfered with Sfh protein-dependent [³H]-PtdIns transfer activities at concentrations some 200-fold greater than the corresponding IC₅₀s measured for Sec14 (40μM SMI; **Figure 11e**). The indifference of Sfh proteins to NPPM challenge *in vitro* demonstrates a clear selectivity of these molecules for Sec14 as Sfh proteins share 23%-64% primary sequence identity and 43%-89% primary sequence similarity with Sec14. While this point is further examined below, the fact that Sfh1-mediated transfer activities were not inhibited by NPPMs deserves emphasis. These data underscore the exquisite selectivity of the NPPMs for Sec14 as the functionally enigmatic Sfh1 is the closest known homolog to Sec14 (64% primary sequence identity) (Schaaf, Dynowski et al. 2011).

NPPM structure activity relationships

Forty-six NPPM-like molecules were evaluated for structure-activity relationships (SAR) for Sec14 inhibition *in vitro* and *in vivo*. The cumulative SAR data assigned the relative importance of each NPPM functional group to activity as Sec14 inhibitor ($IC_{50} < 10 \mu M$ *in vitro* activity threshold). Those results are summarized in **Figure 13a** and in **Figures 10** and **12**. SAR reported an obligatory requirement for *ortho*-Cl in the Cl-nitrophenyl (*i.e.* activated aryl halide) moiety of NPPMs (**Figures 10, 12 and 13b**). Either removal of the Cl- group (compare 4130-1276 to 5355-152 [**6**]), or shift of the Cl- to the *para* position (compare 4130-1276 to 5658-722 [**7**]), increased the IC_{50} for Sec14 inhibition by >500-fold (**Figure 13b,d**). The linker ketone that connects the Cl-nitrophenyl and piperazinyl groups was also important. Modification of this group reduced NPPM potency *in vitro* by 30-fold (compare 6748-481 and 5263-433 [**8**]). The NO_2 -group contributed to NPPM potency as its removal resulted in an approximately 10-fold increase in the IC_{50} for Sec14 PtdIns-transfer activity (compare 6748-481 and 5357-399 [**9**]; **Figure 13d**).

With regard to the apolar end of the NPPM, addition of hydrophobic functional groups to the fluorobenzene tail enhanced potency by approximately 4-fold (compare 5348-909 [**10**] with 6748-481, 4130-1276, 67170-49, 7276-196 [**11**] and 6828-980 [**12**]; **Figure 10 and Figure 12**). Extending the linker that bridges the piperazinyl and fluorobenzene groups by only a single carbon also reduced NPPM potency (5348-909 *vs.* 5356-684 [**13**]; **Figure 12**).

No.	Accession #		[³ H]-PtdIns Transfer IC ₅₀ (μM)
13	5356-684		>20*
14	BBV34896-755		36.8 ± 5
15	BBV34846-244		0.0997 ± 0.0056
16	Z1082669-326		0.174 ± 0.0174
17	BBV34846-247		0.173 ± 0.035
18	5348-723		11.06 ± 1.13
19	5356-628		>100*
20	5356-350		22 ± 3.1
21	5567-782		56.5 ± 6.6
22	5353-036		0.768 ± 0.071
23	7329-906		0.589 ± 0.051
24	5355-139		>100*

No.	Accession #		[³ H]-PtdIns Transfer IC ₅₀ (μM)
25	5528-054		~100*
37	5261-847		31.04 ± 10.35
38	5344-323		>100*
39	5651-199 2573-0382		>100*
40	5570-428		~100*
41	6113-178		>20.0*
42	5656-333		>100*
43	5353-383		>100*
44	6031-920		>100*
45	5653-520		>100*
46	5347-864		>100*

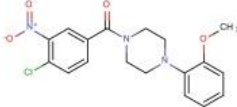
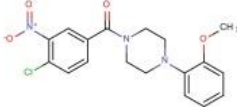
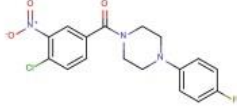
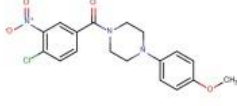
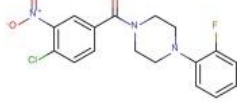
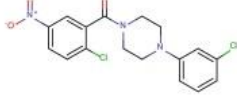
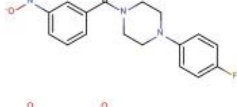
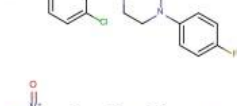
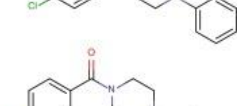
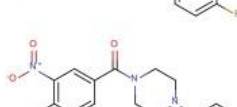
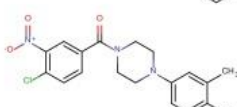
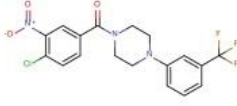
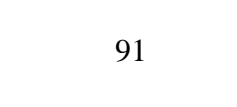
No.	Accession #		[³ H]-PtdIns Transfer IC ₅₀ (μM)
1	5276-937 4130-1278		1.07 ± 0.125
2	4130-1276		0.283 ± 0.030
3	67170-49		0.175 ± 0.026
4	6748-481		0.211 ± 0.019
5	5564-701		>100 ^a
6	5355-152		>100 ^a
7	5658-722		>100 ^a
8	5263-433		5.68 ± 0.50
9	5357-399		2.55 ± 0.230
10	5348-909		0.877 ± 0.095
11	7276-196		0.186 ± 0.025
12	6828-980		0.386 ± 0.048

Figure 12. *In vitro* SAR analyses.

(a) Sec14-catalyzed [³H]-PtdIns transfer was monitored *in vitro* using purified recombinant Sec14 in the presence of the indicated SMI. Relative [³H]-PtdIns transfer compares Sec14 activity in presence of NPPM relative to the vehicle control (DMSO; see Methods) in assays where Sec14 concentration was clamped at 287nM. IC₅₀s are represented as the mean ± the 95% confidence interval of three independent experiments performed in triplicate. IC₅₀s highlighted by (a) represent single concentration measurements where the IC₅₀s exceeded the indicated value.

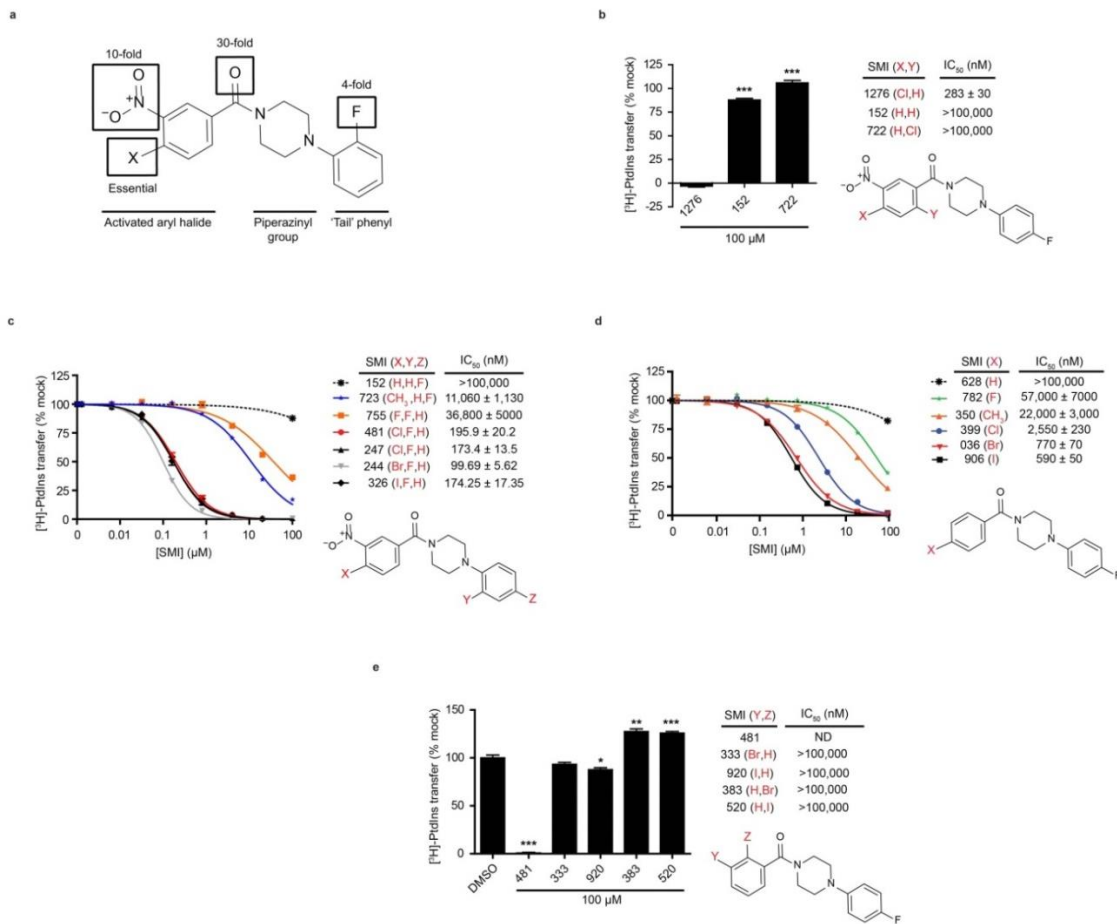


Figure 13. NPPM SAR relationships.

(a) A summary of the contributions of each highlighted functional group of NPPM 6748-481 to potency as Sec14 inhibitor is depicted. Data represent a compilation, and superimposition onto the 6748-481 scaffold, of IC₅₀ measurements for Sec14-catalyzed [³H]-PtdIns transfer activity for each SMI listed in Figure 12. (b-f) Chemical-induced inhibition of Sec14-catalyzed [³H]-PtdIns transfer activity was monitored in the presence of the indicated SMI. Chemical identities for functional groups X,Y and Z are identified for each SMI tested, and are highlighted in red. Relative [³H]-PtdIns transfer compares activity in presence of compound relative to the “no-drug” control (DMSO) in assays where Sec14 concentration was clamped at 287nM. [³H]-PtdIns input ranged from 7,542-13,002 cpm per assay, with background ranging from 282-1,317 cpm and transfer efficiency (% of total input) ranged from 11% to 32%. Values indicate the mean ± s.e.m of triplicate determinations from three independent experiments. IC₅₀ values represent the 95% confidence interval or for single concentration points a predicted IC₅₀. Statistical comparisons of values used the “unpaired two-tailed t-test” where P***<0.0001, P**=0.0024 and P*=0.0089.

Sec14 inhibition and chemical nature of the NPPM halide

The obligate requirement for *ortho*-Cl on the activated aryl halide of Sec14-active NPPM raised the question of whether chemical nature of the halide influences NPPM potency. A variable aryl halide series, represented by compounds BBV34896-755 (**14**), BBV34846-244 (**15**) and Z1082669-326 (**16**), was assembled, and 6748-481 was resynthesized for inclusion in the series (BBV34846-247 [**17**]). Comparisons of the NPPM potencies for inhibition of Sec14 PtdIns-transfer activity demonstrated the Cl-, Br- and I- derivatives (4130-1276 and 6748-481; BBV34846-244; Z1082669-326, respectively) exhibited potencies superior to those of the H-, CH₃- or F-derivatives (5355-152, 5348-723 [**18**], BBV34896-755, respectively). In rank order: Br-NPPM > I-NPPM ≥ Cl-NPPM (6748-481; BBV34846-247) >> F-NPPM, CH₃-NPPM, H-NPPM (**Figures 12 and 13c**). Consistent with the *in vitro* data, the -Cl, -Br and -I versions were potent growth inhibitors, whereas the -H, -CH₃ and -F derivatives were not (**Figure 10**).

Six 'NO₂-less' derivatives differing in halide chemistry and/or position, were similarly evaluated (5356-628 [**19**], 5356-350 [**20**], 5567-782 [**21**], 5357-399, 5353-036 [**22**], 7329-906 [**23**], 5355-139 [**24**], 5528-054 [**25**]; **Figures 10, 12 and 13d**). The relative potencies of these compounds as Sec14 inhibitors were also directly proportional to the atomic mass and lipophilicities of the *ortho*-halide, and inversely proportional to halide electronegativity: I-NPPM > Br-NPPM > Cl-NPPM >> CH₃-NPPM > F-NPPM > H-NPPM (**Figures 12 and 13d**). The requirement for a properly positioned halide for SMI activity was similarly conserved (**Figures 12 and 13e**). Results from parallel *in vivo* experiments recapitulated the *in vitro* data. The IC₅₀s for the -Cl, -Br and -I compounds for wild-type

yeast were $28 \pm 5\mu\text{M}$, $7.7 \pm 1.5\mu\text{M}$ and $5.2 \pm 1\mu\text{M}$, respectively, whereas the -H, -CH₃ and -F derivatives were inactive ($\text{IC}_{50\text{s}} > 200\mu\text{M}$; **Figure 10**).

NPPM docking pose within the Sec14 phospholipid-binding pocket

NPPMs are amphipathic molecules that efficiently partition into apolar environments ($C_{\log\text{P}} \sim 3.0$). The chemical properties of Sec14-active NPPMs, when coupled with the fact that the compounds inhibit both Sec14 PtdIns- and PtdCho-transfer activities, suggested the NPPMs load into the hydrophobic pocket during phospholipid exchange. To gain more precise insights into how Sec14 binds NPPMs, a virtual binding surface ($\sim 1400\text{\AA}^2$) was modeled (see Methods). This surface formed a boundary for unconstrained docking routines using 6748-481 as query NPPM (**Figure 14**; see Methods). Multiple independent simulations, using different docking platforms, produced a solution set of >3000 potential binding poses that reduced themselves into 6 representative modes. These modes shared certain features with regard to Sec14 interactions with 6748-481, but these exhibited unique features as well (**Figure 15a-f** and **Figure 16a,b**).

Two pose classes (modes 1,2 and modes 3,4) represented mirror images of each other where orientations of bound 6748-481 were rotated 180° around the long axis of the NPPM. Another pose class (modes 5,6) shifted the 6748-481 binding site further down the hydrophobic pocket (**Figure 15a-f**). The 6 representative modes were mapped for Sec14::NPPM interactions, and the fingerprints highlight how modes 5,6 slide the 6748-481 binding site down the Sec14 pocket relative to modes 1,2 and 3,4 (**Figure 15g**). Moreover, the interaction fingerprints highlighted how mode 5,6 poses pressed NPPM polar groups into

hydrophobic environments. This unappealing feature, when coupled with lack of experimental support for these poses (see below), led us to reject mode 5,6 poses from further consideration.

A feature common to modes 1,2 and 3,4 is intercalation (in flipped orientation) of the 6748-481 fluorobenzene tail into the narrow hydrophobic cleft lined by Sec14 residues L₂₃₂, F₂₂₈, F₂₂₅, I₂₄₀, F₂₂₁, L₁₇₉, I₂₁₄, and M₁₇₇ (**Figure 15a-g and Figure 16a**). The fluoro-benzyl moiety wedges between the side chains of F₂₂₈ on one side and F₂₁₂ and M₁₇₇ on the other -- thereby consolidating a network of hydrophobic and π - π stacking interactions. A second common feature is inter-digitation of the 6748-481 chloro-nitrophenyl group in a hydrophilic subdomain of the Sec14 pocket where it is set within H-bonding distance (1.5-3.5Å) to residues framing the Sec14 PtdCho headgroup-coordinating substructure (S₁₇₃, Y₁₁₁, Y₁₂₂, Y₁₅₁; **Figure 15g**). All modes predict NPPM-binding is sterically incompatible with PtdIns/PtdCho-binding (**Figure 16b**).

Modes 1,2 were distinguished from modes 3,4 by the orientation of the 6748-481 ketone. Mode 1,2 poses anchored the ketone via H-bond interactions with S₂₀₁, whereas mode 3,4 poses projected ketone interactions with Y₁₅₁. Modes 1 and 2 were distinguished from each other by their mirror-image orientation of the activated aryl halide. Mode 1 poses anchored the nitro- group by interactions with residues S₁₇₃/Y₁₂₂ and the halide with Y₁₁₁/S₁₇₃. Mode 2 poses featured nitro- and halide interactions with S₁₇₃ and Y₁₁₁/Y₁₂₂, respectively. Mode 3 poses assigned interactions of the nitro- and halide groups with residues S₁₇₃ and Y₁₁₁, respectively, whereas mode 4 poses projected that both the nitro- and halide groups engage residues S₁₇₃/Y₁₁₁. In total, the solution sets predict a number of interactions between the Sec14 residues S₁₇₃, Y₁₁₁, Y₁₂₂, Y₁₅₁ with the activated aryl halide of the NPPM

(albeit in flipped orientations), and anchor the NPPM's ketone group to S₂₀₁ or Y₁₅₁.

Together these solution sets provide several models that can be distinguished through the introduction of rational mutations into Sec14 to monitor for the disruption of NPPM::Sec14 interaction pairs.

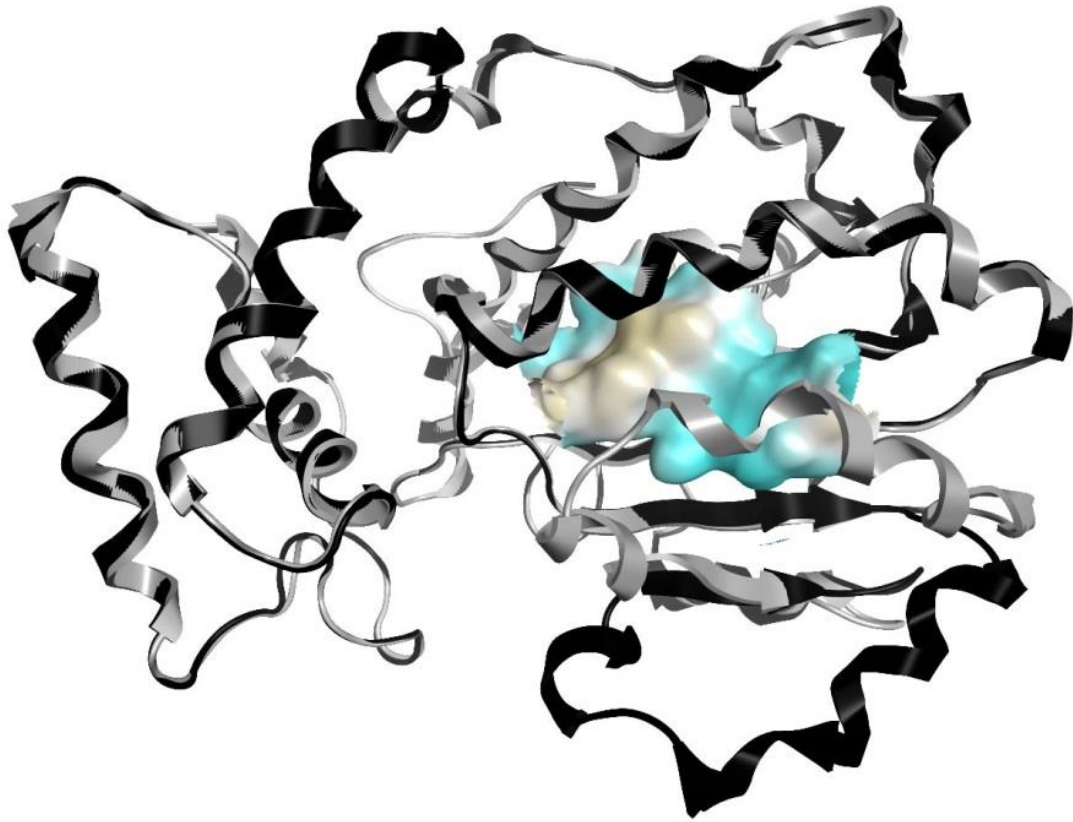


Figure 14 Homology model of a closed Sec14 conformer.

The Sec14 primary sequence was threaded onto a holo-Sfh1 structure (pdb 3B7N) and a virtual cavity surface was defined (see Methods). The open Sec14 structure (black) and the closed Sec14 model (gray) are shown. The virtual surface is rendered using a hydrophobicity scale ranging from blue (hydrophobic) to tan (hydrophilic).

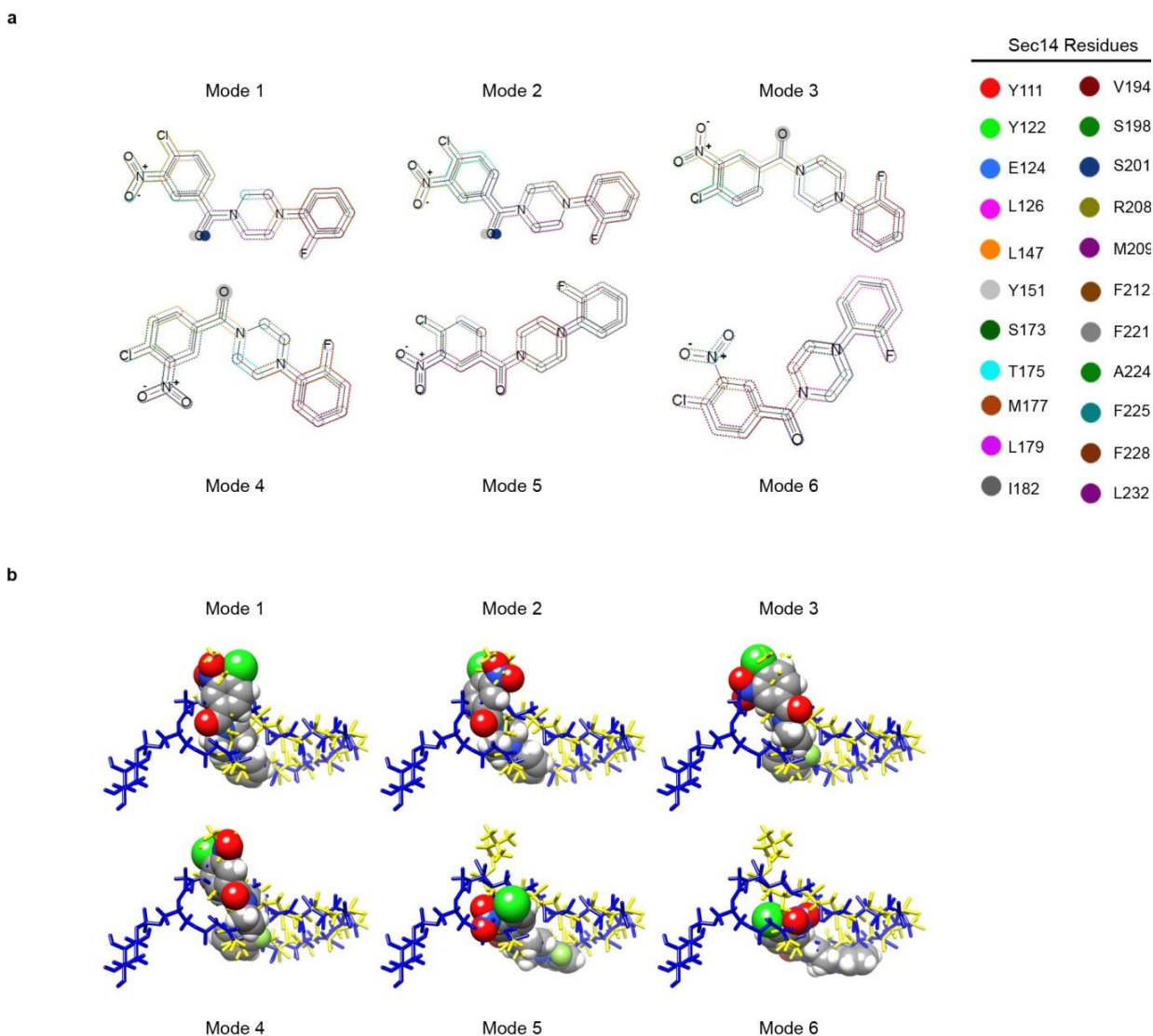


Figure 16 Interaction fingerprints of representative 6748-481 docking poses. (a) Composites of 6748-481 binding modes 1-6 produced from GOLD and Glide docking simulations are shown (see Figure 3), and Sec14 interactions are depicted on the 6748-481 structure using MOE (see Methods). The interaction territories of the indicated Sec14 residues with the NPPM are color coded. (b) 2-Dimensional diagrammatic representations of binding modes 1-6 (ball diagrams, as indicated) are shown relative to PtdIns (blue) and PtdCho (yellow) binding space within the Sec14 cavity. Phospholipids are rendered in stick diagram. NPPMs are color-coded according to element; carbon (grey), oxygen (red), nitrogen (blue), hydrogen (white), and halide (green).

NPPM-resistant Sec14 proteins

The various NPPM binding models make distinguishing experimental predictions which guided design of Sec14 missense substitutions predicted to diminish NPPM binding without affecting PtdIns/PtdCho exchange activity or biological function. The mutant Sec14 proteins were subsequently purified and assayed for PtdIns transfer activity. Residue S₁₇₃ was of particular interest as it was consistently identified as the highest scoring NPPM-interacting residue in docking simulations. Indeed, the S₁₇₃C missense substitution rendered Sec14 completely resistant to inhibition by NPPM 6748-481 *in vitro* (**Figure 17a-c**). Sec14^{S173C} PtdIns-transfer activity was indifferent to 6748-481 challenge even at concentrations approaching the solubility limit of the NPPM (>736-fold more resistant than Sec14). Because the S→C missense substitution is chemically subtle, these data provide strong evidence for a critical interaction between S₁₇₃ and 6748-481 (**Figure 17a-c**). The resistance properties of Sec14^{S173C} translated to the other Sec14-active NPPMs (**Figure 18a**). Reductions in 6748-481 sensitivity were also scored for Sec14^{S201C}, Sec14^{Y111A} and Sec14^{Y151A}. The PtdIns-transfer activities of these proteins were 22-, 337- and 140-fold less sensitive to 6748-481 inhibition, respectively, whereas Sec14^{Y111F}, Sec14^{Y122A}, Sec14^{M177C} and Sec14^{Y122F} showed only 3- to 5-fold reductions in the same (**Figure 17a-c**). Sec14^{Y151F} presented an interesting case as the mutant protein displayed modestly enhanced sensitivity to 6748-481 *in vitro* (**Figure 17a-c**).

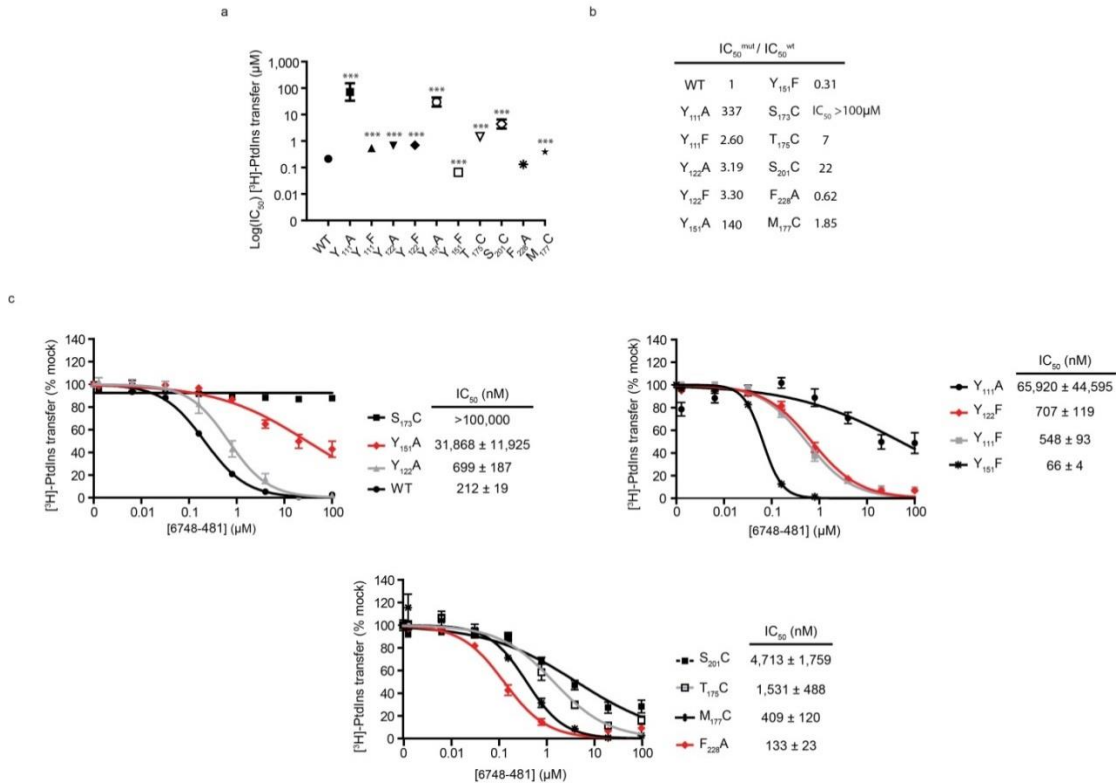


Figure 17. Sec14 mutants resistant to NPPM inhibition.

Sec14-catalyzed transfer of [³H]-PtdIns was measured using purified recombinant Sec14 proteins (287nM) in the presence of 6748-481. (a) Relative [³H]-PtdIns transfer compares activities in presence of 6748-481 relative to the “no-drug” control (DMSO; see Methods). Input ranged from 9,227-16985 cpm per assay, with background ranging from 160-724 cpm. Transfer efficiencies were as follows: Sec14 (24-32%), Sec14^{Y111A} (5-13%), Sec14^{Y111F} (38-41%), Sec14^{Y122A} (13-15%), Sec14^{Y122F} (18-27%), Sec14^{Y151A} (31-40%), Sec14^{Y151F} (31-40%), Sec14^{S173C} (22-24%), Sec14^{T175C} (5-16%), Sec14^{S201C} (6-11%), Sec14^{M177C} (8-10%) and Sec14^{F228A} (18-27%). (b) NPPM-resistance of each of the indicated Sec14 missense mutants relative to Sec14 is listed. (c) NPPM inhibition curves are shown for the indicated Sec14 derivatives. Values indicate the mean ± s.e.m of triplicate determinations from at least three independent experiments. IC₅₀ values represent the 95% confidence interval. Statistical comparisons of WT to mutant IC₅₀ values used the “extra sum-of-squares F-test” where P***<0.0001.

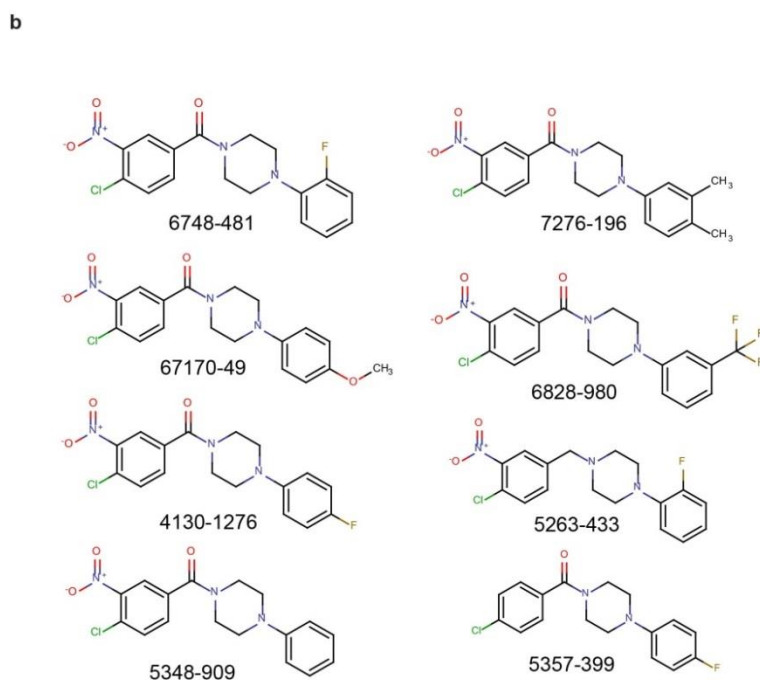
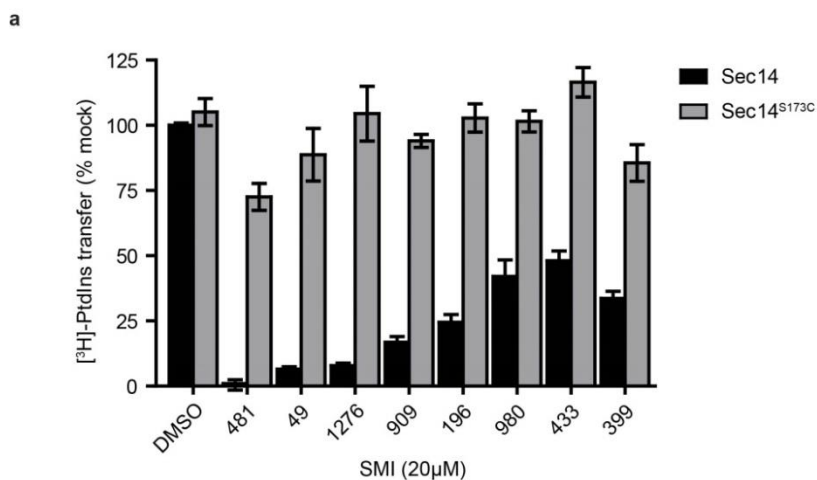


Figure 18. Sec14^{S173C} is resistant to inhibition by NPPMs.

(a) [³H]-PtdIns transfer assays using Sec14^{S173C} or Sec14 (287nM) were run in the presence of 20μM of the indicated SMI. Input [³H]-PtdIns ranged from 9110-13928 cpm per assay, with protein-independent background transfer ranging from 422-681 cpm. Transfer efficiencies were as follows: Sec14 (24-32%), Sec14^{S173C} (22-24%) and Sec14^{T175C} (5-16%). Values represent the mean ± s.e.m of triplicate determinations from three independent experiments. (b) Molecular structures of SMIs used are shown.

NPPMs and *sec14-1^{ts}* at non-permissive temperature induce a G2 cell-cycle arrest

Although *sec14-1^{ts}* has been extensively studied, quantitative measurements of potential cell-cycle disruptions have, to our knowledge, to our knowledge has never been measured. To determine if *sec14-1^{ts}* (CTY1-1A) at non-permissive temperature (37°C) or active-NPPM induce cell cycle arrest, CTY1-1A was incubated at 37°C for three hours or in the presence of the active compounds NPPM 481, NPPM 49 or the inactive-NPPM 701 for three hours at 30°C (**Figure 19**). Inactivation of Sec14 resulted in an accumulation of G2 arrested cells in the active drugs and at 37°C but not in the inactive drug or DMSO at 30°C (**Figure 19**).

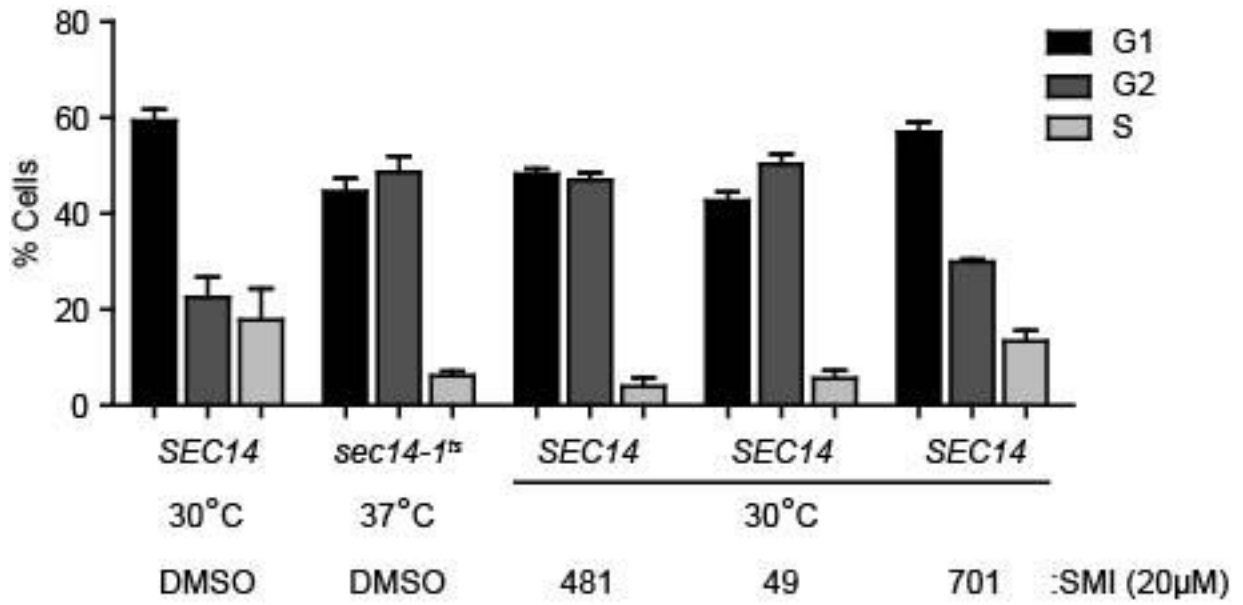


Figure 19. Active-NPPMs phenocopy *sec14-1^{ts}* cell cycle arrest

Wild type (CTY182) or *sec14-1^{ts}* (CTY1-1A) yeast were grown at 30°C in 2% glucose containing YPD media overnight to mid logarithmic phase ($\lambda_{600}=0.5$). The indicated strains were treated as indicated for three hours. Cells were fixed and treated with propidium iodide and their DNA quantity was assayed by FACS (see methods). Values indicate the % of cells in their respective growth phase from three independent experiments.

Sec14 is the sole essential NPPM target in cells

Two lines of evidence demonstrated that Sec14 represents the sole essential NPPM target in cells. First, yeast expressing Sec14^{S173C} were resistant to challenge with 6748-481 (**Figure 20a**). Additionally, the expression of several mutations at S173 and T175 were also resistant to 6748-481 (**Figure 20b**). The second came from exploitation of ‘bypass Sec14’ mutants that no longer require Sec14 for viability. Genetic inactivation of the CDP-choline pathway for PtdCho biosynthesis (*cki1Δ*), or of the oxysterol binding protein homolog Kes1 (*kes1Δ*), effects ‘bypass Sec14’ (Cleves, McGee et al. 1991; Cleves, McGee et al. 1991; Fang, Kearns et al. 1996; Li, Rivas et al. 2002). Both *cki1Δ* and *kes1Δ* cells were indifferent to 6748-481, 67170-49 or 4130-1276 (**Figure 20c,d**).

a

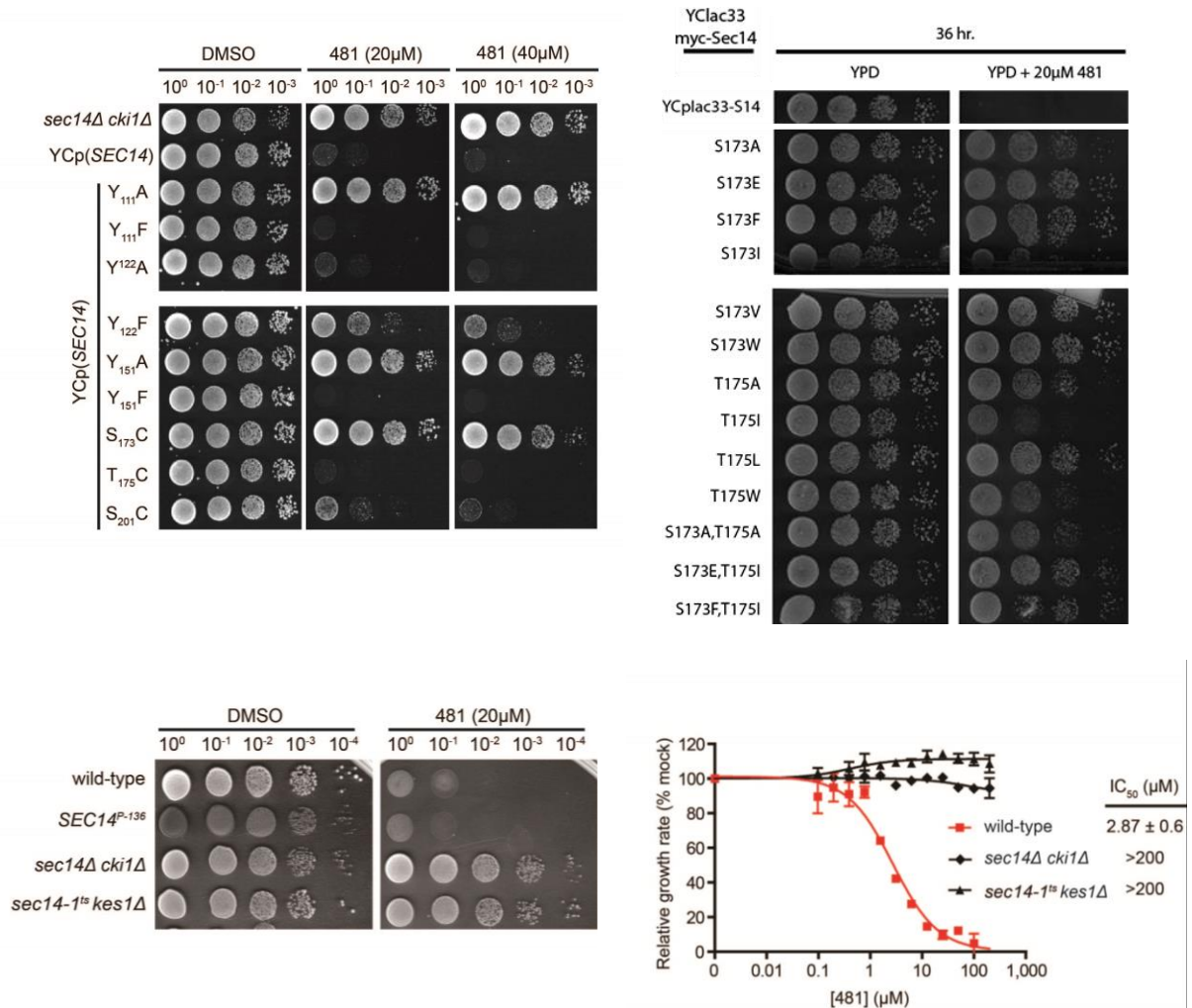


Figure 20. Sec14 is the sole essential cellular target of bioactive NPPMs.

(a) Expression of NPPM-resistant Sec14 derivatives renders cells insensitive to NPPM-mediated growth arrest. Yeast expressing physiological levels of Sec14 [YCp(*SEC14*); top row], or the indicated Sec14 variant, as the sole source of Sec14 in the cell, were diluted in a 10-fold series onto YPD agar containing DMSO, 20μM or 40μM 6748-481, as indicated. Plates were incubated at 30°C for 48h. (b) Experiment was conducted as in (a) with the addition of multiple S173 and T175 mutants. (c) ‘Bypass Sec14’ mutants are NPPM-resistant. Congenic WT (CTY182), *SEC14^{P-136}* (CTY374), and the *sec14Δ cki1Δ* (CTY303) and *sec14-1^{ts} kes1Δ* (CTY159) ‘bypass Sec14’ mutants, were analyzed as in (a). (d) Chemical-induced growth inhibition of the indicated strain by 6748-481 was measured in a dose-response regime. Relative growth (y-axis) compares growth rate in presence of NPPM to that of the vehicle control (DMSO; see Methods). Data are plotted as a function of NPPM concentration (x-axis). Values indicate the mean ± s.e.m from 3 independent experiments. IC₅₀ values represent the 95% confidence interval.

NPPMs induce phospholipase D activity in vegetative yeast

Phospholipase D (PLD) consumes H₂O and PtdCho in *trans*-phosphatidylation reactions that produce choline and phosphatidic acid. Activation of this enzyme in yeast is typically reserved for diploid cells engaged in a developmental program of meiosis in response to nutrient stress (Honigberg, Conicella et al. 1992; Rose, Rudge et al. 1995). Curiously, Sec14-deficiencies subvert this tight developmental regulation and elicit precocious phospholipase D activation in vegetative haploid cells. Such potentiation of phospholipase D activity is not observed upon functional ablation of individual PtdIns 4-OH kinase isoforms, or of other PtdIns-4-phosphate effector functions we have tested (our unpublished data). Yet, all ‘bypass Sec14’ mechanisms require this enhanced phospholipase D activity (Sreenivas, Patton-Vogt et al. 1998; Li, Routt et al. 2000; **Figure 21a**). As phospholipase D activation is a hallmark cellular signature of Sec14 deficiencies, we tested whether NPPM-intoxication of vegetative yeast cells induced phospholipase D activity in vegetative cells in the face of a physiologically normal Sec14 load.

Enhanced phospholipase D activity was recorded upon NPPM challenge as measured by phospholipase D-dependent release of free choline from cells (**Figure 21b**). In these experiments, ‘bypass Sec14’ strain *cki1Δ* mutants were employed as the associated choline kinase deficiency renders *cki1Δ* cells incapable of recycling free choline back into PtdCho synthesis via the cytidine-diphosphate choline salvage pathway. Additionally, it allows the examination of phospholipase D activity in NPPM-resistant background. Salvage failure supports unobstructed accumulation of the choline liberated by phospholipase D action (Henry, Kohlwein et al. 2012). As phospholipase D is a PtdIns(4,5)P₂-dependent enzyme *in vitro* (Rose, Rudge et al. 1995), similar to that observed in mammals (Hammond, Altshuller

et al. 1995; Colley, Sung et al. 1997). The observation that phospholipase D activity is induced by chemical inhibition of Sec14 suggested bioactive NPPMs impose selective defects on cellular phosphoinositide signaling that mimic those observed in the genetic inactivation of Sec14 *in vivo*.

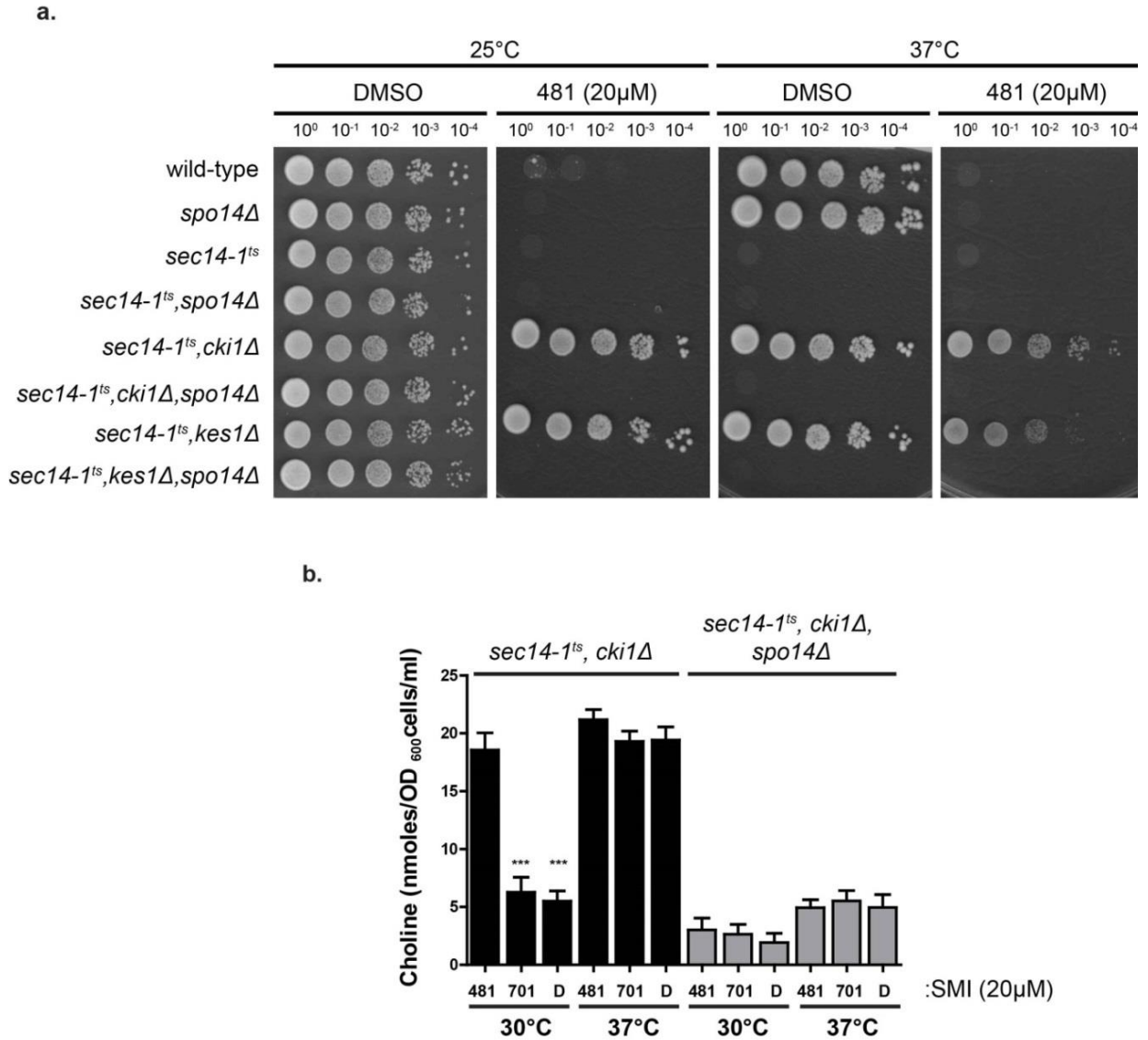


Figure 21. NPPM intoxication stimulates phospholipase D activity in vegetative yeast.

(a) Wild-type, *spo14Δ*, *sec14-1^{ts}*, or “bypass-Sec14” mutants and their corresponding *spo14Δ* yeast were spotted in 10-fold serial dilution on YPD plates \pm 20 μ M 6748-481, as indicated, and plates incubated for 48h at 25°C or 37°C. (b) *sec14-1^{ts}, cki1Δ* and *sec14-1^{ts}, cki1Δ, spo14Δ* strains were quantified for free choline release in the presence of 6748-481, 5564-701 or a “no-drug” DMSO vehicle control and incubated for 2h at 25°C or 37°C. Values represent the mean \pm s.e.m calculated from triplicate determinations from at least three independent experiments. P*** <0.0001 (two-tailed t-test, Graphpad). D=DMSO.

NPPM intoxication and genetic ablation of Sec14 activity evoke similar phenotypes

Sec14 promotes membrane trafficking through the TGN/endosomal system by coordinating PtdCho metabolism with production of PtdIns(4)phosphate (Cleves, McGee et al. 1991; Fang, Kearns et al. 1996; Mousley, Tyeryar et al. 2008). Thermal inactivation of Sec14 (*i.e.* by shift of *sec14-1^{ts}* mutants to 37°C) provoked accumulation of cargo-engorged TGN/endosomes in the cytoplasm (**Figure 22**). These morphological phenotypes were recapitulated in wild-type and *SEC14^{P-136}* cells upon challenge with NPPMs 6748-481, 67170-49 or 4130-1276. Mock challenge with DMSO, or with the inactive 5564-701 control, had no such effect (**Figure 22**). The *kes1Δ* and *cki1Δ* ‘bypass Sec14’ mutants were phenotypically unaffected when confronted with normally inhibitory concentrations of 6748-481, 67170-49, or 4130-1276 (**Figure 23**). Similarly, cells reconstituted for Sec14^{S173C} expression were phenotypically unperturbed by NPPM challenge relative to the mock challenge (**Figure 24**).

The trafficking defects induced by poisoning cells with Sec14-active NPPMs were also on display when transport and/or recycling of specific cargo through the TGN/endosomal system was analyzed. Endocytic transport of an internalized pool of the bulk membrane tracer FM4-64 to the limiting vacuole membrane (**Figure 25**), and recycling to the cell surface from TGN/endosomes of endocytosed Snc1 v-SNARE, was retarded when cells were cultured in the presence of 6748-481, 67170-49 or 4130-1276. Mock challenge with DMSO, or with the inactive 5564-701 control, had no such effect (**Figure 26**). Trafficking of secretory invertase to the cell surface was similarly impaired in the face of 6748-481, 67170-49, or 4130-1276 challenge, but not by challenge with 5564-701 or DMSO (**Figure 27**). Furthermore, the *kes1Δ* ‘bypass Sec14’ mutation fully rescued the NPPM-

induced FM4-64, GFP-Snc1, and invertase trafficking defects (**Figure 28**). When cells expressing Sec14^{S173C} were treated with Sec14-active NPPMs, invertase secretion was again observed to be substantially resistant to inhibition by these compounds (**Figure 29**).

The effects of NPPM challenge on transit of vacuolar carboxypeptidase Y (CPY) through the TGN/endosomal system were monitored by a regimen of pulse-chase radiolabeling. Impaired trafficking from ER or TGN compartments is diagnosed by enhanced accumulation of CPY precursor forms (p1 and p2, respectively (Stevens, Esmon et al. 1982). Indeed, pools of p1CPY, and particularly of p2CPY, accumulated when *sec14-1^{ts}* yeast were shifted to the restrictive temperature of 37°C, and upon treatment of WT or *SEC14^{P-136}* cells with NPPMs 6748-481, 67170-49 or 4130-1276 (**Figure 30**). Neither DMSO, nor 5564-701, impaired CPY transport from ER or TGN/endosomal compartments in wild-type or *SEC14^{P-136}* cells--as evidenced by quantitative conversion of CPY to the mature form during the course of chase (**Figure 30**). The inhibitory effects of Sec14-active NPPMs on CPY trafficking were both dose- and time-dependent (**Figure 31**), and were only poorly reversible. This property of poor reversibility was on display upon NPPM-washout conducted in the presence of cycloheximide to prevent new Sec14 synthesis. As shown in **Figure 32**, precursor CPY forms failed to chase to mCPY – even after a 2hr washout period in the presence of cycloheximide. Finally, NPPM 6748-481, 67170-49, and 4130-1276-mediated inhibition of CPY transit through the secretory pathway to the vacuole was efficiently reversed in *kes1Δ* and *cki1Δ* ‘bypass Sec14’ mutants (**Figure 33 a,b**), and in cells expressing Sec14^{S173C} as their sole Sec14 source (**Figure 33c**).

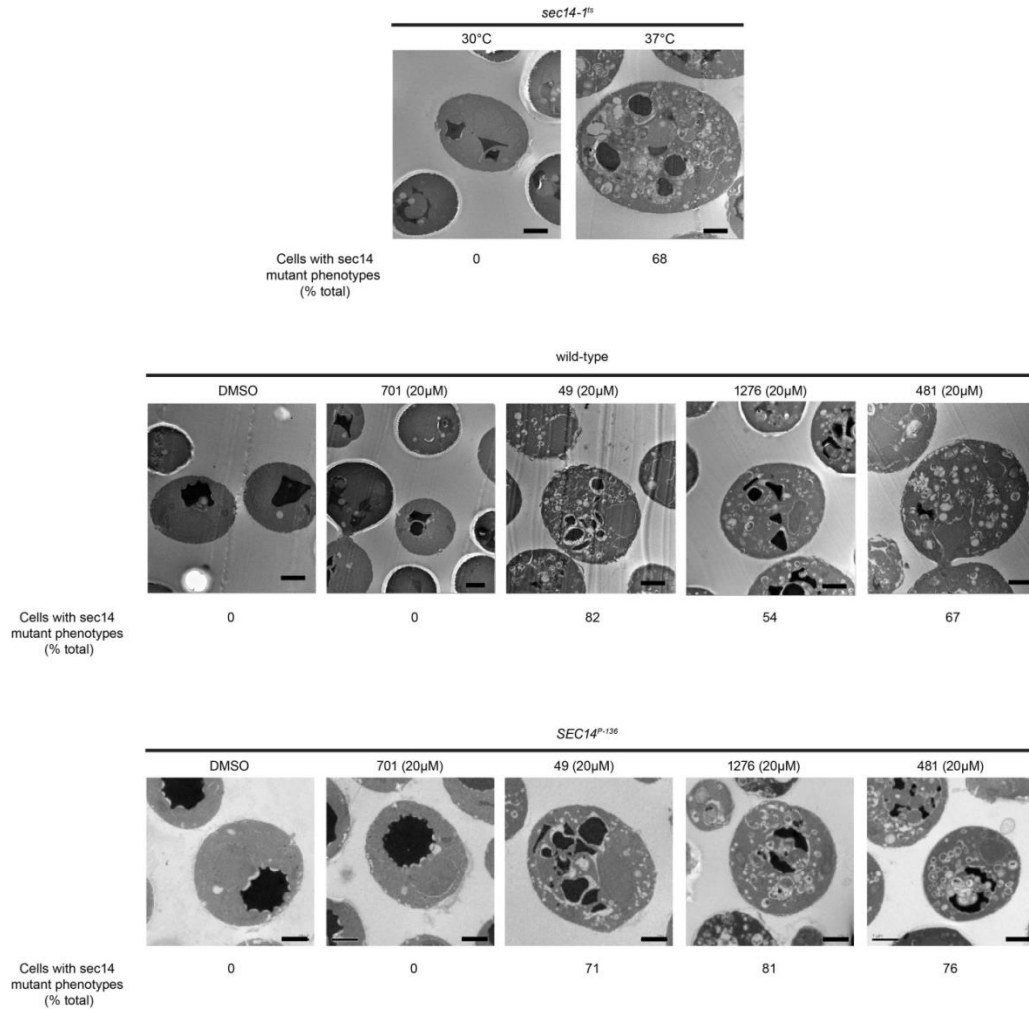


Figure 22. NPPMs induce accumulation of TGN/endosomal compartments.

WT (CTY182), *sec14-1^{ts}* (CTY1-1A), and *SEC14^{P-136}* (CTY374) yeast strains were cultured in YPD medium to mid-logarithmic phase at 30°C, then shifted to a restrictive temperature for *sec14-1^{ts}* mutants (37°C), or treated with NPPM (20μM) or DMSO for 2h, as indicated. The morphological phenotype associated with Sec14 insufficiency was assessed by thin section transmission electron microscopy, and is characterized by the accumulation, in the cytoplasm, of toroid structures that represent trafficking-defective cargo-engorged TGN/endosomal compartments. Penetrance of the membrane trafficking defects was scored for each condition and is expressed as a ratio of (# cells with *sec14*-like mutant phenotypes)/(total cells counted). Between 24 and 79 cells were evaluated for each condition.

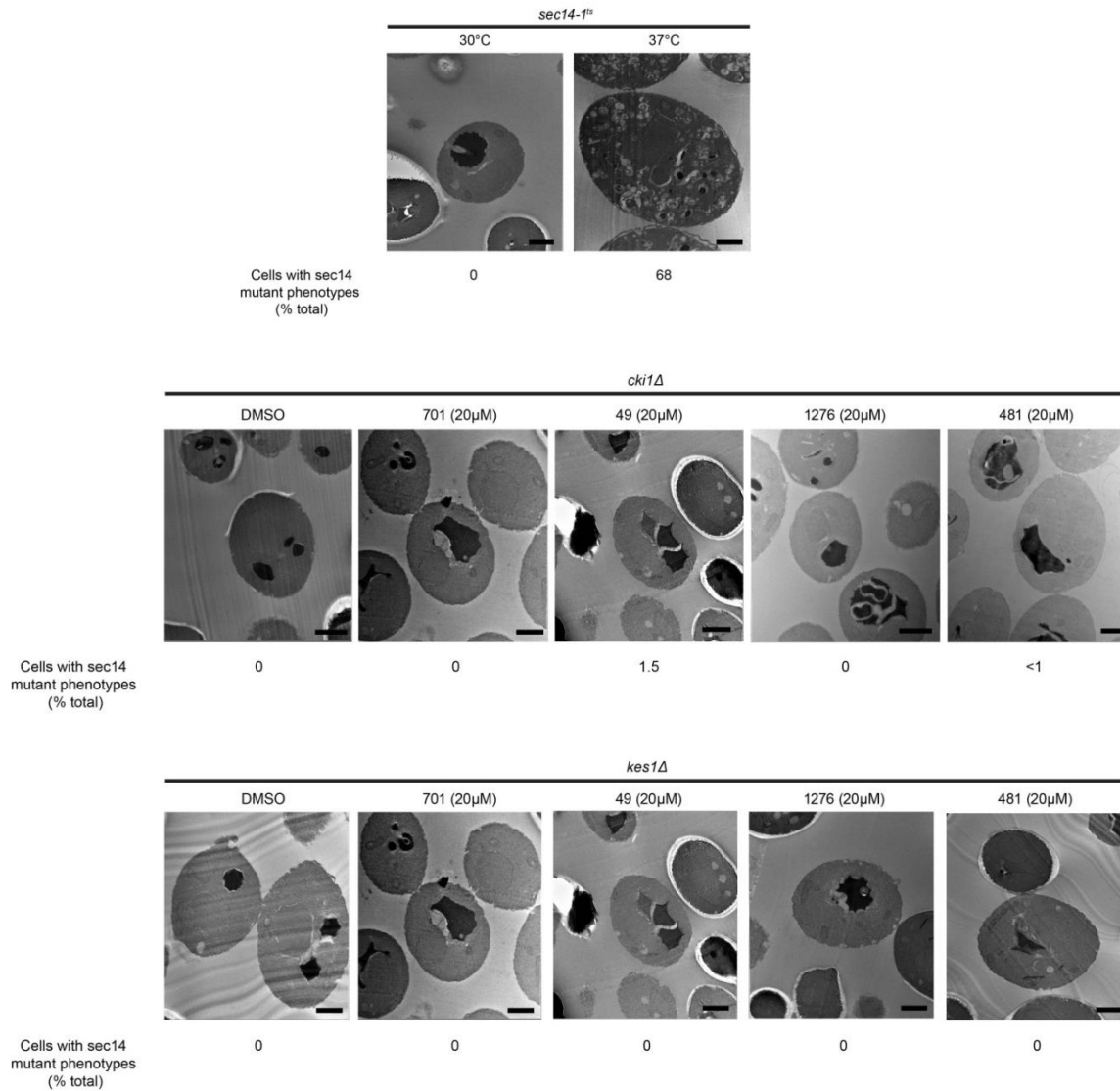


Figure 23. ‘Bypass Sec14’ are resistant to NPPM-induced accumulation of defective TGN/endosomal compartments.

Isogenic *sec14-1^{ts}* (CTY1-1A), *kes1Δ* (CTY159), and *cki1Δ* (CTY160) ‘bypass Sec14’ strains were cultured in YPD medium to mid-logarithmic phase at 30°C, then shifted to a restrictive temperature for *sec14-1^{ts}* mutants (37°C), or treated with NPPM (20μM) or DMSO for 2h, as indicated. Interpretation of the EM micrographs is detailed in the legend to **Figure 23**. Penetrance of the membrane trafficking phenotypes was scored for each experiment and is expressed as a ratio of (# cells with *sec14^{ts}*-like trafficking phenotypes)/(total cells counted). Between 26 and 123 cells were evaluated for each condition.

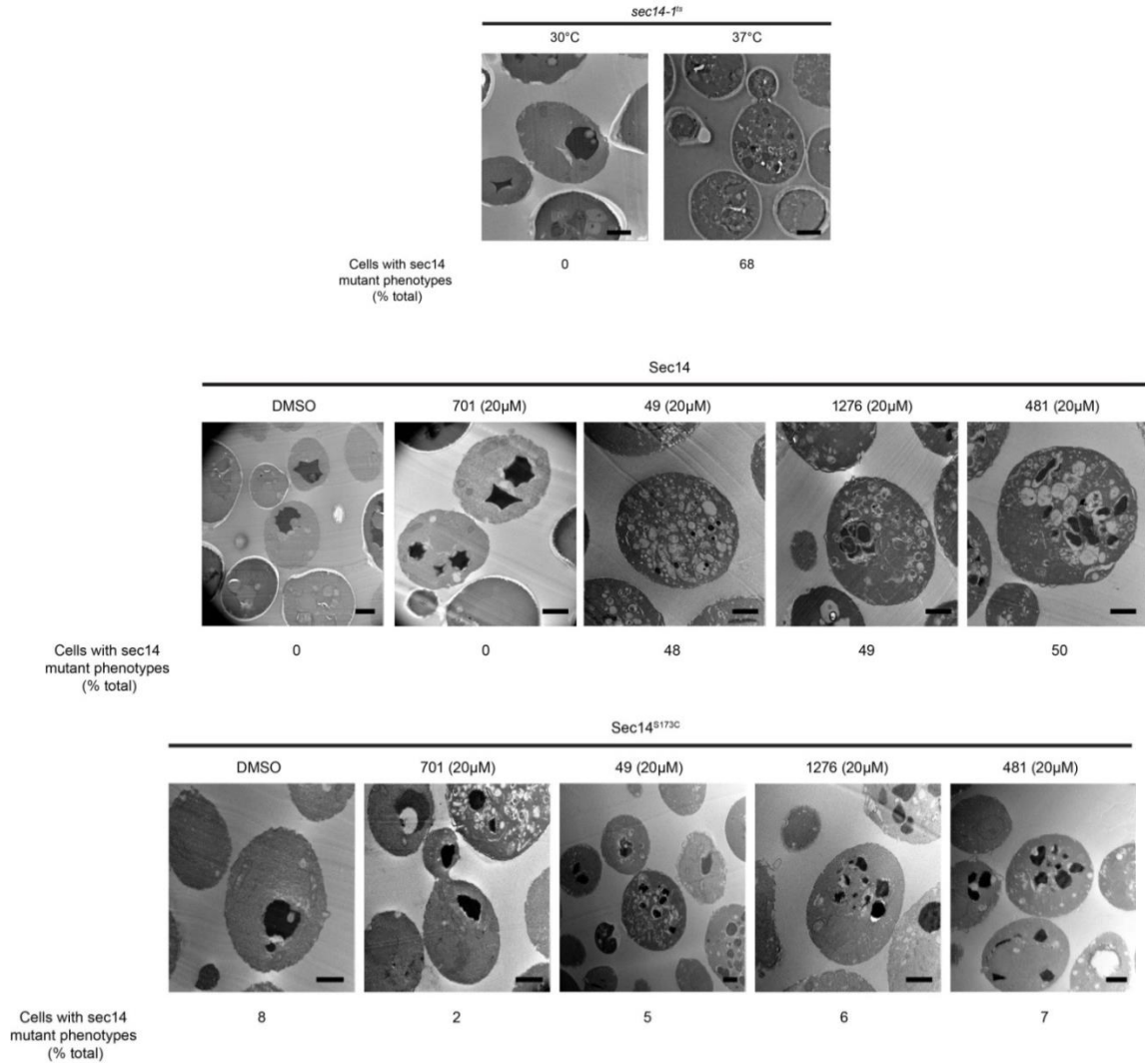


Figure 24. *SEC14*^{S173C} cells are resistant to NPPM-induced accumulation of defective TGN/endosomal compartments.

Thin-section electron microscopy. A yeast strain (CTY558) expressing either Sec14 or Sec14^{S173C}, as their sole Sec14-source, and congenic wild-type (CTY182), or *sec14-1^{ts}* strains (CTY1-1A), were cultured in YPD medium to mid-logarithmic phase at 30°C. Cultures were then shifted to 37°C, or treated with NPPM (20µM) or DMSO, for 2h, as indicated. Individual cells were scored as having WT or *sec14*-mutant-like morphologies. Incidence of cells with membrane trafficking defects for each condition is reported as a function of number of cells counted. Between 12 and 81 cells were evaluated for each condition.

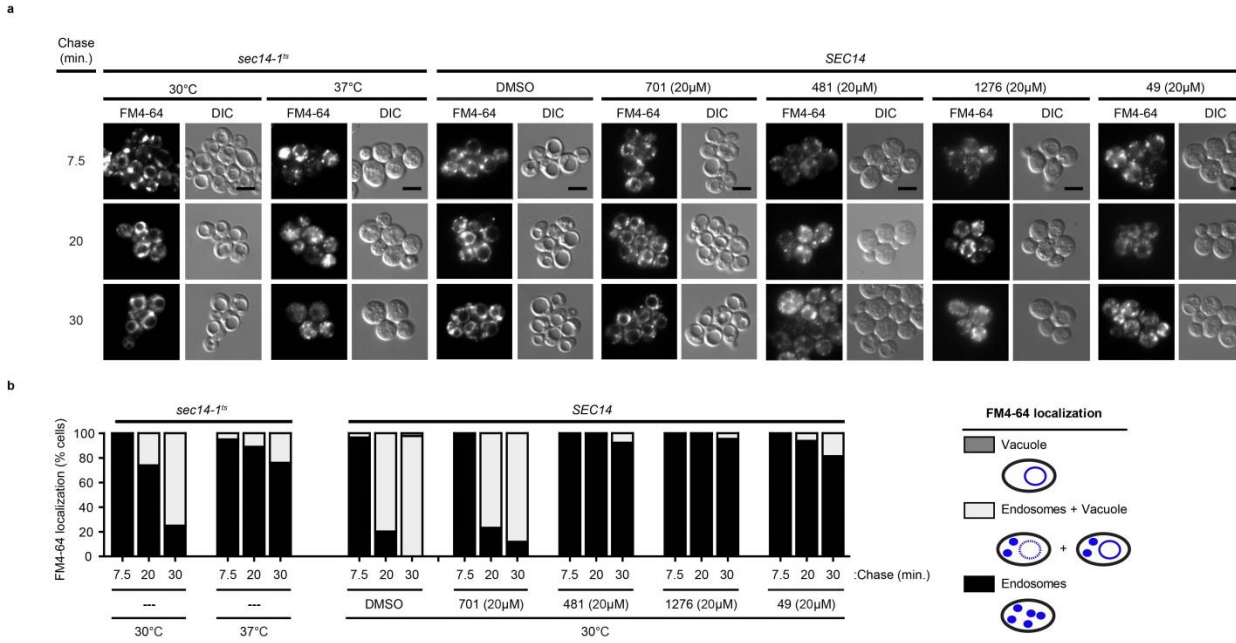
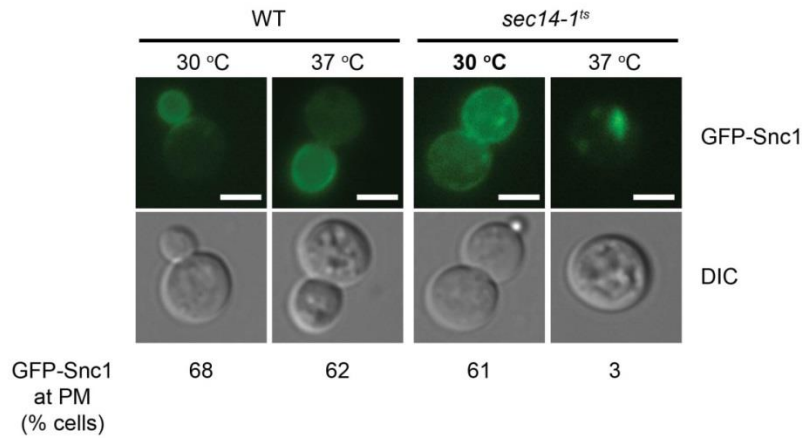


Figure 25. NPPMs induce defects in bulk endocytosis.

(a) Isogenic wild-type (CTY182) or *sec14-1^{ts}* (CTY1-1A) yeast strains were grown in YPD media to mid-logarithmic phase at 30°C with or without 3h shift to 37°C, or NPPM treatment (20µM) at 30°C, as indicated. Cells were pulsed with the endocytic tracer FM4-64 (10µM) for 20 min., washed into fresh media without dye, chased for the indicated times, then poisoned with NaN_3/NaF (1mM final, each) on ice, and their FM4-64 profiles imaged. Bar, 5µm. (b) Quantification of FM4-64 profiles in (a). Penetrance of FM4-64 localization profiles is represented as % of total cells examined ($n \geq 200$).

a



b

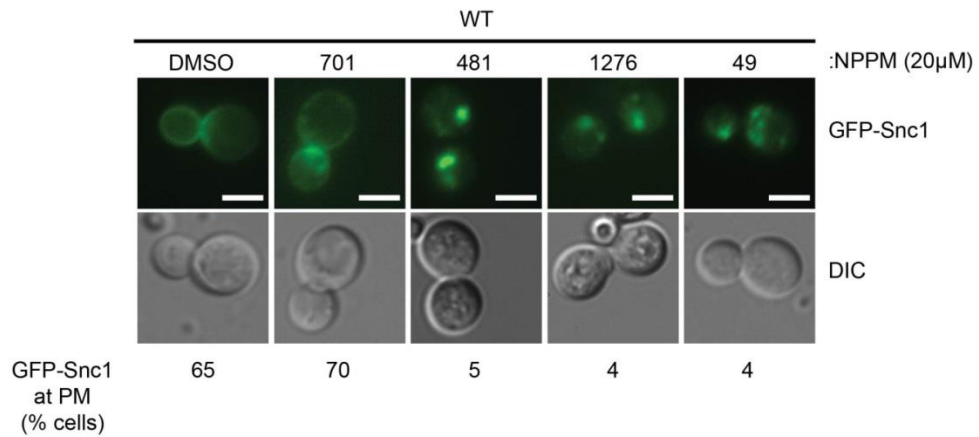


Figure 26. Endocytic recycling of GFP-Snc1 is retarded in NPPM-intoxicated cells.

(a) Isogenic WT (CTY182) and *sec14-1^{ts}* (CTY1-1A) strains were cultured in YPD medium to mid-logarithmic phase at 30°C, and then shifted to a restrictive temperature for 2h. Defective recycling is characterized by an accumulation of GFP-Snc1 in TGN/endosomal puncta, whereas the normal steady-state location for the reporter is on the plasma membrane. Bar, 5μm. (b) WT yeast were cultured as in (a) with the exception that cells were treated with NPPM (20μM) for 2h at 30°C, as indicated. Penetrance of GFP-Snc1 localization in plasma membrane or TGN/endosomes is quantified as % of total cells examined (n ≥ 300). Bar, 5μm.

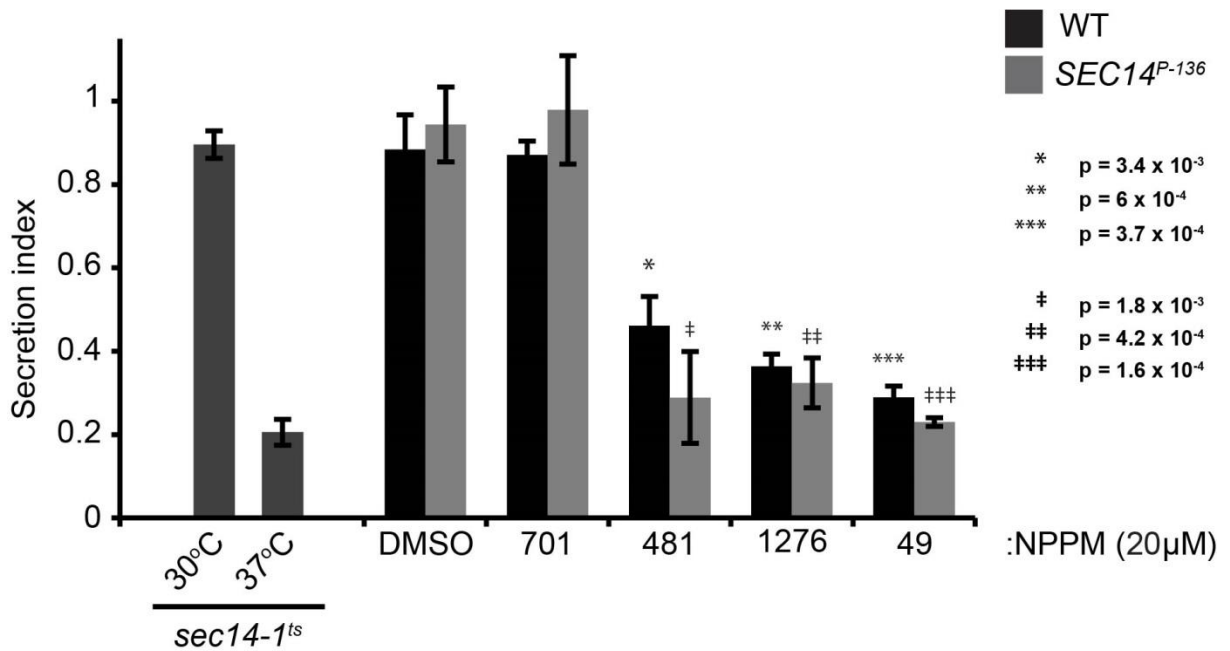


Figure 27. Sec14-active NPPMs block invertase secretion.

(a) Invertase secretion indices for *sec14-1^{ts}* yeast (CTY1-1A) incubated at 30°C and 37°C report secretory efficiency under Sec14-proficient and -deficient conditions, respectively. WT (CTY182) and *SEC14^{P-136}* (CTY374) yeast strains were challenged with NPPM (20µM) for 1h prior- and 2h post-induction of secretory invertase synthesis by shift to low glucose medium. Statistics relate the experimental condition to the corresponding DMSO control (two-tailed unpaired *t*-test, p-values indicated).

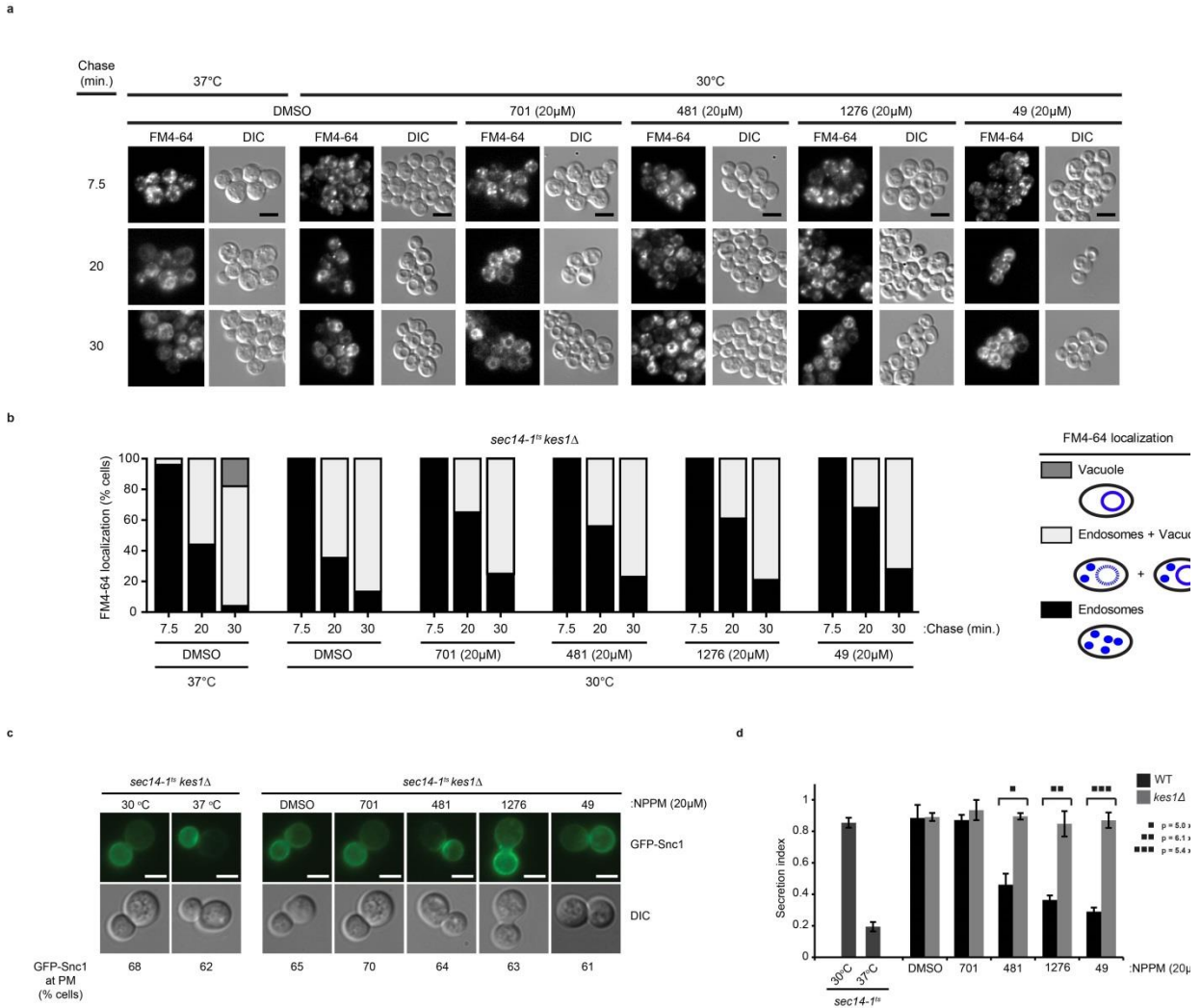


Figure 28. ‘Bypass Sec14’ mutations correct NPPM-induced trafficking defects.

When challenged with normally toxic concentrations of Sec14-active NPPMs, the *kes1Δ* ‘bypass Sec14’ mutant (CTY159) efficiently trafficked FM4-64 (panels **a** and **b**), endocytic recycling of GFP-Snc1 (panel **c**), and invertase secretion (panel **d**). The *kes1Δ* data in this panel were collected at the same time as partner experiments shown in **Figure 28** so the same *sec14^{ts}* and WT data are used in this Figure. For all image panels, bar=5µm. The data were performed at the same time as the partner data sets presented in **Figures 25, 26** and **27**, respectively, and quantifications were performed as so described.

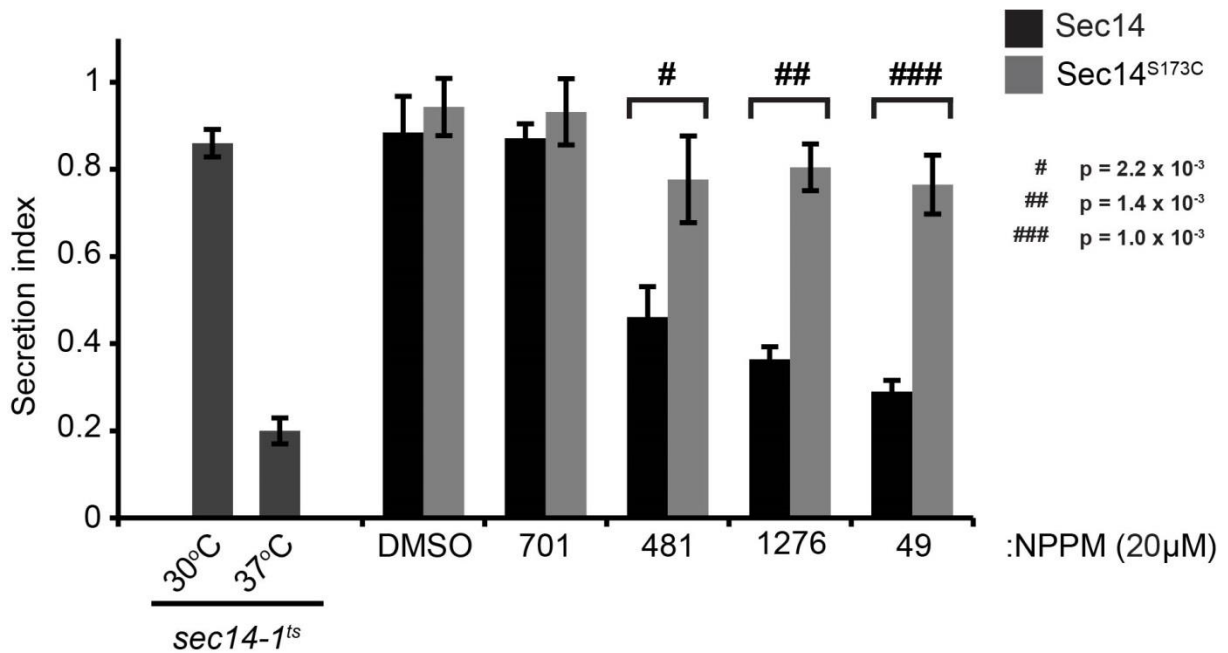


Figure 29. Sec14^{S173C} yeast secrete invertase in the face of Sec14-active NPPMs.

Culture conditions for imposing Sec14 deficiencies by temperature shift or NPPM challenge are as in **Figure 27**. Invertase secretion indices for a *sec14-1^{ts}* strain incubated at 30°C or 37°C report the secretory efficiency under Sec14-proficient and -deficient conditions, respectively. The isogenic wild-type (CTY182) strain provides a positive control for both conditions. A wild-type strain (CTY182) expressing NPPM-sensitive Sec14, and its congenic partner (CTY558) expressing the NPPM-resistant Sec14^{S173C} as sole Sec14 source, were challenged with the indicated NPPM (20µM) for 1h prior to, and 2h following, induction of secretory invertase synthesis. Statistics compare the indicated wild-type and Sec14^{S173C} NPPM-treated conditions (two-tailed unpaired *t*-test; p-values indicated). The Sec14^{S173C} data in this panel were collected at the same time as partner experiments shown in **Figure 27** so the same *sec14^{ts}* and wild-type data are used in this Figure.

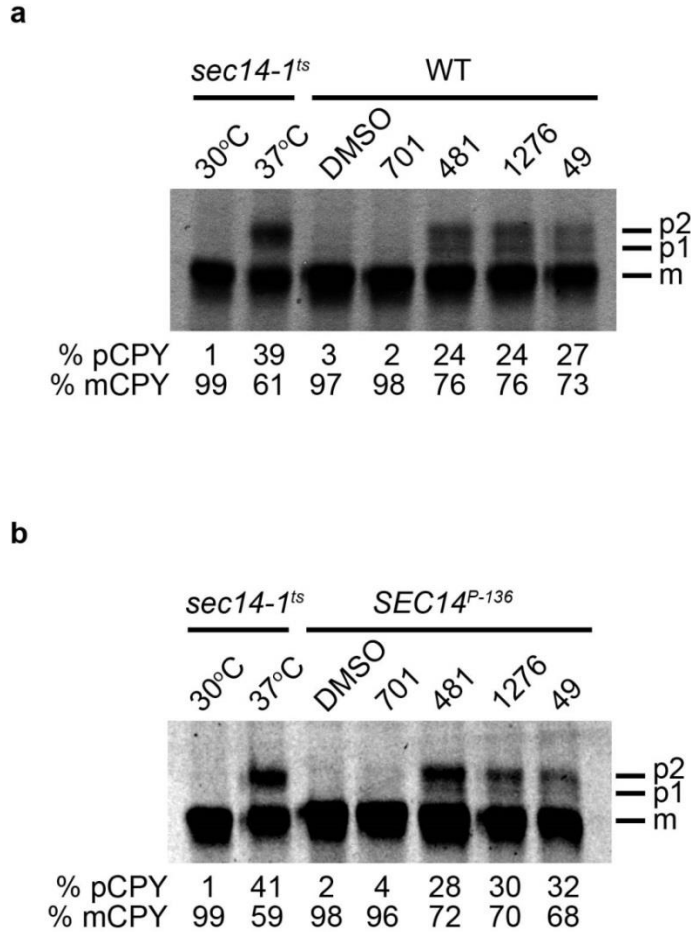


Figure 30. Sec14-active NPPMs induce CPY trafficking defects.

Isogenic wild-type (CTY182) or *sec14-1^{ts}* yeast (CTY1-1A) were grown to mid- logarithmic phase in YPD media. CPY trafficking of WT (at 30°C or after shift to 37°C for 2hrs) and *sec14-1^{ts}* yeast strains (at 30°C) report CPY transit through the secretory pathway under Sec14-proficient conditions. Shift of *sec14-1^{ts}* yeast to 37°C for 2hrs reports CPY trafficking under Sec14-deficient conditions. In parallel, wild-type (**a**) and *SEC14^{P-136}* yeast (**b**) were grown at 30°C, and subsequently challenged with NPPM (20μM) or DMSO for 2hrs. Cells were radiolabeled with [³⁵S]-amino acids for 20 min., a 30 min chase was run, samples were processed, and immunoprecipitates evaluated by SDS-PAGE and autoradiography (see Methods). Precursor p1CPY and p2CPY forms and the fully processed vacuolar mCPY forms are identified. Quantification of pCPY forms (p1 + p2) as percentages of total CPY species are given at bottom for each condition.

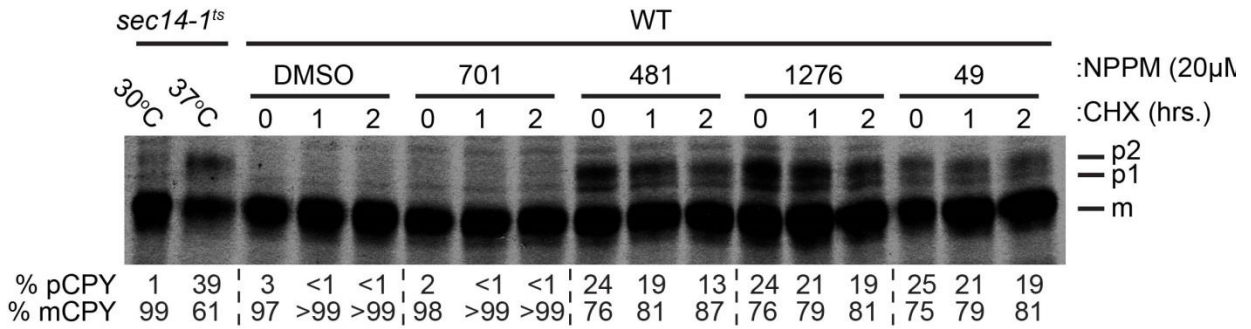
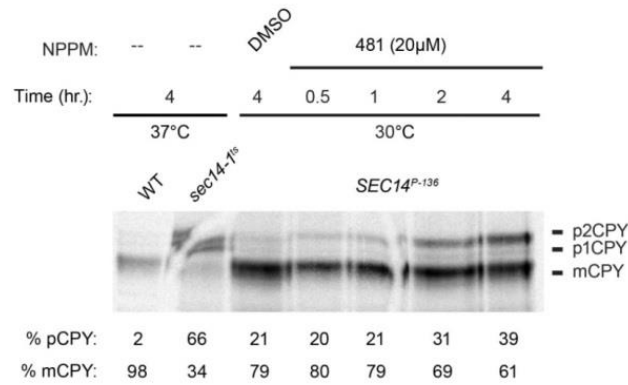


Figure 31. NPPM induced CPY trafficking defects are poorly reversible.

WT (CTY182) or *sec14-1^{ts}* yeast (CTY1-1A) were grown to mid-logarithmic phase at 30°C and treated with NPPM (20μM), DMSO, or shifted to 37°C, for 2h as indicated at top. Cells were radiolabeled with [³⁵S]-amino acid (20μCi/ml) for 20 min. and chase was initiated with excess unlabeled methionine and cysteine (final concentration, 1%) for 30 min. Subsequently, cells were transferred to fresh media without inhibitor and incubated at 30°C in the presence of cyclohexamide (100μg/ml) to inhibit new Sec14 synthesis. The incubation was terminated at the indicated times by addition of ice-cold trichloroacetic acid (final concentration, 5%). Core glycosylated proCPY (p1), fully glycosylated proCPY (P2), and the matured vacuolar mCPY forms are identified. Quantification of pCPY forms (p1 + p2) as percentages of total CPY species are given at bottom for each condition.

a



b

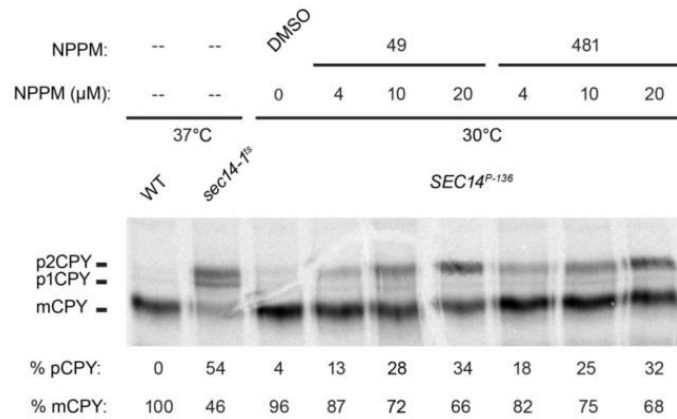


Figure 32. NPPM-induced CPY trafficking block is dose-and time-dependent.

(a) Isogenic WT and *sec14-1^{ts}* yeast strains (CTY182, CTY1-1A) were grown to mid-logarithmic phase at 30 $^{\circ}$ C and shifted to 37 $^{\circ}$ C to provide reference CPY trafficking profiles under Sec14-sufficient and -deficient conditions, respectively. In parallel, *SEC14^{P-136}* yeast were cultured in the presence of 6748-481 (20 μ M) for increasing times at 30 $^{\circ}$ C, as indicated at top. Cells were subsequently radiolabeled at the indicated temperatures for 30 min, and CPY species evaluated by SDS-PAGE and autoradiography. Precursor and mature forms of CPY are identified. Quantification of pCPY forms (p1 + p2) as percentages of total CPY species are given at bottom for each condition. (b) Similar experiment as in (a) except 6748-481 and 67170-49 concentrations were varied, as indicated at top. Quantification of pCPY forms (p1 + p2) as percentages of total CPY species are given at bottom for each condition.

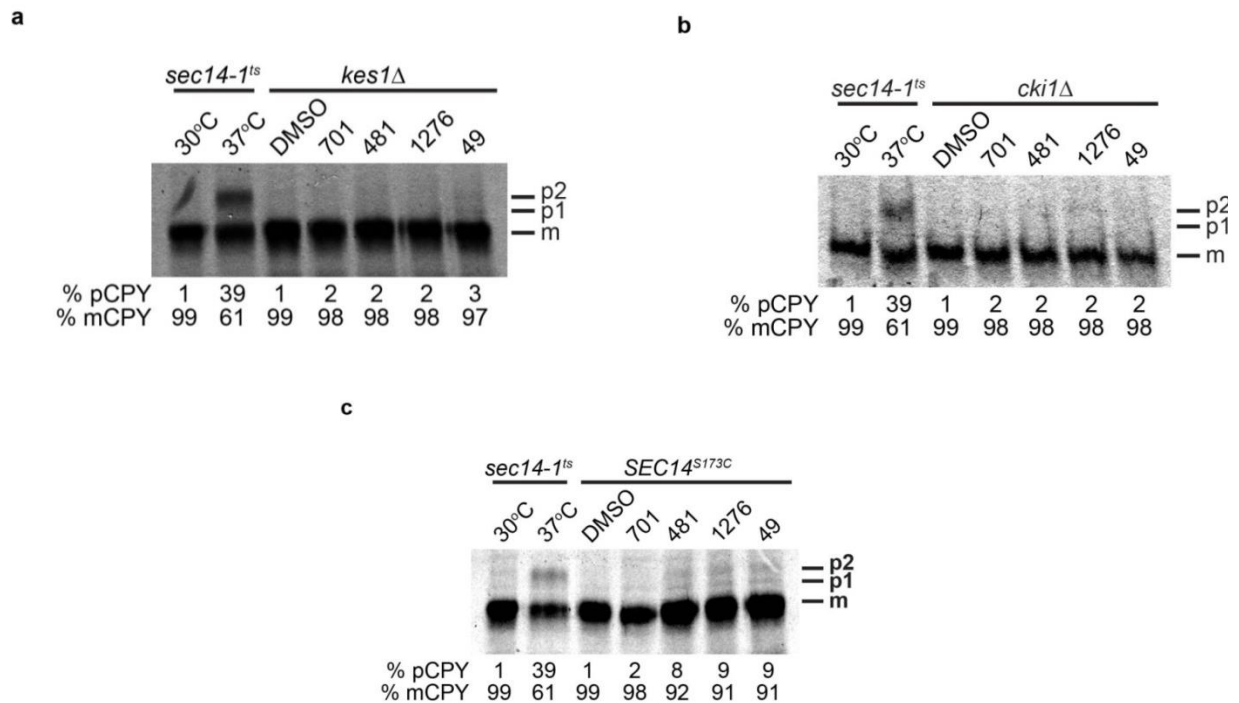


Figure 33. ‘Bypass Sec14’ mutations and Sec14^{S173C} expression alleviate NPPM-induced CPY trafficking defects.

(a) *sec14-1^{ts}* yeast (CTY1-1A) were grown to mid-logarithmic phase at 30°C and shifted to 37°C for 2hrs to provide reference CPY trafficking profiles under Sec14-sufficient and –deficient conditions, respectively. The isogenic *kes1Δ* ‘bypass Sec14’ mutant (CTY159) was grown to mid-logarithmic phase at 30°C and challenged with NPPM (20μM) or DMSO for 2hrs, as indicated at top. Cells were radiolabeled with [³⁵S]-amino acids (20μCi/ml) for 20 min. Chase was initiated with excess unlabeled methionine and cysteine (final concentration, 1%), then terminated after 30 min with ice-cold trichloroacetic acid (final concentration, 5%). Precursor and mature forms of CPY are identified. Quantifications of pCPY forms (p1 + p2) are reported as percentages of total CPY species at bottom for each condition. (b) Experiment was carried out as in (a) with the isogenic *cki1Δ* ‘bypass Sec14’ mutant (CTY160). (c) Experiment was carried out as in (a) with a yeast strain CTY558/YCp(*SEC14^{S173C}*) expressing Sec14^{S173C} as sole Sec14 source. Quantifications of pCPY forms (p1 + p2) are reported as percentages of total CPY species at bottom for each condition.

NPPMs discriminate between chemically distinct phosphoinositide pools

Sec14 potentiates the activities of both of the essential yeast PtdIns 4-OH kinases *in vivo* (*i.e.* Stt4 and Pik1) (Hama, Schnieders et al. 1999; Phillips, Sha et al. 1999; Rivas,

Kearns et al. 1999; Schaaf, Ortlund et al. 2008). We therefore tested whether bulk PtdIns(4)P production in cells was sensitive to inhibition by Sec14-active NPPMs. In these experiments, *sac1* mutants inactivated for the major yeast PtdIns(4)P phosphatase were employed because these mutants accumulate PtdIns(4)P to high levels (Guo, Stolz et al. 1999; Rivas, Kearns et al. 1999). This accumulation provides the dual benefits of simplifying measurements of PtdIns(4)P biosynthetic rates, and by increasing the statistical power of PtdIns(4)P quantification.

Challenge with 6748-481, 67170-49, 4130-1276, reduced bulk PtdIns(4)P levels by approximately 40% compared to the levels recorded when cells were challenged with DMSO or inactive NPPM 5564-701 controls (**Figure 34a,b**). Neither challenge with 6748-481, nor with 5564-701, exerted significant reductions in bulk PtdIns(3)P or PtdIns(4,5)P₂ levels when compared to challenge with vehicle alone (**Figure 34c,d**).

The selectivity of NPPM effects on phosphoinositide homeostasis in wild-type yeast cells was similarly on display in vital imaging assays using isomer-selective biosensors. To probe status of cellular PtdIns(4,5)P₂ pools, we monitored intracellular distribution of the GFP-2xPH^{PLC γ 1} PtdIns(4,5)P₂ biosensor. This reporter localized to the yeast plasma membrane in the expected PtdIns(4,5)P₂-dependent manner--as evidenced by biosensor release into the cytoplasm upon inactivation of a temperature-sensitive version of the single yeast PtdIns(4)P 5-OH kinase (*Mss4*; **Figure 35**). In accord with [³H]-inositol radiolabeling data, GFP-2xPH^{PLC γ 1} remained bound to the plasma membrane—even after a 3hr incubation of cells with Sec14-active SMIs. Moreover, release of GFP-2xPH^{PLC γ 1} from the plasma membrane was not observed upon individual inactivation of the other PtdIns kinases.

The status of TGN/endosomal PtdIns(4)P pools was queried using two different biosensors; GFP-GOLPH3 and GFP-2xPH^{Osh2} (Roy and Levine 2004; Baird, Stefan et al. 2008; Wood, Schmitz et al. 2009). Optimal association of these reporters with punctate TGN/endosomal compartments is both Sec14- and Pik1-dependent as evidenced by their enhanced release from these organelles upon shift of *sec14^{ts}*, and particularly *pik1^{ts}*, mutants to non-permissive temperatures (**Figure 36**). Intoxication of yeast with 6-748-481, 67170-49, or 4130-1276 similarly released GFP-2xPH^{Osh2} from TGN/endosomal structures into the cytoplasm. The effect on GFP-GOLPH3 localization was different, however, in that both genetic and NPPM-mediated inactivation of Sec14 effected what was primarily a structural transformation of the GFP-GOLPH3 compartment accompanied by some release of the reporter to the cytoplasm (**Figure 36**). As expected, the appropriate membrane association profiles for both reporters were unaffected in cells devoid of PtdIns(3)P and PtdIns(3,5)P₂ (*vps34Δ*; **Figure 36**).

In addition to the Sec14- and Pik1-dependent TGN/endosomal PtdIns(4)P pool, GFP-2xPH^{Osh2} also scored an Stt4-dependent pool of this phosphoinositide in the plasma membrane (**Figure 36c,d**). The dual localization of this biosensor revealed a compartmental pool-specificity for NPPM-mediated interference of PtdIns(4)P signaling. Challenge of WT cells with 6748-481, 67170-49 or 4130-1276 (but not 5564-701 or DMSO) released GFP-2xPH^{Osh2} from TGN/endosomal compartments without obviously compromising biosensor targeting to the plasma membrane (**Figure 36c,d**). We had previously shown that *kes1Δ* phenotypically rescues the growth defects of *pik1^{ts}*, but not *stt4^{ts}*, mutants at semi-permissive temperatures (Li, Rivas et al. 2002)—identifying Kes1 as an antagonist of Pik1-dependent PtdIns(4)P signaling. Consistent with those findings, the *kes1Δ* ‘bypass Sec14’ mutant

presented undiminished GFP-2xPH^{Osh2} association with TGN/endosomal membranes in the face of 6748-481, 67170-49, or 4130-1276 challenge (**Figure 37**) suggesting that Kes1 disruption rescues NPPM-induced trafficking defects through PtdIns(4)P signaling events *in vivo*.

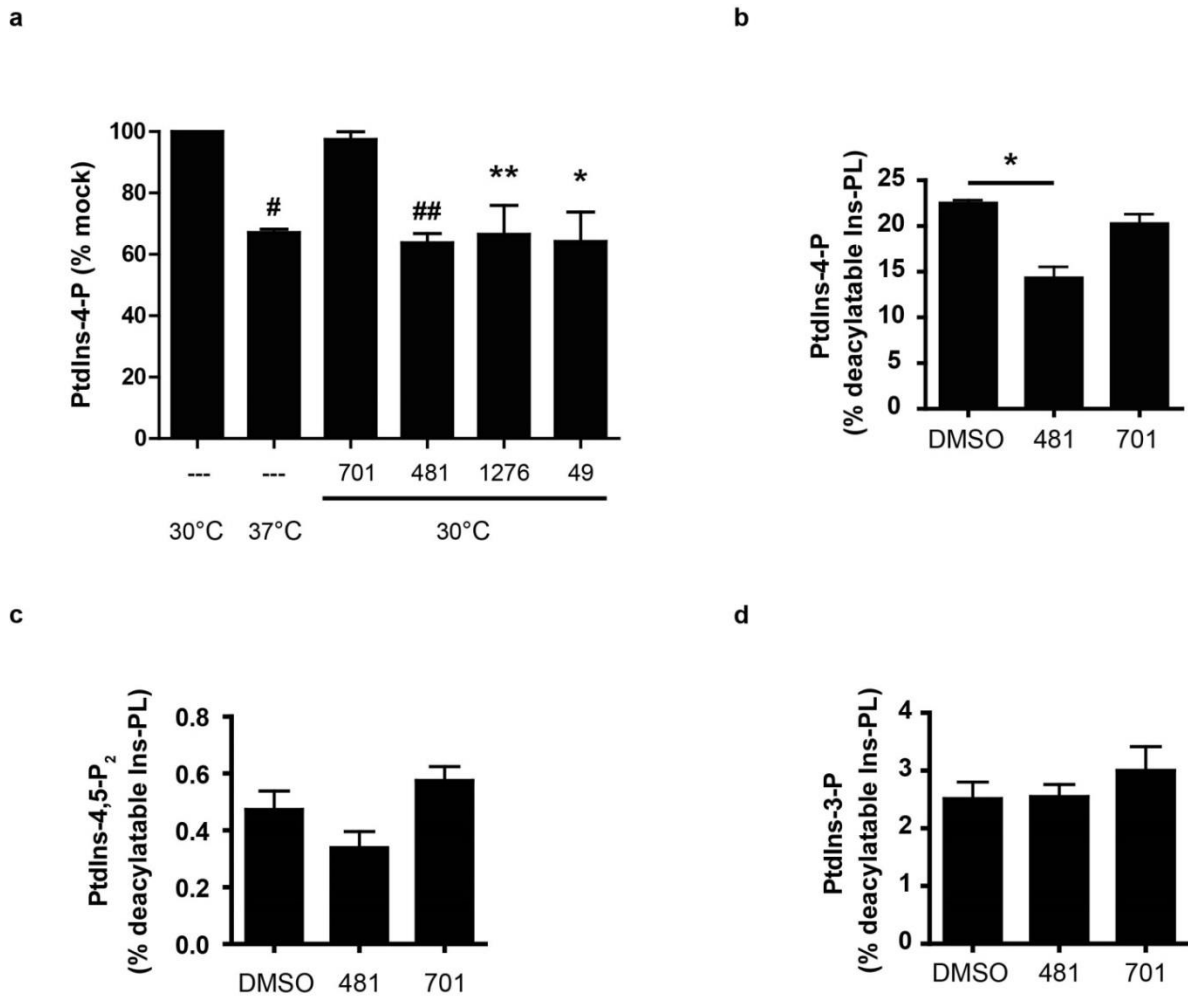
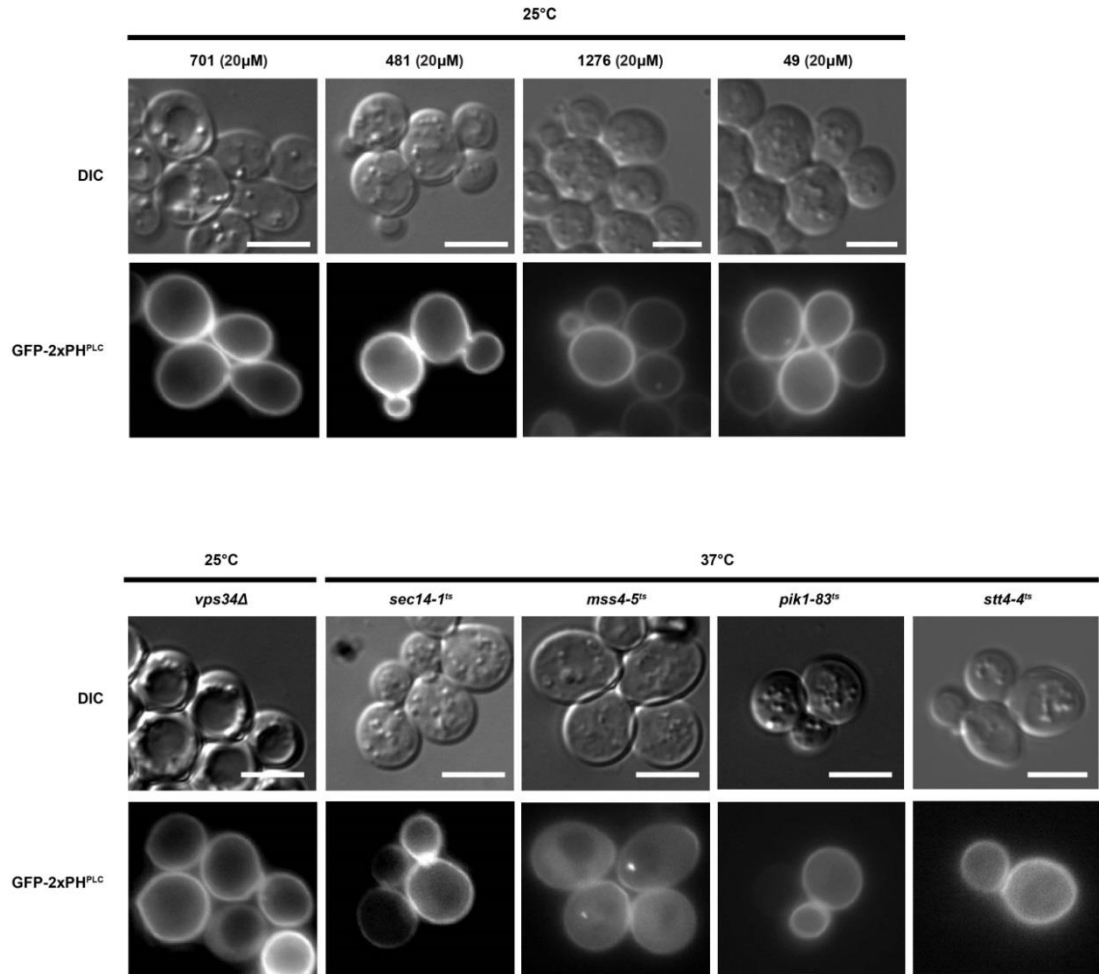


Figure 34. Sec14-active NPPMs target specific phosphoinositide classes.

sac1Δ yeast (CTY100) were radiolabeled with [³H]-Ins (10μCi/ml) for 24 hours at 30°C, and treated ± NPPM (20μM) or DMSO for 3hr, as indicated. (a) Lipids were extracted and resolved by TLC or (b) the glycerophosphoinositols (groPtdIns) were collected from lipid extracts, resolved by strong ion-exchange HPLC, and radioactivity in each phosphoinositide class measured. (b) PtdIns(4)P (c) PtdIns(4,5)P₂ and (d) PtdIns(3)P are quantified. Statistical significance compared the NPPM conditions to DMSO control using two-tailed t-test (P<0.05; n = 3; Graphpad, see Methods).

a



b

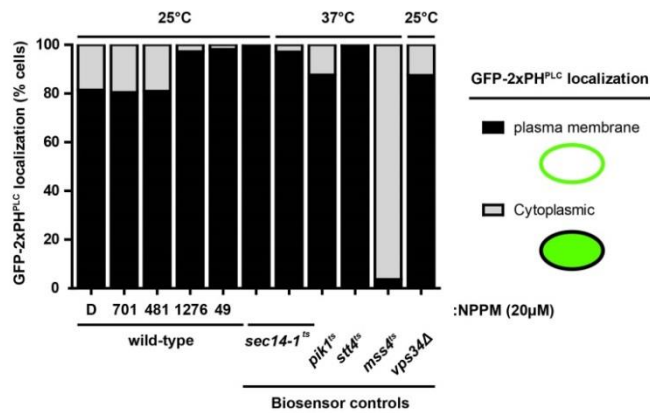


Figure 35. GFP-2xPH^{PLCδ1} plasma membrane association is unperturbed by challenge with Sec14-active NPPMs.

(a) Top panels: wild-type yeast (CTY182) were intoxicated with indicated SMIs (20 μ M) for 3h at 25 $^{\circ}$ C and GFP-2xPH^{PLC δ 1} images collected (bar = 5 μ m). GFP-2xPH^{PLC δ 1} profiles were scored as PM or diffuse cytoplasmic (see below). Bottom panels: Data from a set of control experiments run in parallel with NPPM challenge experiments are shown. Indicated PtdIns kinase mutants expressing GFP-2xPH^{PLC δ 1} were shifted to 37 $^{\circ}$ C for 3h--except *mss4-5^{ts}* which was shifted to 37 $^{\circ}$ C for 30 min. The *vps34 Δ* strain was analyzed at 25 $^{\circ}$ C as it is unconditionally defective for synthesis of all 3-OH phosphorylated phosphoinositides. (b) Incidence of GFP-2XPH^{PLC} plasma membrane and endosomal localization profiles is quantified as % of total cells examined (n \geq 300) for all conditions in (a). D=DMSO.

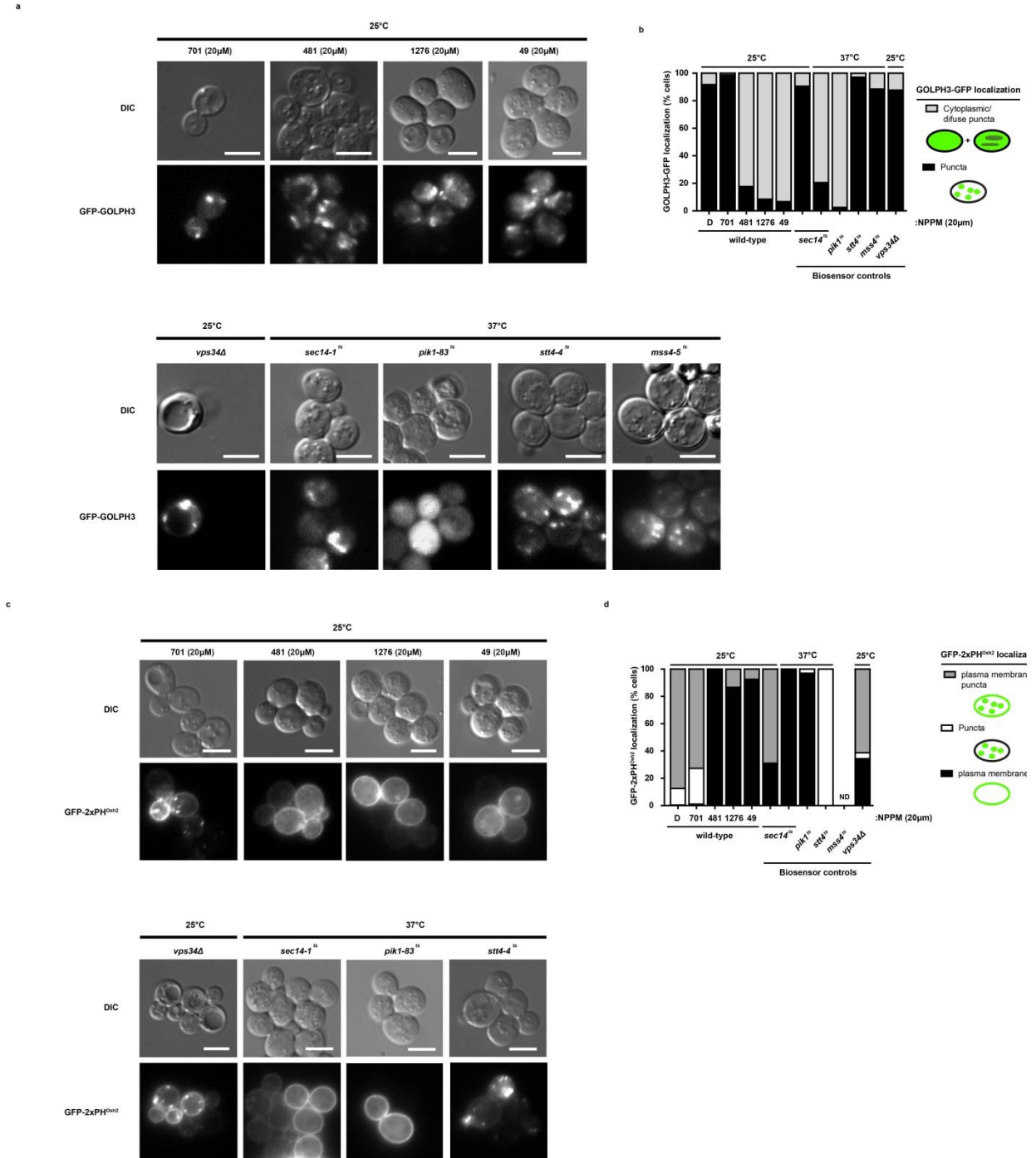
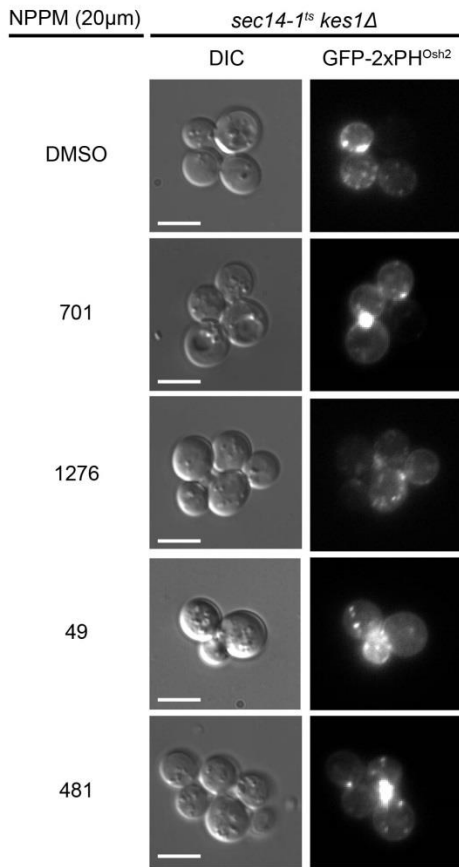


Figure 36. PtdIns(4)P biosensors.

(a) GFP-2xPH^{Osh2} registers Stt4-generated PtdIns(4)P pools at the plasma membrane (see *stt4-4^{ts}* control) and Pik1- and Sec14-dependent pools in punctate TGN/endosomal compartments (*pik1-83^{ts}* and *sec14-1^{ts}* controls). Indicated PtdIns kinase mutants expressing GFP-2xPH^{Osh2} were shifted to 37°C for 3h. The *vps34Δ* strain was analyzed at 25°C as it is unconditionally defective for synthesis of all 3-OH phosphorylated phosphoinositides. The *mss4-5^{ts}* condition was not analyzed in these experiments as we were unable

to generate viable *mss4-5^{ts}* mutants that expressed GFP-2xPH^{Osh2}. **(b)** GFP-2xPH^{Osh2} distribution was scored, and >300 cells were evaluated for each condition. GFP-2xPH^{Osh2} distributions were classified as PM, punctate, or both. Data are expressed in three values scored from the same cell set--a PM value (cells showing PM localization profiles/total #cells evaluated) x 100, a TGN/endosomal value (cells showing punctate localization profiles/total #cells evaluated) x 100 or both (cells showing PM and punctate profiles/total #cells evaluated) x 100. ND--not determined. **(c)** Cultures were grown as in (a) except *mss4-5^{ts}* yeast expressing GFP-GOLPH3 were shifted to 37°C for 30 min. GFP-GOLPH3 normally associates with punctate TGN/endosomal compartments at steady-state. *sec14-1^{ts}* mutants distended the compartment at 37°C with some release of GFP-GOLPH3 from TGN/endosomal membranes - - a phenotype recapitulated by NPPM-intoxicated cells (see below). **(d)** GFP-GOLPH3 distributions were scored as punctate, or not, or all conditions in (c). Data are expressed as (cells showing punctate localization profiles/total #cells evaluated) x 100%. At least 300 cells were scored for each condition.

a



b

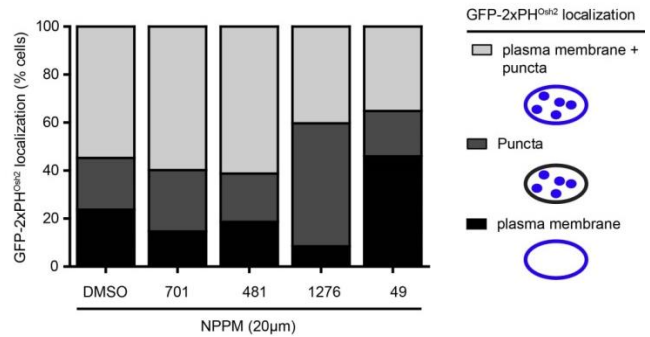


Figure 37. GFP-2xPH^{Osh2} localization to membranes is unperturbed in *kes1Δ* ‘bypass Sec14’ mutants by challenge with Sec14-active NPPMs. (a) A *kes1Δ* ‘bypass *sec14*’ strain (CTY159) expressing GFP-2xPH^{Osh2} was cultured to mid-logarithmic growth phase in uracil-free 3% glucose-containing minimal medium supplemented with 1% casamino acids at 25°C. Cells were treated ± NPPM (20μM) for 3h at 25°C and the GFP-2xPH^{Osh2} profiles imaged. Steady-state distribution of GFP-2xPH^{Osh2} to PM and punctate TGN/endosomal compartments was evident under all conditions tested (bar = 5μm). (b) Quantification of localization profiles is expressed in three values scored from the same cell set--a PM value (cells showing PM localization profiles/total #cells evaluated) x 100, a TGN/endosomal value (cells showing punctate localization profiles/total #cells evaluated) x 100 or both (cells showing PM and punctate profiles/total #cells evaluated) x 100. At least 300 cells were scored for each condition. These experiments were performed in parallel to those described in **Figure 36 c,d**.

NPPMs discriminate between local PtdIns(4)P signaling pathways

The [³H]-inositol metabolic labeling and biosensor imaging results described above speak to the pool specificity with which Sec14-active SMIs disrupted phosphoinositide signaling as a function of chemical identity [PtdIns(4)P vs. PtdIns(4,5)P₂], and PtdIns(4)P signaling as a function of intracellular compartment (TGN/endosomes vs. plasma membrane). Is the pool specificity even more discriminating? The distinct biological activities of Sec14 and the Sec14-like Sfh4 protein provided a test of whether Sec14-active NPPMs distinguish between functionally diversified PtdIns(4)P signaling pathways that operate in the same general endomembrane system. Sec14 and Sfh4 both control PtdIns(4)P production in TGN/endosomes. Unlike Sec14, Sfh4-dependent PtdIns(4)P signaling supports phosphatidylserine (PtdSer) decarboxylation to phosphatidylethanolamine (PtdEtn) in those compartments (**Figure 38a**; Wu, Routt et al. 2000). As PtdEtn is an essential lipid, loss of Sfh4 activity results in an Etn auxotrophy when the functionally redundant mitochondrial PtdSer decarboxylase 1 pathway is also incapacitated (*psd1Δ* mutants; **Figure 38b**, rows 3,5).

Because Sfh4 is not inhibited *in vitro* by NPPMs that potently inactivate Sec14, we examined whether Sec14-active SMIs respect the PtdIns(4)P pool-selectivities of these distinct PITP-dependent metabolic circuits. Thus, *psd1Δ* cells were reconstituted for Sec14^{S173C} expression (to circumvent growth defects associated with NPPM-mediated inactivation of Sec14), and the strains were intoxicated with 6748-481. The NPPM challenge failed to impose Etn auxotrophy onto the *PSDI* control, or onto the isogenic *psd1Δ* derivative (**Figure 38b**, rows 3,4)—thereby demonstrating that Sfh4 retained biological activity in the face of this NPPM.

These *in vivo* results were independently supported by [³H]-serine metabolic radiolabeling experiments that directly measured Sfh4-dependent decarboxylation of PtdSer to PtdEtn in TGN/endosomes. NPPM 6748-481 challenge of *psd1Δ* mutants did not compromise this decarboxylation *in vivo*—thereby confirming intrinsic Sfh4 resistance to Sec14-active NPPMs. This result was observed regardless of whether *psd1Δ* mutants expressed Sec14 (TGN/endosomal trafficking is blocked in this condition) or Sec14^{S173C} (cells remain competent for TGN/endosomal trafficking in this condition; **Figure 38c**). Taken together, the data establish that NPPM intoxication of yeast failed to interfere with Sfh4-dependent PtdIns(4)P signaling in TGN/endosomes—even as this challenge strongly impaired Sec14-dependent PtdIns(4)P signaling in the same endomembrane system.

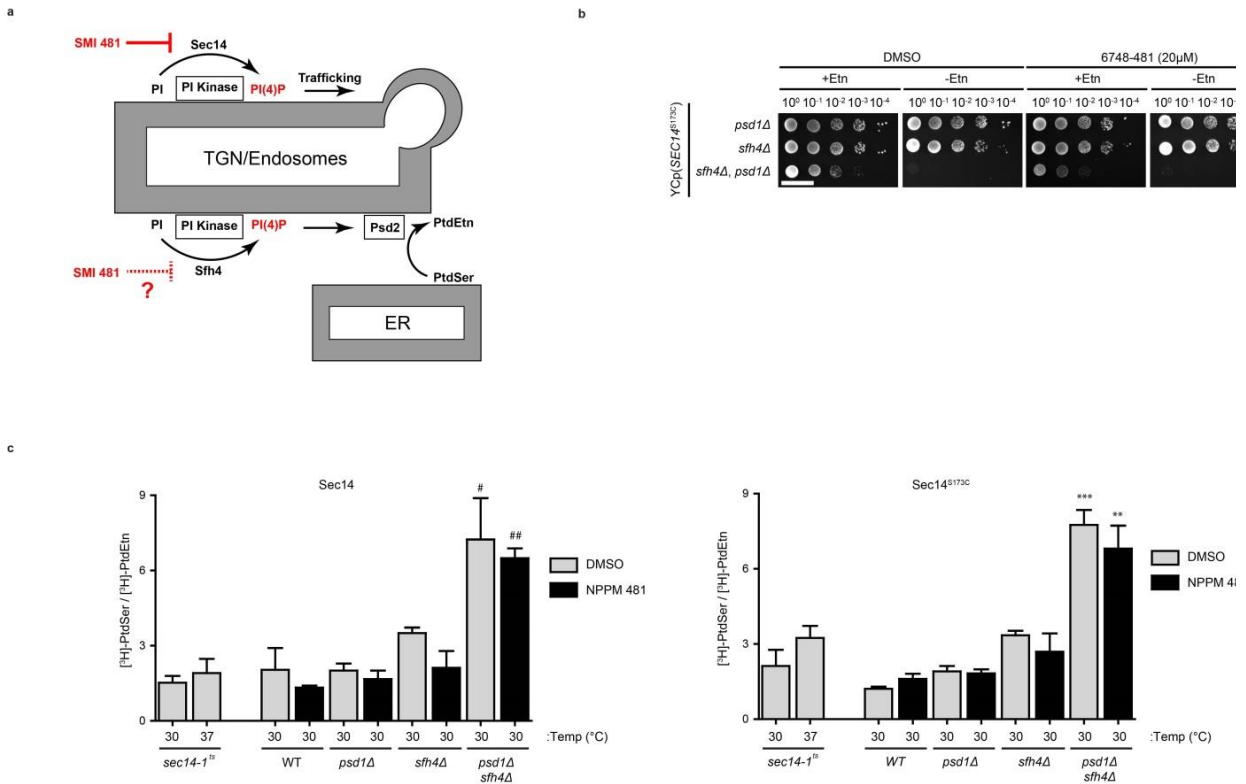


Figure 38. NPPMs discriminate between Sec14- and Sfh4-mediated PtdIns(4)P signaling.

(a) Sec14 and Sfh4 control distinct PtdIns(4)P signaling pathways in TGN/endosomal compartments. The Sec14-pathway couples PtdIns 4-OH kinase action with vesicle biogenesis, whereas the Sfh4 pathway couples PtdIns 4-OH kinase action with decarboxylation of PtdSer to PtdEtn. The decarboxylation reaction is catalyzed by Psd2 and is posited to involve a membrane contact site that bridges the endoplasmic reticulum (ER) with TGN/endosomes. (b) WT (CTY182), *sfh4Δ* (PYY40), or *sfh4Δ psd1Δ* (PYY30) yeast expressing Sec14 [YCP(*URA3*)] or the NPPM-resistant Sec14^{S173C} [YCP(*SEC14*^{S173C})] were spotted in 10-fold dilution series on uracil-free minimal agar ± ethanolamine (1mM), with or without 6748-481 (20μM), as indicated. Plates were incubated for 96h at 30°C. (c) To monitor PtdSer decarboxylation, WT (CTY182), *sec14-1^{ts}* (CTY1-1A), *psd1Δ* (PYY23), *sfh4Δ* (PYY40), or *sfh4Δ psd1Δ* (PYY30) cells expressing either Sec14 or Sec14^{S173C} (as indicated) were cultured in YNB uracil-free media containing ethanolamine (2mM) at 30°C. Mid-logarithmic growth phase cultures ($\lambda_{600}=0.3$) were incubated in the presence of [³H]-serine (3.3μCi/ml) for a total of six hours. At hour three, cells were presented with 6748-481 (20μM), DMSO, or shifted to non-permissive temperature (37°C), as appropriate. Lipids were extracted and resolved by thin layer chromatography (see Methods). PtdSer and PtdEtn species were harvested, quantified by liquid scintillation counting, and data expressed as the indicated

precursor/product ratio. Values represent the mean \pm s.e.m from at least 3 independent experiments. Defects in Sfh4-dependent conversion of PtdSer to PtdEtn are diagnosed by the high PtdSer/PtdEtn ratios characteristic of the *psd1 Δ sfh4 Δ* double mutant control strains. Statistical comparisons of values used the ‘unpaired two-tailed t-test’ relative to DMSO control, where # (P = 0.0495), ## (P = 0.002), ** (P = 0.0051), *** (P = 0.0004).

Discussion of NPPM-like Sec14-directed inhibitors

Herein, we translate the cell biological concept that PITPs represent highly discriminating portals for interrogating phosphoinositide signaling to the realm of chemical biology. We describe the first validated small molecule inhibitors of a PITP, and demonstrate an exquisite *in vivo* specificity of action for such compounds. We further propose a chemical mechanism for how these SMIs exert their inhibitory effects. These studies deliver a strong proof-of-concept that PITP-directed SMIs offer new prospects for intervening with cellular phosphoinositide signaling pathways, and in doing so with selectivities superior to those delivered by: **(i)** contemporary PtdIns-kinase-targeted strategies, or **(ii)** Rapalog-driven depletion of compartment-specific pools of a particular phosphoinositide class.

The data identify NPPMs as Sec14-directed inhibitors. Consistent with this assignment, intoxication of cells with Sec14-active NPPMs comprehensively recapitulates the morphological and cell biological phenotypes associated with loss of Sec14 function *in vivo*. That Sec14 is the sole essential NPPM target in yeast is established by the NPPM-resistance of: **(i)** cells whose viability relies on expression of mutant NPPM-resistant Sec14 proteins, **(ii)** ‘bypass Sec14’ mutants, and **(iii)** yeast whose viability is supported by expression of Sec14-like PITPs naturally resistant to NPPMs (*i.e.* Sfh2, Sfh4 or Sfh5). Moreover, the ability of NPPM to cleanly discriminate between Sfh4- and Sec14-dependent functions in the same endomembrane system demonstrates a strict PITP and PtdIns(4)P signaling pool specificity for these compounds in a physiologically relevant context.

NPPM-mediated inhibition of Sec14 is accompanied by the indifference of Sec14 mutants defective in NPPM binding, and of the Sfh1- Sfh5 PITPs, to high concentrations of these compounds. These findings convincingly demonstrate that NPPMs do not exert their Sec14-targeted effects via non-specific membrane-active mechanisms. Rather, NPPMs inactivate the Sec14 protein itself. The data are most consistent with NPPMs loading into the Sec14 hydrophobic pocket during a phospholipid exchange cycle and effecting a poorly reversible inhibition of both PtdIns- and PtdCho-transfer activities. Docking simulations forecast that bound NPPM invades the space occupied by the PtdIns- and PtdCho-acyl chains, engages with Sec14 residues essential for PtdCho headgroup coordination. This steric invasion of PtdIns/PtdCho-binding space by NPPMs accounts for how these molecules inactivate Sec14.

The likelihood that NPPMs engage Sec14 pocket residues essential for coordinating the PtdCho headgroup offers a coherent rationale for why the Sfh2, Sfh3, Sfh4 and Sfh5 PITPs are indifferent to NPPM challenge. That is, these Sec14-like PITPs do not conserve the structural elements required for PtdCho headgroup coordination (**Figure 39**), and therefore lack the elements required for coordination of the aryl-halide moiety of the NPPM in the binding reaction. Sfh1 presents an interesting conundrum in that it is highly homologous to Sec14 (64% and 89% primary sequence identity and similarity, respectively), and this Sec14-like PITP conserves the functional PtdCho-binding unit critical for NPPM binding. Yet, Sfh1 is intrinsically resistant to inhibition by NPPMs. This issue is further discussed below. The Sfh1 paradox notwithstanding, all Sfh PITPs conserve the PtdIns-binding 'barcode' (Schaaf, Ortlund et al. 2008; Nile, Bankaitis et al. 2010). Therefore, the structural engineering of Sec14-like PITPs holds out prospects not only for developing highly

selective inhibitors (as shown here), but also for developing broader range inhibitors which target PtdIns-headgroup binding substrates.

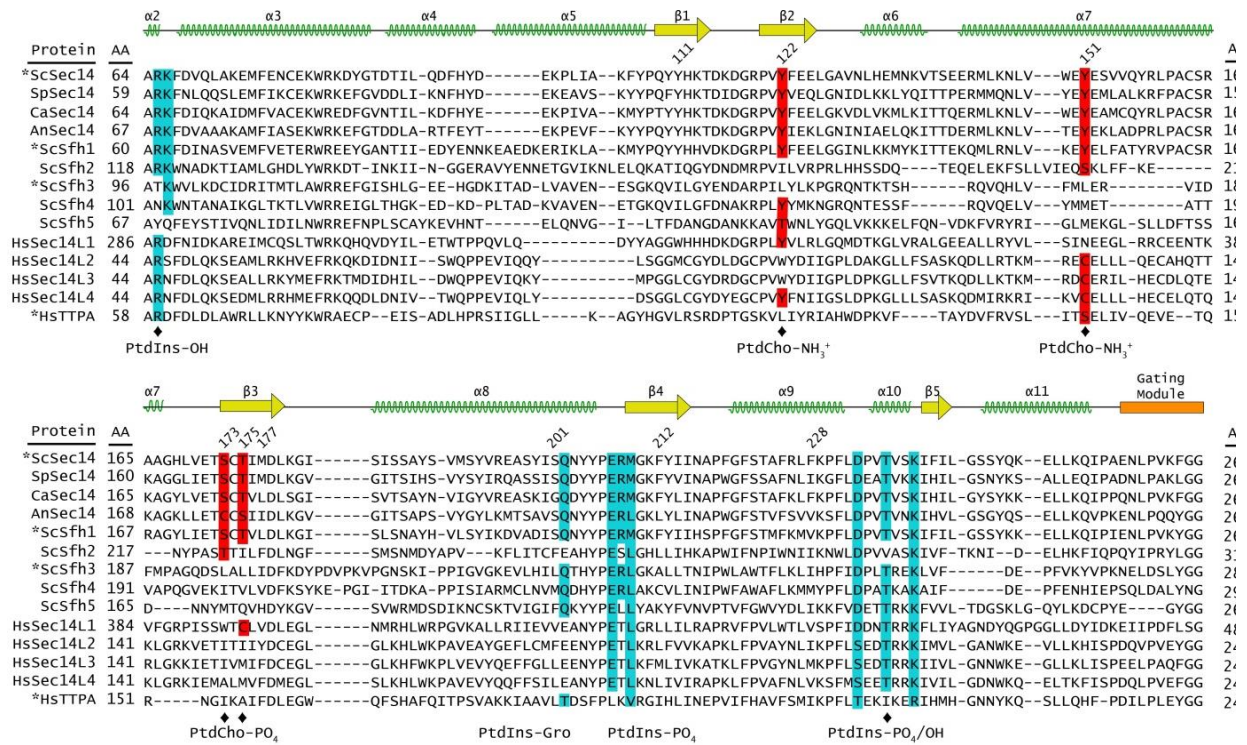


Figure 39. The Sec14 PtdIns and PtdCho binding barcodes.

(a) T-Coffee alignments of selected Sec14-superfamily members (identified at left; proteins for which crystal structures are available are identified with an asterisk) were superimposed onto the Sfh1 crystal structure using secondary structural elements as guide (diagrammed at top). Residues critical for PtdIns headgroup and glycerol (Gro) backbone coordination are boxed and shaded in cyan. Residues critical for PtdCho headgroup coordination are highlighted in red. Residues that contribute to the definition of acyl chain space for both PtdIns and PtdCho are marked with “♦”. AA=amino acid; Sc=*Saccharomyces cerevisiae*; Sp=*Schizosaccharomyces pombe*; Ca=*Candida albicans*; An=*Aspergillus nidulans*, Hs=*Homo sapiens*.

SAR analyses establish an obligatory requirement for an *ortho*-halide in Sec14-active NPPMs, and indicate an important role for the NO₂- group. The chemical properties of such activated aryl halides suggest two potential mechanisms for how NPPMs effect poorly reversible inhibition of Sec14. The first involves aromatic nucleophilic substitution (ANS) reactions where strong *e*⁻-withdrawing groups on the NPPM (NO₂, Cl, C=O) collaborate to form an activated aryl halide that presents an electrophilic ring carbon unusually susceptible to attack by a Lewis base. Nucleophilic attack decomposes the aromatic ring and produces a resonance-stabilized carbanion. This Meisenheimer intermediate ultimately resolves into a covalent Sec14::NPPM adduct with halide as leaving group (Sykes 1986; **Figure 40**). Sec14 harbors four residues (Y₁₁₁, Y₁₂₂, Y₁₅₁, S₁₇₃) positioned within 3-4 Å of the halogen group that could potentially act as nucleophiles (Sykes 1986), but the relative potencies of the compounds in the *ortho*-halide NPPM series are most consistent with halogen bonding mechanisms (**Figure 41a**).

The second, ‘halogen bonding’, or ‘short oxygen-halogen interactions’, are non-covalent interactions which confer specificity and affinity for halogenated ligands (Auffinger, Hays et al. 2004; Lu, Wang et al. 2009). These mechanisms require organization of an electropositive ‘ σ -hole’ on the charge surface of the halogen—an organization enhanced by vicinal *e*⁻-withdrawing groups (*e.g.* -NO₂). Halogen bonding mechanisms predict NPPM potencies of -I > -Br > -Cl with -F, -CH₃ and -H being inactive. This rank order reflects the propensities of larger halide atoms to adopt anisotropic distributions of electrostatic potentials (Metrangolo and Resnati 2001; Auffinger, Hays et al. 2004). The plausibility of halogen bonding mechanisms for NPPM-mediate inhibition of Sec14 is supported by correlation of the activities of NPPM molecules as Sec14 inhibitors with features of NPPM

electrostatic surface potentials. These simulations project the activated aryl halide groups of NPPMs can form σ -holes, and that the magnitudes of these σ -holes (and NPPM potencies as Sec14 inhibitors) are inversely proportional to halide electronegativity (**Figure 41a**).

The halogen bonding hypothesis allows us to refine our projections of NPPM binding space in the Sec14 pocket. Taking SAR and Sec14 mutagenesis data into account, we propose NPPM occupancy in the Sec14 pocket is anchored by S₁₇₃ engagement with *ortho*-halide via a halogen bond, NO₂-group engagements with Y₁₁₁ and Y₁₅₁, an H-bond interaction of the ketone group with S₂₀₁, and intercalation of the NPPM fluorobenzene group between residues F₂₂₈ of the helical gate and F₂₁₂/M₁₇₇ of the Sec14 pocket floor (**Figure 41b,c**). Proof of a halogen-bonding mechanism requires structural data, however, as the cardinal signature is a ‘short’ halide-oxygen bond whose length is less than the sum of the halide and oxygen van der Waals radii (Metrangolo and Resnati 2001; Auffinger, Hays et al. 2004; Lu, Wang et al. 2009).

Washout data indicate a poor reversibility for NPPM-mediated inhibition of Sec14 *in vivo*. How does non-covalent NPPM binding in the Sec14 pocket exert such an inhibition? NPPM-mediated bridging of the pocket floor and gate sub-structures might tether these elements too strongly for Sec14 to spring the gate for ligand exchange upon membrane association. Alternatively, NPPM may decouple the conformational switch elements required for gate opening for ligand exchange by disturbing the H₂O network that lubricates the pocket surface (Ryan, Temple et al. 2007)--thereby locking Sec14 in a ‘closed’ NPPM-bound state.

Why do Sec14 and Sfh1 exhibit such different NPPM-sensitivities given the high Sec14/Sfh1 homology? Our current view is that subtle alterations in pocket geometry underlie the differential NPPM-sensitivities of these proteins. The Sec14 pocket constricts tightly in the region where the apolar end of the NPPM is projected to bind--thereby fostering extensive interactions that anchor NPPM binding to Sec14. The corresponding region of the Sfh1 pocket is more expansive, however, and we posit Sfh1 cannot anchor that domain of the NPPM and therefore cannot stably bind the small molecule. Indeed, docking simulations consistently fail to produce coherent solutions for NPPM binding within the Sfh1 pocket. Either way, the remarkable differences in Sec14 and Sfh1 NPPM-sensitivities highlight the exquisite P1TP selectivities of these SMIs.

The collective data project Sec14-active NPPMs as valuable tool compounds in several respects. First, the powerful genetic technologies afforded by the yeast system notwithstanding, these SMIs allow circumvention of the tedious process of incorporating *sec14^{ts}* mutations into large sets of isogenic yeast strains for purposes of executing genome-scale functional interaction screens. Second, the SMIs allow ‘tuning’ of Sec14 activity in cells--thereby providing a chemically-induced means for analyzing cellular responses to graded levels of Sec14 function. Third, these SMIs are useful reagents in biochemical reconstitutions of membrane trafficking. Optimal exploitation of such systems is frequently hindered by misbehavior, during purification, of biochemical fractions derived from mutant cells. Chemical inactivation of Sec14 enables surgical manipulation of assays fully reconstituted with wild-type components.

Taken together, our results firmly establish P1TPs as tractable pharmacological targets. As the non-enzymatic activities of these proteins complicate high-throughput

screening efforts, we believe cell-based phenotypic screens constitute the most attractive strategy for discovering new chemical modulators of PITP activities. It is from this applied perspective that we have assembled a versatile platform for rational discovery of SMIs directed against a target PITP of the investigator's choosing. The platform exploits yeast 'tester' strains whose survival obligatorily requires target PITP activity. The screen is conducted in multiplex format where distinct PITPs are simultaneously interrogated for inhibition along with sentinel 'bypass Sec14' strains that control for 'off-target' effects. This design feature incorporates internal specificity controls into the screen for rapid target validation.

As PITPs are ubiquitously distributed across the *Eukaryota* (Phillips, Vincent et al. 2006), a yeast-based PITP-directed screening platform offers a promising instrument for drug discovery. For example, because expression of the structurally-unrelated mammalian StART-like PITPs rescues Sec14 defects in yeast (Skinner 1993), the platform can be repurposed for discovery of SMIs that target these mammalian PITPs. PITP-directed inhibitors also empower exploration of phosphoinositide signaling in organisms intractable to genetic approaches. Many such organisms are pathogens, and we have identified new classes of PITP-directed SMIs that inhibit dimorphic transitions of pathogenic fungi—*i.e.* inhibit the very developmental processes essential to success of these organisms as infectious agents.

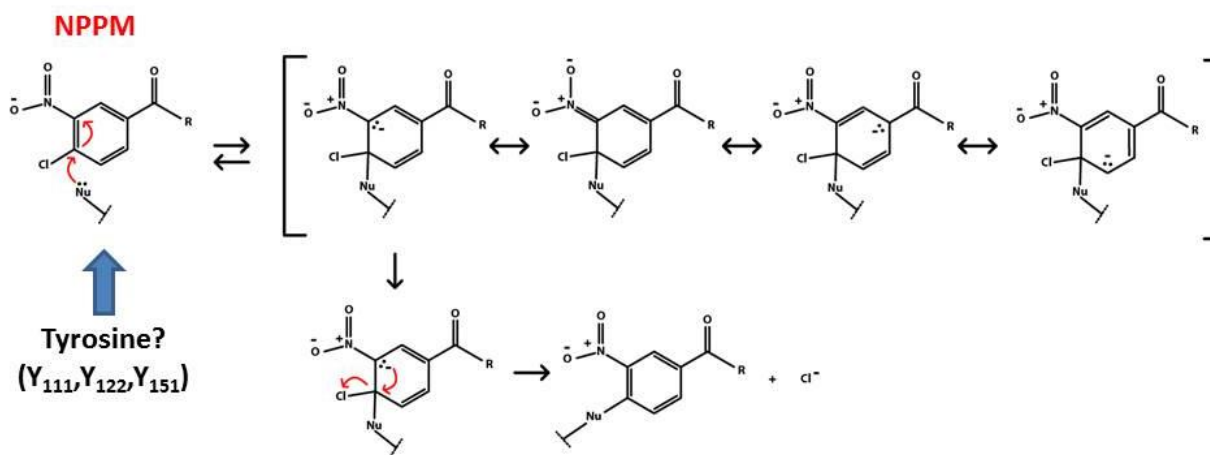


Figure 40. Aromatic nucleophilic substitution of NPPMs.

Aromatic nucleophilic substitution proceeds via a Meisenheimer intermediate and culminates in a covalent Sec14::NPPM adduct. Potential nucleophiles for initiating Meisenheimer chemistry are shown. Nu=nucleophile.

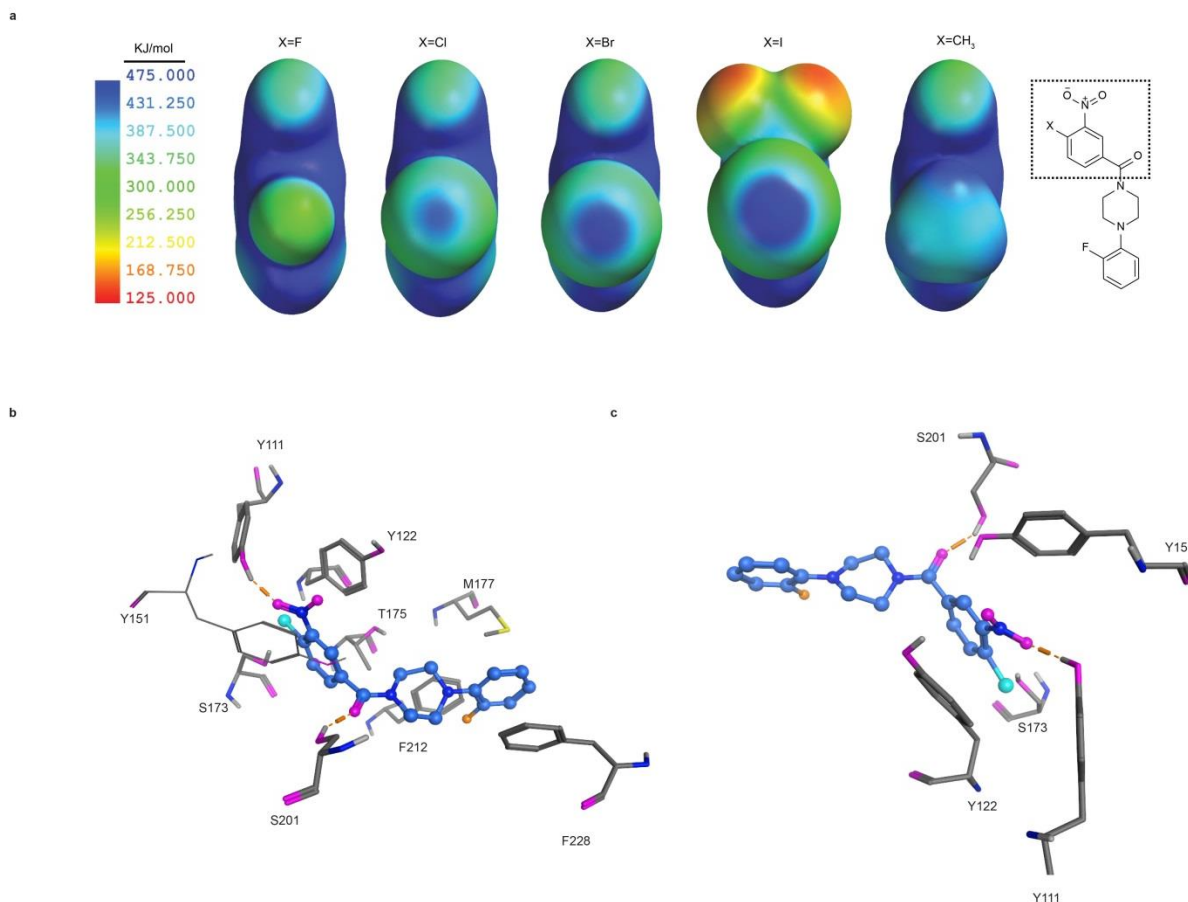


Figure 41. Mechanism for NPPM-mediated inhibition of Sec14.

(a) Simulations of the electrostatic potentials of the indicated NPPM activated aryl halides predict formation of progressively larger electropositive σ -holes in the -Cl, -Br and -I activated aryl halides, respectively. The -CH₃ and -F derivatives are forecast to be incapable of forming significant σ -holes. (b) NPPM binding mode 2 is most consistent with the various data and is depicted within the Sec14 hydrophobic pocket. Hydrogen bonds (magenta), carbon (blue), oxygen (red), nitrogen (dark blue), chlorine and fluorine (green). (c) A focused view of NPPM binding mode 2 highlighting Sec14 residues which form the PtdCho headgroup coordinating substructure, and whose alteration renders Sec14 resistant to NPPM inhibition. Hydrogen bonds (magenta), carbon (blue), oxygen (red), nitrogen (dark blue), chlorine and fluorine (green).

Results: alternative Sec14-directed SMIs

Chemicogenetic profiles identified additional scaffolds predicted to inhibit Sec14 function *in vivo* (**Figure 42a**). All chemical scaffolds identified through the chemogenomic screen and those assembled with SAR analysis were further classified on the basis of structural similarity by applying a fragment-based hierarchical algorithm in ISIDA/Cluster (see Methods). Through this analysis we subdivided all assembled compounds into 12 structurally similar groups based on chemical similarity (**Figure 42b**). Three of these scaffolds: identified 9131112, 9097855 and 9053361, were tested for their ability to inhibit Sec14-mediated PtdIns transfer activity (**Figure 43**) and yeast growth (**Figure 44**). Based on this data these additional scaffolds appear to be promising lead SMIs that specifically inhibit Sec14 and potentially other Sec14-like proteins.

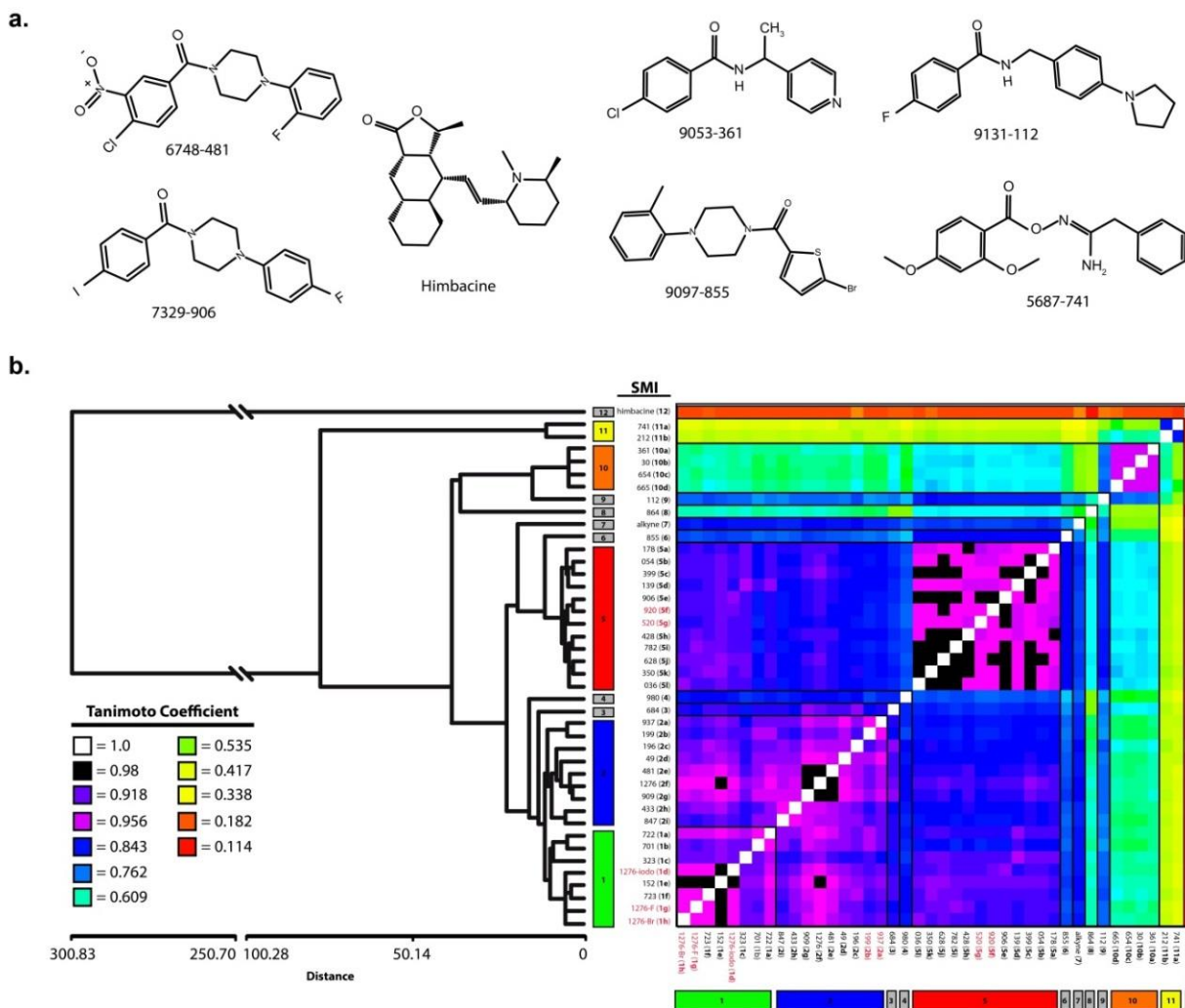


Figure 42. Hierarchical analysis of SAR reveals 12 structural clusters
 SMI clustering by chemical similarity. **(a)** Representative 2D chemical structures of the indicated small molecule inhibitors. **(b)** Heat map representing the tanimoto coefficient (*i.e.* similarity) matrix (right; see methods) between compounds and the corresponding dendrogram (left): The map is colored according to the chemical similarity between compounds (black-blue-violet, high similarity; yellow-red, low similarity). Clusters with high levels of chemical similarity can be identified on the diagonal of the matrix. Clusters 1-12 are indicated by colored boxes and SMI identity are located between the dendrogram and heat map. Compound numbers colored in red were not tested. **(c)** Values were calculated using the ISIDA/Cluster program (<http://infochim.u-strasbg.fr>) (Fourches, Barnes et al. 2010).

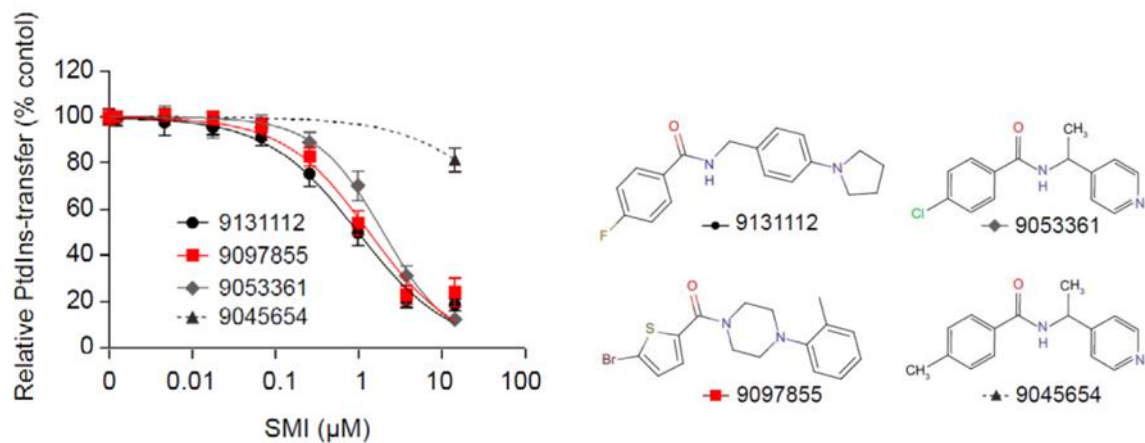


Figure 43. Inhibition of Sec14-mediated PtdIns transfer activity.

Transfer of radiolabelled phosphatidylinositol (PtdIns), as a percent of the untreated control (y-axis), measured in the presence of 9131-112, 9097-855, 9053-361 and 9045-654 (an inactive derivative) at the indicated concentrations (x-axis). Error bars represent the standard deviation of three independent experiments performed in triplicate.

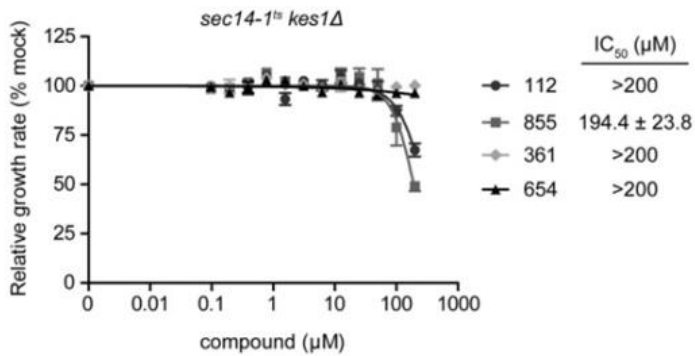
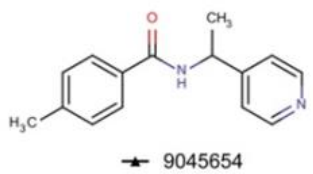
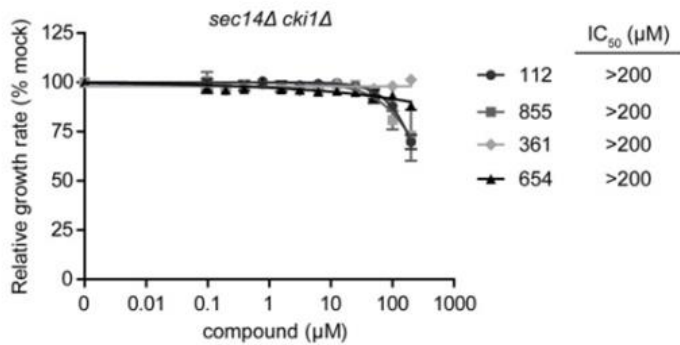
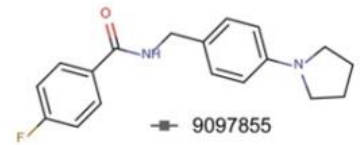
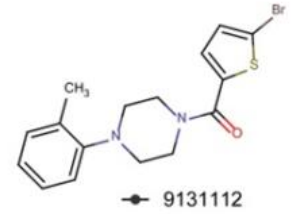
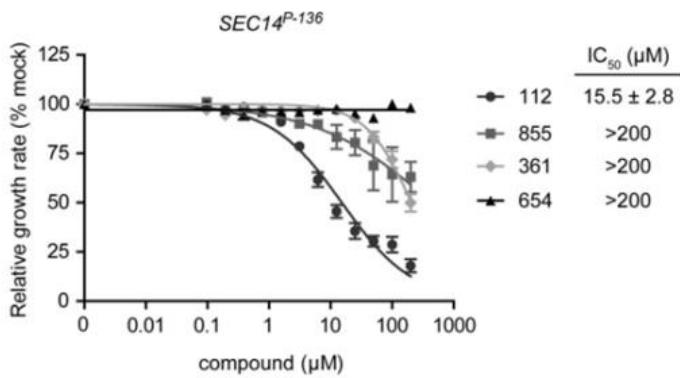
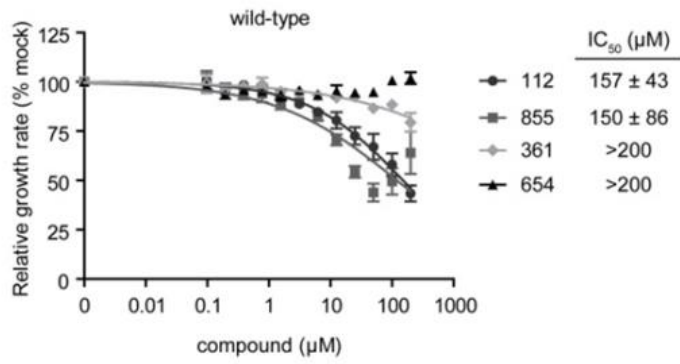


Figure 44. Resistance of Sec14 inhibitors to genetic ‘bypass Sec14’ mutants.

Growth rate relative to the no-drug control (vehicle only; y-axis) was measured in increasing concentrations of 9131-112, 9097-855, 9053-361 and 9045-654 (x-axis) concentration. Results for wild-type (CTY182; top panel), a *SEC14* promoter mutant (CTY374; *SEC14*^{P-136}), in which steady-state Sec14 protein levels are reduced ~7 fold relative to wild-type (second panel), the *SEC14* bypass mutants, *cki1Δ* (CTY303; third panel) and *kes1Δ* (CTY159; bottom panel) are shown. Plotted are the mean of 3 replicates; error bars represent the standard error of the mean (s.e.m.). IC₅₀s represent the 95% confidence interval. Chemical structures are shown on the right.

The natural product himbacine is an active Sec14-inhibitor

Interestingly, the natural product himbacine was identified as a potential Sec14-directed small molecule inhibitor (our unpublished results). Himbacine is an alkaloid that was originally isolated from the bark of the Australian magnolias (**Figure 45**). It is an inhibitor of the Muscarinic acetylcholine receptor M2 and subsequently became of interest for Alzheimer research (Chackalamannil, Doller et al. 2004). Currently an analogue of himbacine is in clinical trials as a thrombin receptor antagonist (Chackalamannil, Wang et al. 2008). There are currently no reported interactions with himbacine and any Sec14-like protein. Given the number of clinical trials that have utilized himbacine it will be useful to identify other binding partners of this natural product.

To determine if himbacine inhibits Sec14 we utilized a similar validation approach to that used in Chapter 2. The analysis was more limited primarily resulting from limited commercial structural analogues and the high cost of himbacine. Our results were as follows: first, himbacine inhibits yeast growth in a dose-dependent manner and changes

appropriately when the Sec14 cellular-load is altered (**data not shown**). Second, ‘bypass Sec14’ yeast are insensitive to himbacine, demonstrating that Sec14 is likely himbacine’s sole-essential target (**data not shown**). Third, himbacine inhibits Sec14-mediated transfer of PtdIns *in vitro* with an IC_{50} of 1164 ± 80 nM (**Figure 46**). Finally, we introduced point mutations into the hydrophobic cavity of Sec14 that endowed himbacine resistance *in vitro* (**Figure 47**). *In silico* docking simulations were unable to resolve coherent docking modes of himbacine (**data not shown**). Because of this limitation, we introduced large changes at the Sec14 PtdCho headgroup recognition site that maintains PtdIns transfer activity but abolishes PtdCho exchange activity [Sec14^{S173I,T175I} (referred to as II) and Sec14^{S173A,T174A} (referred to as AA; Schaaf, Ortlund et al. 2008)]. This data suggests that himbacine occupies space near the PtdCho recognition-site. Detailed mutagenesis analyses are forthcoming.

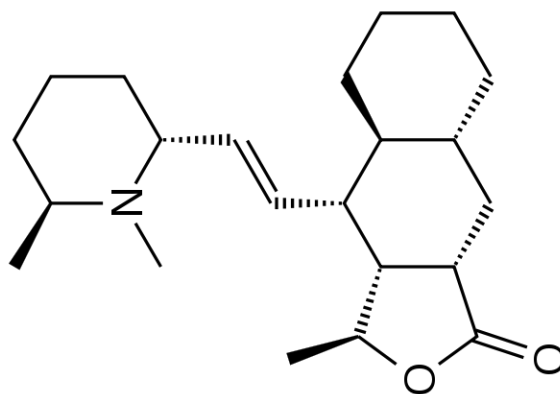


Figure 45. The structure of himbacine.

Chemical structure of himbacine. MW=345.27 g/mol

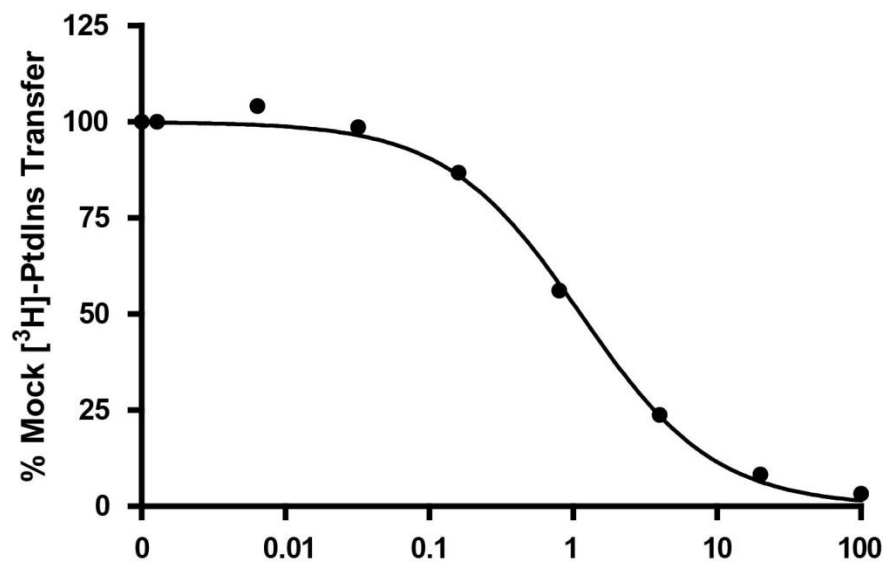


Figure 46. Himbacine inhibits Sec14-mediated PtdIns transfer activity *in vitro*.

Transfer of [³H]-PtdIns as a percent of the untreated control (y-axis), measured in the presence of himbacine at the indicated concentrations (x-axis; in μM). Sec14p activity is clamped at 287nM with a mass of 10μg. The IC₅₀ of himbacine is 1164±80nM and represents the 95% confidence interval.

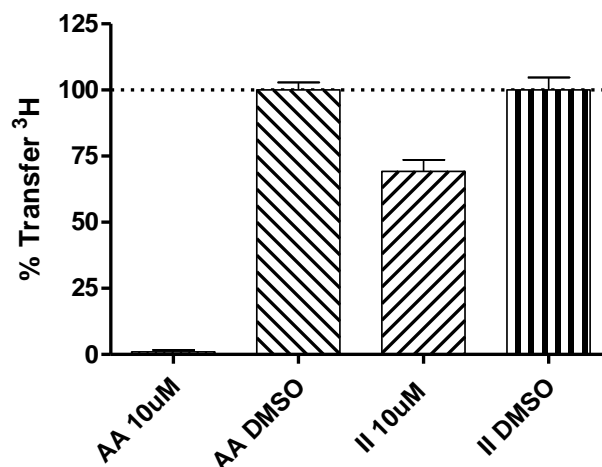


Figure 47. Mutations in the PtdCho binding site of Sec14 confer Himbacine-resistance.

Transfer of radiolabelled phosphatidylinositol (PtdIns), as a percent of the untreated control (y-axis), measured in the presence of 10 μ M himbacine or the vehicle control. Sec14^{S173A,T175A} or Sec14^{S173L,T175I} was clamped at 287nM. Error bars represent the standard error mean of one experiment done in triplicate.

Sec14 inhibitors show inhibitory activity against pathogenic yeast in the *Candida* genus

From a previous chemical screen: SMI 741 or 2-(4-chlorophenyl)-N'-[(2,4-dimethoxybenzoyl) oxy]ethanimidamide, was identified along with NPPM 1278 as a potential inhibitor of Sec14 (Hoon, Smith et al. 2008). Subsequently we selected several SMIs to conduct a limited SAR analysis and isolated SMI 212 as a putative inactive derivative of SMI 741 (**Figure 48**). We demonstrated that SMI 741 shows activity against *S.cerevisiae* with an *in vivo* IC₅₀ of 8.7 \pm 1.4 μ M (**data not shown**) and an *in vitro* IC₅₀ of 1.16 \pm 0.11 μ M (**Figure 49**). Surprisingly, SMI 212 which had a poor ability to inhibit Sec14 *in vitro* (IC₅₀ 74.58 \pm 17.41) had a similar *in vivo* profile in wild-type yeast (CTY182). Additionally, the three 'bypass Sec14' strains *kes1 Δ* , *cki1 Δ* and *sac1 Δ* (CTY159, CTY160, and CTY100, respectively) all had *in vivo* IC₅₀s of ~50 μ M, suggesting that these compounds

have off-target activity in *S.cerevisiae*. Interestingly, the yeast Sec14p homologue in *Candida albicans*, CaSec14, is likely an essential gene; however, its role in dimorphic transition is not clear (Monteoliva, Sanchez et al. 1996).

To monitor SMI 741's potential as an antifungal agent, SMI 741 was incubated with *Candida albicans* in YPD media containing 10% FBS at 37°C to promote dimorphic transitions. We demonstrated that SMI 741 has the ability to inhibit dimorphic transitions in *Candida albicans* (**Figure 50**) and several other species within the *Candida* genus (**Table 3; data not shown**). Interestingly, *Candida galbrata*, a pathogenic species closely related to *Saccharomyces cerevisiae* is also inhibited by NPPM 481 (**Table 3; data not shown**). This data suggests that NPPM 481 may act as a potent antifungal therapeutic in some *Candida* species as an inhibitor of Sec14 or Sec14-like protein. As we discussed in **Chapter 2**, the dimorphic transition of *Yarrowia lipolytica* is controlled by Sec14^{YL} and shows a similar string of pearls phenotype as observed under SMI 741 intoxication. Together this data suggests that these compounds deserve additional attention to probe their applicability as inhibitors of CaSec14 and potentially as therapeutic agents.

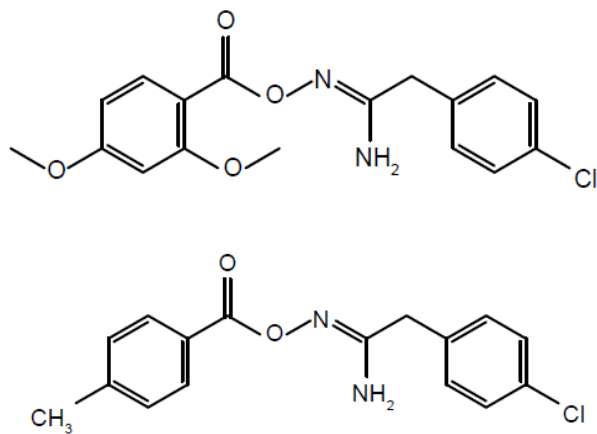


Figure 48. Chemical structure of SMI 741

Figure 48 shows the chemical structure of SMI 741 or 2-(4-chlorophenyl)-N'-[(2,4-dimethoxybenzoyl)oxy]ethanimidamide (left) and SMI 212 or 2-(4-chlorophenyl)-N'-[(2,4-dimethoxybenzoyl)oxy]ethanimidamide (right).

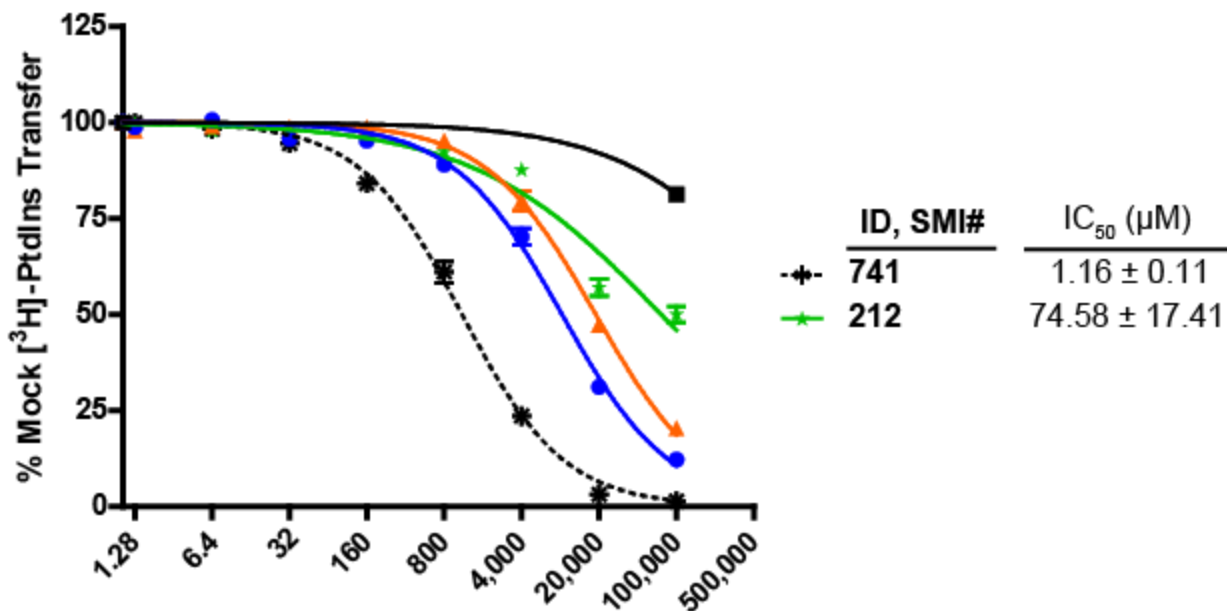


Figure 49. Inhibition of *Saccharomyces cerevisiae* Sec14 *in vitro* by SMI 741

Transfer of [³H]-PtdIns as a percent of the untreated control (y-axis), measured in the presence of the indicated SMI at the indicated concentrations (x-axis; in μM). Sec14p is clamped at 287nM with a mass of 10μg. The IC₅₀ is indicated to the right and represents the 95% confidence interval. Error bars represent the s.e.m. of three independent experiments.

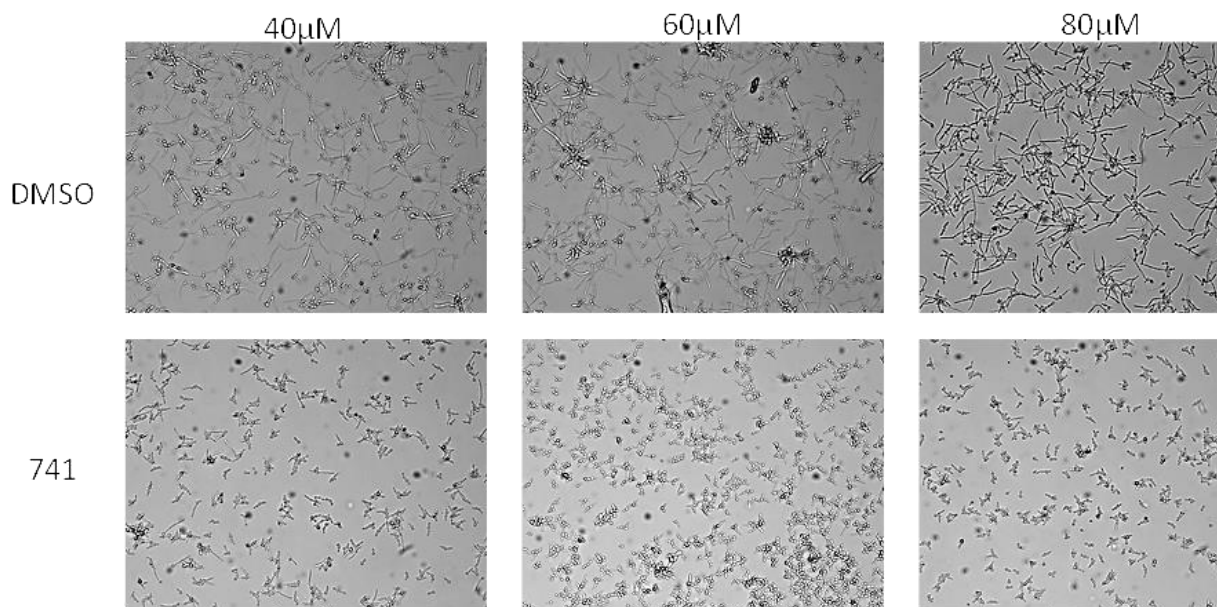


Figure 50. SMI 741 inhibits dimorphic transitions in *Candida albicans*.

An overnight culture of *Candida albicans* was grown in 2% glucose YPD at 30°C and transferred to the same media supplemented with 10% FBS at 37°C to initiate dimorphic transition. At that time SMI 741 or the vehicle control (DMSO) was added, and the cells were imaged 6 hours later with differential interference contrast (DIC) microscopy. The IC₅₀ of inhibiting the dimorphic transition was approximately 40µM.

Table 3. SMI 741 inhibits dimorphic transitions in <i>Candida albicans</i>			
Candida species	Drug	Dymorphic Transition?	Dimorphic inhibition with Drug?
<i>Candida albicans</i>	741	YES	YES
<i>Candida tropicalis</i>	741	YES	YES
<i>Candida parapsilesis</i>	741	YES	YES
<i>Candida krusei</i>	741	YES	YES
<i>Candida kefyr</i>	741	YES	YES
<i>Candida galbrata</i>	481	NO	Inhibits growth
Cultures grown at 37°C in YPD containing 2% glucose and 10% FBS			

Discussion: alternative sec14-directed inhibitors

Many fungal pathogens are capable of reversibly transitioning between blastospore and hyphal growth phases, termed a dimorphic transition. Dimorphic transitions are proposed to promote pathogenic activities of fungi; however, it is likely only one of many contributing factors (Brown and Gow 1999; Gow, Brown et al. 2002). To investigate Sec14's role in dimorphic transitions, the model system *Yarrowia lipolytica* was employed, demonstrating that the Sec14p's homologue, Sec14^{YL}, is a non-essential (probably due to additional isoforms), Golgi-associated protein that modulates *Y.lipolytica*'s dimorphic transition (Lopez, Nicaud et al. 1994). This transition is regulated by the delivery of plasma membrane and cell envelope proteins that are specific for mycelial growth. Interestingly, this defect is bypassed through the addition of the neutral lipid, oleic acid (Titorenko, Ogrydziak et al. 1997) which enlarges lipid droplets and lowers the ratio of TAG to sterol esters in *Y.lipolytica* (Athenstaedt, Jolivet et al. 2006).

Candida infections or candidemia, represent a large cause of nosocomial infections in the United States, resulting in an estimated annual mortality rate between 2800 and 11,200 deaths. Of the *Candida* species, the majority of infectious episodes are caused by *Candida albicans* (Pfaller and Diekema 2007). *C.albicans* is a commensal, dimorphic fungus, often found in the human gastrointestinal tract. Most commonly, mucosal membranes are the sites of infection resulting in oropharyngeal, esophageal and vaginal candidiasis; however, more severe systemic infections can occur. All individuals are susceptible to infection although contributing factors include wide spectrum antibiotics, corticosteroids, hormone therapy, and HIV (Calderone 2002).

Additionally, multiple Sec14-like and mammalian PTP protein have been cloned from *Dictyostelium discoideum* that can bind and transfer PtdIns and PtdCho (Swigart, Insall et al. 2000). Recently, a novel Sec14-like protein was identified in *Taenia solium* or Sec14Tsol. *T.solium* is an infectious parasite found in humans and porcine that can cause cysticercosis or neurocysticercosis. Sec14Tsol binds phospholipids and is localized to the Golgi membranes of the metacestode tegument, suggesting a potential role in host interactions (Montero, Gonzalez et al. 2007; Sinha and Sharma 2009). Although antifungal agents exists against *C.albicans* (Sobel 2008) and cysticides for *T.solium* (Sinha and Sharma 2009); none probe the hydrophobic patch of Sec14, providing an attractive, and essentially virgin territory to combat these pathogens.

Together this data suggests that a wide range of chemical structures are capable of inhibiting Sec14 activity *in vivo* and *in vitro*. These compounds will require additional validation for their use as tool or therapeutic agents. However, we have identified a number of lead compounds that may provide information for the development of novel SMIs directed against Sec14-like proteins.

Materials and methods

Molecular graphics and chemical drawing

Molecular graphics and analyses were performed with the UCSF Chimera package (version 1.8; <http://www.cgl.ucsf.edu/chimera/>; Pettersen, Goddard et al. 2004). Marvin was used for drawing, displaying and characterizing chemical structures, substructures and reactions, Marvin 5.10.0 and 5.11.4, 2012, ChemAxon (<http://www.chemaxon.com>). Docking poses and cavity surfaces were generated using MOE suite (2011.10; Chem. Comp. Group Inc., Montreal, Canada).

Yeast strains, media and reagents

Yeast media and transformation methods are described (Sherman 1983). Restriction endonucleases were from New England Biolabs (Ipswich, MA), standard reagents from Sigma (St. Louis, MO) or Fisher Scientific (Norcross, GA), and all phospholipids were purchased from Avanti Polar Lipids Inc. (Alabaster, AL). [³⁵S]-Translabel was purchased from MP Biomedicals (Irvine, CA). Yeast strain genotypes are listed in **Table 9** and plasmids in **Tables 10 and 11**.

Small molecule inhibitors

The compounds shown in **Figure 8** were from ChemDiv (San Diego, CA). SMIs BBV34896-755, BBV34846-244, Z1082669-326, BBV34846-247, BBV34847-734 were synthesized by UORSY/Ukrorgsyntez Ltd. (Riga Latvia). Himbacine was purchased from

Enzo Life Sciences. Unless otherwise noted, all other compounds were purchased from ChemBridge Chemical Store, San Diego, CA (www.hit2lead.com). SMIs were dissolved in DMSO (Fisher, D128-500) to a final stock concentration of 20mM and stored in the dark at room temperature.

Chemogenomic screening

Pools of bar-coded homozygous and heterozygous deletion strains were grown in YPD + 25mM HEPES (pH 6.8) supplemented with 4130-1276 (6.7 μ M) for 5 and 20 generations, respectively. Genomic DNA extraction, PCR amplification of molecular barcodes, and Genflex tag16k array hybridization/scanning (Affymetrix), and analysis of chemogenomic data, were as described (Hoon, Smith et al. 2008). Quantile normalized fluorescence values for each tag were log₂-transformed, and z-scores calculated: Tag z-score = [(average of controls)-(experimental value)]/(std. dev. of controls); where the controls were 12 replicate samples of pools treated with DMSO. The z-score for each strain is the average of the two tags associated with that strain, and represents the sensitivity value.

Docking simulations

Several independent docking platforms were used. These included; GOLD [CCDC] (Jones, Willett et al. 1997); Glide (Friesner, Murphy et al. 2006); QM Polarized Ligand Docking [QM-PLD] (Cho, Guallar et al. 2005). Details are presented in the Methods section.

GOLD docking

Computational docking used the genetic algorithm-based ligand docking program GOLD (version 3.0.25; Jones, Willett et al. 1995; Jones, Willett et al. 1997). GOLD exhaustively explores ligand conformations and provides limited flexibility to protein side chains with -OH groups by reorienting the hydrogen bond donor and acceptor groups. The GOLD scoring function is based on favorable conformations found in Cambridge Structural Database, and on empirical results of weak chemical interactions. The active site was defined by a single solvent accessible point near the center of the protein active site, a radius of ~10 Å, and the GOLD cavity detection algorithm. GOLD docking was carried out without constraints to obtain an unbiased result and to explore all possible ligand binding modes. Ligand was docked in independent runs, 50 solutions were produced for each run, (except for one where 20 were generated), as opposed to the default of 10, and early termination of ligand docking was switched off. All other parameters were as the defaults. All ligands were docked using the same parameters.

Hydropathic scoring

The HINT (Hydropathic INTERactions) scoring function was used to analyze docking solutions (version 3.11S b; Meng, Kuntz et al. 1994; Abraham, Kellogg et al. 1997). HINT evaluates each atom-atom interaction in a biomolecular complex using a parameter set derived from solvation partition coefficients for 1-octanol/water. The thermodynamic parameter $\text{Log } P_{o/w}$ can be directly correlated with free energy. HINT describes specific interactions between two molecules as:

$$B = \sum \sum b_{ij} = \sum \sum (a_i S_i a_j S_j R_{ij} T_{ij} + r_{ij})$$

where a is the hydrophobic atom constant derived from $\text{Log}_{o/w}$, S is the solvent accessible surface area, T is a function that differentiates polar-polar interactions (acid–acid, acid–base or base–base), and R , r are functions of the distance between atoms i and j as previously described (Abraham, Kellogg et al. 1997). The binding score, b_{ij} , describes the specific atom–atom interaction between atoms i and j , whereas B describes the total interaction. For selection of the optimum docked conformation and to further differentiate the relative binding efficacy of the NPPM ligands, interaction scores were calculated for each pose found by docking. The protein and ligands were partitioned as distinct molecules. ‘Essential’ hydrogen atoms, that is, only those attached to polar atoms (N, O, S, P), were explicitly considered in the model and assigned HINT constants. The inferred solvent model, where each residue is partitioned based on its hydrogen count, was applied. The solvent accessible surface area for the amide nitrogens was corrected with the ‘+20’ option.

Glide docking

Protein and ligands were prepared using Protein Preparation Wizard and LigPrep module of Maestro 9.2 Interface of Schrodinger Suite (Schrodinger Suite 2012; Glide version 5.8). Receptor Grids were generated without using any constraints and standard settings were used. Docking was performed using Standard Glide and QM-PLD modules with SP and XP scoring function respectively (Friesner, Banks et al. 2004; Halgren, Murphy et al. 2004; Cho, Guallar et al. 2005; Friesner, Murphy et al. 2006). No similarity, torsional and inter-molecular interaction (hydrogen bonding or hydrophobic) constraints were used. Ligand was

docked flexibly with nitrogen inversions and ring sampling turned on with post-docking minimization.

PLIF

Protein-Ligand Interaction Fingerprint (PLIF) was calculated within MOE suite (2011.10; Chem. Comp. Group Inc., Montreal, Canada; Labute 2001; Clark, Labute et al. 2006; Clark and Labute 2007). PLIF was calculated between a closed Sec14 conformer and 6 representative binding modes produced by the docking runs. The protein Ligand Interaction Fingerprint (PLIF) is a method to encapsulate the interaction between ligands and proteins using a fingerprint scheme. To generate PLIF within MOE, maximum 250 bits were used with Min Score 1 turned off and keeping the Min Score 2 to its default value.

Hierarchical cluster analysis

The clustering of a chemical data set consists of merging compounds into independent clusters that include chemically similar molecules as determined by their tanimoto score. We employed the Sequential Agglomerative Hierarchical Nonoverlapping (SAHN) method implemented in the ISIDA/Cluster program (<http://infochim.u-strasbg.fr>; Fourches, Barnes et al. 2010). The ISIDA/Cluster allows visualization of molecular structures in each cluster to draw the heat map of the tanimoto coefficient similarity matrix, as well as the dynamic dendrogram of compound clusters.

FACS sorting

Cells were grown to mid-logarithmic phase ($OD_{\lambda_{600}}=0.5$) and either subjected to a temperature shift or SMI intoxication for 3h. Cells were sonicated for 10 sec. and resuspended in 70% ethanol overnight at room temperature. Cells were washed twice in 50mM Tris-HCl pH=7.8, and resuspended in 200 μ g of RNaseA overnight at 37°C. Cells were then resuspended in 50mM Tris-HCl pH=7.8 and 2.5mg of pepsin for 30 min. at 37°C. Subsequently, cells were washed in 200 mM Tris-HCl pH7.5, 211 mM NaCl, 78 mM MgCl₂, and resuspended in 0.55ml of the same buffer containing 16 μ g/ml of propidium iodide. Prior to FACS sorting cells were again sonicated for 10 seconds to break up clumped cells. Cells were analyzed with a Becton Dickinson LSRII and the data was analyzed with FlowJo (Tree Star, v 7.6.5) and fit to the Dean-Jett-Fox algorithm. Values are given as a percentage of cells counted.

Protein purification

Recombinant proteins were purified essentially as described (Schaaf, Ortlund et al. 2008). In summary, pET28b-His₈-Sec14, pET28b-His₈-Sfh1, pET28b-His₈-Sfh3 and pET28b-His₈-Sfh4 were grown in *E.coli* BL21 (DE3; New England BioLabs Inc, Ipswich, MA). Sfh2 and Sfh5 expression was driven by pQE30-His₆-Sfh2 and pQE30-His₆-Sfh5 vectors in *E.coli* strain KK2186 (Li, Routt et al. 2000). Recombinant proteins of interest were bound to TALON metal affinity beads (Clontech, Mountain View, CA), and eluted with imidazole (10mM-200mM gradient) and dialyzed (Prod # 68100, Thermo Scientific, Rockford, IL). In the case of Sec14, dialysis was against 300mM NaCl, 25mM Na₂HPO₄

(pH=7.5), 5mM β -mercapthoethanol. Purified Sfh proteins were dialyzed against the same buffer with the exception that 50mM Na_2HPO_4 was used. Proteins mass was quantified by SDS-PAGE with BSA standard and A_{280} .

Rat liver microsomes

Rat liver microsomes containing [^3H]-PtdIns were produced as previously described (Paulus and Kennedy 1960). In summary, six rats were euthanized and their livers removed, blended and dounce homogenized 10 times in a 30% SET buffer (pH 7.4, 250 mM Sucrose, 5mM Tris-HCL, 1mM EDTA). The slurry was centrifuged for 10 min. at 1000xg and the supernatant was centrifuged for 90 min. at 95,000xg. The pellet was resuspended in 80 ml cold pH=7.4, 20mM Tris-KCL. 0.8mL of 1M MnCl_2 was added containing 100 μCi of [^3H]-inositol and incubated for 2hr at 37°C. The slurry was centrifuged for 1hr at 95,000xg and the supernatant was decanted. The pellet was serially centrifuged, resuspended and washed in 10mM Tris-HCL, 2mM inositol pH=8.6, then 1mM Tris-HCL, 2mM inositol, pH=8.6, and finally resuspended in cold SET buffer.

PtdIns-transfer assays

[^3H]-PtdIns-transfer assays were performed using established methods (Schaaf, Ortlund et al. 2008). In assays involving SMI, purified recombinant PITP was pre-incubated in the presence of acceptor membranes, buffer (300mM NaCl, 25mM Na_2HPO_4 , pH 7.5) and SMI for 30 min. at 37°C prior to initiating the assay by addition of radiolabeled donor membranes. Fractional transfer of [^3H]-PtdIns was normalized to mock DMSO controls.

Nonlinear regression was applied to the dataset to calculate the best fit equation using $[Y=100/(1+10^{((\text{LogIC}_{50}-X)*\text{HillSlope}))}]$ in Graphpad Prism v5.0. Statistical comparisons of inhibition was calculated using “extra sum-of-squares F-test” in Graphpad prism v 5.00.

Statistical analyses

Curve fitting and t-test were performed using GraphPad Prism version 5.00 for Windows, GraphPad Software, La Jolla California USA (www.graphpad.com) unless otherwise noted. General data handling was carried out in Excel 2010 (v14.0.4734.1000, 32-bit; Microsoft Corporation). Statistical comparisons of [³H]-PtdIns transfer activities and growth inhibition were calculated using the “extra sum-of-squares F-test” in Graphpad prism v 5.00.

Growth rate analyses

Growth assays were conducted in 96 well microtiter plates. In **Figures 8 and 9**, optical densities were measured every 15 min. over the course of 20 hours using a GENios microplate reader (Tecan). All other growth rates were determined as follows. Cells were cultured to mid-logarithmic growth phase in YPD medium (2% glucose) and diluted to $\lambda_{600\text{nm}}=0.1$ in media appropriately supplemented with SMI or DMSO. Cultures were incubated in 96 well plates in a final volume of 250 μ l of YPD (2% glucose) for 10-16 hours between 30°C and 32°C. ODs were measured every 15 min. at $\lambda_{610\text{nm}}$ (BioTek Synergy 2) or $\lambda_{595\text{nm}}$ (PerkinElmer VictorX3 3030 Multilabel Plate Reader). Doubling times were calculated and

normalized to an internal DMSO control. Nonlinear regression was applied to the dataset to calculate the best fit equation using $[Y=100/(1+10^{((\text{LogIC}_{50}-X)*\text{HillSlope}))}]$ in Graphpad Prism v5.0. IC₅₀ values represent the 95% confidence interval from at least three independent experiments unless otherwise noted. Statistical comparison of SMI-mediated growth inhibition were determined using the “extra sum-of-squares F-test” in Graphpad prism v 5.00.

[³H]-Serine labeling of yeast cells

[³H]-Serine radiolabeling of yeast strains was performed as previously described (Wu, Routt et al. 2000), with modification. The indicated strains were grown overnight at 30°C in uracil- and serine-free minimal media containing glucose (3%), ethanolamine (2mM), and sub-cultured to a $\lambda_{600\text{nm}}=0.3$. Cells were metabolically radiolabeled for 3h with 3.33 $\mu\text{Ci/ml}$ L-[³H]-serine (ART 0246; American Radiolabeled Chemicals Inc., St. Louis, MO), and either shifted to 37°C, or challenged with 6748-481 (20 μM) or DMSO for 3h, as appropriate. Labeling was terminated upon addition of ice-cold trichloroacetic acid (10% final concentration), and samples were incubated on ice for 30 min. Pellets were washed 2X with cold ddH₂O and re-suspended in ddH₂O: absolute ethanol (1:4, v/v) at 100°C for 45 min. The aqueous phase was re-extracted with CHCl₃:CH₃OH:0.2M KCl (4:4:3.3 v/v/v). The organic phase was washed 2X with PBS: CH₃OH (9:10, v/v), dried under N₂ gas, and the lipid film re-suspended in CHCl₃:CH₃OH (2:1, v/v) with 1mg/ml of butylated hydroxytoluene. Lipids were resolved by Silica Gel H thin layer chromatography (Analtech, Newark, DE) in a CHCl₃:2-propanol:0.25% KCl:triethylamine (30:9:6:18, v/v/v/v) solvent

system. Plates were sprayed with 0.2% (w/v) 8-anilino-1-naphthalenesulfonic acid, and lipids visualized under UV illumination. Individual lipid species were identified by internal standards (Avanti Lipids), collected, and radioactivity quantified by liquid scintillation counting. Sample loads were normalized by total cpm.

Choline release assay

Yeast strains were cultured to mid-logarithmic growth phase at 30°C in choline-free yeast nitrogen base (Difco 2015-08-31) supplemented with uracil, histidine and glucose (2%). Yeast were washed twice with ddH₂O, resuspended in fresh choline-free media and challenged with SMI, DMSO and/or temperature shift to 37°C, as appropriate. After 2h, cells were pelleted by centrifugation, the culture supernatant were collected and filtered through a 0.45µm (pore size) filter. Free choline was determined using a choline oxidase-coupled Trinder reaction where H₂O₂ (produced via enzymatic oxidation of choline by choline oxidase; Sigma C5896) was reacted with phenol, 4-aminoantipyrine (Sigma A4382) and peroxidase (Sigma P6782). The resulting quinoneimine was quantified spectrophotometrically at $\lambda_{490\text{nm}}$. Standard curves relating choline concentration (Acros A4382) to quinoneimine production were used to extract absolute choline concentrations (Warnick 1986; Li, Routt et al. 2000).

Homology modeling of sec14 closed conformation

A homology model for the closed conformer of Sec14 was generated using the Modeller program (Šali and Blundell 1993) based on the templates of the open conformer of Sec14 (PDB ID 1AUA; Sha, Phillips et al. 1998) and the closed conformer of Sfh1 bound to PtdIns (PDB ID 3B7N; Schaaf, Ortlund et al. 2008). Gate residues in the Sec14 open conformation (I₂₁₅ – Y₂₄₇) were removed from that template structure prior to modeling whereas the corresponding gate residues in the closed conformation in Sfh1/PtdIns were retained. In addition, residues Ala 84–Gln 111 on the far side of the binding pocket from the gate were removed from the Sfh1 template prior to modeling since they were structurally divergent from the corresponding Sec14 residues.

Site-directed mutagenesis

Site-directed mutations were generated using QuickChangeTM (Stratagene) as recommended by the manufacturer. Primer sequences are available from the authors by request.

Transmission electron microscopy

Yeast were grown to an OD_{600 nm}=0.5 and cultures were either shifted to 37°C for 2 hours or challenged with 20µM SMI for 2 hours at 30°C. Cells were fixed in 3% glutaraldehyde, converted to spheroplasts, stained with 2% OsO₄ and 2% uranyl acetate, dehydrated in a 50%, 70%, 90% ethanol series, and washed in 100% ethanol and 100% acetone, respectively. Cell pellets were embedded into Spurr's resin at 60°C for 48h and

sectioned (Adamo, Moskow et al. 2001). Thin sections produced from strains in the *SEC14^{P-136}* (CTY374) background were imaged at 80 kV on a Tecnai 12 electron microscope (FEI, Hillsboro, OR), and images captured using Gatan micrograph with version 3.9.3 software (Gatan, Pleasanton, CA). All other samples were visualized on a Jeol 1200 EX TEM operated at an accelerating voltage of 100 kV. Images were captured at calibrated magnifications using an optically coupled 3k slow scan CCD camera (model 15C, SIA, Duluth, GA) and Maxim DL imaging software.

Metabolic labeling and immunoprecipitation

Samples were prepared as previously described with modification (Phillips, Sha et al. 1999; Rivas, Kearns et al. 1999). Strains were grown in minimal media lacking methionine and cysteine to mid-logarithmic phase ($OD_{600nm} \sim 0.5$). Where indicated, cultures were treated with 20 μ M SMI or shifted to 37°C for 2h and radiolabeled with 20 μ Ci/ml [³⁵S]-amino acids (Translabel; MP Biomedicals). Chase was initiated by addition of unlabeled methionine and cysteine (2 mM each, final concentration) and terminated with trichloroacetic acid (5% wt/vol, final concentration). CPY immunoprecipitation, SDS-polyacrylamide gel electrophoresis (PAGE), and autoradiography were performed as described (Young, Craven et al. 2001). In washout experiments, cultures were pulse-radiolabeled and subjected to chase. Cells were then pelleted (30sec at 4,000rpm), washed 2X with fresh YPD medium, resuspended in YPD containing cyclohexamide (100 μ g/ml), and further incubated for the indicated times at 30°C. Subsequently, cells were poisoned with trichloroacetic acid (5% wt/vol, final concentration) and samples further processed as described above.

Phosphoinositide analyses

Strains CTY182 (wild-type) or CTY100 (*sec14-1^{ts}*, *sac1Δ*) were grown overnight in uracil-free minimal media containing 3% glucose, 1% case amino acids and labeled to steady state for at least 20h with 10 μ Ci/ml [3 H]-*myo*-inositol (ART 0116A; American Radiolabeled Chemicals Inc., St. Louis, MO). Cells were either shifted to 37°C, or challenged with NPPM or DMSO vehicle for 3h, as appropriate. Labeling was terminated with trichloroacetic acid (5% final concentration) and samples incubated on ice for 30 min. Cells were pelleted (10,000 rpm for 1 min), washed twice in 500 μ l of cold ddH₂O, and resuspended in 500 μ l 4.5% perchloric acid. Approximately, 300 μ l of 0.5mm glass beads were added and cells disrupted by vigorous agitation for 10 min in 1 min bursts with 1 min rest on ice.

In experiments where inositol-glycerophospholipids were deacylated and resolved by strong anion exchange HPLC, bulk lipids were extracted as previously described with modification (Stolz, Kuo et al. 1998). Lipids were extracted in 2x 250 μ l of CH₃CH₂OH:ddH₂O:(C₂H₅)₂O:C₄H₉OH (15:15:5:1 vol/vol), dried under N₂ gas, and deacylated (Clarke and Dawson 1981) by resuspension in 300 μ l of CH₃OH:ddH₂O:C₄H₉OH:CH₃NH₂ (0.8:0.6:0.2:0.35 vol/vol) and incubation for 30 min. at 53°C. 100 μ l of cold CH₃CH₂CH₂OH was added to the solution, the liquid centrifuged to dryness under vacuum, and the dessicate resuspended in 400 μ l ddH₂O. The solution was extracted 2X with 750 μ l 1-butanol:petroleum ether:ethyl formate (20:4:1 v/v/v), adjusted to 10mM (NH₄)₃PO₄, (pH 3.5), and soluble glycerophosphoinositols resolved and quantified by HPLC (Stolz, Kuo et al. 1998; Guo, Stolz et al. 1999; Rivas, Kearns et al. 1999).

In experiments where phosphoinositides were quantified by thin layer chromatography, the lysate from disrupted cells was collected and centrifuged at 13,000 rpms for 10 min., the pellet washed with 500 μ l of 100mM EDTA (pH 7.4), and resuspended in 500 μ l of CHCl₃:CH₃OH:HCL (2:1:0.007). A two-phase system was produced by addition of 100 μ l of 0.6M HCl, the sample vortexed for 5 min., and sample centrifuged for 5 min. (13,000 rpm). The organic phase was collected, washed 2X with 250 μ l of CH₃OH:0.6M HCl:CHCl₃ (1:0.94:0.06), dried under N₂ gas and resuspended in 50 μ l CHCl₃. Samples were resolved by thin layer chromatography on Partisil LK6DF 60Å silica gel plates (Whatman, Cat# 4866-821) using a CHCl₃:CH₃OH:ddH₂O:NH₄OH (1:0.83:0.15:0.1) solvent system. Lipids were visualized by autoradiography and quantified with ImageJ (version 1.47t, National Institute of Health; Schneider, Rasband et al. 2012).

Fluorescence imaging

N-[3-Triethylammoniumpropyl]-4-[*p*-diethylaminophenylhexatrienyl] pyridinium dibromide (FM4-64; Invitrogen, Carlsbad, CA) staining was performed essentially as described (Vida and Emr 1995). Cells were grown to mid-logarithmic phase (OD_{600 nm}=0.5) in YPD medium at 30°C, then either shifted to 37°C for 2h or treated with 20 μ M SMI at 25°C for 2 h. Subsequently, cells were pulsed with 10 μ M FM4-64 (Invitrogen) for 15 min. washed 2X in YPD media matched to the appropriate drug or temperature condition. Labeling was terminated at indicated times by washing cells in NaN₃/NaF (1mM final concentration of each) and placing samples on ice prior to imaging.

Cultures for GFP-Snc1 imaging were grown in synthetic defined medium lacking uracil at 30°C. Cells processed for imaging of phosphoinositide biosensors were collected from liquid cultures grown in uracil-free YNB supplemented with 3% glucose and 1% casamino acids at 25°C by centrifugation at 4,000 rpm for 1 min, and resuspended into fresh uracil-deficient medium prior to analysis. Cells were immobilized onto a thin layer of growth medium with 20% gelatin (G-2500, Sigma-Aldrich), sealed under a coverslip with Valap, and examined at 25°C as described (Coffman, Nile et al. 2009). The imaging system employed a CFI plan apochromat lambda 100x oil immersion objective lens NA 1.45 mounted on a Nikon Ti-U microscope base (Nikon, Melville, NY) interfaced to a Photometrics CoolSNAP HQ2 high sensitivity monochrome CCD camera (Roper Scientific, Ottobrunn, Germany) or an Andor Neo sCMOS CCD camera (Andor Technology, Belfast, UK). A Lumen 200 Illumination System (Prior Scientific Inc., Rockland, MA.) was used in conjunction with a B-2E/C (465-495nm/515-555nm;EX/EM) or G-2E/C (528-553nm/590-650nm;EX/EM) filter set (Nikon, Melville, NY). Images were captured using the Nikon NIS Elements software package (Nikon, Melville, NY, version 4.10) and exported as .TIF files. Image analyses were performed using ImageJ (version 1.47t, National Institute of Health; Schneider, Rasband et al. 2012) and figures were constructed using Adobe Illustrator and Adobe Photoshop CS6 (version 15.0.0).

Simulation of charge distribution on activated aryl halides

Wave function calculations were carried out using the PC Spartan package (Wavefunction Inc. Irvine, CA; version 10 1.1.0). Starting geometries were obtained using

Spartan's interactive building mode, and pre-optimized using the MMFF force field. Wave functions were approximated using the Hartree-Fock method at the 3-21G^(*) gaussian basis set. Electrostatic potentials were generated onto surfaces of molecular electron densities (0.002 electrons per Å³).

Invertase secretion assays

Total and extracellular invertase activities were determined by modification of a previously described assay (Bankaitis, Malehorn et al. 1989). Cells were grown to mid-logarithmic phase in YPD (2% glucose) at 30°C. Cultures were split and cells were cultured at 30°C ± NPPM (20µM) or DMSO or 37°C for 1h in YPD (2% glucose), as indicated. Cells were then pelleted (2000g), washed twice with pre-warmed YPD (0.1% glucose), resuspended in the low glucose YPD medium, and incubated as before for 1.5h. To halt trafficking, samples were adjusted to 10mM NaN₃, and incubated on ice. The samples were washed 3X with 500µl ice-cold 10mM NaN₃ and re-suspended in 500µl of the same. The samples were split into 10mM NaN₃ buffers ± 0.2 % Triton X-100 (final) with the Triton-solubilized fractions also being subjected to one cycle of freeze-thaw to generate the permeabilized cell fraction. The partner non-permeabilized and permeabilized samples were used to determine extracellular and total invertase activities, respectively, using the assay of Goldstein and Lampen (Goldstein and Lampen 1975). Invertase units were expressed as nmoles of glucose produced per min. at 30°C.

Sequence alignment

Protein sequences were acquired from the Universal Protein Resource (Consortium 2012), aggregated using UGENE (version 1.10.1; <http://ugene.unipro.ru/>; Okonechnikov, Golosova et al. 2012), and aligned with the T-Coffee module using the default settings (Notredame, Higgins et al. 2000). Homologous sequences were superimposed onto structural models (PDB IDs 1AUA, 1OLM, 3B7Z, 4FMM) to highlight the PtdIns/PtdCho lipid binding barcode (Schaaf, Ortlund et al. 2008; Nile, Bankaitis et al. 2010).

NPPM chemogenomic interactions

Interactions were determined according to their Gene Ontology (GO) descriptors (Ashburner, Ball et al. 2000). Data sets from chemogenomic profiling were analyzed and enriched gene sets were chosen that had Z-scores greater than 4. Gene-sets that did not pass enrichment threshold are not shown.

Table 4. Chapter two summary
Validation of Sec14-directed small molecule inhibitors
<ul style="list-style-type: none">• Validation of Sec14 as a direct target for NPPMs.• Sec14 is the sole essential cellular NPPM target.• Demonstration of the exquisite phosphoinositide and PtdIns(4)P pathway selectivity shown by these compounds <i>in vivo</i>.

- **Demonstration of the suitability of PITPs as novel targets for specific dissection of phosphoinositide signaling pathways in eukaryotic cells.**

CHAPTER 3: MEASURING AND MODULATING PHOSPHOINOSITIDE SIGNALING IN CELLS

Overview

Phosphatidylinositol phosphates (PIPs) regulate virtually all aspects of cellular function and have been intensely studied for decades. The study of phosphoinositide signaling has been facilitated by the development of tools to monitor and alter cellular PtdIns phosphate levels, activity, and localization. In this Chapter, I will discuss methods used to track and modify PIPs *in vivo*. Additionally, I will discuss many of the tools currently being employed for the attenuation of PIP signaling with focus on small molecule inhibitors of PIP-modifying enzymes. As I discussed in Chapter 1, phosphatidylinositol transfer proteins (PITPs) provide attractive targets for chemical intervention as they channel the activity of phosphatidylinositol kinases. These proteins are also disrupted in a number of inherited mammalian diseases and are essential in a number of pathogenic organisms. In Chapter 2, I designed novel and specific inhibitors of the prototype Sec14-like PITP, demonstrating that even highly homologous Sec14-like PITPs can be selectively inhibited. In conclusion, I will discuss the future discovery of Sec14-like PITPs and proteins that genetically interact with Sec14 using yeast as a platform to interrogate diverse chemical libraries for novel SMIs.

Introduction

All glycerophospholipids in yeast, including the major phospholipids, phosphatidylinositol (PtdIns), phosphatidylserine (PtdSer), phosphatidylethanolamine (PtdEtn), and phosphatidylcholine (PtdCho) are all derived from phosphatidic acid (PtdOH) (Henry, Kohlwein et al. 2012). Each of these lipids is composed of two fatty acid molecules esterified to a glycerol backbone at the *sn*-1 and *sn*-2 positions (**Figure 51**). In the case of PtdIns, a *myo*-inositol is linked to a phosphatidic acid backbone linked by a phosphate group. PtdIns can then be phosphorylated on its inositol headgroup at the 3, 4 and/or 5 position(s) (D-3, D-4 or D-5, respectively) generating five unique combinations in yeast, and seven in mammals (Michell 2008; **Figure 52**). PtdIns represents approximately 10-20 mol% of total cellular phospholipids where PtdIns(4)P and PtdIns(4,5)P₂ are only ~0.1-1 mol% which translates to approximately 2-5% of all PtdIns and the other PIP derivatives are significantly less abundant (Balla 2013). Even though PIPs represent a relatively minor lipid species, they play critical roles in virtually all aspects of cell biology (Balla and Balla 2006; Di Paolo and De Camilli 2006; Bankaitis, Mousley et al. 2010; Balla 2013).

Phosphoinositides are found on the cytoplasmic face of membranes, and through the combinatorial phosphorylation of their inositol ring become discriminating platforms for the recruitment of PIP-binding domains and thus initiate signaling events (Lemmon 2003; Lemmon 2008). PIP-mediated signaling events are critical to normal cellular function and are deranged in numerous human diseases, making their study a topic of intense research. To maintain PIP homeostasis and diversification, cells have evolved numerous enzymes for their regulation: PtdIns hydroxyl kinases, PtdIns phosphate phosphatases, PtdIns transfer proteins (PITPs) and PtdIns-lipases (see **Chapter 1**; Balla 2013). To facilitate the study of these

enzymes and PIPs, multiple techniques have been developed. In this chapter I discuss techniques used to monitor and disrupt PIPs with focus on the chemical modulation of PIP-modifying enzymes. Additionally, I will expand upon the studies in Chapter 2 and discuss several screening methods we developed to identify novel chemical inhibitors of currently ‘undrugged’ enzymes involved in a variety of lipid-signaling pathways.

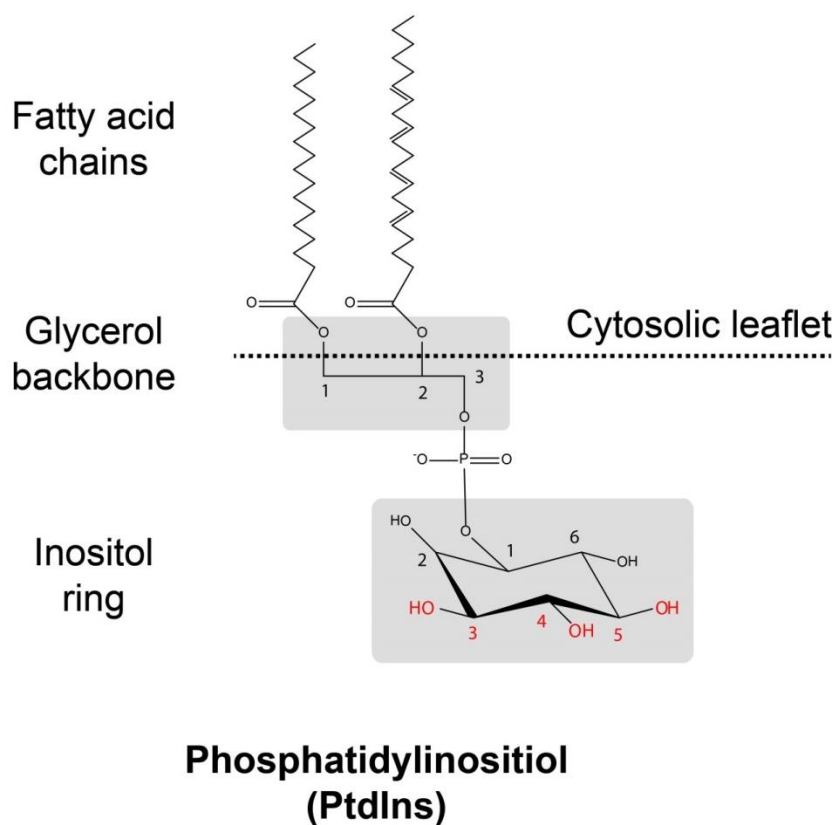


Figure 51 Structure of phosphoinositides

Phosphatidylinositol (PtdIns) is an acidic phospholipid with a phosphatidic acid backbone where *myo*-inositol is linked via a phosphate group. PtdIns can then be phosphorylated at the 3, 4 and/or 5 position(s) on the inositol ring (indicated in red) generating phosphatidylinositol phosphates (PIPs).

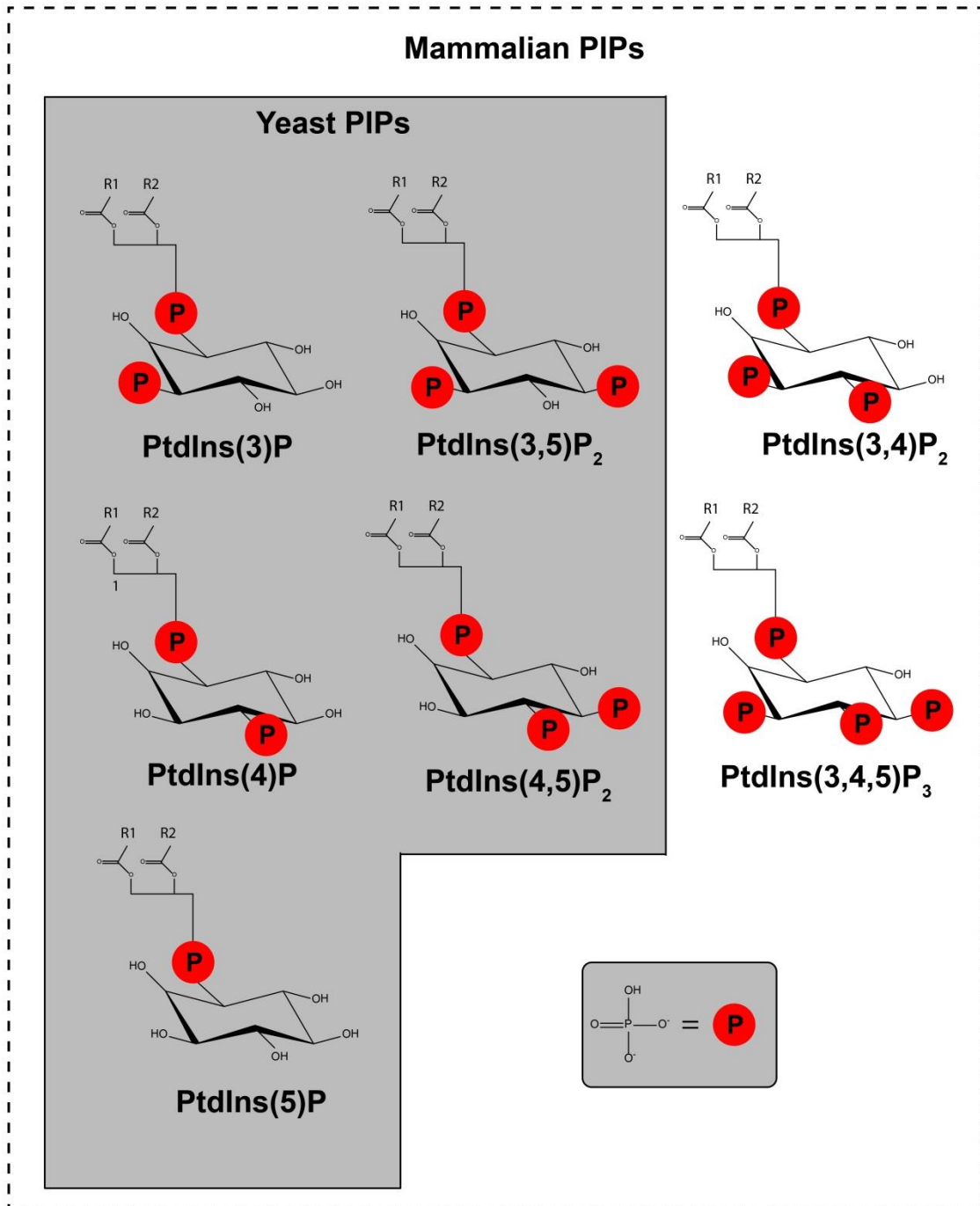


Figure 52. PIP diversity in yeast and mammals
 Variation of phosphoinositides in *Saccharomyces cerevisiae* and mammalian cells. Indicated are the different PIP species found in yeast (gray box) and mammals (all shown PIPs).

Methods to monitor phosphatidylinositol phosphate status

Cells are composed of more than 1000 unique lipid species, all of which contribute to cellular function, making the study, and isolation of desired lipid species difficult simply by their sheer diversity (van Meer 2005). Phosphatidylinositol phosphates (PIPs) constitute a relatively minor lipid species in this mixture, are highly dynamic, have diverse phosphorylation and acyl-chain composition. Because of these factors, the PIP signal to noise ratio is low and requires a robust toolset to monitor their distribution, dynamics and mass, to infer their signaling role(s). Here I detail several of the most common methods used to monitor PIPs through both direct and indirect methods. For more detailed explanations and protocols, the reader is referred to several resources (Balla, Szentpetery et al. 2009; Christie 2010; Davison, Bankaitis et al. 2012; Wymann and Schultz 2012).

Direct measurement of phosphatidylinositol phosphates

The biochemical measurement of PIP levels is accomplished through a variety of methods. Most commonly, radioactive compounds including inorganic phosphate (^{32}Pi or ^{33}Pi) or [2- ^3H]-*myo*-inositol] are incubated with cells, tissue, or whole animals followed by lipid extraction and analysis (Guillou, Stephens et al. 2007; Kim, Shanta et al. 2010). After the desired incubation time and conditions, the material is harvested and the lipids are extracted. Typically extraction employs a chloroform/methanol extraction followed by an acidified (HCl or citric acid) solvent extraction (Guillou, Stephens et al. 2007; Kim, Shanta et al. 2010; Nile, Tripathi et al. 2014). Lipids are often subsequently resolved using thin layer chromatography (TLC; van Dongen, Zwiers et al. 1985) or alternatively, the

glycerolphospholipids can be chemically deacylated with methylamine and the radioactive inositol headgroups isolated (Clarke and Dawson 1981; Guo, Stolz et al. 1999; Rivas, Kearns et al. 1999; Guillou, Stephens et al. 2007; Nile, Tripathi et al. 2014). Following extraction, the inositol headgroup is separated by high-performance liquid chromatography (HPLC) using strong anion-exchange chromatography and radioactivity is detected (*e.g.* β -RAM from LabLogic; Guo, Stolz et al. 1999; Rivas, Kearns et al. 1999; Guillou, Stephens et al. 2007). This technique separates the radioactive inositol headgroups by charge characteristics and is often favored due to its increased reproducibility and quantitative nature. Techniques involving radioactivity often require: long incubations, expensive reagents, specialized equipment, are rarely compatible with the analysis of clinical samples (*e.g.* biopsies, etc.), and typically only monitor steady-state PIPs. Additionally, the radiolabeling of PIPs measures only active-PIPs undergo turnover potentially missing 'dormant' pools.

Several non-radioactive methods exist to monitor PIPs. These methods often suffer from reduced sensitivity compared to radioactive methods and they are less commonly used in the field. First, phospholipids can be separated by TLC and visualized by charring densitometry (Fewster, Burns et al. 1969; Baron, Cunningham et al. 1984). Second, lipids are: isolated, deacylated, and the inositol-phosphates then separated by strong anion-exchange HPLC and then detected with metal/indicator complexes (Mayr 1988). This system monitors absorbance response when the metal is displaced and provides ~ 1 pmol detection, but not all anions can be resolved (Mayr 1988). A more recent technique is to separate the deacylated PIPs after strong-anion HPLC and monitor the PIP-species using suppressed conductivity. The major anionic lipid species detected by suppressed conductivity included PA, PIP, and PIP₂, and these were detected with a 'practical detection

limit' of approximately 100pmol, however, the D-3 isoforms of monophosphorylated and bisphosphorylated PtdIns were measured as the shoulders of peaks. This technique suffers from decreased sensitivity of approximately 1-2 log units compared to isotopic methods (Nasuhoglu, Feng et al. 2002). Currently, there is a push to develop enzyme-coupled detection methods, however these systems still require optimization for their general use (Guillou, Stephens et al. 2007).

Mass spectrometry

Mass spectrometry (MS) systems are becoming increasingly sensitive and are being employed to monitor system-level lipid-profiles or 'lipidomics' with the intent to identify biomarker signatures and measure global lipid profiles (Wenk 2005; Wakelam, Pettitt et al. 2007; Ivanova, Milne et al. 2009). 'Lipidomics' has applied a number of methods to address this question including electrospray ionization (ESI)-MS, atmospheric pressure chemical ionization (APCI)-MS, and matrix-assisted laser desorption/ionization (MALDI)-MS (Wenk 2005). Theoretically, MS will provide a method to measure global nonradioactive PIP levels based on their phosphorylation status and also their acyl-chain characteristics (Wenk, Lucast et al. 2003). Additionally, it may eventually be possible to develop MALDI-MS based methods with acceptable tissue-level PIP localization (Kielkowska, Niewczas et al. 2014).

The low abundance of PIPs coupled with their acidic nature introduces a number of technical challenges. Techniques have been developed to monitor PIPs by MS using ESI-MS, MALDI-TOF-MS, and FAB-MS (Wakelam, Pettitt et al. 2007; Kim, Shanta et al. 2010; Kielkowska, Niewczas et al. 2014). These techniques often allow the parallel profiling of

many phospholipid family members including PIPs; however, PIP and PIP₂ are not differentiated from family members (*e.g.* PIP [PtdIns(3)P vs. PtdIns(4)P vs. PtdIns(5)P] or PIP₂ [PtdIns(3,4)P₂ vs. PtdIns(3,4)P₂ vs. PtdIns(3,4)P₂]; Kielkowska, Niewczas et al. 2014). Although information regarding acyl chain composition can be extracted, PIPs can only be defined as PIP, PIP₂ or PIP₃ while using current MS-based methods and the results will be skewed towards the most abundant PIP in each class (Kielkowska, Niewczas et al. 2014). Therefore PIP₃ is the only PIP species that can be unambiguously assigned acyl-chain compositions (Wakelam and Clark 2011). MS-based methodology to measure PIPs is an emerging, and technically detailed field so the reader is referred to several reviews for additional information (Kim, Shanta et al. 2010; Wenk 2010; Wakelam and Clark 2011; Sparvero, Amoscato et al. 2012; Kielkowska, Niewczas et al. 2014).

Isomer-specific PIP antibodies

Isomer-specific PIP antibodies have been developed as a method to provide superior spatial resolution relative to more global PIP-detection methods, such as radiochemical labeling and mass spectrometry. Unfortunately, their use typically requires fixation and often relegated their use as validation of more sophisticated PIP-monitoring systems. I will not discuss anti-PIP antibodies in detail and the reader is referred to manuscripts that have utilized anti-PIP antibodies. Several commercial antibodies are available that detect: PtdIns(3)P (Nobukuni, Joaquin et al. 2005; Dowling, Vreede et al. 2009; Zornetta, Brandi et al. 2010), PtdIns(4)P (Weber, Ragaz et al. 2006; Blagoveshchenskaya, Cheong et al. 2008), PtdIns(3,4)P₂ (Bae, Ding et al. 2010), PtdIns(4,5)P₂ (Hirono, Denis et al. 2004; Leloup, Shao

et al. 2010), PtdIns(3,5)P₂ (Touchberry, Bales et al. 2010) and PtdIns(3,4,5)P₃ (Weiner, Neilsen et al. 2002). In addition to their role in PIP-localization, anti-PIP antibodies are being explored as therapeutic agents to treat diseases, such as the human immunodeficiency virus (HIV; Brown, Karasavvas et al. 2007).

PtdIns phosphate binding domains

The inositol headgroup of phosphatidylinositol phosphates (PIPs) are exposed to the cytoplasmic face of membranes, where they can selectively recruit PIP-binding domains based on their phosphorylation status and subsequently modulate downstream signaling events (Lemmon 2008). To circumvent the limitations associated with antibodies, a number of groups over the last 20 years have engineered PIP binding domains to monitor the isomer-specific PIP-landscape by fusing these proteins to reporters such as fluorescent proteins or quantum dots (Qdots; Lemmon 2008; Irino, Tokuda et al. 2012). These isomer-specific PIP ‘biosensors’ allow the visualization of intracellular PIP localization with high spatial and temporal resolution, providing significant insights into PIP localization and their response to cellular modifications. Here we will highlight several phosphoinositide binding domains including: PH, PX, TUBBY, BAR, PTB, BATS, SYLF, GLUE and EHD domains. For several examples of PIP-binding domains, the reader is referred to **Table 5**. This is not an exhaustive examination of PIP-binding domains and the reader(s) is referred to review articles that cover these domains in significant biological and structural detail (Stahelin, Scott et al. ; Kutateladze 2007; Lemmon 2008; Moravcevic, Oxley et al. 2012).

Table 5. List of PtdIns phosphate binding domains				
Name of Domain	Gene	Primary Lipid Species	Other Binding Partners	Reference
	Plexstrin	PtdIns(4,5)P ₂	PtdIns(4)P PtdIns(3)P	(Harlan, Hajduk et al. 1994)
Plexstrin homology (PH) domain	DAPP1	PtdIns(3,4,5)P ₃ , PtdIns(3,4)P ₂		(Dowler, Currie et al. 2000)
	Grp1	PtdIns(3,4,5)P ₃		(Dowler, Currie et al. 2000)
	PLCδ1	PtdIns(4,5)P ₂	Ins(1,4,5)P ₃	(Lemmon, Ferguson et al. 1995; Dowler, Currie et al. 2000)
	TAPP1	PtdIns(3,4)P ₂		(Dowler, Currie et al. 2000)
	TAPP2	PtdIns(3,4)P ₂		(Dowler, Currie et al. 2000)
	FAPP1	PtdIns(4)P + ARF		(Dowler, Currie et al. 2000)
	PEPP1	PtdIns(3)P		(Dowler, Currie et al. 2000)
	AtPH1	PtdIns(3)P		(Dowler, Currie et al. 2000)
	Centaurin-β2	PtdIns(3,5)P ₂		(Dowler, Currie et al. 2000)
	Evectin-2	PtdIns(3,4,5)P ₃		(Dowler, Currie et al. 2000)
	LL5a	All PIPs		(Dowler, Currie et al. 2000)
	LL5B	All PIPs		(Dowler, Currie et al. 2000)
	Plekstrin-2	Multiple		(Dowler, Currie et al. 2000)
	PH30	Multiple		(Dowler, Currie et al. 2000)
		OSBP	PtdIns(4)P	
	Akt	PtdIns(3,4)P ₂ PtdIns(3,4,5)P ₃		(Franke, Kaplan et al. 1997)
	Slm1	PtdIns(4,5)P ₂ and DHS1-P for proper binding		(Tabuchi, Audhya et al. 2006; Gallego, Betts et al. 2010)

FYVE domains	EEA1	PtdIns(3)P		(Stenmark, Aasland et al. 1996; Kutateladze 2006)
BATS		PtdIns(4,5)P ₂ PtdIns(3)P		(Fan, Nassiri et al. 2011)
SYLF	SH3YL1	PtdIns(3,4,5)P ₃ PtdIns(4,5)P ₂ PtdIns(3,5)P ₂		(Hasegawa, Tokuda et al. 2011)
DHR		PtdIns(3,4,5)P ₃		(Premkumar, Bobkov et al. 2010)
PHD		PtdIns(5)P		(Huang, Zhang et al. 2007)
Tubby domain	TUB	PtdIns(4,5)P ₂ PtdIns(3,4)P ₂ PtdIns(3,4,5)P ₃		(Santagata, Boggon et al. 2001; Szentpetery, Balla et al. 2009)
Phox homology (PX) domain		PtdIns(3)P	PtdIns(4,5)P ₂ PtdIns(3,4)P ₂	(Seet and Hong 2006)
FERM		PtdIns(4,5)P ₂		(Frame, Patel et al. 2010)
PTB domain		PtdIns(4,5)P ₂		(DiNitto and Lambright 2006)
PTB	Disabled-1	NPXY peptide and PtdIns		(Stolt, Jeon et al. 2003)
Eps15 homology (EHD) domain	EHD1	PtdIns(3,4)P ₂ , PtdIns(4,5)P ₂ , PtdIns(3,5)P ₂ , PtdIns(4)P PtdIns(5)P PtdIns(3,4,5)P ₃		(Blume, Halbach et al. 2007; Naslavsky, Rahajeng et al. 2007; Jović, Kieken et al. 2009)
EHD	EHD2	PtdIns(4)P PtdIns(3,4)P ₂ , PtdIns(4,5)P ₂ , PtdIns(3,4,5)P ₃		(Blume, Halbach et al. 2007; Daumke, Lundmark et al. 2007)
EHD	EHD3	PtdIns(4)P PtdIns(4,5)P ₂		Blume, Halbach et al. 2007)
EHD	EHD4	PtdIns(4)P PtdIns(4,5)P ₂		Blume, Halbach et al. 2007)

PH domains

PH (pleckstrin homology) domains were the first identified PIP-binding domains with high specificity and affinity (Haslam, Koide et al. 1993; Mayer, Ren et al. 1993). There are at least 303 proteins in humans and 32 in *S.cerevisiae* that contain PH domains, making the PH-domain the 11th most common domain (Lemmon 2007; Lemmon 2008). PH domains consist of approximately 100-120 amino acids and were originally identified as regions with sequence homology to pleckstrin (Harlan, Hajduk et al. 1994) a substrate of protein kinase C (PKC) in platelets (Tyers, Haslam et al. 1989) that can bind PtdIns(4,5)P₂. However, the specific binding of PtdIns(4,5)P₂ was not shown until the examination of the PLCδ1 PH-domain (Garcia, Gupta et al. 1995; Lemmon, Ferguson et al. 1995). Subsequent studies demonstrating that other PH domains also have PIP-binding ability, including PtdIns(3,5)P₂, PtdIns(4,5)P₂, and PtdIns(3,4,5)P₃ (Lemmon, Ferguson et al. 1995; Dowler, Currie et al. 2000). Importantly, a number of PH domains bind PtdIns(3,4,5)P₃ and or PtdIns(3,4)P₂ that propagate PtdIns(3,4,5)P₃ signaling cascades including PI4L/Akt (Franke, Kaplan et al. 1997; Stokoe, Stephens et al. 1997) and phosphoinositide-dependent kinase-1 (PDK1; Stephens, Anderson et al. 1998; Currie, Walker et al. 1999; Komander, Fairservice et al. 2004). Even though PH domains are commonly thought to be primarily PIP-binding domains, only approximately 10% of PH-domains bind PIPs. Alternative binding partners including protein-protein and lipid binding interactions and these alternative functions continue to be investigated (Lemmon 2007; Lemmon 2008).

As of this writing there are ~161 solved PH-domain structures submitted to the protein database (PDB; Pfam Accession Number PF00169). Several classic examples of PH-domain crystal structures include PLCδ1 (Ferguson, Lemmon et al. 1995), Dapp1-PH, Grp1-

PH (Ferguson, Kavran et al. 2000) in addition to number of other structures (DiNitto and Lambright 2006). Based on these structures it was determined that PH-domains share low sequence homology even though they have significant structural similarity. In general, PH domains consist of a 7 stranded β -sandwich (β 1 through β 7) which is capped by a COOH-terminal α -helix where the open end is linked by three variable loops (β 1- β 2; β 3- β 4 and β 6- β 7). PH domains have a wide range of PIP binding affinities where the PIP headgroup recognition is primarily mediated by the length, and sequence of these variable loops, and in particular, the β 1 to β 2 loop. The β 1- β 2 loop lines the PH-domain pocket, and contains the conserved sequence motif $KX_n(K/R)XR$, where the basic residues provide the majority of the PIP headgroup interactions (Isakoff, Cardozo et al. 1998; Lemmon and Ferguson 2000; DiNitto and Lambright 2006; Lemmon 2007; Lemmon 2008). A number of PH-domains have been utilized as isomer-specific PIP biosensors including, but not limited to, PLC δ ₁-PH, Osh2-PH, and GOLPH3 to monitor PIP distribution and dynamics in cells (see **Chapter 2**) (Stefan, Audhya et al. 2002; Roy and Levine 2004; Baird, Stefan et al. 2008; Wood, Schmitz et al. 2009). Detailed reviews describing biosensor applications, structural analysis, and alternative PH-domain activities are available (Lemmon 2007; Lemmon 2008).

PX domains

The PX (Phox Homology) domain was originally identified and named after the two phagocytic NADPH oxidase (phox; phagocytic oxidase) subunits, p40^{phox} and p47^{phox} (Ponting 1996). Since its discovery in 1996, more than 47 mammalian and 15 yeast proteins have been identified that contain a PX-domain (Kutateladze 2007; Lemmon 2008). The

majority of these domains are incorporated into sorting nexins some of which are commonly involved in the retrograde-transport of resident *trans*-Golgi proteins from endosomes specifically, through the retromer (Seet and Hong 2006; Cullen 2008; Cullen and Korswagen 2012). Proteins that contain PX-domains are primarily found associated PtdIns(3)P-enriched endosomal vesicles and vacuoles (Cozier, Carlton et al. 2002; Kutateladze 2007); however, they have also been shown to bind PtdIns(3,4)P₂, PtdIns(3,5)P₂, PtdIns(4,5)P₂ and PtdIns(3,4,5)P₃ (Kanai, Liu et al. 2001; Song, Xu et al. 2001).

The PX domain consists of approximately 130 amino-acids and is structurally conserved in eukaryotes (Hiroaki, Ago et al. 2001; Kutateladze 2007). Multiple PX-domains have been solved and share common structural elements despite poor sequence homology [*e.g.* (Bravo, Karathanassis et al. 2001; Kutateladze 2007)]. For more biological and structural details regarding PX domain containing-proteins and structural rationale for PIP binding the reader is referred to several reviews (Kutateladze 2007; Lemmon 2007; Lemmon 2008; Kutateladze 2010; Cullen and Korswagen 2012).

GLUE domains

The NH₂-terminal GLUE (GRAM-Like Ubiquitin-binding in EAP45) domain from the yeast Vps36, was crystalized to 1.9Å (PDB ID code 2CAY) revealing a ‘split’ PH domain and shares similarity to the GRAM domain (Teo, Gill et al. 2006). The Vps36 GLUE domain forms a non-canonical lipid binding site that is distinct from other PH domains (Teo, Gill et al. 2006). Subsequently, Vps36 was crystalized in complex with Vps22 and Vps25 (ESCRT-II complex; Im and Hurley 2008). This Vps36 GLUE domain

contains a large sequence insertion containing two Npl4-type zinc finger domains, NZF1 and NZF2 (Teo, Gill et al. 2006). The GLUE domain of Vps36 was shown to bind PtdIns(3)P (affinity $\sim 0.1 \mu\text{M}$), PtdIns(4)P, PtdIns(3,4)P₂, PtdIns(3,5)P₂, and is the primary membrane-targeting domain for the ESCRT-II complex in yeast (Teo, Gill et al. 2006). Mutations in the GLUE domain were shown to inhibit lipid binding and caused defects in the sorting of ubiquitinated cargo (Teo, Gill et al. 2006). The mammalian Vps36 orthologue, Eap45, strongly bound PtdIns(3,4,5)P₃ and PtdIns(3,4)P₂ and weakly binds PtdIns(3,5)P₂ *in vitro* as assayed by lipid-overlay (Slagsvold, Aasland et al. 2005). Given the poor isoform-specificity of the GLUE domain it is unlikely that it will develop into a useful isoform-specific PIP biosensor.

Tubby domains

The *tubby* mouse is a naturally occurring mutation at the splice-site junction of the 3' coding exon (Stubdal, Lynch et al. 2000) isolated at the Jackson Laboratory as an autosomal recessive mouse that shows maturity-onset obesity (Coleman and Eicher 1990), blindness and deafness (Ohlemiller, Hughes et al. 1995). Through positional cloning efforts, *Tub* was identified as the phenotype-inducing gene (Kleyn, Fan et al. 1996; Noben-Trauth, Naggert et al. 1996). *TUB* is the founding member of the tybby-like proteins or TULPs. These proteins are found in diverse organisms throughout the animal- and plant-kingdoms (Boggon, Shan et al. 1999; Santagata, Boggon et al. 2001). The biological-significance, structural-differences, and cellular distribution of TULPs will not be discussed here, and we refer the reader to published review articles (Carroll, Gomez et al. 2004; Mukhopadhyay and Jackson 2011).

Tub protein family-members are defined as having a highly conserved carboxy-terminal domain of approximately 260 amino acids, referred to as the 'tubby domain' with a less-conserved NH₂-termini that resembles the activation domains from known transcription factors (Boggon, Shan et al. 1999). The crystal structure of the mouse protein Tub was solved, revealing a 12-stranded, anti-parallel, closed β -barrel that surrounds a central α -helix (site of the *tubby* mutation) that forms most of the hydrophobic core (PDB# 1C8Z; 1.90 Å; Boggon, Shan et al. 1999). Tub localizes to the plasma membrane and through lipid-binding assays was demonstrated to interact with PtdIns(4,5)P₂, PtdIns(3,4)P₂, and PtdIns(3,4,5)P₃ but not PtdIns(3,5)P₂ or any monophosphorylated phosphoinositide species through its -COOH-terminal 'tubby' domain. Analysis further suggests that Tub acts as a membrane-bound transcription regulator that translocates to the nucleus in response to PLD-dependent phosphoinositide hydrolysis, providing a direct link between G-protein signaling and the regulation of gene expression (Santagata, Boggon et al. 2001).

To provide structural insights into the PIP:Tub interactions, the crystal structure of Tub from mouse was solved in complex with L- α -glycerophospho-D-*myo*-inositol(4,5)P₂ (Santagata, Boggon et al. 2001). This PIP₂ derivative binds to a positively charged cavity in the *tubby* domain. The co-crystal structure revealed that the conserved residue K320 intercalates the the 4- and 5-phosphates of the inositol headgroup whereas R363 coordinates with the inositol ring at the 3-position and the side-chain NH₂ group of N310 hydrogen-bonds to the oxygen atoms at the 4- and 5-phosphoester position (Santagata, Boggon et al. 2001). These observations were confirmed through site directed-mutagenesis followed by lipid-binding assays that demonstrated that PIP₂:Tubby interactions were abrogated (PDB# 1I7E; 1.95 Å)(Santagata, Boggon et al. 2001). The 'specific' PIP₂ binding activity of Tub's

tubby domain has been exploited for use as a biosensor and it is reported to have a higher affinity for PIP₂ than the commonly used PH^{PLC δ 1} biosensor (Field, Madson et al. 2005; Nelson, Nahorski et al. 2008; Quinn, Behe et al. 2008; Szentpetery, Balla et al. 2009).

BATS domains

Fan et al. recently described a novel lipid binding domain from last 80 COOH-terminal amino acids of the Barkor/Atg14(L) protein. This region is referred to as the BATS domain and is the minimal subunit required to target the class III phosphatidylinositol 3-OH kinase complex to early autophagic structures (Fan, Nassiri et al. 2011). Bioinformatic analysis suggests that 19 amino acids of the BATS domain form a classic amphipathic α -helix wheel with hydrophobic and hydrophilic residues that align on adjacent sides of the α -helix. The GST-BATS domain was shown to favor membranes enriched in PtdIns(3)P and PtdIns(4,5)P₂ but not PtdIns(4)P or PtdIns(5)P as measured by liposome binding assays. This domain is preferentially recruited to membranes with high curvature enriched in PtdIns(3)P but not PtdIns(4,5)P₂ (Fan, Nassiri et al. 2011).

PROPPINs

Atg18 defines the prototype 500 amino acid β -propeller protein in *S.cerevisiae* that binds phosphoinositides and was named PROPPIN (β -propellers that bind phosphoinositides) (Michell, Heath et al. 2006; Lemmon 2008). Additional PROPPINs were shown to bind

monophosphorylated PIPs and PtdIns(3,4)P₂, *in vitro* (Jeffries, Dove et al. 2004; Strømhaug, Reggiori et al. 2004; Michell, Heath et al. 2006)

SYLF domains

The SYLF domain (also called DUF500) has been proposed to be a novel lipid binding domain named after SH3YL1 (SH3 domain containing Ysc84-like 1 protein), Ysc84p/Lsb4, Lsb3, and plant and plant FYVE domains that contain it (Hasegawa, Tokuda et al. 2011). The SYLF domain is highly conserved and found in Gram-negative bacteria, also in eukaryotes such as mammals and green plants. Proteins that contain SYLF domains are found as stand-alone proteins or in combination with more complicated multi-subunit proteins (Hasegawa, Tokuda et al. 2011). The SYLF domain of SH3YL1 is an approximately 220 amino acids and binds PtdIns(3,5)P₂, PtdIns(4,5)P₂, and PtdIns(3,4,5)P₃ and to a lesser extent PA (Hasegawa, Tokuda et al. 2011). Although the crystal structure has not been solved, the lipid binding capacity of this domain was isolated to positively charged residues on a putative amphipathic NH₂-terminal helical structure (residues 9-23). Point mutations or deletion to this putative α -helical structure in SYLF reduced lipid binding (Hasegawa, Tokuda et al. 2011).

EH domains

The Eps15 homology (EH) domain was originally identified as a 70-100 amino acid conserved NH₂-terminal region of Eps15 and is conserved from yeast to mammals

(Confalonieri and Di Fiore 2002; Miliaras and Wendland 2004; Naslavsky and Caplan 2011). Through bioinformatics analysis it was determined that there are at least 50 proteins that contain EH-domains (Confalonieri and Di Fiore 2002; Naslavsky and Caplan 2011). A number of EH domain structures have been solved by NMR (de Beer, Carter et al. 1998; Koshiya, Kigawa et al. 1999; Whitehead, Tessari et al. 1999; Enmon, de Beer et al. 2000; Kim, Cullis et al. 2001) and crystallography (Daumke, Lundmark et al. 2007). EH domain proteins are formed by two EF-hand motifs (loop-helix-loop), connected by a short antiparallel β -sheet, and the residues that form the α -helices are conserved in the majority of EH domains (~60% similarity) (Miliaras and Wendland 2004). EF-hands have Ca^{2+} binding properties although not all EH-domain proteins maintain Ca^{2+} binding (Confalonieri and Di Fiore 2002). For more detailed descriptions of the structure and variations between EHD domains the reader is referred to several reviews on the subject (Confalonieri and Di Fiore 2002; Miliaras and Wendland 2004; Naslavsky and Caplan 2011).

In addition to various protein binding partners (Confalonieri and Di Fiore 2002; Miliaras and Wendland 2004; Naslavsky and Caplan 2011), EHD domains have recently been shown to bind phosphoinositides *in vitro*. All four COOH-terminal EHD domain containing proteins (EHD1-EHD4) in mammals bind phosphatidylinositol phosphates with varying specificity *in vitro* (Blume, Halbach et al. 2007; Daumke, Lundmark et al. 2007; Naslavsky, Rahajeng et al. 2007; Jović, Kieken et al. 2009). These domains were shown to bind phosphatidylinositol phosphates with low affinity *in vitro* likely because oligomerization is required for optimal membrane binding (Lee, Zhao et al. 2005). The crystal structure of the mouse EHD2 domain was recently crystalized and provided some rational as to how these EHD domains interact with PIPs. It was suggested that the primary

membrane binding site is localized to poly-basic cluster within the $\alpha 9$ helix of EHD2 dimers (Daumke, Lundmark et al. 2007). Additionally, the COOH-terminal EHD proteins may induce membrane curvature and may contribute to their *in vivo* function (Daumke, Lundmark et al. 2007). Given the poor specificity it is unlikely that these domains will provide a useful tool construct to PIPs *in vivo*.

FERM domains

The FERM (4.1/ezrin/radixin/moesin) domain is typically found at the NH₂-terminal of FERM-containing proteins (Chishti, Kim et al. 1998). FERM domain containing proteins are often associated with the cytoskeleton and plasma membrane (Chishti, Kim et al. 1998). There are approximately 50 FERM-containing proteins across 30 genes in the human genome (Frame, Patel et al. 2010). Applying sequence alignment of FERM domains from human, *Caenorhabditis elegans*, and *Dictyostelium discoideum* these proteins were segregated into three groups and classified by their predominant members: (i) talin and kindlin (ii) ERM (ezrin/radixin/moesin), guanine nucleotide exchange factors (GEFs), kinases and phosphatases and (iii), myosin and Krev interaction trapped (KRIT) proteins (Frame, Patel et al. 2010).

The FERM domain is a cysteine-rich hydrophobic molecule that is composed of approximately 300 amino acids. The crystal structure of several FERM domains have been solved including ezrin (PDB # 1NI2; Smith, Nassar et al. 2003), moesin (Pearson, Reczek et al. 2000; Edwards and Keep 2001), and radixin (Hamada, Shimizu et al. 2000). Using these structures, the FERM domain was divided into three sub-domains, that when combined, form

a three-lobed clover shape. These lobes are classified as F1, F2 and F3: F1 is the NH₂-terminal lobe which resembles ubiquitin, F2 is the ‘central lobe’ which resembles an acyl-CoA binding protein, and F3 is the COOH-terminal lobe which contains a pleckstrin homology-phosphotyrosine binding (PH-PTB) domain (Hamada, Shimizu et al. 2000; Pearson, Reczek et al. 2000). FERM domains have been isolated and bind several PIPs including PtdIns(3,4)P₂, however each FERM domain is unique and must be individually tested (Moleirinho, Tilston-Lunel et al. 2013). There is a large base of literature on FERM domains, and FERM-domain containing proteins and the reader is referred to several review articles (Chishti, Kim et al. 1998; Fehon, McClatchey et al. 2010.; Frame, Patel et al. 2010; Arpin, Chirivino et al. 2011; Moleirinho, Tilston-Lunel et al. 2013).

BAR domains

BAR (Bin-Amphiphysin-Rvs) domains are highly conserved domains that are found in a number of proteins involved in membrane dynamics, filopodia formation, and endocytosis, (Razaq, Robinson et al. 2001; Lee, Marcucci et al. 2002; Lemmon 2008; Cullen and Korswagen 2012). The BAR domain is approximately 260 amino acids that form dimers with a crescent or ‘banana’ shape (Peter, Kent et al. 2004). Since the original crystal structure, a number of structures have been crystalized that display with variations on the classic ‘banana shape’, including ‘Zeppelins’, and ‘tildes’ (Masuda and Mochizuki 2010). BAR domains have been shown to induce membrane deformation in PtdIns(4,5)P₂ containing vesicles *in vitro* and are thought to act as sensors of membrane curvature (e.g. Snx1; Peter, Kent et al. 2004; van Weering, Verkade et al. 2012). For additional information regarding BAR domains, and various variations such as I-BAR, and F-BAR domains, the reader is

referred to several review articles (Gallop and McMahon 2005; Lemmon 2008; Itoh and Takenawa 2009; Ahmed, Goh et al. 2010; Bhatia, Hatzakis et al. 2010; Campelo, Fabrikant et al. 2010; Madsen, Bhatia et al. 2010; Masuda and Mochizuki 2010; Cvrckova 2013).

FYVE domains

Vps34 was originally identified as *VPT29* (vacuolar protein targeting) mutant in *S.cerevisiae* (Robinson, Klionsky et al. 1988). Subsequently, Vps34 was identified as a homologue of the class III mammalian phosphoinositide 3-OH kinase (PI3K; Schu, Takegawa et al. 1993). The disruption of Vps34 has been linked to a number of protein sorting (Herman and Emr 1990; Schu, Takegawa et al. 1993) and autophagic defects (Kihara, Noda et al. 2001). Insights into the mechanism of action were initially made using proteins recruited by PtdIns(3)P in wortmannin treated cells (PtdIns 3-OH kinase inhibitor) and, for example, the detection of EEA1 loss of endosomal localization upon wortmannin treatment (early endosomal autoantigen 1; Patki, Virbasius et al. 1997). Subsequent studies linked Vps34-mediated PtdIns(3)P production and the recruitment of EEA1 with proper vacuolar sorting (Stenmark, Aasland et al. 1996; Burd and Emr 1998; Patki, Lawe et al. 1998). Upon examination of EEA1, it was shown that the EEA1 FYVE domain mediated the PtdIns(3)P-specific recruitment of EEA1 to PtdIns(3)P enriched endosomes (Burd and Emr 1998; Gaullier, Simonsen et al. 1998; Patki, Lawe et al. 1998). Together, this made a mechanistic link between: PtdIns(3)P synthesis, EEA1 recruitment to the membrane-cytoplasmic interface, and endosomal trafficking (Hayakawa, Hayes et al. 2007).

The binding of EEA1 FYVE domain is comprised of a cysteine-rich Zn²⁺ finger binding domain composed of approximately 60-70 amino acids (Stenmark, Aasland et al. 1996; Misra and Hurley 1999). FYVE's name is derived from the first letter of the first four proteins it was originally identified in: Fab 1, YOTB, Vac 1, and EEA1 (Mu, Callaghan et al. 1995; Stenmark, Aasland et al. 1996). FYVE domains have been divided into two classes: those that specifically bind PtdIns(3)P and those that have an undetermined function (Tibbetts, Shiozaki et al. 2004). Even though proteins that contain FYVE domains are expected to bind PtdIns(3)P and thus endosomes many do not (Hayakawa, Hayes et al. 2007). This variation has been attributed to: the propensity of FYVE domains to oligomerize, their ability to insert into membranes, and their varied electrostatic potentials (Hayakawa, Hayes et al. 2007). Given the high specificity of FYVE domains for PtdIns(3)P they make excellent biosensors for tracking PtdIns(3)P localization in cells.

FYVE domains are found in numerous eukaryotic proteins from yeast to man (Banerjee, Basu et al. 2010). Humans are predicted to have approximately 38 gene products that contain FYVE domains (Hayakawa, Hayes et al. 2007; Lemmon 2008). The crystal structure of several FYVE domains have been solved including the *S.cerevisiae* Vps27p, *Drosophila* Hrs, human EEA1, CARP2 and LMS1 (Misra and Hurley 1999; Mao, Nickitenko et al. 2000; Dumas, Merithew et al. 2001; Kutateladze and Overduin 2001; Tibbetts, Shiozaki et al. 2004). General features of FYVE domains reveal two double-stranded antiparallel β sheets and a C-terminal α -helix (Kutateladze 2007). The FYVE-domain fold is stabilized by the binding of two Zn²⁺ atoms that bind to four CxxC motifs (Kutateladze 2007). For more details regarding FYVE domains the reader is referred to the following reviews (Stahelin, Scott et al. ; Hayakawa, Hayes et al. 2007; Kutateladze 2007; Lemmon 2008).

PIP biosensors and FRET

Fluorescence/Förster resonance energy transfer (FRET) a phenomenon first predicted by Förster in 1946 that describes the non-radioactive energy transfer from a ‘donor’ fluorophore to an ‘acceptor’ fluorophore that stimulates acceptor-fluorescence (Stryer and Haugland 1967; Cheng 2006). The energy transfer observed in FRET is largely dependent on two factors. First, as the distance of the FRET-pairs increases, the FRET efficiency is inversely proportional to the sixth power of the distance between the ‘donor’ and ‘acceptor’ fluorophores (*i.e.* $1/r^6$; Miller 2005). Second, the relative orientation of the FRET-pairs also influences FRET efficiency. Although this is a simplistic view of the variables, the general principal is that only fluorescent macromolecules-pairs in close proximity (low nm range) will induce FRET (Miller 2005). These features allow for the calculation of distance between any two FRET-pairs and led to FRET being used as a ‘molecular-’ or ‘spectroscopic ruler’ (Stryer and Haugland 1967). Subsequently genetically encoded FRET pairs were developed to monitor Ca^{2+} signaling in cells (Miyawaki, Llopis et al. 1997) and opened up a powerful ‘new’ technique that could be applied to a variety of systems (e.g. yeast, cell culture, whole animal, etc.). For more general information on FRET, the reader is referred to several resources that describe this technique in more detail [e.g. (Miller 2005; Cheng 2006; Padilla-Parra and Tramier 2012; Zadran, Standley et al. 2012; Ueda, Kwok et al. 2013)].

Multiple FRET-based systems have been developed to monitor PIP interactions. For example, the CFP- $\text{PH}^{\text{PLC}\delta 1}$ and YFP- $\text{PH}^{\text{PLC}\delta 1}$ domains have been used to monitor $\text{PtdIns}(4,5)\text{P}_2$ depletion in the plasma membrane of mammalian cells upon PLC activation. This increased temporal resolution and reduced excitation damage to the cells (van Rheenen, Mulugeta Achame et al. 2005). Additionally, techniques to monitor $\text{PtdIns}(3,4,5)\text{P}_3$ using

lipid-binding domains, coupled with FRET have also been utilized (Margolin 2000; Sato, Ueda et al. 2003; Sato 2006; Ueda and Hayashi 2013). FRET pairs have also been constructed for PtdIns(4)P, PtdIns(3,4)P₂, PtdIns(4,5)P₂ and DAG to monitor PIP-turnover and cell migration in MDCK cells (Nishioka, Aoki et al. 2008).

Coincidence detection

It's becoming apparent that the simplistic view of a single lipid binding one lipid binding domain excludes a number of co-binding elements. Multiple lipid binding domains have been shown to require multiple binding events either from various lipid species or other protein domains for robust membrane recruitment. Coincidence detection (i.e. multiple signaling cues working together to direct localization) is not covered here and the reader is referred to several manuscripts discussing coincidence detection and PIP binding domains (Stahelin, Scott et al. ; Wenk and De Camilli 2004; Behnia and Munro 2005; Carlton and Cullen 2005; Di Paolo and De Camilli 2006; Lemmon 2008).

Modulation of cellular phosphatidylinositol phosphates

Fundamental to our understanding of phosphatidylinositol phosphate (PIP) signaling is the ability to selectively disrupt PIP-signaling pathways through both direct and indirect methods. Traditionally, employed techniques include physical application of lipids, antibodies, genetic alteration(s) and pharmacological intervention of phosphatidylinositol phosphate metabolizing-enzymes. More recent methodologies include genetically encoded light- and chemical-induced enzyme-localization constructs that enhance the spatial and temporal resolution of PIP-attenuation relative to more traditional methods. In this section, I discuss common methods used to attenuate PIP-signaling with an emphasis on chemical modulators of PIP-modifying enzymes. For additional information surrounding the disruption of PIP signaling the reader is referred to these resources (Chang-Ileto, Frere et al. 2012; Wymann and Schultz 2012).

Addition of exogenous phosphatidylinositol phosphates

In principal, the simplest method to modify cellular PIP composition is to add exogenous PIPs to the culture media. Phosphatidylinositol phosphates have an intrinsic anionic characteristic that makes it relatively difficult for them to penetrate the electrical potential of -60mV to -70mV at the plasma membrane (Ozaki, DeWald et al. 2000; Wymann and Schultz 2012) and thus, the intracellular environment. To circumvent this limitation, various PIPs have been incorporated into polyamine carriers to “ferry” PIPs across the cell membrane (Ozaki, DeWald et al. 2000). Additionally, these polyamine carriers have been used to deliver PIP-mimetics that inhibit various PIP-modifying enzymes (see below).

Several PIP species have been loaded into cells using polyamine carriers and subsequently their localization, metabolism, and effects on signal transduction pathways have been monitored (Ozaki, DeWald et al. 2000). Alternatively, PIPs can pass through the plasma membrane by utilizing ‘bioactivatable’ protecting groups (Schultz 2003), or lipid micelles can be directly injected into cells, a technique which has been used to monitor diffusion patterns of PtdIns(4,5)P₂ (Golebiewska, Nyako et al. 2008).

More sophisticated PIP derivatives are those that incorporate functional groups to ‘cage’ PIPs thereby keeping them biologically inactive until ‘uncaged’ by light. These ‘cage’ techniques provide superior control over the spatial and temporal activity of PIPs by modulation of the intensity, localization and frequency of light applied to cells (Mentel, Laketa et al. 2011). Additionally, ‘caged’-PIPs allows cells to stabilize the PIP cellular-distribution and if bioactive protecting groups were used for cellular entry, also gives cells time to metabolize (i.e. remove) these groups (Mentel, Laketa et al. 2011). However, the ability of ‘caged’-PIPs to mimic natural lipids is not well studied and their expense is often prohibitive. Several ‘caged’-lipid derivatives have been developed including PtdIns(3)P [cgPtdIns(3)P] (Subramanian, Laketa et al. 2010), PtdIns(3,4,5)P₃ [cgPtdIns(3,4,5)P₃/AM] (Mentel, Laketa et al. 2011) and although not a PIP, DAG (Nadler, Reither et al. 2013). The ‘caged’ PtdIns(3)P when applied to cells induced rapid endosomal fusion, suggesting that PtdIns(3)P is sufficient to drive an EEA1-dependent fusion (Subramanian, Laketa et al. 2010). In the case of cgPtdIns(3,4,5)P₃/AM, it was shown to be cell permeable, photoactivatable, membrane ruffling and PH-domain translocating when activated in cells (Mentel, Laketa et al. 2011). Finally, the ‘caged’ DAG derivative was used to determine the

influence of fatty acid chain length on PKC-dependent signaling (Nadler, Reither et al. 2013).

Various ‘metabolically stable’ (ms) PIPs have been generated to separate direct PIP effects from downstream metabolic products. Multiple ‘metabolically-stabilized’ PIP-derivatives have been developed for: PtdIns(3)P (Xu, Lee et al. 2006), PtdIns(4)P (He, Gajewiak et al. 2011), PtdIns(5)P (Huang, Zhang et al. 2007) and PtdIns(3,4,5)P₃ (Zhang, Markadieu et al. 2006; Zhang, Xu et al. 2006). Together these methods provide varying degrees of control over the application of exogenously added lipids. However, they are all limited in their ability to control PIP- localization, are expensive and are often difficult to obtain.

Genetic modulation of PIP modifying enzymes

Genetic modulation of PIP-modifying enzymes has been instrumental in the elucidation of PIP-signaling events and the identification of PIP-modifying enzymes. Methods to genetically attenuate PIPs included the attenuation of PIP-modifying enzyme by: overexpression (Mousley, Yuan et al. 2012), RNAi (Prasad and Decker 2005; Reagan-Shaw and Ahmad 2006) and organismal deletion(s) (Di Cristofano, Pesce et al. 1998; Sasaki, Suzuki et al. 2002). Ideally the genetic disruption will quickly and selectively disrupt the PIP-modifying enzyme of choice by either reducing or increasing the level of PIP-modifying enzymes. However, these methods are slow to implement (e.g. days), and thus, provide cells with time to reroute signaling networks, adapt to their new conditions and potentially mask results—especially acute responses. Temperature-sensitive (ts) mutations solve some of

these limitations; we will limit our discussion to this class of genetic modulators as it's most relevant to Chapter 2.

Instrumental to the understanding of PIP-modifying enzymes has been the generation of conditional mutants, and in particular temperature sensitive (ts) alleles. These mutations inactivate a protein at 'nonpermissive temperature' (e.g. 37°C in *S.cerevisiae*) but are active at 'permissive' temperature (e.g. 25-30°C in *S.cerevisiae*). Temperature sensitive mutations are often highly conservative (e.g. single point mutations) that introduce structural instability into a protein that become critically unstable at their 'non-permissive' temperature, to the point of inactivity. These mutations have provided a powerful toolbox to study essential gene function in a number of model systems: *Schizosaccharomyces pombe* (Nurse, Thuriaux et al. 1976), *Saccharomyces cerevisiae* (Hartwell 1974), Chinese Hamster cells (Roscoe, Robinson et al. 1973) and *Caenorhabditis elegans* (Ward and Miwa 1978). Temperature sensitive genes are typically essential, and by definition, are poorly-buffered by redundant pathways that code for an important cellular function (Hartman, Garvik et al. 2001). These genes are often highly conserved in evolution, making their study in lower organisms highly relevant to cell biology (Hughes 2002). The isolation of temperature-sensitive mutations in *S.cerevisiae* have provided insights into a variety of cellular activities that translate from yeast to mammals including: cell cycle (Howell and Lew 2012), secretion (Barlowe and Miller 2013), nutrient-signaling (Loewith and Hall 2011), lipid metabolism (Henry, Kohlwein et al. 2012), DNA repair (Boiteux and Jinks-Robertson 2013) and PIP-signaling (Robinson, Klionsky et al. 1988; Bankaitis, Malehorn et al. 1989; Audhya, Foti et al. 2000).

The number of methods and manuscripts that genetically manipulate PIP-regulating proteins is vast and will not be covered in detail here. However, despite their wide use they

suffer from various limitations: (i) the generation of tools is time-consuming (ii) modifications require application to each genetic background (iii) cells have time to adapt to modifications. Temperature sensitive systems are also not ideal: (i) generation of temperature sensitive mutations is often a limiting factor in their application, especially in multicellular organisms (Harris and Pringle 1991). (ii) The detection of minor defects at 'permissive' temperature is difficult, (iii) analysis is conducted at sub-optimal temperature(s) and (iv) they are often limited to essential genes. For these and other reasons, it's desirable to use a system that will modify PIP pools quickly, specifically and with a high degree of spatial and temporal resolution. Several tools that provide these traits are chemical- and light-induced protein targeting technologies (CID and LID, respectively).

Chemical- and light-induced enzyme targeting

Continuous disruption of PIPs as described above can result in a number of compensatory mechanisms in cells (*e.g.* alter lipid metabolism, effector proteins, bypass mutations, etc.). Because of this cellular compensation, observed outcomes may represent artifacts complicating experimental interpretation. Additionally, many PIP responses are short lived and these acute disruptions will be missed. To circumvent these limitations, genetically encoded drug- or light-induced (*i.e.* optogenetics) dimerization systems were developed to allow the rapid dose-dependent recruitment of PIP-modifying enzymes (*e.g.* kinases and phosphatases) to subcellular regions of interest. Additionally, these systems allow for gain-of-function studies by localizing desired proteins to a site of interest. Several variations of these systems exist to modulate cellular activities including gene expression,

endocytosis, and cargo sorting (Chang-Ileto, Frere et al. 2012). Major advances have been applied to neurobiology and have been reviewed in detail elsewhere (Zhang, Wang et al. 2007; Deisseroth 2011; Yizhar, Fenno et al. 2011; Chow, Han et al. 2012; Mei and Zhang 2012; Pathak, Vrana et al. 2013). I will not describe these systems in detail and the reader is directed to review articles for additional details (Chang-Ileto, Frere et al. 2012; Wymann and Schultz 2012).

Pharmacological intervention of phosphoinositide signaling

Although CID and LID technologies are superior relative to more traditional genetic methodologies in several ways, they require significant genetic modification, optimization and are not available for genetically intractable systems. An alternative PIP-modifying enzyme is the application of pharmacological modulators (*i.e.* compounds that activate or inactivate a target). Chemical modulators provide a dose-dependent, specific, acute, potent and in some cases reversible tool to modulate the activity of a chosen target; however, the majority of these compounds are target-inactivators (*i.e.* loss-of-function studies; see below). Additionally, these chemical modulators can often transition between model systems (*e.g.* *Saccharomyces cerevisiae*, *Schizosaccharomyces pombe*, *Caenorhabditis elegans*, *Toxoplasma gondii*, etc.) and cell types (*e.g.* Schneider 2, HeLa, etc.)—assuming the appropriate controls have been conducted (*e.g.* cells contain the target, etc.). Here I describe several pharmacological agents that are directed against PIP-modifying enzymes and when applicable highlighting how inadequate validation of chemical modulators can confuse the interpretation of experimental results.

Small molecule inhibitor validation in *S.cerevisiae*

Effective chemical modulators (*e.g.* SMIs) require proper validation prior to their use. Although this seems obvious, it's often the exception as opposed to the rule. Results obtained from inadequately validated inhibitors cannot be interpreted with confidence, and thus, will add confusion and uncertainty into the literature. Several common problems associated with poorly-validated SMIs are: multiple SMI targets, isoform cross-reactivity, general cytotoxic activity, metabolic effects and the lack of mechanistic understanding of the SMI. For example, in a PubMed search conducted in March 2014, the commonly used phospholipase C (PLC) inhibitor, U-73122 resulted in more than 1600 results (and an unknown number of citations). U-73122 has a number of off-targets, and to my knowledge has never been shown to directly inhibit PLC. This exemplifies the importance of properly validating a chemical modulator; otherwise, your experimental data cannot be validated and 1600 manuscripts with data of unknown relevance. Although it's almost impossible to obtain absolute confidence regarding SMI-validation, every attempt should be made within the chemical biology field to raise the standards of 'validated' chemical modulators. As I describe below, many 'specific' SMIs are poorly validated; often a result of investigator oversight or historical classification that has been misinterpreted over time. Great care must be used when selecting a chemical modulator for your application, with substantial primary literature research to determine what is, and is not known.

Below are 'rules' that I developed/used in Chapter 2 (and a few I could not achieve in the NPPM-validation regime) to assist the investigator in determining the quality of a chemical-modulator. These 'rules' were developed for essential proteins in *Saccharomyces cerevisiae*; however, many are applicable to multiple systems. If possible, the investigator

should determine if their protein of interest complements a homologous yeast protein.

Although this is not always possible, it will allow additional assays to detect SMI off-targets especially those of essential proteins (Hughes 2002).

1. SMI intoxication phenocopies genetic inactivation of protein.
2. SMI-sensitivity is proportional to target-protein cellular-load.
3. SMI inhibits recombinant protein in a dose-dependent manner
4. Do SMIs inhibit closely related proteins?
5. Inactive SMIs are not active in 1-4.
6. SAR provides predictive capability towards chemical SMI modification(s).
7. SMI::Protein interactions are observed (*e.g.* co-crystal, NMR, mass spec, etc.).
8. Rational mutations in recombinant protein endow resistance to SMI.
9. Cells made dependent on SMI-resistant protein are resistant to SMI.
10. When available, SMI target protein bypass mutations are SMI resistant.

Inhibitors of PIP signaling pathways

Phosphatidylinositol phosphates recruit various PIP-binding proteins that subsequently regulate multiple downstream signaling events. The phosphorylation status, localization and lifetime of these PIPs mediate how and what signals are propagated. To maintain appropriate signaling networks the PIP phosphorylation status is tightly regulated through the coordination of PtdIns kinases, phosphatases and lipases. Multiple diseases have

been associated with the derangement of these PIP-regulating proteins such as cancer, insulin resistance and viral replication. Since this field is expanding rapidly, I will only briefly discuss the biological role of these proteins and focus on their chemical modulation. For additional information the reader is referred to excellent review articles that cover both the biological and historical details when appropriate.

Akt/PKB inhibitors

Akt, also known as protein kinase B (PKB) is a serine/threonine-specific protein kinase that regulates multiple cellular events including, apoptosis, cell proliferation, transcription, protein synthesis and cell migration. Since Akt promotes cell survival and inhibits apoptosis it has become a promising target for chemical intervention. Multiple ATP-competitive, PIP-analogue and allosteric Akt-inhibitors have been developed, primarily with the intent of generating cancer therapeutics. The generation of Akt/PKB-directed SMIs is a major area of investigation; however, since Akt does not directly modify PIPs I direct the reader to review articles on Akt and Akt inhibitors (Cheng, Lindsley et al. 2005; Lindsley 2010; Wang, Zhang et al. 2011; Mahajan and Mahajan 2012).

PtdIns-3-kinases inhibitors

Phosphatidylinositol 3-OH kinase (PI3K) catalyze the phosphorylation of the D-3 position of the inositol ring of PtdIns. PI3K enzymes are divided into three classes: Class I PI3Ks are composed of an 110kDa catalytic domain (α , β , γ , and δ) which is encoded by four

genes in mammals. Five genes encode the regulatory domains for Class I PI3Ks p85a, p101 and p84/p87. Class II PI3Ks are 150-180 kDa proteins that exist in three isoforms (α , β , and γ) and there is a single Class III PI3K in mammals. The PI3K pathway influences multiple cellular activities and when it becomes deranged mammalian disease occur including cancers (Balla 2013). Under normal conditions the second messenger PtdIns(3,4,5)P₃ is maintained at low concentration in the plasma membrane (Palmieri, Nowell et al. 2010). Upon the activation of receptor tyrosine kinases (RTK), phosphatidylinositol-3-kinase(s) (PI3K) is recruited to the cytoplasmic face of the plasma membrane generating PtdIns(3,4,5)P₃ from PtdIns(4,5)P₂ (Balla 2013). As a result, multiple PtdIns(3,4,5)P₃ binding proteins are recruited to the plasma membrane (*e.g.* PH-domains). Some of these recruited proteins include the phosphoinositide kinase 1 (PDK1; Stephens, Anderson et al. 1998; Currie, Walker et al. 1999; Komander, Fairservice et al. 2004) and protein kinase B (Akt; Franke, Kaplan et al. 1997; Stokoe, Stephens et al. 1997) which facilitates their downstream activity. The literature surrounding the PI3K/Akt pathway is massive and the reader is directed to review articles that cover this subject in depth (Vanhaesebroeck, Stephens et al. 2012; Balla 2013).

Yeast have a single Class III PI3K, Vps34 which phosphorylates the inositol headgroup of PtdIns to generate PtdIns(3)P (Auger, Carpenter et al. 1989; Stack and Emr 1994). Vps34 (first identified as Vpt29) was identified in a screen to identify vacuolar protein sorting (Vps) defects (Robinson, Klionsky et al. 1988). Vps34 is the sole source of all D-3 phosphorylated PIPs in yeast as *vps34Δ* cells do not contain D-3 phosphorylated PIPs (Auger, Carpenter et al. 1989; Schu, Takegawa et al. 1993; Wenk, Lucast et al. 2003). Vps34p specifically catalyzed the D-3 phosphorylation of PtdIns but not PtdIns(4)P or

PtdIns(4,5)P₂ *in vitro* (Schu, Takegawa et al. 1993; Stack and Emr 1994; Stack, DeWald et al. 1995). Vps34p is recruited to TGN/endosomes from the cytoplasm through interactions with the protein kinase Vps15p which forms a complex enhances kinase activity (Herman, Stack et al. 1991; Stack, Herman et al. 1993; Stack, DeWald et al. 1995). Regulatory proteins such as Rab5 and Rab7 bind to Vps15 and promote the recruitment to membranes and the activity of Vps34/Vps15 (Murray and Backer 2005; Shin, Hayashi et al. 2005; Simonsen and Tooze 2009). Mammals contain a single Class III PI3K which is associated with p150 the human orthologue of Vps15 (Volinia, Dhand et al. 1995; Panaretou, Domin et al. 1997). Vps34 has a number of in yeast including localizing vacuolar proteins, vacuolar segregation (Herman and Emr 1990) and autophagy (Kihara, Noda et al. 2001) and in mammals it has been shown to regulate endocytic sorting (Christoforidis, McBride et al. 1999), autophagy (Vergne and Deretic 2010), transport to lysosomes through MVB (Schu, Takegawa et al. 1993), endosome to TGN transport through the retromer (Burda, Padilla et al. 2002). Additionally, Vps34 it has been shown to have roles in the nutrient sensing through the mTOR pathway (Byfield, Murray et al. 2005; Nobukuni, Joaquin et al. 2005) and signal downstream of heterotrimeric GTP-binding protein-coupled receptors (Slessareva, Routt et al. 2006). The structure of the *Drosophila melanogaster* Vps34 was solved without its C2 domain which is not required for its catalytic activity *in vitro* (Miller, Tavshanjian et al. 2010). This structure reveals that the overall fold of the protein containing a solenoid helical domain, forming a compact unit with many inter-domain contacts (Miller, Tavshanjian et al. 2010). The literature surrounding PI3Ks is expansive and the reader is referred to excellent review articles that cover these proteins in much greater detail (Vanhaesebroeck, Stephens et al. 2012; Balla 2013; Fruman and Rommel 2014).

The recruitment and activation of phosphatidylinositol-3-kinase (PI3K) to the plasma membrane is an early event in the PI3K/Akt pathway and thus, its chemical inactivation is an attractive avenue to modulate PI3K/Akt signaling, several of which are in clinical trials (Kurtz and Ray-Coquard 2012). Informed by the solution of multiple PI3K structures, high throughput screening, the utilization of medicinal chemistry and *in silico* methodologies, the list of PI3K inhibitors has greatly expanded from the first two identified inhibitors, wortmannin (Arcaro and Wymann 1993; Wymann and Arcaro 1994) and LY294002 (Vlahos, Matter et al. 1994). Wortmannin is a steroid metabolite originally isolated from *Penicillium wortmannin* (Brian, Curtis et al. 1957) and was shown to inhibit respiratory burst in neutrophils and monocytes (Baggiolini, Dewald et al. 1987). Subsequently, wortmannin was demonstrated to inhibit PI3K (Arcaro and Wymann 1993) through covalent modification at Lys802 within the ATP binding site of p110 α (Wymann, Bulgarelli-Leva et al. 1996) and Lys833 in p110 γ (Stoyanova, Bulgarelli-Leva et al. 1997; Walker, Pacold et al. 2000). LY294002 is a morpholine derivative of quercetin, a naturally occurring bioflavonoid which reversibly inhibits PI3K at the ATP binding site (Vlahos, Matter et al. 1994). Because wortmannin inhibits through covalent modification, its IC₅₀ is approximately 5nM, whereas LY294002 is ~1.4 μ M (Vlahos, Matter et al. 1994; Wymann and Arcaro 1994). Wortmannin is unstable in solution unlike LY294002, although both compounds have numerous off-targets including mTOR (Brunn, Williams et al. 1996) and myosin light chain kinase (MLCK) (Hu, Zaloudek et al. 2000). LY294002 also has a number of off targets including casein kinase 2 (CK2), SmMLCK (Davies, Reddy et al. 2000) and skin-related toxic side effects (Hu, Zaloudek et al. 2000; Kong and Yamori 2008). Because of limitations in specificity, pharmacology and potency significant efforts have been devoted to designing

wortmannin and LY294002 derivatives in addition to novel classes of PI3K-directed inhibitors. Because of the large number and diversity of PI3K inhibitors the reader is referred to reviews that specifically focus on this area (Kong and Yamori 2008; Workman, Clarke et al. 2010; Wymann and Schultz 2012; Welker and Kulik 2013).

PTEN PtdIns 3-Phosphatase inhibitors

PTEN (phosphatase and tensin homologue) is a tumor suppressor that was identified as a loss of function (LOF) cancer hot spot on human chromosome 10q23 (Steck, Pershouse et al. 1997). PTEN contains a HCXXGXXRS/T phosphatase signature similar to that found in protein tyrosine phosphatases (PTPase), suggesting that PTEN was a protein phosphatase (Li, Yen et al. 1997). It appears that the most relevant biological activity of PTEN is as a PIP phosphatase that is directed against the D-3 position where it has preferential activity against PtdIns(3,4,5)P₃ *in vivo* and *in vitro* (Myers, Stolarov et al. 1997; Maehama and Dixon 1998). Through this PIP phosphatase activity PTEN negatively regulates PI3K/Akt signaling pathways (Hopkins, Hodakoski et al. 2014). Additionally, PTEN's activity is thought to play a role through protein phosphatase and non-catalytic activities although these activities are less well understood (Myers, Stolarov et al. 1997; Freeman, Li et al. 2003; Shen, Balajee et al. 2007; Leslie, Maccario et al. 2009; Liu and Bankaitis 2010; Tibarewal, Zilidis et al. 2012). PTEN is composed of a two-domains, a NH₂-terminal phosphatase domain followed by a loop to a C2 domain, a class 1 PDZ binding motif and a putative PtdIns(4,5)P₂ binding domain on the catalytic subunit (Lee, Yang et al. 1999; Gericke, Munson et al. 2006). PTEN's preference for PIPs is explained by the solution of its structure where the NH₂-

terminal phosphatase domain is enlarged relative to the canonical protein phosphatase catalytic motif which is surrounded by three basic residues CX₅RT/S (Lee, Yang et al. 1999). It's this enlarged region that allows PTEN to specifically dephosphorylate the D-3 position of PtdIns(3,4,5)P₃ (Lee, Yang et al. 1999).

PTEN negatively regulates PtdIns(3,4,5)P₃ signaling in cells and functions as a tumor suppressor by downregulating the PI3K/Akt signaling pathways (Hopkins, Hodakoski et al. 2014). When PTEN is disrupted, PtdIns(3,4,5)P₃ levels increase and recruits the Ser/Thr kinase Pdk1. Subsequently, Pdk1 phosphorylates the Akt kinase which is also recruited to PtdIns(3,4,5)P₃ membranes through its PH domain. Through this PtdIns(3,4,5)P₃/PI3K/Akt signaling pathway cell promoting pro-proliferation and anti-apoptotic activity—tumor suppressor. Its function as a tumor suppressor is primarily attributed to the negative regulation of the PI3K/AKT signaling pathways and thus promote uncontrolled cell growth and prevents cell death (Cantley and Neel 1999; Rameh and Cantley 1999; Cantley 2002; Downes, Ross et al. 2007; Liu, Boukhelifa et al. 2009). Mutations in PTEN result in a number of inherited human diseases including Cowden's disease, Bannayan-Zonana syndrome and Lhermitte-Duclos disease (Hollander, Blumenthal et al. 2011; Pilarski, Burt et al. 2013). Loss of PTEN is also found in a number of spontaneous cancers including gliomas, melanomas, thyroid and breast (Hollander, Blumenthal et al. 2011). For these reasons, the chemical modulation of PTEN is highly desirable due to the large implications for human health. The literature surrounding PTEN is expansive and the reader is referred to review articles that discuss this topic in much greater detail (Liu and Bankaitis 2010; Hollander, Blumenthal et al. 2011; Hopkins, Hodakoski et al. 2014).

PTEN-directed SMIs have utility as tool compounds for loss-of-function studies in various systems. Additionally, reduced PTEN activity has been linked to enhanced glucose uptake and has been proposed as a target for enhanced insulin sensitivity in insulin-resistant individuals (Lazar and Saltiel 2006). As discussed above, PTEN is a potent tumor suppressor where even heterozygous deletion of PTEN results in increased rates of tumor formation in mice (Di Cristofano, Pesce et al. 1998), making the therapeutic application of PTEN inhibitors inherently risky (Lazar and Saltiel 2006). Vanadate is a widely used competitive and reversible inhibitor of protein tyrosine phosphatases (PTPase) (Cuncic, Detich et al. 1999; Bhattacharyya and Tracey 2001). Vanadate derivatives such as peroxovanadium (pV) and dimethylhydroxylamine have also been used as PTPase inhibitors (Posner, Faure et al. 1994; Cuncic, Desmarais et al. 1999). Because PTPases share significant homology with PTEN (Li, Yen et al. 1997), vanadate and vanadate derivatives were tested as potential PTEN inhibitors. Subsequently, several of these derivatives, namely bisperoxovanadium (bpV) had preferential PTEN inhibitory activity although it also inhibited PTP- β and PTP-1 β with IC_{50} s of 14 ± 2.3 nM, 4.9 ± 0.9 μ M and 25.3 ± 2.9 μ M *in vitro*, respectively (Schmid, Byrne et al. 2004). BpV has been used by several groups as a ‘specific’ inhibitor of PTEN (Morohaku, Hoshino et al. 2013); however, this terminology is inappropriate as bpV has cross reactivity with multiple cysteine-based phosphatases such as PTP- β , SAC1, myotubularin (MTM1) and Sopb (Rosivatz, Matthews et al. 2006). Using bpV as lead-compound, vanadate scaffolds complexed with organic ligands produced a vandyl complexed to hydroxypicolinic acid (VO-OHPic $IC_{50} = 35 \pm 2.0$ nM against PTEN, *in vitro*) was reported to be a more selective inhibitor of PTEN relative to other cysteine-based phosphatases *in vivo* and *in vitro* (Rosivatz, Matthews et al. 2006). Subsequent studies, gave

insight into the mechanism of VO-OHpic showing that it's a reversible and noncompetitive inhibitor of PTEN (Mak, Vilar et al. 2010). VO-OHpic has been used in multiple studies including PTEN's role in PI3K-dependent signaling (Papakonstanti, Ridley et al. 2007), PTEN-induced senescence (Alimonti, Nardella et al. 2010) and cardiac function (Zu, Shen et al. 2011).

Chemical modulators of SHIP phosphatase

As with PTEN, both SHIP1 and SHIP2 negatively regulate PtdIns(3,4,5)P₃ signaling pathways although through their 5-phosphatase activity to generates PtdIns(3,4)P₂. The misregulation of SHIP proteins through either their activation or inactivation produces a number of beneficial or detrimental phenotypes making them attractive targets for chemical modulation (Viernes, Choi et al. 2013). The literature regarding SHIP proteins is expansive and the reader is referred to several excellent review articles (Bunney and Katan 2010; Liu and Bankaitis 2010; Viernes, Choi et al. 2013). Here I will discuss several of the recent advances in chemicals that activate SHIP1 and those that inhibit SHIP1, SHIP2 or are pan-SHIP inhibitors.

To identify SHIP1 agonists, crude extracts of marine invertebrates were screened *in vitro* for SHIP1-catalyzed conversion of ins(1,3,4,5)P₄ to ins(1,3,4)P₃. From this screen, Yang et al. identified SHIP1-activating activity in the MeOH extract of *Dactylospongia elegans* that were collected from Papua New Guinea. By utilizing assay-guided fractionation, pelorol was identified as the active compound (Yang, Williams et al. 2005). Subsequent studies generated the pelorol derivative, tolyl (AQX-016A) which had improved

biological activity (Yang, Williams et al. 2005; Ong, Ming-Lum et al. 2007; Meimetis, Nodwell et al. 2012). Due to AQX-016A's unfavorable medicinal chemistry, the catechol-free derivative AQX-MN100 was developed which has similar potency profile to that of AQX-016A although with more favorable chemistry (Goclik, König et al. 2000; Ong, Ming-Lum et al. 2007). These inhibitors are allosteric activators of SHIP1 and provided the first experimental evidence that SHIP1 activators function as anti-inflammatory agents *in vivo* and *in vitro* (Ong, Ming-Lum et al. 2007). Clinical trials have been initiated with non-plorol SHIP1 activators that showed an approximately ~20% increase in SHIP1 activity, inhibited cytokines and was effective at treating pulmonary inflammation in mice (Stenton, Mackenzie et al. 2013; Stenton, Mackenzie et al. 2013; Viernes, Choi et al. 2013). Other SHIP1 agonists have been identified such as Australin E and cyclic depsipeptides; however, these will not be discussed here (Williams, Amlani et al. 2010; Li, Carr et al. 2011; Viernes, Choi et al. 2013).

SHIP1 inhibitors have been developed that utilize metabolically stabilized PtdIns(3,4,5)P₃. Derivatives were synthesized that replace the D-3 or D-5 phosphate group with a phosphorothioate (PT) or methylenephosphonate (MP) to generate 3-PT, 3-MP- (Zhang, Markadieu et al. 2006), 5-PT-, 5-MP-PtdIns(3,4,5)P₃ (Zhang, Markadieu et al. 2006) and 3,4,5-P₃PtdIns(3,4,5)P₃.(Zhang, Xu et al. 2008). PT's are phospho-mimetics that have reduced rates of enzyme-mediated hydrolysis (Lampe, Liu et al. 1994). These derivatives do not perfectly mimic PtdIns(3,4,5)P₃ as the P=O replaced by P=S results in a lost hydrogen-bond acceptor and altered its pKa (Murray and Atkinson 1968; Hampton, Brox et al. 1969). It was shown that the 5-PT- and 5-MP-PtdIns(3,4,5)P₃ derivatives were ineffective against both SHIP2 and PTEN phosphatase activity *in vitro* (Zhang, He et al. 2010). *In vitro*, 5-MP-PtdIns(3,4,5)P₃ and 3,4,5-PT₃-PtdIns(3,4,5)P₃ showed approximately 50% inhibition against

SHIP1 with approximately 20% inhibition of SHIP2, and no inhibition of PTEN phosphatase activity as measured by the dephosphorylation of Ins(3,4,5)P₃ *in vitro*. Another class of inhibitor was later identified by utilizing a fluorescent polarized-based high-throughput screen the SHIP1 inhibitor, 3 α -aminocholestane (3AC). 3AC inhibited SHIP1 with an IC₅₀ of 10 μ M with no inhibition observed for SHIP2 or PTEN *in vitro* (Brooks, Fuhler et al. 2010). 3AC demonstrated cytotoxicity towards hematologic cancers *in vitro* and multiple myeloma (MM) in an *in vivo* mouse model (Brooks, Fuhler et al. 2010; Fuhler, Brooks et al. 2012) suggesting that it may be a potential anti-cancer lead compound.

SHIP2 inhibitors have been developed including biphenyl 2,3',4,5',6-pentakisphosphate which is composed of five phosphate groups on two rings and inhibits the catalytic domain of human type-I InsP₃ 5-phosphatase and SHIP2 (both involved in insulin signaling). Type-I InsP₃ 5-phosphatase and SHIP2 are inhibited with IC₅₀s of 7.9 \pm 0.7 μ M and 1.8 \pm 0.2 μ M, respectively, as measured by the dephosphorylation of Ins(1,3,4,5)P₄ *in vitro* (Vandeput, Combettes et al. 2007). Suwa et al., identified the thiophene-based SMI, AS1949490, a SHIP2-specific inhibitor that selectively and competitively inhibits both human (IC₅₀=0.62 \pm 0.02 μ M) and mouse SHIP2 (IC₅₀=0.34 \pm 0.1 μ M) *in vitro* (Suwa, Yamamoto et al. 2009). SHIP1 has an IC₅₀ of approximately 12 μ M whereas human PTEN, synaptojanin and myotubularin are not inhibited by AS1949490 *in vitro* (Suwa, Yamamoto et al. 2009). Treatment with AS1949490 activates intracellular insulin signaling while decreasing both fasting and post-partial blood glucose in *diabetes (db/db)* mice (Kobayashi, Forte et al. 2000; Suwa, Yamamoto et al. 2009). Subsequently, Suwas et al., conducted additional characterization and identified the SHIP2 inhibitor, AS1938909, that has increased selectivity for SHIP2 compared to SHIP1 while maintaining similar potency for SHIP2

(Suwa, Kurama et al. 2010). Recently, the phosphatase domain of SHIP2 was crystalized in complex with biphenyl-derived polyphosphate, biphenyl 2,3',4,5',6-pentakisphosphate (BiPh(2,3',4,5',6)P₅) to 2.1 Å (Suwa, Kurama et al. 2010). Interestingly, this group did molecular dynamics simulations with AS1938909 and demonstrated that it can bind in the region where BiPh(2,3',4,5',6)P₅ binds and propose SMI analogues to increase fidelity (Mills, Persson et al. 2012). Utilizing a high-throughput affinity selection-mass spectrometry screen, three classes of SHIP2 inhibitors were identified; however, the pyrazole-based SHIP2 inhibitor NGD-61338 was highlighted (Annis, Cheng et al. 2009). NGD-61338 is a competitive inhibitor with a predicted target-specific binding of one (Annis, Cheng et al. 2009).

Ichihara et al., utilized the structures of both AS1949490 (Suwa, Yamamoto et al. 2009) and NGD-61338 (Annis, Cheng et al. 2009) for *in silico* ligand-based drug design (LBDD) to identify novel SHIP2 inhibitors (Ichihara, Fujimura et al. 2013). LBDD compiled the three-dimensional structures of the two known SHIP2-directed inhibitors to generate a total of 18,193,092 alignments. Subsequently, the top 63 highest scoring alignments were clustered into four modes which informed the synthesis of the four lead compounds. Through SAR analysis, 28 compounds were synthesized for downstream testing cell-based testing (Ichihara, Fujimura et al. 2013). Of these compounds, twelve out of the twenty eight inhibited insulin-induced Akt phosphorylation in tissue-culture where several from each of the four classes inhibited this activity, suggesting that the designed scaffolds are potential SHIP2 inhibitors (consistent with their parent inhibitors). The most potent inducer of Akt phosphorylation was N-[4-(4-chlorobenzyloxy) pyridin-2-yl]-2-(2,6-difluorophenyl)-acetamide or CPDA which also partially rescued abnormal glucose metabolism in diabetic

mice (*db/db*; Ichihara, Fujimura et al. 2013). Although this data is suggestive that SHIP2 is inhibited by CPDA, evidence was not provided that demonstrates direct-inhibition of SHIP2 or specificity relative to other phosphatases (*e.g.* SHIP1). Multiple groups have generated SHIP2-directed lead compounds that utilize high-throughput affinity selection-mass spectrometry (inhibitor NGD-61338; Annis, Cheng et al. 2009), competitive fluorescence polarization assays (Drees, Weipert et al. 2003) and microfluidics (Rowe, Hale et al. 2006).

Three pan-SHIP inhibitors were identified in a high-throughput screen for SHIP inhibitors (Brooks, Fuhler et al. 2010). These inhibitors, 1PIE, 2PIQ and 6PTQ have IC_{50} s ($\mu\text{mol/L}$) for SHIP1/SHIP2 of 30/30, 500/500, 63/35 *in vitro*, respectively (Fuhler, Brooks et al. 2012). Additionally, none of these three inhibitors inhibited the inositol polyphosphate 5-phosphatase OCRL-1 (INPPP5F). As with the SHIP1 inhibitor 3-AC MM cells were also inhibited by the pan-SHIP inhibitors; however the cells were more sensitive to the pan-SHIP inhibitors. For additional information regarding SHIP proteins and SMIs that target them the reader is referred to review articles on the subject (Hamilton, Ho et al. 2011; Kerr 2011; Fernandes, Iyer et al. 2013; Viernes, Choi et al. 2013). Viernes et al., is an excellent historical account of SHIP modulators and the rationale for the development of SHIP modulators (Viernes, Choi et al. 2013).

Screening for synaptojanin inhibitors

Synaptojanin 1 is a phosphatidylinositol phosphate phosphatase that displays enriched expression in the nervous system whereas its isoform, synaptojanin 2, is broadly expressed (McPherson, Takei et al. 1994; Nemoto, Wenk et al. 2001). Synaptojanin 1 consists of two

splice variants, synaptojanin-145 and synaptojanin-170 where synaptojanin-145 is highly expressed in nerve terminals (Ramjaun and McPherson 1996). Synaptojanin interacts with clathrin-coated endocytic intermediates and functions in the clathrin-mediated endocytosis of synaptic vesicles (McPherson, Garcia et al. 1996; Ramjaun and McPherson 1996; Haffner, Takei et al. 1997). Synaptojanins are composed of: an NH₂-terminal region homologous to the yeast Sac1p [reviewed in (Liu and Bankaitis 2010)], a central inositol 5-phosphatase domain, a COOH-terminal region with a Src homology 3 (SH3) domain, three NPF-repeats and an AP2-binding site (Montesinos, Castellano-Muñoz et al. 2005). The Synaptojanin Sac1-domain hydrolyzes PtdIns(3)P, PtdIns(4)P, and PtdIns(3,5) *in vitro* (Guo, Stolz et al. 1999); however, its *in vivo* substrate is unknown. The central PtdIns 5-phosphatase domain hydrolyzes both PtdIns(4,5)P₂ and PtdIns(3,4,5)P₃ at the D-5 position with PtdIns(4,5)P₂ being its primary physiological substrate (McPherson, Garcia et al. 1996; Cremona, Di Paolo et al. 1999; Guo, Stolz et al. 1999; Chang-Ileto, Frere et al. 2011). It's this conversion of PIP₃ to PIP₂ that is thought to be synaptojanin's primary physiological role (Cremona, Di Paolo et al. 1999). The COOH-terminal region of synaptojanin domain interacts with multiple proteins involved in clathrin-mediated vesicles (Montesinos, Castellano-Muñoz et al. 2005; Liu and Bankaitis 2010). Defects in Synaptojanin has recently been linked to early onset Parkinsonism disorder (Quadri, Fang et al. 2013). In 2010 Montesinos et al., developed a high-throughput assay to identify small molecule inhibitors of synaptojanin. This assay monitors the phosphatase activity of recombinant synaptojanin, through the detection of free phosphate through the fluorescence of resorufin after a series of oxidative reactions initiated by free phosphate. No synaptojanin inhibitors have yet been published (McIntire, Lee et al. 2013). For additional information regarding synaptojanin the reader is

referred to the following texts (Montesinos, Castellano-Muñoz et al. 2005; Liu and Bankaitis 2010).

Inhibitors of PtdIns-4-kinases

PtdIns 4-OH kinases catalyze the phosphorylation of PtdIns at the D-4 position of its inositol headgroup to generate PtdIns(4)P through the consumption of PtdIns and ATP. PtdIns represents approximately 10-20% (mol%) of total cellular phospholipids, where PtdIns(4)P and PtdIns(4,5)P₂ constitute approximately 2-5% of total PtdIns (Balla, Baukal et al. 1988; Di Paolo and De Camilli 2006; Balla 2013). PtdIns(4)P is commonly considered a *trans*-Golgi marker; however, it regulates multiple activities including the recruitment of membrane trafficking components (Santiago-Tirado and Bretscher 2011; Balla 2013), viral replication (Bishe, Syed et al. 2012; Delang, Paeshuyse et al. 2012) and it is reported to be misregulated in some cancers (Altan-Bonnet and Balla 2012; Waugh 2012). Additionally, PtdIns(4)P is the precursor of two important PIPs, PtdIns(4,5)P₂ and PtdIns(3,4,5)P₃ and thus, pools of PtdIns(4)P are found at both the plasma membrane in addition to TGN/endosomes (Roy and Levine 2004).

PtdIns 4-OH kinases are divided into two families; Type II and Type III kinases, based on their biochemical properties, activity in cellular fractions and sensitivity to wortmannin (Balla 2013). Type I PtdIns 4-OH kinase are no longer included as they were subsequently identified as PtdIns 3-OH kinase (Whitman, Downes et al. 1988). *Saccharomyces cerevisiae* contains a single Type II PtdIns 4-OH kinase Lsb6, whereas vertebrates express two isoforms, PI4KII α and PI4KII β (Han, Audhya et al. 2002; Balla

2013). Lsb6 was originally identified as a binding partner of Las17p using a yeast two-hybrid assays (Madania, Dumoulin et al. 1999) which is the yeast homologue of the Wiskott-Aldrich Syndrome protein (WASP; Li 1997). WASP is linked to immune-deficiencies and defects in blood cell morphogenesis (Derry, Ochs et al. 1994). Lsb6p is non-essential, associates with the plasma membrane and vacuolar membranes (Han, Audhya et al. 2002). Lsb6 null strains do not display obvious growth-defects or defects in PIP synthesis (Han, Audhya et al. 2002). Lsb6 null strains display impaired endosome motility; however, yeast expressing the catalytically-dead Lsb6p, rescue endosomal defects, indicating that the endosomal motility defects are PtdIns(4)P-independent (Chang, Han et al. 2005). The mammalian Type II enzymes, PI4KII β and PI4KII α are primarily localized to internal TGN/endosomal membranes (Balla, Tuymetova et al. 2002). PtdIns(4)P generated through PI4KII α recruits clathrin adapter proteins to TGN/endosomes such as GGAs (Wang, Sun et al. 2007), AP-1 (Wang, Wang et al. 2003) and AP-3 to endosomes (Salazar, Craige et al. 2005). In general, little is known about the PI4KII β isoform (Balla and Balla 2006; Balla 2013).

The first PI4Ks to be cloned were Pik1 and Stt4, both Type III kinases from *Saccharomyces cerevisiae* (Flanagan, Schnieders et al. 1993; Yoshida, Ohya et al. 1994). Pik1 and Stt4 have non-redundant functions despite generating the same lipid product, distinguishing their activity by their localization to distinct membrane compartments (Audhya, Foti et al. 2000); however, Lsb6 overexpression partially suppresses *stt4 Δ* yeast (Han, Audhya et al. 2002). Stt4 was originally identified as a protein affecting staurosporine sensitivity (Yoshida, Ohya et al. 1994). STT4 is an essential gene, whose product Stt4p is a ~215 kDa membrane associated protein (Yoshida, Ohya et al. 1994; Audhya and Emr 2002).

Disruption of *Stt4* causes multiple defects which include impaired cell wall integrity, actin organization, vacuolar morphology (Audhya, Foti et al. 2000) and sphingolipid metabolism (Tabuchi, Audhya et al. 2006). *Stt4p* localizes to the plasma membrane through *Sfk1p* (Suppressor of Four Kinase), and regulates Rho/Pkc1-mediated MAP kinase cascade (Audhya and Emr 2002). Yeast's other type II PI4K, *PIK1* is an essential gene whose protein product, *Pik1p* is a soluble 125kD protein that primarily localizes to the Golgi and nucleus (Flanagan and Thorner 1992; Garcia-Bustos, Marini et al. 1994; Walch-Solimena and Novick 1999). The temperature sensitive *pik1* alleles have a number of defects at non-permissive temperature, including: normal secretion, Golgi and vacuole membrane dynamics, endocytosis (Audhya, Foti et al. 2000) and autophagy (Wang, Yang et al. 2012). Together with *Stt4*, these two enzymes generate the majority of *PtdIns(4)P* in yeast cells where each contribute about half of the *PtdIns(4)P* (Audhya, Foti et al. 2000). However, overexpression of one enzyme cannot complement the other, demonstrating unique activities for their respective *PtdIns(4)P* pools (Audhya, Foti et al. 2000). For *Pik1* to support cell viability *Pik1* must localize to both TGN/endosomal membranes and the nucleus. Membranes localization of *Pik1* is mediated by *Frq1* (a homologue of the neuronal calcium sensor (NCS)), where it binds to *Pik1*'s NH₂-termini (Hendricks, Qing Wang et al. 1999; Strahl, Hama et al. 2005).

The mammalian Type III *PtdIns* 4-OH kinases *PIK4III α* , is the orthologue of the yeast *Stt4* (Yoshida, Ohya et al. 1994). This protein is primarily localized to the plasma membrane of mammalian cells and its main function is to supply plasma membrane *PtdIns(4)P* (Balla, Kim et al. 2008). A number of recent reports have linked the disruption of *PI4KIII α* with reduced viral replication of the hepatitis C (HCV), making *PIK4III α* a new 'hot' drug target. For more details regarding *PtdIns* 4-OH kinases, the reader is referred to a

number of excellent reviews on the subject (Balla 2007; Santiago-Tirado and Bretscher 2011; Altan-Bonnet and Balla 2012; Balla 2013). PI4K inhibitors will provide useful tool compounds and are promising targets to inhibit viral propagation and other infections organism such as Plasmodium. The number and quality of PI4K inhibitors is limited and significant efforts are only starting to be devoted to their discovery.

The PtdIns 3-OH kinase inhibitors, wortmannin and LY294002 inhibit PtdIns 4-OH kinase at levels in excess of those needed to inhibit PtdIns 3-OH kinase activity (Nakanishi, Catt et al. 1995; Downing, Kim et al. 1996; Sorensen, Linseman et al. 1998; Balla and Balla 2006). Both the alpha and beta isoforms of PI4KIII are sensitive to both Wortmannin with an IC_{50} ~50-300nM and to LY294002 which inhibits PI4KIII α and PI4KIII β with IC_{50a} of ~50-100 μ M or 100 μ M, respectively (Nakanishi, Catt et al. 1995; Downing, Kim et al. 1996; Meyers and Cantley 1997; Sorensen, Linseman et al. 1998; Balla and Balla 2006). The more potent inhibitory activity of these compounds towards PI3K (see above) makes the data interpretation of experiments utilizing wortmannin or LY294002 to inhibit PI4KIII's uninterruptable. Additionally, phenylarsine oxide (PAO) has been used as an inhibitor of PIP synthesis (Schaefer, Wiedemann et al. 1994; Wiedemann, Schafer et al. 1996; Balla and Balla 2006). PAO inhibit PIP synthesis that and prevents the release of catcholamine from chromaffin cells presumably through the inhibition of PI4K (Wiedemann, Schafer et al. 1996). Subsequently, it was reported that PAO inhibits the endocytosis of muscarinic cholinergic receptors through the inhibition of PI4K in neuroblastoma cells (Sorensen, Linseman et al. 1998). The incubation of PAO also inhibits *N*-formyl-methionyl-leucyl-phenylalanine (fMLP)-stimulated respiratory burst and a PMA-induced respiratory burst (Yue, Liu et al. 2001). Because PMA is a 'direct activator' of PLC, it was suggested that

PAO is a non-specific inhibitor of PI4K activity likely making the data obtained using PAO uninterrupted (Yue, Liu et al. 2001). Additionally, it is reported that both mammalian PI4KIIIs are insensitive to PAO ($IC_{50} > 100 \mu M$) whereas PI4KIII α and PI4KIII β have IC_{50} s of 1-5 μM and $\sim 30 \mu M$, respectively (Balla and Balla 2006). Resveratrol is a naturally occurring stilbene (one of two isomers of 1,2-diphenylethene) that is generated by plants in response to injury or fungal infection (Langcake and Pryce 1977) and has been shown to inhibit PI4KII β but not PI3K (IP of p85 or p110) or the yeast Pik1p (vertebrate PI4KIII β) *in vitro*.

Resveratrol has a binding coefficient of $K_d = 7.2 \mu M$ and competes with the PtdIns binding site (Srivastava, Ratheesh et al. 2005). Resveratrol has been shown to bind and inhibit multiple targets including cyclooxygenases, PKC, and COX2 (Slater, Seiz et al. 2003; Murias, Handler et al. 2004; Zykova, Zhu et al. 2008) suggesting that it may not be an ideal inhibitor of PI4K; however, the limited investigations of its interactions with PI4KII β suggest that it may provide superior selectivity compared to wortmannin and LY294002 less than ideal.

Evidence has been accumulating that viral replication utilizes PtdIns 4-OH kinases (Altan-Bonnet and Balla 2012; Bishe, Syed et al. 2012; Delang, Paeshuysse et al. 2012). Because of this connection, multiple groups have intensified screening efforts to identify inhibitors of PtdIns 4-OH kinases. It was previously demonstrated that the mammalian PtdIns 4-OH kinase III α (PI4KIII α) and PI4KIII β are important host factors for the hepatitis C virus (HCV) and potentially other viruses (Balla and Balla 2006; Borawski, Troke et al. 2009; Altan-Bonnet and Balla 2012). These recent 'anti-viral' lead-compounds are relatively new with limited validation and will not be discussed in detail. Several examples of these newly identified SMIs include: quinazolinone (Leivers, Tallant et al. 2013), Thiazolyl-

dihydro-chinazoline (Brandl, Maier et al. 2007; Vaillancourt, Brault et al. 2012), Thiazolyl-dihydro-cyclopentapyrazole (Breitfelder, Maier et al. 2007; Vaillancourt, Brault et al. 2012), AL-9 (Bianco, Reghellin et al. 2012), Enviroxime (Arita, Kojima et al. 2011; van der Schaar, Leyssen et al. 2013), GW5074 (van der Schaar, Leyssen et al. 2013), and others (LaMarche, Borawski et al. 2012; van der Schaar, Leyssen et al. 2013; Waring, Andrews et al. 2014).

Two novel drug classes, imidazopyrazines and quinoxaline were recently identified as antimalarial agents that inhibit the parasite's PI4KIII β . As discussed above on of the functions for PI4KIII β is to regulate intracellular signaling and trafficking in *Plasmodium* of these compounds were tested as anti-malarial drug candidates (McNamara, Lee et al. 2013). Indeed, under drug intoxication the intracellular development of multiple *Plasmodium* species was disrupted at every stage of host infection with IC_{50s} in the low nM range (McNamara, Lee et al. 2013). Treatment with imidazopyrazines blocks late stage parasite development through the disruption of membrane ingression around the daughter merozoites. This is suggested to be a result of altered PtdIns(4)P levels and the disruption of Rab11A-mediated membrane trafficking (McNamara, Lee et al. 2013). Mechanistically, these SMIs are predicted to inhibit the PtdIns 4-OH kinase by binding to the ATP-binding pocket as determined through both ATP-competition assays, mutation-induced resistance, and *in silico* analysis. To monitor for off target activity, an array of approximately 40 human kinases were assayed demonstrating that the parasite kinase is ~1000x more sensitive to drug. Finally, it was demonstrated that the propagation of *Plasmodium* in rodent malaria models was inhibited upon drug treatment (McNamara, Lee et al. 2013). Together McNamara et al., provide compelling data regarding target-validation and its role as a potential anti-malarial therapeutic that targets all life stages of *Plasmodium*.

Inhibitors of phospholipase C

Phospholipase C enzymes (PLC) are divided into two classes based on their substrate specificity: those that act on phosphatidylinositol (PtdIns-PLC) or phosphatidylcholine (PtdCho-PLC; Balla 2013). Here I will only discuss PtdIns-PLC enzymes as they are most relevant to our discussion on PIP-regulation. PtdIns-PLC enzymes catalyze the cleavage of the polar head group of inositol-containing phospholipids including PtdIns, PtdIns(4)P and PtdIns(4,5)P₂ at the phosphodiester bond proximal to the glycerol backbone generating Ins(1)P, Ins(1,4)P₂, and Ins(3,4,5)P₃, respectively (Ryu, Suh et al. 1987) and cyclic inositol phosphates (Kim, Ryu et al. 1989). All of these substrates when degraded generate diacylglycerol (DAG; Ryu, Suh et al. 1987) which itself is involved in multiple downstream signaling pathways including the promotion of protein kinase C (PKC) phosphorylation (Lipp and Reither 2011). The primary substrate of PLC is PtdIns(4,5)P₂ to generate DAG and Ins(1,4,5)P₃ which binds Ins(1,4,5)P₃ receptors. Subsequently, Ca²⁺ is released from the endoplasmic reticulum and in conjunction with DAG is responsible for many downstream signaling events (Kadamur and Ross 2013). Ins(3,4,5)P₃ receptors are conserved from humans to *C.elegans* although they are not found in yeast (Taylor, Genazzani et al. 1999). Instead in yeast Ins(1,4,5)P₃ is the precursor for water soluble inositol polyphosphates (IPs) which regulate multiple cellular processes including gene expression, mRNA export, DNA repair and telomerase maintenance (York 2006; Tsui and York 2010).

Mammalian PtdIns-PLC proteins contain a core conserved structure that is comprised of a pleckstrin homology (PH) domain, four tandem EF-hand domains, a split TIM barrel,

and a C2 domain (Kadamur and Ross 2013). The catalytic site, and the Ca^{2+} binding site, is contained on the TIM barrel (Kadamur and Ross 2013). PtdIns-PLC proteins are conserved proteins and are found in bacteria, yeast, flies, and mammals (Vines 2012; Kadamur and Ross 2013). In yeast, a single cytoplasmic PtdIns-PLC variant (PLC1; most similar to mammalian $\text{Plc}\delta$) is present and is specific for $\text{PtdIns}(4,5)\text{P}_2$. Deletion of PLC1 in yeast, results in a number of defects including: reduced growth rate, impaired cell wall integrity, impaired management of osmotic stress and difficulties in the utilization of non-glucose carbon sources (Flick and Thorner 1993; Yokoyama, Matsui et al. 1993; Rebecchi and Pentylala 2000). Mammals contain thirteen PtdIns-PLC isozymes which are divided into six isotypes (β , γ , δ , ϵ , ζ , and η) based on their structure, activity and localizations (Balla 2013; Kadamur and Ross 2013). The literature associated with PtdIns-PLC enzymes is extensive and it will not be described in depth. Instead, the reader is referred to review articles that provide additional depth (Rhee and Choi 1992; Rebecchi and Pentylala 2000; Balla 2013; Kadamur and Ross 2013).

PLC enzymes regulate the activity and level of important signaling molecules key to cellular survival. The generation of PLC-specific inhibitors will greatly help advance our understanding of these enzymes; however, none that meet my validation criteria exist. Several putative small molecule inhibitors have been developed that are directed against PLC with varying selectivity towards PLC isozymes. The most commonly used SMI U-73122, is a sterol mimetic that inhibits PtdIns-PLC activity as measured by platelet aggregation stimulated by collagen ($\text{IC}_{50}=0.6\mu\text{M}$) or thrombin ($\text{IC}_{50}=5\mu\text{M}$; Bleasdale, Thakur et al. 1990; Smith, Sam et al. 1990). As control, the close structural analogue U-73343 was used that differs in that U-73343 contains an N-alkylsuccinimide moiety in place of the N-

alkymaleimide found in U-73122 (Bleasdale, Thakur et al. 1990). This structural modification suggests that the inhibitory activity of U-73122 is likely the result of the electrophilic maleimide (Bleasdale, Thakur et al. 1990). Maleimides react with sulfhydryl groups (-SH) at near neutral pH and form stable thioether linkages which may explain the numerous off targets associated with this SMI (Lutter and Kurland 1975). As of this writing there is limited evidence that U-73122 directly inhibits PLC.

U-73122 has a number of off targets including: telomerase (Chen, Sheng et al. 2006), 5-lipoxygenase synthesis induced by cell stress (Feißt, Albert et al. 2005), histamine H1 receptor (Hughes, Gibson et al. 2000), calcium channels (Pulcinelli, Gresele et al. 1998), sarcoplasmic/endoplasmic reticulum calcium ATPase pump in smooth muscle (MacMillan and McCarron 2010), cardiac phospholipase D by a PIP₂-dependent mechanism (Burgdorf, Schafer et al. 2010), exocytotic signaling pathways in rat peritoneal mast cells (RPMCs) (Gloyna, Schmitz et al. 2005), Kir3 and BK channels (Klose, Huth et al. 2008). Other reports suggest that U-73122 has preferential activity towards PLC β (Vines 2012) where others claim it's an activator of hPLC β 3, hPLC γ 1 and hPLC β 2 as measured in a cell-free, mixed micelle system (Klein, Bourdon et al. 2011). The reliance on U-73122 in the literature has been extensive with thousands of papers relying on this SMI as an inhibitor of PtdIns-PLC and as a probe for PLC's involvement in phenotypic and cellular responses. Most experiments use U73122 to monitor downstream events of PLC activation (*e.g.* intracellular calcium release) coupled with the lack of data for direct inhibition and the reported off-targets, great care should be used when interpreting results obtained from the use of the SMI U-73122.

Recently, a high-throughput screen based on the fluorogenic substrate reporter WH-15, identified three novel PLC inhibitors (Huang, Barrett et al. 2013). These inhibitors, aurintricarboxylic acid (ATA), 3013 and 3017 inhibited PLC δ 1 with IC_{50s} of 0.53 \pm 0.36 μ M, 7.3 \pm 2.1 μ M and 8.0 \pm 0.3 μ M *in vitro*, respectively as measured by a fluorescent-based assay (Huang, Barrett et al. 2013). Additionally, PLC γ 1 and PLC β 3 were inhibited to a similar extent *in vitro*, suggesting that all three inhibitors bind to the conserved PLC binding pocket (Huang, Barrett et al. 2013). The compound ATA has been shown to inhibit several enzymes including DNA topoisomerase II (Benchokroun, Couprie et al. 1995), the cytosine deaminase APOBEC3G (Li, Shandilya et al. 2011) and the kinase c-Met (Milanovic, Radtke et al. 2012) indicating that ATA will not become a useful tool compound (Huang, Barrett et al. 2013). Additionally, the other two compounds, 3013 and 3017 have limited solubility, moderate potency with no reports in the literature suggesting that more research will need to be done to determine if these SMIs will become useful tool compounds (Huang, Barrett et al. 2013). The natural product Manoalide irreversibly inhibits PLC, PLA2 and calcium channels (Bennett, Mong et al. 1987; Wheeler, Sachs et al. 1987; Potts, Faulkner et al. 1992). The natural product Thielavin B, derived from *Thielavia terricola* inhibits PLC, prostaglandin biosynthesis, telomerase activity, cell wall transglycosylation inhibitors, and glucose-6-phosphatase (G6Pase; Kitahara, Endo et al. 1981; Mani, Sancheti et al. 1998; Togashi, Ko et al. 2001; Sakemi, Hirai et al. 2002). The cytotoxic ether lipid mimetic Edelfosine (ET-18-OCH₃) direct inhibitor of Swiss 3T3 fibroblast and BG1 ovarian adenocarcinoma cell cytosolic phosphoinositide selective phospholipase C (PIPLC) (Powis, Seewald et al. 1992). However, there are a number of alternative targets for ET-18-OCH₃ indicating that this ether lipid is not a suitable inhibitor of PLC (Mollinedo, Gajate et al. 2004). It's clear that there

are not currently any PLC or PLC isozyme-specific inhibitors available to the community highlighting the need to identify new and specific tool compounds.

Inhibitors of inositol monophosphatase (IMPase)

Inositol monophosphatases (IMPase; EC 3.1.3.25) are highly conserved enzymes found in archaeobacteria (Chen and Roberts 1998), plants (Gillaspy, Keddie et al. 1995), and mammals (Hallcher and Sherman 1980; Gee, Ragan et al. 1988). IMPases are members of the phosphodiesterase family of enzymes, are homodimers and require Mg^{2+} for catalyzing the dephosphorylation of Ins(1)P, Ins(3)P and Ins(4)P (Hallcher and Sherman 1980; Majerus, Connolly et al. 1988). IMPase may also have a number of alternative cellular functions including Zn^{2+} -dependent tyrosine phosphatase activity, carbohydrate metabolism and protein dephosphorylation (Miller and Allemann 2007). Multiple IMPase structures have been solved, revealing that the monomer consists of alternating layers of α -helices and β -sheets forming a penta-layered $\alpha\beta\alpha\beta\alpha$ core structure (Bone, Springer et al. 1992).

Lithium has been used effectively to treat bipolar disorder; however, lithium has at least 10 targets (Can, Schulze et al. 2014) and two reported at clinical concentrations (0.6-1mM serum levels): glycogen synthase 3 β (O'Brien and Klein 2009) and IMPase (Hallcher and Sherman 1980; Gee, Ragan et al. 1988; Atack, Cook et al. 1993). Lithium inhibits recombinant IMPase and increase Ins(1)P levels in the brain (Hallcher and Sherman 1980; Sherman, Gish et al. 1986; Berridge, Downes et al. 1989) through an uncompetitive mechanism that also displaces Mg^{2+} (*i.e.* it becomes more effective as substrate levels increase; Hallcher and Sherman 1980; Gee, Ragan et al. 1988; Atack, Cook et al. 1993).

Myo-inositol is primarily generated from two sources: (i) the cyclization of glucose-6-phosphate (Eisenberg 1967) or (ii) the dephosphorylation of inositol monophosphate by IMPase (Berridge, Downes et al. 1982). Regardless of where inositol originates, IMPase is required for the final biosynthetic step prior to inositol's incorporation into CDP-DAG and the generation of PtdIns for downstream PIP-signaling (Agranoff, Bradley et al. 1958; Chen and Charalampous 1966; Gee, Ragan et al. 1988; Nahorski, Ragan et al. 1991). From this work, it was hypothesized that lithium reduces free *myo*-inositol and thus, PtdIns signaling which may restore overactive neurotransmitter signaling associated with mania. This model is now referred to as the 'inositol depletion hypothesis' (Berridge, Downes et al. 1982; Berridge, Downes et al. 1989; Schloesser, Huang et al. 2008). For a historical account and more details regarding the 'inositol depletion hypothesis' the reader is referred to several texts (Berridge, Downes et al. 1989; Schloesser, Huang et al. 2008).

Lithium is toxic at twice the therapeutic dosage and has a number of side effects including weight gain, thirst, tremors and kidney damage (Cade 1949). Coupled with the uncertainty of lithium's *in vivo* effect is the possibility that IMPase inhibition is not specific (*e.g.* glycogen synthase 3 β) therefore multiple SMIs have been developed against IMPase. All IMPase-directed SMIs demonstrate poor bio-availability except one (Miller and Allemann 2007; Singh, Halliday et al. 2013). To provide focus, I will exclude all bio-unavailable compounds except the original series. The initial IMPase-directed SMIs constructed contain phosphate groups but were ineffective *in vivo*. Through iterative modification, the drug L-690,330 was developed and is still in use (Baker, Carrick et al. 1991; Kulagowski, Baker et al. 1991; Atack, Cook et al. 1993; Shtein, Toker et al. 2013). L-690,330 is a competitive inhibitor (*i.e.* as substrate increases, the drug becomes less

effective) of IMPase *in vitro* and in cell culture (Atack, Cook et al. 1993). However L-690,330 had poor *in vivo* characteristics relative to lithium, likely a result of poor blood brain barrier penetration and solubility (Atack, Cook et al. 1993). This poor blood-brain barrier penetration was attributed to the inherent cell permeability issues associated with the bisphosphonate functional groups in L-690,330 (Atack, Cook et al. 1993). In an attempt to fix the ‘defect’ in L-690,330, the tetrapivaloyloxymethyl ester pro-drug L-690,488 was developed (Atack, Prior et al. 1994). However, administered L-690,488 was not detected in either serum or brain, suggesting that L-690,488 was unable to leave the injection site; relegating its use to *in vitro* applications (Atack, Prior et al. 1994). Recently through the use of intracerebroventricular (icv) administration of L-690,330-loaded liposomes has allowed its use in animal models to attenuate brain IMPase activity (Shtein, Toker et al. 2013).

Singh et al. recently reported the identification the first bio-available lithium-mimetic, ebselen (Singh, Halliday et al. 2013). To identify ebselen, they expressed human IMPase in bacteria and screened the NIH Clinical Collection library (Austin, Brady et al. 2004; Singh, Halliday et al. 2013). Ebselen inhibited human ($IC_{50}=1.5\mu M$) and mouse IMPase *in vitro* and requires an electrophilic selenium group to initiate the covalent and irreversible inhibition of IMPase. Ebselen reduced the agonist-induced cortically mediated 5-HT₂ receptor-dependent head twitch in a dose-dependent manner suggesting that ebselen inhibited IMPase *in vivo* (a PIP-dependent process), similar to that of lithium (Barnes and Sharp 1999; Singh, Halliday et al. 2013). Ebselen passed the blood brain barrier, reduce inositol levels and rescues bipolar-associated behavioral phenotypes in mice. These behavioral phenotypes are restored upon the delivery of intracerebroventricular inositol as observed with lithium treatments in rats

(Kofman and Belmaker 1990; Singh, Halliday et al. 2013). Together ebsele offers a novel and exciting new lead compound for the treatment of bipolar disorder.

Conclusions and future directions

Utilizing counter-ligand and pocket geometry to identify isomer-specific PITP inhibitors

Chapter 1 describes how the disruption of PITPs results in multiple inherited mammalian diseases and how these proteins are utilized as essential virulence factors for pathogenic organisms. Primary amino acid alignments and the solution of Sec14-like crystal structures reveal a highly conserved structure--the Sec14-fold. Based on this data, it's apparent that the binding site for PtdIns, but not the counter ligand is conserved throughout the Sec14-superfamily (**Figure 4**). Disease causing mutations in many PITPs are located at the counter-ligand binding site and can easily explain protein dysfunction. For example, mutations in the α -tocopherol binding site in α TTP; however, multiple mutations are often occupy a distant site and were not so explained until recently. Many of these mutations align with the PtdIns binding barcode, although these proteins were not thought to bind or exchange PtdIns/PIP because most of these proteins were isolated based on their ability to bind and transfer their counter ligand (e.g. α -tocopherol). These disruptive mutations in the PtdIns barcode suggest the divergent Sec14-like PITPs also use a two-ligand heterotypic exchange mechanism similar to those found in Sec14/Sfh1. This model is supported by the recent crystallization of α TTP bound to PtdIns(3,5)P₂ or PtdIns(4,5)P₂, where PIP₂ mimics the distinct PtdIns binding observed in Sfh1 and Sec14. As expected, mutations in the PtdIns head-group binding site disrupts PIP₂ binding/transfer, which is essential for α TTP *in vivo*

activity (Kono, Ohto et al. 2013), as we predicted (Schaaf, Ortlund et al. 2008; Nile, Tripathi et al. 2014). Together this data supports the conservation of the ‘nanoreactor’ model from yeast to mammalian Sec14-like PITPs (Nile, Bankaitis et al. 2010{Schaaf, 2008 #1008). From these and other studies it’s apparent that Sec14-like proteins have three ‘hot-spots’ where point-mutations inactivate Sec14-like PITPs: **(i)** the PtdIns/PIP head-group binding site **(ii)** the counter-ligand binding site (*e.g.* PtdCho, α -tocopherol, etc.) or **(iii)** the gating module (*e.g.* G₂₆₆D in *sec14-1^{ts}*; **Figure 4**).

The study of PITPs has been hindered by the lack of chemical modulators directed against them. To my knowledge there has been no directed-efforts to identify chemical modulators of PITPs, likely because Sec14-like proteins appear to be challenging targets for chemical intervention, because: **(i)** there are at least 20 conserved family members in mammals making isoform-specific chemical modulation difficult **(ii)** PITPs have a large hydrophobic cavity that may bind non-specifically to hydrophobic molecules and **(iii)** no previous chemical modulators of PITPs have been identified. However, these ‘weaknesses’ as I describe below provide rationale for developing chemical modulators with high degree of selectivity—even between the two closest homologues, Sec14 and Sfh1.

Variation between the counter-ligand binding site easily explains why NPPMs differentiate between Sec14 and other yeast Sec14-like proteins (*e.g.* Sfh2, Sfh3, Sfh4 and Sfh5, **Figure 11**) because the PtdCho binding site is not conserved. Unexpectedly, Sec14’s closest homologue, Sfh1 is insensitive to NPPMs which was not predicted based on primary sequence alone (**Figure 11, Figure 15**). Utilizing *in silico* cavity-search-routines coupled with NPPM-docking simulations, reveal that NPPMs don’t form coherent solution sets in Sfh1’s hydrophobic cavity. We attribute this to an elongated hydrophobic patch relative to

Sec14 which eliminates π - π and hydrophobic interactions with the NPPM's phenyl tail, thereby destabilizing the NPPM-headgroup interactions at the PtdCho recognition site (**Figure 53**). Although we have not yet identified inhibitors directed against other Sec14-like proteins, this work provides evidence that isomer-specific chemical modulators of highly-similar Sec14-like proteins is probable by utilizing: (i) counter-ligand recognition site and (ii) the variable geometry of the hydrophobic cavity. Additionally, by taking advantage of the conserved PtdIns binding site may allow for the development of pan-Sec14 inhibitors; expanding the repertoire of useful tools to study these proteins.

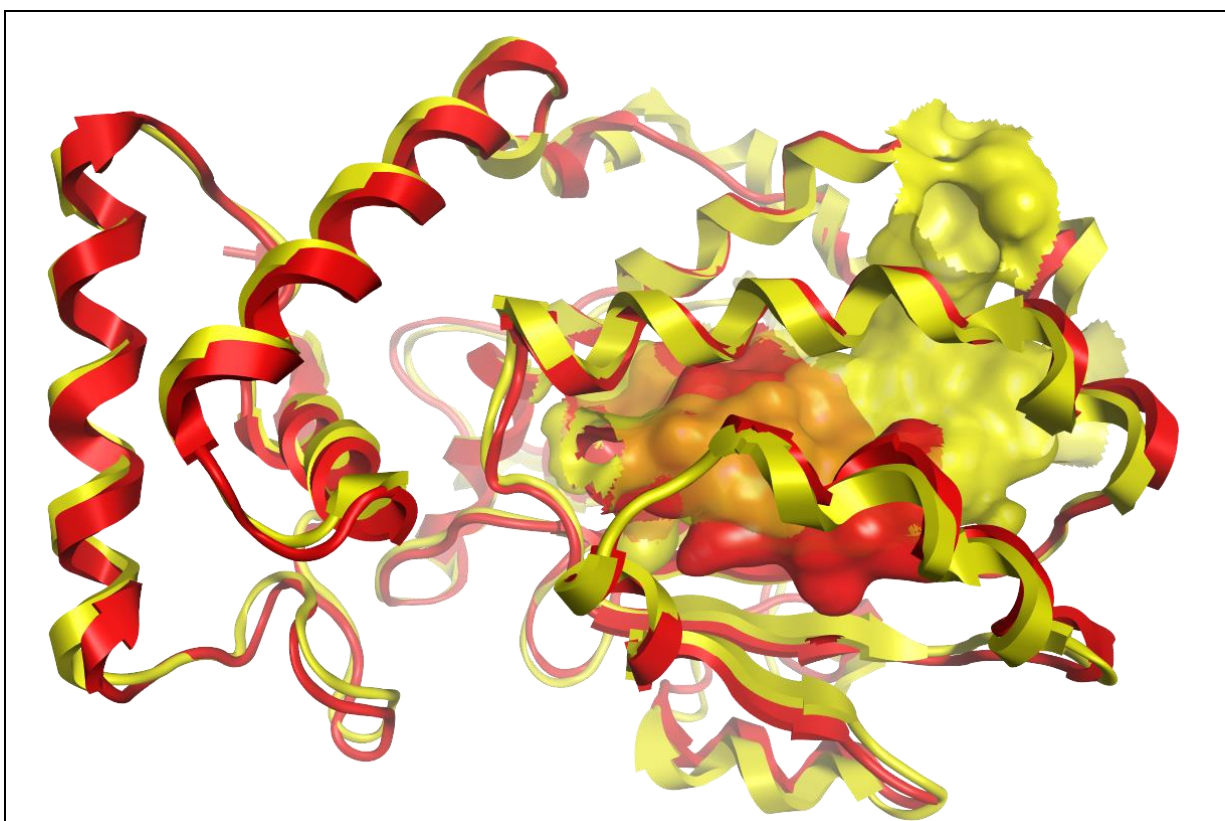


Figure 53. Sfh1 has an elongated hydrophobic cavity

Displayed are the Sfh1 (yellow) and the closed Sec14 homology (red) ribbon structures. The hydrophobic cavity is defined *in silico* and are displayed for both Sec14 (red) and the elongated hydrophobic cavity of Sfh1 (yellow).

Identification of SMIs directed against PITPs

PITPs are ubiquitously distributed across the *Eukaryota*, and are essential for the viability of pathogenic organisms such as *Candida albicans*, *Plasmodium* and humans. The fact that many of these PITPs genetically complement the yeast Sec14 can be exploited as yeast can be made into a screening platform for a desired PITP then screened for growth defects in the presence of diverse chemicals. Lead compounds can then be easily validated as described in Chapter 2. Importantly, this system also allows us to identify inhibitors of the structurally-unrelated mammalian START-like PITPs which also rescue Sec14 defects in yeast. Through this procedure I expect that we will identify multiple SMIs of interest against diverse PITPs.

SMIs against ‘bypass Sec14’ proteins and phospholipase D

The isolation of spontaneous suppressors of the *sec14-1^{ts}* allele (i.e. ‘bypass Sec14’) was instrumental in connecting Sec14’s PtdIns(4)P signaling cues and flux through the CDP-choline pathway (discussed in **Chapter 1**). These ‘bypass Sec14’ mutations suppress both the genetic and chemical inactivation of Sec14 (Nile, Tripathi et al. 2014; **Figure 20**; see **Chapter 1**). These genes are divided into three pathways which include the oxysterol binding protein Kes1, the PtdIns(4)P phosphatase (Sac1) and members of the CDP-Choline pathway (see **Chapters 1** and **Chapter 2**). Taking advantage of the PITP activator screen described above, inhibitors of ‘bypass Sec14’ proteins will also be isolated. This screen relies on the recovery of yeast growth, thereby eliminating many of the technical and signal/noise difficulties associated with high-throughput loss-of-function screens.

Additionally, a series of *sec14-1^{ts}* and ‘bypass Sec14’ double mutants can be screened for inhibitors of PLD (PLD is required for ‘bypass Sec14’ activity) by monitoring loss of growth in ‘bypass Sec14’ yeast. ‘Bypass Sec14’ inhibitors can be easily separated from PITP activators because ‘bypass Sec14’ inhibitors will no longer function in the phospholipase D deletion background whereas the activators should (*spo14Δ*; **Figure 21**). Although this is only a cursory test, it will provide confidence that the SMIs in question are worth additional validation and will inform the experimenter where the chemical modulator is acting.

Closing remarks

Phosphatidylinositol transfer proteins are highly conserved proteins that are found throughout the Eukaryota. Throughout evolution Sec14-like PITPs have retained their ability to bind and transfer PtdIns/PIPs, whereas the counter ligand(s) and associated binding sites have diversified to cover a variety of molecules such as α -tocopherol in the case of α TTP. We believe that it’s this second ligand that provides the signaling cue for the Sec14-like protein to stimulate PIP synthesis *in vivo*. Because these proteins are highly conserved based on their primary amino acid sequence and they contain a large hydrophobic cavity, Sec14-like PITPs have not been considered viable targets for chemical modulation. In Chapter 2, I describe how these characteristics can work in our favor to develop highly specific and potent SMIs that target the counter-ligand binding site and utilize subtle architectural differences in the hydrophobic cavity. By targeting PITPs we can more specifically inhibit specific arms of PIP signaling relative to the more traditional kinase inhibitors discussed in Chapter 3. As described above, most inhibitors that target PtdIns kinases target the

conserved ATP binding site making isomer cross-reactivity a common problem. However, unlike the kinase, we have multiple sites of variability within Sec14-like PITPs to design inhibitor that target specific isomers or if desirable, pan-Sec14 inhibitors. In conclusion, I have developed the first SMIs that target any PITP and have developed a rapid validation protocol for the development of novel inhibitors. Additionally, I propose utilizing what I have learned about drug validation and what we know about Sec14's genetic interactions to isolate chemical modulators of multiple proteins from diverse organisms that include: (i) PITPs (ii) OSBPs (iii) PtdIns(4)P phosphatases, (iv) phospholipase D and (v) members of the CDP-choline pathway.

Table 6. Yeast Strains

<u>Strains</u>	<u>Genotype</u>	<u>Origin</u>
CTY1-1A	<i>MATa ura3-52 lys2-801 his3Δ-200 sec14-1^{ts}</i>	(Bankaitis, Malehorn et al. 1989)
CTY 100	<i>MATa ura3-52 lys2-801 his3Δ-200 sec14-1^{ts} sac1-26^{CS}</i>	(Rivas, Kearns et al. 1999)
CTY159	<i>MATa ura3-52 lys2-801 his3Δ-200 sec14-1^{ts} kes1-1</i>	(Cleves, McGee et al. 1991)
CTY160	<i>MATa ura3-52 his3Δ-200 sec14-3 cki1-1</i>	(Cleves, McGee et al. 1991)
CTY182	<i>MATa ura3-52 lys2-801 his3Δ-200 SEC14</i>	(Bankaitis, Malehorn et al. 1989)
CTY303	<i>MATa ura3-52 lys2-801 his3Δ-200 sec14Δ::HISG cki1-1</i>	(Li, Routt et al. 2000)
CTY374	<i>MATa trpΔ his3Δ-200 lys2-801 ade2-101 sec14Δ1::HIS3 ura3-52::[sec14-ΔP136/URA3]</i>	(Salama, Cleves et al. 1990)
CTY558	<i>MATa ade2 ade3 leu2 his3Δ ura3-52 sec14Δ1::HIS3 pCTY11</i>	(Phillips, Sha et al. 1999)
CTY1568	<i>MATa leu2 ura3 his3 trpΔ lys2-800 suc2Δ stt4Δ::HIS3 YCp[stt4-4 LEU2]</i>	Jeremy Thorner
CTY1708	<i>MATa ade2-101 his3Δ-200 leu2-Δ1 trp1-Δ1 ura3-52 lys2-801α pik1-83::TRP</i>	Jeremy Thorner
HO1	<i>MATa HO/ho::KanMX3</i>	(Hoon, Smith et al. 2008)
ANY104	<i>MATa ade2 ade3 leu2 his3Δ ura3-52 sec14Δ1::HIS3 YCplac33(SEC14)</i>	(Nile, Tripathi et al. 2014)
ANY115	<i>MATa ade2 ade3 leu2 his3Δ ura3-52 sec14Δ1::HIS3 YCplac33(SEC14^{Y111A})</i>	(Nile, Tripathi et al. 2014)
ANY116	<i>MATa ade2 ade3 leu2 his3Δ ura3-52 sec14Δ1::HIS3 YCplac33(SEC14^{Y111F})</i>	(Nile, Tripathi et al. 2014)
ANY117	<i>MATa ade2 ade3 leu2 his3Δ ura3-52 sec14Δ1::HIS3 YCplac33(SEC14^{Y122A})</i>	(Nile, Tripathi et al. 2014)
ANY118	<i>MATa ade2 ade3 leu2 his3Δ ura3-52</i>	(Nile, Tripathi et al. 2014)

	<i>sec14Δ1::HIS3 YCplac33(SEC14^{Y122F})</i>	
ANY119	<i>MATa ade2 ade3 leu2 his3Δ ura3-52 sec14Δ1::HIS3 YCplac33(SEC14^{Y151A})</i>	(Nile, Tripathi et al. 2014)
ANY120	<i>MATa ade2 ade3 leu2 his3Δ ura3-52 sec14Δ1::HIS3 YCplac33(SEC14^{Y151F})</i>	(Nile, Tripathi et al. 2014)
ANY114	<i>MATa ade2 ade3 leu2 his3Δ ura3-52 sec14Δ1::HIS3 YCplac33(SEC14^{S173C})</i>	(Nile, Tripathi et al. 2014)
ANY137	<i>MATa ade2 ade3 leu2 his3Δ ura3-52 sec14Δ1::HIS3 YCplac33(SEC14^{T175C})</i>	(Nile, Tripathi et al. 2014)
ANY122	<i>MATa ade2 ade3 leu2 his3Δ ura3-52 sec14Δ1::HIS3 YCplac33(SEC14^{S201C})</i>	(Nile, Tripathi et al. 2014)
ANY160	<i>MATa mss4Δ::KanMX ura3-52 his3-Δ200 ade pRS315(mss4-5^{ts})</i>	(Nile, Tripathi et al. 2014)
ANY185	<i>MATa mss4::URA3 pRS315(mss4-5^{ts})</i>	(Nile, Tripathi et al. 2014)
ANY219	<i>MATa his3Δ1 leu2Δ0 ura3Δ0 lys2Δ0 vps34Δ::KanMX4</i>	Research Genetics
PYY23	<i>MATa ura3-52 lys2-801 his3Δ-200 psd1::KanMX4</i>	(Nile, Tripathi et al. 2014)
PYY30	<i>MATa ura3-52 lys2-801 his3Δ-200 sfh4Δ::HIS psd1Δ::NAT1</i>	(Nile, Tripathi et al. 2014)
PYY40	<i>MATa ura3-52 lys2-801 his3Δ-200 sfh4Δ::KanMX4</i>	(Nile, Tripathi et al. 2014)
PYY68	<i>MATa ura3-52 lys2-801 his3Δ-200 psd1Δ::KanMX4 cki1Δ::NAT1</i>	(Nile, Tripathi et al. 2014)
PYY69	<i>MATa ura3-52 lys2-801 his3Δ-200 psd1Δ::KanMX4 kes1Δ::NAT1</i>	(Nile, Tripathi et al. 2014)

Table 7. Protein Expression Plasmids.

Plasmid	Description	Citation
pRE644	pQE30(<i>His₆-SFH2</i>)	(Li, Routt et al. 2000)
pRE745	pQE30(<i>His₆-SFH5</i>)	(Li, Routt et al. 2000)
pRE1201	pET28b(<i>His₈-SEC14</i>)	(Schaaf, Ortlund et al. 2008)
pRE1227	pET28b(<i>His₈-SFH1</i>)	(Schaaf, Ortlund et al. 2008)
pRE1270	pET28b(<i>His₈-SEC14^{S173C}</i>)	(Nile, Tripathi et al. 2014)
pRE1271	pET28b(<i>His₈-SEC14^{T175C}</i>)	(Nile, Tripathi et al. 2014)
pRE1272	pET28b(<i>His₈-SEC14^{M177C}</i>)	(Nile, Tripathi et al. 2014)
pAN1	pFU#1	Personal Collection
pAN2	pFU#2	Personal Collection
pAN3	pET28b(reverse transcriptase)	Personal Collection
pAN4	Taq	Personal Collection
pAN5	Lyticase	Personal Collection
pAN6	pRS416(GFP-GOLPH3)	Chris Burd
pAN7	pbluScript	Personal Collection
pAN31	pET28b(<i>His₈-SEC14^{Y111F}</i>)	(Nile, Tripathi et al. 2014)
pAN32	pET28b(<i>His₈-SEC14^{Y111A}</i>)	(Nile, Tripathi et al. 2014)
pAN33	pET28b(<i>His₈-SEC14^{Y122F}</i>)	(Nile, Tripathi et al. 2014)
pAN34	pET28b(<i>His₈-SEC14^{Y122A}</i>)	(Nile, Tripathi et al. 2014)
pAN35	pET28b(<i>His₈-SEC14^{Y151F}</i>)	(Nile, Tripathi et al. 2014)
pAN36	pET28b(<i>His₈-SEC14^{Y151A}</i>)	(Nile, Tripathi et al. 2014)
pAN37	pET28b(<i>His₈-SEC14^{Y111F,Y122F}</i>)	Personal Collection

pAN38	pET28b(<i>His₈-SEC14</i> ^{Y111F,Y151F})	Personal Collection
pAN39	pET28b(<i>His₈-SEC14</i> ^{Y122F,Y151F})	Personal Collection
pAN40	pET28b(<i>His₈-SEC14</i> ^{Y111F,Y122F,Y151F})	Personal Collection
pAN41	pET28b(<i>His₈-SEC14</i> ^{S201A})	Personal Collection
pAN42	pET28b(<i>His₈-SEC14</i> ^{F228A})	(Nile, Tripathi et al. 2014)
pAN43	pET28b(<i>His₈-SEC14</i> ^{F228Y})	Personal Collection
pAN44	pET28b(<i>His₈-SEC14</i> ^{F228I})	Personal Collection
pAN45	pET28b(<i>His₈-SEC14</i> ^{F228L})	Personal Collection
pAN46	pET28b(<i>His₈-SEC14</i> ^{E124L})	Personal Collection
pAN86	pGEX4T(<i>SAC1</i>)	John York
pAN87	pGEX4T(<i>Sac1</i> ^{C392S})	Personal Collection
pAN120	pET28b(<i>His₈-SFH3</i>)	(Ren, Schaaf et al. 2011)
pAN121	pET28b(<i>His₈-SFH4</i>)	(Nile, Tripathi et al. 2014)
pAN138	pET28b-(<i>His₈-SEC14</i> ^{S201C})	(Nile, Tripathi et al. 2014)

Table 8. Yeast Expression Plasmids

Plasmid	Description	Citation
pDR195	YEp(<i>URA3</i>)	(Rentsch, Laloi et al. 1995)
YCplac33	YCp(<i>URA3</i>)	(Gietz and Sugino 1988)
pRS315	YCp(<i>LEU2</i>)	(Sikorski and Hieter 1989)
pRS426	YEp(<i>URA3</i>)	(Sikorski and Hieter 1989)
pCTY11	YEp(<i>LEU2,ADE3,SEC14</i>)	(Lopez, Nicaud et al. 1994)
pCTY1600	YCplac33(<i>URA3</i>)	(Schaaf, Ortlund et al. 2008)
pCTY1611	YCplac33(<i>myc-SEC14</i>)	(Schaaf, Ortlund et al. 2008)
pCTY1651	YCplac33(<i>myc-SEC14^{S173C}</i>)	(Nile, Tripathi et al. 2014)
pCTY1652	YCplac33(<i>myc-SEC14^{T175C}</i>)	(Nile, Tripathi et al. 2014)
pAN6	pRS416(<i>GFP-GOLPH3</i>)	(Wood, Schmitz et al. 2009)
pAN11	YCplac33(<i>myc-SEC^{Y111F}</i>)	(Nile, Tripathi et al. 2014)
pAN12	YCplac33(<i>myc-SEC^{Y111A}</i>)	(Nile, Tripathi et al. 2014)
pAN13	YCplac33(<i>myc-SEC14^{Y122F}</i>)	(Nile, Tripathi et al. 2014)
pAN14	YCplac33(<i>myc-SEC14^{Y122A}</i>)	(Nile, Tripathi et al. 2014)
pAN15	YCplac33(<i>myc-SEC14^{I22V}</i>)	Personal Collection
pAN16	YCplac33(<i>myc-SEC14^{Y151F}</i>)	(Nile, Tripathi et al. 2014)
pAN17	YCplac33(<i>myc-SEC14^{Y151A}</i>)	(Nile, Tripathi et al. 2014)
pAN18	YCplac33(<i>myc-SEC14^{Y151L}</i>)	Personal Collection
pAN19	YCplac33(<i>myc-SEC14^{Y111F,Y122F}</i>)	Personal Collection
pAN20	YCplac33(<i>myc-SEC14^{Y122F,Y151F}</i>)	Personal Collection
pAN21	YCplac33(<i>myc-SEC14^{Y111F,Y151F}</i>)	Personal Collection
pAN22	YCplac33(<i>myc-SEC14^{Y111F, Y122I, Y151F}</i>)	Personal Collection
pAN23	YCplac33(<i>myc-SEC14^{E124Q}</i>)	Personal Collection
pAN24	YCplac33(<i>myc-SEC14^{E124L}</i>)	Personal Collection
pAN25	YCplac33(<i>myc-SEC14^{F228Y}</i>)	Personal Collection
pAN26	YCplac33(<i>myc-SEC14^{F228A}</i>)	Personal Collection
pAN27	YCplac33(<i>myc-SEC14^{F228I}</i>)	Personal Collection
pAN28	YCplac33(<i>myc-SEC14^{F228L}</i>)	Personal Collection

pAN29	YCplac33(<i>myc-SEC14^{S201A}</i>)	Personal Collection
pAN30	YCplac33(<i>myc-SEC14^{S201C}</i>)	(Nile, Tripathi et al. 2014)
pAN49	<i>YIplac211(myc-p⁻¹³⁶-SEC14)</i>	Personal Collection
pAN50	<i>YIplac211(myc-p⁻¹³⁶-SEC14^{S173C})</i>	Personal Collection
pAN51	<i>YIplac211(myc-p⁻¹³⁶-SEC14^{S173A})</i>	Personal Collection
pAN52	<i>YIplac211(myc-p⁻¹³⁶-SEC14^{T175C})</i>	Personal Collection
pAN53	<i>YIplac211(myc-p⁻¹³⁶-SEC14^{T175A})</i>	Personal Collection
pAN54	<i>YIplac211(myc-p⁻¹³⁶-SEC14^{Y151A})</i>	Personal Collection
pAN55	<i>YIplac211(myc-p⁻¹³⁶-SEC14^{S201C})</i>	Personal Collection
pAN56	<i>YIplac211(myc-p⁻¹³⁶-SEC14^{S201A})</i>	Personal Collection
pAN57	<i>YIplac211(myc-p⁻¹³⁶-SEC14^{Y111A})</i>	Personal Collection
pAN58	<i>YIplac211(myc-p⁻¹³⁶-SEC14^{Y111F})</i>	Personal Collection
pAN61	<i>YIplac211(myc-p⁻¹³⁶-SEC14^{Y151F})</i>	Personal Collection
pAN62	<i>YIplac211(myc-p⁻¹³⁶-SEC14^{V154F})</i>	Personal Collection
pAN63	<i>YIplac211(myc-p⁻¹³⁶-SEC14^{M177C})</i>	Personal Collection
pAN65	<i>YIplac211(myc-p⁻¹³⁶-SEC14^{A197V})</i>	Personal Collection
pAN66	<i>YIplac211(myc-p⁻¹³⁶-SEC14^{F228A})</i>	Personal Collection
pAN67	<i>YIplac211(myc-p⁻¹³⁶-SEC14^{F228V})</i>	Personal Collection
pAN132	pRS416(<i>mRFP-EEA1^{FYVE}</i>)	Emr Lab
pAN133	pRS424 (<i>GFP-EEA1^{FYVE}</i>)	Emr Lab
pAN134	pRS426(<i>GFP-PLC^{PH}</i>)	(Stefan, Audhya et al. 2002)
pAN135	pRS426(<i>GFP-2xPH^{PLCδ1}</i>)	(Stefan, Audhya et al. 2002)
pAN142	pRS426(<i>GFP-2xPH^{Osh2}</i>)	(Baird, Stefan et al. 2008)
pAN156	pRS315(<i>mss4-5^{ts}</i>)	(Nile, Tripathi et al. 2014)
pAN160	pDR195(<i>SEC14</i>)	(Schaaf, Ortlund et al. 2008)

FUNDING SOURCES

This work was supported by the Robert A. Welch Foundation (VAB) and grant GM44530 (VAB) from the NIH. RWD was supported by the NIH (HG003317). G. Giaever and C. Nislow were supported by the NHGRI (5RO1-003317-08) and the Canadian Cancer Society (020380). The Texas A&M Laboratory for Molecular Simulation provided software, support and computer time. Glen E. Kellogg and eduSoft LC donated HINT software,

REFERENCES

- Abraham, D. J., G. E. Kellogg, et al. (1997). "Hydropathic analysis of the non-covalent interactions between molecular subunits of structurally characterized hemoglobins." Journal of Molecular Biology **272**(4): 613-632.
- Adamo, J. E., J. J. Moskow, et al. (2001). "Yeast Cdc42 functions at a late step in exocytosis, specifically during polarized growth of the emerging bud." The Journal of Cell Biology **155**(4): 581-592.
- Agranoff, B. W., R. M. Bradley, et al. (1958). "The enzymatic synthesis of inositol phosphatide." Journal of Biological Chemistry **233**(5): 1077-1083.
- Ahmed, S., W. I. Goh, et al. (2010). "I-BAR domains, IRSp53 and filopodium formation." Seminars in Cell & Developmental Biology **21**(4): 350-356.
- Akihiro, H., A. Makoto, et al. (1997). "Affinity for α -tocopherol transfer protein as a determinant of the biological activities of vitamin E analogs." FEBS Letters **409**(1): 105-108.
- Alb, J. G., Jr., S. E. Phillips, et al. (2002). "Genetic ablation of phosphatidylinositol transfer protein function in murine embryonic stem cells." Mol. Biol. Cell **13**(3): 739-754.
- Alb, J. G., Jr., S. E. Phillips, et al. (2007). "The pathologies associated with functional titration of phosphatidylinositol transfer protein α activity in mice." J. Lipid Res. **48**(8): 1857-1872.
- Alb, J. G. J., J. D. Cortese, et al. (2003). "Mice lacking phosphatidylinositol transfer protein-alpha exhibit spinocerebellar degeneration, intestinal and hepatic steatosis, and hypoglycemia." J. Biol. Chem. **278**(35): 33501-33518
- Alimonti, A., C. Nardella, et al. (2010). "A novel type of cellular senescence that can be enhanced in mouse models and human tumor xenografts to suppress prostate tumorigenesis." The Journal of clinical investigation **120**(3): 681-693.
- Alonso, A., J. Sasin, et al. (2004). "Protein Tyrosine Phosphatases in the Human Genome." **117**(6): 699-711.
- Altan-Bonnet, N. and T. Balla (2012). "Phosphatidylinositol 4-kinases: hostages harnessed to build panviral replication platforms." Trends in biochemical sciences **37**(7): 293-302.

- Annis, D. A., C. C. Cheng, et al. (2009). "Inhibitors of the lipid phosphatase SHIP2 discovered by high-throughput affinity selection-mass spectrometry screening of combinatorial libraries." Combinatorial Chemistry & High Throughput Screening **12**(8): 760-771.
- Aoyama, T., S. Hata, et al. (2009). "Cayman ataxia protein caytaxin is transported by kinesin along neurites through binding to kinesin light chains." J Cell Sci **122**(22): 4177-4185.
- Aparicio, J. M., A. Belanger-Quintana, et al. (2001). "Ataxia with isolated vitamin E deficiency: case report and review of the literature." Journal of Pediatric Gastroenterology & Nutrition **33**(2): 206-210
- Aravind, L., A. F. Neuwald, et al. (1999). "Sec14p-like domains in NF1 and Dbl-like proteins indicate lipid regulation of Ras and Rho signaling." Current Biology **9**(6): R195-R197.
- Arcaro, A. and M. P. Wymann (1993). "Wortmannin is a potent phosphatidylinositol 3-kinase inhibitor: the role of phosphatidylinositol 3,4,5-trisphosphate in neutrophil responses." The Biochemical journal **296**: 297-301.
- Arita, M., H. Kojima, et al. (2011). "Phosphatidylinositol 4-Kinase III Beta Is a Target of Enviroxime-Like Compounds for Antipoliiovirus Activity." Journal of virology **85**(5): 2364-2372.
- Arita, M., K. Nomura, et al. (1997). " α -Tocopherol transfer protein stimulates the secretion of α -tocopherol from a cultured liver cell line through a brefeldin A-insensitive pathway." Proceedings of the National Academy of Sciences of the United States of America **94**(23): 12437-12441.
- Arpin, M., D. Chirivino, et al. (2011). "Emerging role for ERM proteins in cell adhesion and migration." Cell adhesion & migration **5**(2): 199-206.
- Ashburner, M., C. A. Ball, et al. (2000). "Gene ontology: tool for the unification of biology. The Gene Ontology Consortium." Nature genetics **25**(1): 25-29.
- Atack, J. R., S. M. Cook, et al. (1993). "In Vitro and In Vivo Inhibition of Inositol Monophosphatase by the Bisphosphonate L-690,330." Journal of neurochemistry **60**(2): 652-658.
- Atack, J. R., A. M. Prior, et al. (1994). "Effects of L-690,488, a prodrug of the bisphosphonate inositol monophosphatase inhibitor L-690,330, on phosphatidylinositol cycle markers." Journal of Pharmacology and Experimental Therapeutics **270**(1): 70-76.

- Athenstaedt, K., P. Jolivet, et al. (2006). "Lipid particle composition of the yeast *Yarrowia lipolytica* depends on the carbon source." Proteomics **6**(5): 1450-1459.
- Audhya, A. and S. D. Emr (2002). "Stt4 PI 4-kinase localizes to the plasma membrane and functions in the Pkc1-mediated MAP kinase cascade." Developmental cell **2**(5): 593-605.
- Audhya, A., M. Foti, et al. (2000). "Distinct roles for the yeast phosphatidylinositol 4-kinases, Stt4p and Pik1p, in secretion, cell growth, and organelle membrane dynamics." Molecular biology of the cell **11**(8): 2673-2689.
- Auffinger, P., F. A. Hays, et al. (2004). "Halogen bonds in biological molecules." Proceedings of the National Academy of Sciences of the United States of America **101**(48): 16789-16794.
- Auger, K. R., C. L. Carpenter, et al. (1989). "Phosphatidylinositol 3-kinase and its novel product, phosphatidylinositol 3-phosphate, are present in *Saccharomyces cerevisiae*." Journal of Biological Chemistry **264**(34): 20181-20184.
- Austin, C. P., L. S. Brady, et al. (2004). "NIH molecular libraries initiative." Science **306**(5699): 1138-1139.
- Bae, Y. H., Z. Ding, et al. (2010). "Profilin1 regulates PI(3,4)P₂ and lamellipodin accumulation at the leading edge thus influencing motility of MDA-MB-231 cells." Proceedings of the National Academy of Sciences.
- Baggiolini, M., B. Dewald, et al. (1987). "Inhibition of the phagocytosis-induced respiratory burst by the fungal metabolite wortmannin and some analogues." Experimental cell research **169**(2): 408-418.
- Baird, D., C. Stefan, et al. (2008). "Assembly of the PtdIns 4-kinase Stt4 complex at the plasma membrane requires Ypp1 and Efr3." The Journal of cell biology **183**(6): 1061-1074.
- Baker, R., C. Carrick, et al. (1991). "Design and synthesis of 6 α -substituted 2 β ,4 α -dihydroxy-1 β -phosphoryloxycyclohexanes, potent inhibitors of inositol monophosphatase." Journal of the Chemical Society, Chemical Communications(5): 298-300.
- Balla, A. and T. Balla (2006). "Phosphatidylinositol 4-kinases: old enzymes with emerging functions." Trends in cell biology **16**(7): 351-361.
- Balla, A., Y. J. Kim, et al. (2008). "Maintenance of hormone-sensitive phosphoinositide pools in the plasma membrane requires phosphatidylinositol 4-kinase III α ." Molecular biology of the cell **19**(2): 711-721.

- Balla, A., G. Tuymetova, et al. (2002). "Characterization of type II phosphatidylinositol 4-kinase isoforms reveals association of the enzymes with endosomal vesicular compartments." Journal of Biological Chemistry **277**(22): 20041-20050.
- Balla, T. (2005). "Inositol-lipid binding motifs: signal integrators through protein-lipid and protein-protein interactions." J Cell Sci **118**(10): 2093-2104.
- Balla, T. (2007). "Imaging and manipulating phosphoinositides in living cells." The Journal of physiology **582**(3): 927-937.
- Balla, T. (2013). "Phosphoinositides: Tiny Lipids With Giant Impact on Cell Regulation." Physiological Reviews **93**(3): 1019-1137.
- Balla, T., A. J. Baukal, et al. (1988). "Multiple pathways of inositol polyphosphate metabolism in angiotensin-stimulated adrenal glomerulosa cells." Journal of Biological Chemistry **263**(9): 4083-4091.
- Balla, T., Z. Szentpetery, et al. (2009). "Phosphoinositide signaling: new tools and insights." Physiology **24**(4): 231-244.
- Banerjee, S., S. Basu, et al. (2010). "Comparative genomics reveals selective distribution and domain organization of FYVE and PX domain proteins across eukaryotic lineages." BMC genomics **11**: 83.
- Bankaitis, V. A., J. R. Aitken, et al. (1990). "An essential role for a phospholipid transfer protein in yeast Golgi function." Nature **347**(6293): 561-562.
- Bankaitis, V. A., D. E. Malehorn, et al. (1989). "The *Saccharomyces cerevisiae* SEC14 gene encodes a cytosolic factor that is required for transport of secretory proteins from the yeast Golgi complex." The Journal of Cell Biology **108**(4): 1271-1281.
- Bankaitis, V. A., C. J. Mousley, et al. (2010). "The Sec14 superfamily and mechanisms for crosstalk between lipid metabolism and lipid signaling." Trends in Biochemical Sciences **35**(3): 150-160.
- Barlowe, C. K. and E. A. Miller (2013). "Secretory Protein Biogenesis and Traffic in the Early Secretory Pathway." Genetics **193**(2): 383-410.
- Barnes, N. M. and T. Sharp (1999). "A review of central 5-HT receptors and their function." Neuropharmacology **38**(8): 1083-1152.
- Baron, C. B., M. Cunningham, et al. (1984). "Pharmacomechanical coupling in smooth muscle may involve phosphatidylinositol metabolism." Proceedings of the National Academy of Sciences **81**(21): 6899-6903.

- Behnia, R. and S. Munro (2005). "Organelle identity and the signposts for membrane traffic." Nature **438**(7068): 597-604.
- Benchokroun, Y., J. Couprie, et al. (1995). "Aurintricarboxylic acid, a putative inhibitor of apoptosis, is a potent inhibitor of DNA topoisomerase II in vitro and in Chinese hamster fibrosarcoma cells." Biochemical Pharmacology **49**(3): 305-313.
- Bennett, C. F., S. Mong, et al. (1987). "Inhibition of phosphoinositide-specific phospholipase C by manoalide." Molecular Pharmacology **32**(5): 587-593.
- Berridge, M. J., C. P. Downes, et al. (1982). "Lithium amplifies agonist-dependent phosphatidylinositol responses in brain and salivary glands." The Biochemical journal **206**(3): 587-595.
- Berridge, M. J., C. P. Downes, et al. (1989). "Neural and developmental actions of lithium: A unifying hypothesis." Cell **59**(3): 411-419.
- Bezzerrides, V. J., I. S. Ramsey, et al. (2004). "Rapid vesicular translocation and insertion of TRP channels." Nat Cell Biol **6**(8): 709-720.
- Bhatia, V. K., N. S. Hatzakis, et al. (2010). "A unifying mechanism accounts for sensing of membrane curvature by BAR domains, amphipathic helices and membrane-anchored proteins." Seminars in Cell & Developmental Biology **21**(4): 381-390.
- Bhattacharyya, S. and A. S. Tracey (2001). "Vanadium(V) complexes in enzyme systems: aqueous chemistry, inhibition and molecular modeling in inhibitor design." Journal of inorganic biochemistry **85**(1): 9-13.
- Bianco, A., V. Reghellin, et al. (2012). "Metabolism of phosphatidylinositol 4-kinase III α -dependent PI4P is subverted by HCV and is targeted by a 4-anilino quinazoline with Antiviral Activity." PLoS Pathog **8**(3): e1002576.
- Bishe, B., G. Syed, et al. (2012). "Phosphoinositides in the hepatitis C virus life cycle." Viruses **4**(10): 2340-2358.
- Blagoveshchenskaya, A., F. Y. Cheong, et al. (2008). "Integration of Golgi trafficking and growth factor signaling by the lipid phosphatase SAC1." The Journal of cell biology **180**(4): 803-812.
- Bleasdale, J. E., N. R. Thakur, et al. (1990). "Selective inhibition of receptor-coupled phospholipase C-dependent processes in human platelets and polymorphonuclear neutrophils." Journal of Pharmacology and Experimental Therapeutics **255**(2): 756-768.

- Blume, J. J., A. Halbach, et al. (2007). "EHD proteins are associated with tubular and vesicular compartments and interact with specific phospholipids." Experimental cell research **313**(2): 219-231.
- Blumental-Perry, A., C. J. Haney, et al. (2006). "Phosphatidylinositol 4-phosphate formation at ER exit sites regulates ER export." Developmental Cell **11**(5): 671-682.
- Boggon, T. J., W. S. Shan, et al. (1999). "Implication of tubby proteins as transcription factors by structure-based functional analysis." Science **286**(5447): 2119-2125.
- Boiteux, S. and S. Jinks-Robertson (2013). "DNA Repair Mechanisms and the Bypass of DNA Damage in *Saccharomyces cerevisiae*." Genetics **193**(4): 1025-1064.
- Bomar, J. M., P. J. Benke, et al. (2003). "Mutations in a novel gene encoding a CRAL-TRIO domain cause human Cayman ataxia and ataxia/dystonia in the jittery mouse." Nature Genetics **35**(3): 264-269.
- Bone, R., J. P. Springer, et al. (1992). "Structure of inositol monophosphatase, the putative target of lithium therapy." Proceedings of the National Academy of Sciences **89**(21): 10031-10035.
- Bonneau, F., E. D. Lenherr, et al. (2009). "Solubility survey of fragments of the neurofibromatosis type 1 protein neurofibromin." Protein Expr Purif **65**(1): 30-37.
- Borawski, J., P. Troke, et al. (2009). "Class III Phosphatidylinositol 4-Kinase Alpha and Beta Are Novel Host Factor Regulators of Hepatitis C Virus Replication." Journal of virology **83**(19): 10058-10074.
- Bortner, J. D., A. Das, et al. (2009). "Down-Regulation of 14-3-3 isoforms and annexin A5 proteins in lung adenocarcinoma induced by the tobacco-specific nitrosamine NNK in the A/J mouse revealed by proteomic analysis." Journal of Proteome Research **8**(8): 4050-4061.
- Boyd, J. M., S. Malstrom, et al. (1994). "Adenovirus E1B 19 kDa and Bcl-2 proteins interact with a common set of cellular proteins." **79**(2): 341-351.
- Brandl, T., U. Maier, et al. (2007). Thiazolyl-dihydro-chinazoline, Google Patents.
- Bravo, J., D. Karathanassis, et al. (2001). "The crystal structure of the PX domain from p40phox bound to phosphatidylinositol 3-phosphate." Molecular cell **8**(4): 829-839.
- Breitfelder, S., U. Maier, et al. (2007). Thiazolyl-dihydro-cyclopentapyrazole, Google Patents.

- Brian, P. W., P. J. Curtis, et al. (1957). "Wortmannin, an antibiotic produced by *Penicillium wortmanni*." Transactions of the British Mycological Society **40**(3): 365-IN363.
- Briancon-Marjollet, A., A. Ghogha, et al. (2008). "Trio mediates netrin-1-induced Rac1 activation in axon outgrowth and guidance." Mol. Cell. Biol. **28**(7): 2314-2323.
- Brooks, R., G. M. Fuhler, et al. (2010). "SHIP1 Inhibition Increases Immunoregulatory Capacity and triggers apoptosis of hematopoietic cancer cells." The Journal of Immunology **184**(7): 3582-3589.
- Brown, A. J. P. and N. A. R. Gow (1999). "Regulatory networks controlling *Candida albicans* morphogenesis." Trends in Microbiology **7**(8): 333-338.
- Brown, B. K., N. Karasavvas, et al. (2007). "Monoclonal antibodies to phosphatidylinositol phosphate neutralize human immunodeficiency virus type 1: role of phosphate-binding subsites." Journal of virology **81**(4): 2087-2091.
- Brunn, G. J., J. Williams, et al. (1996). "Direct inhibition of the signaling functions of the mammalian target of rapamycin by the phosphoinositide 3-kinase inhibitors, wortmannin and LY294002." The EMBO journal **15**(19): 5256-5267.
- Bunney, T. D. and M. Katan (2010). "Phosphoinositide signalling in cancer: beyond PI3K and PTEN." Nature reviews. Cancer **10**(5): 342-352.
- Bunte, H., M. Schenning, et al. (2006). "A phosphatidylinositol transfer protein alpha-dependent survival factor protects cultured primary neurons against serum deprivation-induced cell death." Journal of Neurochemistry **97**(3): 707-715.
- Burd, C. G. and S. D. Emr (1998). "Phosphatidylinositol(3)-phosphate signaling mediated by specific binding to RING FYVE domains." Molecular cell **2**(1): 157-162.
- Burda, P., S. M. Padilla, et al. (2002). "Retromer function in endosome-to-Golgi retrograde transport is regulated by the yeast Vps34 PtdIns 3-kinase." Journal of cell science **115**(20): 3889-3900.
- Burgdorf, C., U. Schafer, et al. (2010). "U73122, an aminosteroid phospholipase C inhibitor, is a potent inhibitor of cardiac phospholipase D by a PIP2-dependent mechanism." Journal of cardiovascular pharmacology **55**(6): 555-559.
- Burstedt, M., O. Sandgren, et al. (1999). "Bothnia dystrophy caused by mutations in the cellular retinaldehyde-binding protein gene (RLBP1) on chromosome 15q26." Invest. Ophthalmol. Vis. Sci. **40**(5): 995-1000.

- Burton, L. E. and W. W. Wells (1976). "myo-Inositol metabolism during lactation and development in the rat. The prevention of lactation-induced fatty liver by dietary myo-inositol." The Journal of nutrition **106**(11): 1617-1628.
- Burton, L. E. and W. W. Wells (1977). "Characterization of the lactation-dependent fatty liver in myo-inositol deficient rats." The Journal of nutrition **107**(10): 1871-1883.
- Burton, L. E. and W. W. Wells (1979). "myo-inositol deficiency: studies on the mechanism of lactation-dependent fatty liver formation in the rat." The Journal of nutrition **109**(8): 1483-1491.
- Buschdorf, J. P., L. L. Chew, et al. (2008). "Nerve Growth Factor Stimulates Interaction of Cayman Ataxia Protein BNIP-H/Caytaxin with Peptidyl-Prolyl Isomerase Pin1 in Differentiating Neurons." PLoS ONE **3**(7): e2686.
- Byfield, M. P., J. T. Murray, et al. (2005). "hVps34 Is a nutrient-regulated lipid kinase required for activation of p70 S6 kinase." Journal of Biological Chemistry **280**(38): 33076-33082.
- Cade, J. F. (1949). "Lithium salts in the treatment of psychotic excitement." The Medical journal of Australia **2**(10): 349-352.
- Cahill, M. E., Z. Xie, et al. (2009). "Kalirin regulates cortical spine morphogenesis and disease-related behavioral phenotypes." Proceedings of the National Academy of Sciences **106**(31): 13058-13063.
- Calderone, R. A. (2002). Candida and candidiasis. Washington, D.C., ASM Press.
- Campelo, F., G. Fabrikant, et al. (2010). "Modeling membrane shaping by proteins: Focus on EHD2 and N-BAR domains." FEBS letters **584**(9): 1830-1839.
- Can, A., T. G. Schulze, et al. (2014). "Molecular actions and clinical pharmacogenetics of lithium therapy." Pharmacology Biochemistry and Behavior(0).
- Cantley, L. C. (2002). "The phosphoinositide 3-kinase pathway." Science **296**(5573): 1655-1657.
- Cantley, L. C. and B. G. Neel (1999). "New insights into tumor suppression: PTEN suppresses tumor formation by restraining the phosphoinositide 3-kinase/AKT pathway." Proceedings of the National Academy of Sciences **96**(8): 4240-4245.
- Carlton, J. G. and P. J. Cullen (2005). "Coincidence detection in phosphoinositide signaling." Trends in cell biology **15**(10): 540-547.

- Carroll, K., C. Gomez, et al. (2004). "Tubby proteins: the plot thickens." Nature reviews. Molecular cell biology **5**(1): 55-63.
- Carvou, N., R. Holic, et al. (2010). "Phosphatidylinositol- and phosphatidylcholine-transfer activity of PITP β is essential for COPI-mediated retrograde transport from the Golgi to the endoplasmic reticulum." J Cell Sci **123**(8): 1262-1273.
- Chackalamannil, S., D. o. Doller, et al. (2004). "Himbacine analogs as muscarinic receptor antagonists--effects of tether and heterocyclic variations." Bioorganic & Medicinal Chemistry Letters **14**(15): 3967-3970.
- Chackalamannil, S., Y. Wang, et al. (2008). "Discovery of a novel, orally active himbacine-based thrombin receptor antagonist (SCH 530348) with potent antiplatelet activity." Journal of medicinal chemistry **51**(11): 3061-3064.
- Chang-Ileto, B., S. G. Frere, et al. (2011). "Synaptojanin 1-mediated PI(4,5)P₂ hydrolysis is modulated by membrane curvature and facilitates membrane fission." Developmental cell **20**(2): 206-218.
- Chang-Ileto, B., S. G. Frere, et al. (2012). Chapter 10 - Acute manipulation of phosphoinositide levels in cells. Methods in cell biology. P. Gilbert Di and R. W. Markus, Academic Press. **108**: 187-207.
- Chang, F. S., G.-S. Han, et al. (2005). "A WASp-binding type II phosphatidylinositol 4-kinase required for actin polymerization-driven endosome motility." The Journal of cell biology **171**(1): 133-142.
- Charcosset, M., A. Sassolas, et al. (2008). "Anderson or chylomicron retention disease: molecular impact of five mutations in the SAR1B gene on the structure and the functionality of Sar1b protein." Molecular Genetics and Metabolism **93**(1): 74-84.
- Chattopadhyay, I., A. Singh, et al. (2010). "Genome-wide analysis of chromosomal alterations in patients with esophageal squamous cell carcinoma exposed to tobacco and betel quid from high-risk area in India." Mutation Research/Genetic Toxicology and Environmental Mutagenesis **696**(2): 130-138.
- Chen, I.-W. and F. C. Charalampous (1966). "Biochemical studies on inositol: IX. "d-inositol 1-phosphate as intermediate in the biosynthesis of inositol from glucose 6-phosphate and characteristics of two reactions in this biosynthesis." Journal of Biological Chemistry **241**(10): 2194-2199.
- Chen, L. and M. F. Roberts (1998). "Cloning and expression of the inositol monophosphatase gene from methanococcus jannaschii and characterization of the enzyme." Applied and Environmental Microbiology **64**(7): 2609-2615.

- Chen, Y.-J., W.-Y. Sheng, et al. (2006). "Potent inhibition of human telomerase by U-73122." Journal of Biomedical Science **13**(5): 667-674.
- Cheng, J. Q., C. W. Lindsley, et al. (2005). "The Akt/PKB pathway: molecular target for cancer drug discovery." Oncogene **24**(50): 7482-7492.
- Cheng, P.-C. (2006). The contrast formation in optical microscopy. Handbook Of Biological Confocal Microscopy. J. B. Pawley, Springer US: 162-206.
- Chishti, A. H., A. C. Kim, et al. (1998). "The FERM domain: a unique module involved in the linkage of cytoplasmic proteins to the membrane." Trends in biochemical sciences **23**(8): 281-282.
- Cho, A. E., V. Guallar, et al. (2005). "Importance of accurate charges in molecular docking: quantum mechanical/molecular mechanical (QM/MM) approach." Journal of computational chemistry **26**(9): 915-931.
- Chow, B. Y., X. Han, et al. (2012). "Genetically encoded molecular tools for light-driven silencing of targeted neurons." Progress in brain research **196**: 49-61.
- Christie, W. W. (2010). Lipid analysis: Isolation, separation, identification and lipidomic analysis Oily Press Lipid Library.
- Christoforidis, S., H. M. McBride, et al. (1999). "The Rab5 effector EEA1 is a core component of endosome docking." Nature **397**(6720): 621-625.
- Chu, S. H. and D. M. Hegsted (1980). "Myo-inositol deficiency in gerbils: changes in phospholipid composition of intestinal microsomes." The Journal of nutrition **110**(6): 1217-1223.
- Chu, S. H. and D. M. Hegsted (1980). "Myo-inositol deficiency in gerbils: comparative study of the intestinal lipodystrophy in *Meriones unguiculatus* and *Meriones libycus*." The Journal of nutrition **110**(6): 1209-1216.
- Chu, S. W. and R. P. Geyer (1982). "myo-Inositol action on gerbil intestine. Association of phosphatidylinositol metabolism with lipid clearance." Biochimica et biophysica acta **710**(1): 63-70.
- Chuang, J.-Z., Y. Zhao, et al. (2007). "SARA-regulated vesicular targeting underlies formation of the light-sensing organelle in mammalian rods." Cell **130**(3): 535-547.
- Cichowski, K. and T. Jacks (2001). "NF1 tumor suppressor gene function: narrowing the GAP." Cell **104**(4): 593-604.

- Clark, A. M. and P. Labute (2007). "2D depiction of protein–ligand complexes." Journal of Chemical Information and Modeling **47**(5): 1933-1944.
- Clark, A. M., P. Labute, et al. (2006). "2D structure depiction." Journal of Chemical Information and Modeling **46**(3): 1107-1123.
- Clarke, M. W., J. R. Burnett, et al. (2008). "Vitamin E in human health and disease." Critical Reviews in Clinical Laboratory Sciences **45**(5): 417-450.
- Clarke, N. G. and R. M. Dawson (1981). "Alkaline O leads to N-transacylation. A new method for the quantitative deacylation of phospholipids." The Biochemical journal **195**(1): 301-306.
- Clarke, R. A., Z. Zhao, et al. (2009). "New genomic structure for prostate cancer specific gene PCA3 within BMCC1: implications for prostate cancer detection and progression." PLoS ONE **4**(3): e4995.
- Cleves, A., T. McGee, et al. (1991). "Phospholipid transfer proteins: a biological debut." Trends Cell Biol **1**(1): 30-34.
- Cleves, A. E., T. P. McGee, et al. (1991). "Mutations in the CDP-choline pathway for phospholipid biosynthesis bypass the requirement for an essential phospholipid transfer protein." Cell **64**(4): 789-800.
- Cleves, A. E., P. J. Novick, et al. (1989). "Mutations in the SAC1 gene suppress defects in yeast Golgi and yeast actin function." The Journal of Cell Biology **109**(6): 2939-2950.
- Cockcroft, S. and N. Carvou (2007). "Biochemical and biological functions of class I phosphatidylinositol transfer proteins." Biochimica et Biophysica Acta (BBA) - Molecular and Cell Biology of Lipids **1771**(6): 677-691.
- Coffman, V. C., A. H. Nile, et al. (2009). "Roles of Formin Nodes and Myosin Motor Activity in Mid1p-dependent Contractile-Ring Assembly during Fission Yeast Cytokinesis." Molecular Biology of the Cell **20**(24): 5195-5210.
- Coleman, D. L. and E. M. Eicher (1990). "Fat (fat) and tubby (tub): two autosomal recessive mutations causing obesity syndromes in the mouse." The Journal of heredity **81**(6): 424-427.
- Colley, W. C., T.-C. Sung, et al. (1997). "Phospholipase D2, a distinct phospholipase D isoform with novel regulatory properties that provokes cytoskeletal reorganization." Current Biology **7**(3): 191-201.
- Confalonieri, S. and P. P. Di Fiore (2002). "The Eps15 homology (EH) domain." FEBS letters **513**(1): 24-29.

- Consortium, T. U. (2012). "Reorganizing the protein space at the Universal Protein Resource (UniProt)." Nucleic acids research **40**(Database issue): D71-75.
- Cosker, K. E., S. Shadan, et al. (2008). "Regulation of PI3K signalling by the phosphatidylinositol transfer protein PITP α during axonal extension in hippocampal neurons." J Cell Sci **121**(6): 796-803.
- Cozier, G. E., J. Carlton, et al. (2002). "The phox homology (PX) domain-dependent, 3-phosphoinositide-mediated association of sorting nexin-1 with an early sorting endosomal compartment is required for its ability to regulate epidermal growth factor receptor degradation." Journal of Biological Chemistry **277**(50): 48730-48736.
- Cremona, O., G. Di Paolo, et al. (1999). "Essential role of phosphoinositide metabolism in synaptic Vesicle Recycling." Cell **99**(2): 179-188.
- Cullen, P. J. (2008). "Endosomal sorting and signalling: an emerging role for sorting nexins." Nature reviews. Molecular cell biology **9**(7): 574-582.
- Cullen, P. J. and H. C. Korswagen (2012). "Sorting nexins provide diversity for retromer-dependent trafficking events." Nature cell biology **14**(1): 29-37.
- Cuncic, C., S. Desmarais, et al. (1999). "Bis(N,N-dimethylhydroxamido)hydroxooxovanadate inhibition of protein tyrosine phosphatase activity in intact cells: comparison with vanadate." Biochemical Pharmacology **58**(12): 1859-1867.
- Cuncic, C., N. Detich, et al. (1999). "Vanadate inhibition of protein tyrosine phosphatases in Jurkat cells: modulation by redox state." JBIC Journal of Biological Inorganic Chemistry **4**(3): 354-359.
- Currie, R. A., K. S. Walker, et al. (1999). "Role of phosphatidylinositol 3,4,5-trisphosphate in regulating the activity and localization of 3-phosphoinositide-dependent protein kinase-1." Biochem. J. **337**(3): 575-583.
- Curwin, A. J., G. D. Fairn, et al. (2009). "Phospholipid transfer protein Sec14 is required for trafficking from endosomes and regulates distinct trans-Golgi export pathways." Journal of Biological Chemistry **284**(11): 7364-7375.
- Curwin, A. J. and C. R. McMaster (2008). "Structure and function of the enigmatic Sec14 domain-containing proteins and the etiology of human disease." Future Lipidology **3**(4): 399-410.
- Cvrckova, F. (2013). "Formins and membranes: anchoring cortical actin to the cell wall and beyond." Frontiers in plant science **4**: 436.

- D'Angelo, G., M. Vicinanza, et al. (2008). "The multiple roles of PtdIns(4)P - not just the precursor of PtdIns(4,5)P₂." J Cell Sci **121**(12): 1955-1963.
- D'Angelo, I., S. Welti, et al. (2006). "A novel bipartite phospholipid-binding module in the neurofibromatosis type 1 protein." EMBO Rep **7**(2): 174-179.
- Daumke, O., R. Lundmark, et al. (2007). "Architectural and mechanistic insights into an EHD ATPase involved in membrane remodelling." Nature **449**(7164): 923-927.
- Davies, S. P., H. Reddy, et al. (2000). "Specificity and mechanism of action of some commonly used protein kinase inhibitors." Biochem. J. **351**(1): 95-105.
- Davison, J. M., V. A. Bankaitis, et al. (2012). "Devising powerful genetics, biochemical and structural tools in the functional analysis of phosphatidylinositol transfer proteins (PITPs) across diverse species." Methods in cell biology **108**: 249-302.
- de Beer, T., R. E. Carter, et al. (1998). "Structure and Asn-Pro-Phe binding pocket of the Eps15 homology domain." Science **281**(5381): 1357-1360.
- Deeg, C. A., A. J. Raith, et al. (2007). "CRALBP is a highly prevalent autoantigen for human autoimmune uveitis." Clin Dev Immunol **2007**: 39245.
- Deisseroth, K. (2011). "Optogenetics." Nature methods **8**(1): 26-29.
- Delang, L., J. Paeshuyse, et al. (2012). "The role of phosphatidylinositol 4-kinases and phosphatidylinositol 4-phosphate during viral replication." Biochemical Pharmacology **84**(11): 1400-1408.
- Derry, J. M. J., H. D. Ochs, et al. (1994). "Isolation of a novel gene mutated in Wiskott-Aldrich syndrome." Cell **78**(4): 635-644.
- Desfougères, T., T. Ferreira, et al. (2008). "SFH2 regulates fatty acid synthase activity in the yeast *Saccharomyces cerevisiae* and is critical to prevent saturated fatty acid accumulation in response to haem and oleic acid depletion." Biochem J **409**(1): 299-309.
- Di Cristofano, A., B. Pesce, et al. (1998). "Pten is essential for embryonic development and tumour suppression." Nature genetics **19**(4): 348-355.
- Di Donato, I., S. Bianchi, et al. (2010). "Ataxia with vitamin E deficiency: update of molecular diagnosis." Neurological Sciences.
- Di Paolo, G. and P. De Camilli (2006). "Phosphoinositides in cell regulation and membrane dynamics." Nature **443**(7112): 651-657.

- DiNitto, J. P. and D. G. Lambright (2006). "Membrane and juxtamembrane targeting by PH and PTB domains." Biochimica et biophysica acta **1761**(8): 850-867.
- Doria-Lamba, L., E. De Grandis, et al. (2006). "Efficacious vitamin E treatment in a child with ataxia with isolated vitamin E deficiency." European Journal of Pediatrics **165**(7): 494-495.
- Dowler, S., R. A. Currie, et al. (2000). "Identification of pleckstrin-homology-domain-containing proteins with novel phosphoinositide-binding specificities." The Biochemical journal **351**(Pt 1): 19-31.
- Dowling, J. J., A. P. Vreede, et al. (2009). "Loss of myotubularin function results in T-tubule disorganization in zebrafish and human myotubular myopathy." PLoS genetics **5**(2): e1000372.
- Downes, C. P., S. Ross, et al. (2007). "Stimulation of PI 3-kinase signaling via inhibition of the tumor suppressor phosphatase, PTEN." Advances in enzyme regulation **47**(1): 184-194.
- Downing, G. J., S. Kim, et al. (1996). "Characterization of a soluble adrenal phosphatidylinositol 4-kinase reveals wortmannin sensitivity of type III phosphatidylinositol kinases." Biochemistry **35**(11): 3587-3594.
- Drees, B. E., A. Weipert, et al. (2003). "Competitive fluorescence polarization assays for the detection of phosphoinositide kinase and phosphatase activity." Combinatorial Chemistry & High Throughput Screening **6**(4): 321-330.
- Dumas, J. J., E. Merithew, et al. (2001). "Multivalent endosome targeting by homodimeric EEA1." Molecular cell **8**(5): 947-958.
- Edwards, S. D. and N. H. Keep (2001). "The 2.7 Å crystal structure of the activated FERM domain of moesin: an analysis of structural changes on activation" Biochemistry **40**(24): 7061-7068.
- Eisenberg, F. (1967). "D-myoinositol 1-phosphate as product of cyclization of glucose 6-phosphate and substrate for a specific phosphatase in rat testis." Journal of Biological Chemistry **242**(7): 1375-1382.
- Elble, R. J. (1996). "Central mechanisms of tremor." J. Clin. Neurophysiol. **13**(2): 133-144.
- Engelse, M., N. Laurens, et al. (2008). "Differential gene expression analysis of tubule forming and non-tubule forming endothelial cells: CDC42GAP as a counter-regulator in tubule formation." Angiogenesis **11**(2): 153-167.

- Enmon, J. L., T. de Beer, et al. (2000). "Solution structure of Eps15's third EH domain reveals coincident Phe-Trp and Asn-Pro-Phe binding sites." Biochemistry **39**(15): 4309-4319.
- Estrach, S., S. Schmidt, et al. (2002). "The human Rho-GEF trio and its target GTPase RhoG are involved in the NGF pathway, leading to neurite outgrowth." **12**(4): 307-312.
- Fahsold, R., S. Hoffmeyer, et al. (2000). "Minor lesion mutational spectrum of the entire NF1 gene does not explain its high mutability but points to a functional domain upstream of the GAP-related domain." **66**(3): 790-818.
- Fan, W., A. Nassiri, et al. (2011). "Autophagosome targeting and membrane curvature sensing by Barkor/Atg14(L)." Proceedings of the National Academy of Sciences **108**(19): 7769-7774.
- Fang, M., B. G. Kearns, et al. (1996). "Kes1p shares homology with human oxysterol binding protein and participates in a novel regulatory pathway for yeast Golgi-derived transport vesicle biogenesis." The EMBO journal **15**(23): 6447-6459.
- Fardin, P., M. Ognibene, et al. (2009). "Induction of epithelial mesenchymal transition and vasculogenesis in the lenses of Dbl oncogene transgenic mice." PLoS ONE **4**(9): e7058.
- Fazeli, A., S. L. Dickinson, et al. (1997). "Phenotype of mice lacking functional Deleted in colorectal cancer (Dcc) gene." Nature **386**(6627): 796-804
- Fehon, R. G., A. I. McClatchey, et al. (2010). "Organizing the cell cortex: the role of ERM proteins." Nature reviews. Molecular cell biology **11**(4): 276-287.
- Feißt, C., D. Albert, et al. (2005). "The aminosteroid phospholipase C antagonist U-73122 (1-[6-[[17- β -3-Methoxyestra-1,3,5(10)-trien-17-yl]amino]hexyl]-1H-pyrrole-2,5-dione) potently inhibits human 5-lipoxygenase in vivo and in vitro." Molecular Pharmacology **67**(5): 1751-1757.
- Ferguson, K. M., J. M. Kavran, et al. (2000). "Structural basis for discrimination of 3-phosphoinositides by pleckstrin homology domains." Molecular cell **6**(2): 373-384.
- Ferguson, K. M., M. A. Lemmon, et al. (1995). "Structure of the high affinity complex of inositol trisphosphate with a phospholipase C pleckstrin homology domain." Cell **83**(6): 1037-1046.
- Fernandes, S., S. Iyer, et al. (2013). "Role of SHIP1 in cancer and mucosal inflammation." Annals of the New York Academy of Sciences **1280**: 6-10.

- Ferner, R. E., S. M. Huson, et al. (2007). "Guidelines for the diagnosis and management of individuals with neurofibromatosis 1." J Med Genet **44**(2): 81-88.
- Fewster, M. E., B. J. Burns, et al. (1969). "Quantitative densitometric thin-layer chromatography of lipids using copper acetate reagent." Journal of Chromatography A **43**(0): 120-126.
- Field, S. J., N. Madson, et al. (2005). "PtdIns(4,5)P₂ functions at the cleavage furrow during cytokinesis." Current biology : CB **15**(15): 1407-1412.
- Finger, J. H., R. T. Bronson, et al. (2002). "The netrin 1 receptors Unc5h3 and Dcc are necessary at multiple choice points for the guidance of corticospinal tract axons." J. Neurosci. **22**(23): 10346-10356.
- Flanagan, C. A., E. A. Schnieders, et al. (1993). "Phosphatidylinositol 4-kinase: gene structure and requirement for yeast cell viability." Science **262**(5138): 1444-1448.
- Flanagan, C. A. and J. Thorner (1992). "Purification and characterization of a soluble phosphatidylinositol 4-kinase from the yeast *Saccharomyces cerevisiae*." The Journal of biological chemistry **267**(33): 24117-24125.
- Flick, J. S. and J. Thorner (1993). "Genetic and biochemical characterization of a phosphatidylinositol-specific phospholipase C in *Saccharomyces cerevisiae*." Molecular and cellular biology **13**(9): 5861-5876.
- Floyd, J. A., D. A. Gold, et al. (2003). "A natural allele of Nxf1 suppresses retrovirus insertional mutations." Nat Genet **35**(3): 221-228.
- Fourches, D., J. C. Barnes, et al. (2010). "Cheminformatics analysis of assertions mined from literature that describe drug-induced liver injury in different species." Chemical research in toxicology **23**(1): 171-183.
- Frame, M. C., H. Patel, et al. (2010). "The FERM domain: organizing the structure and function of FAK." Nature reviews. Molecular cell biology **11**(11): 802-814.
- Franke, T. F., D. R. Kaplan, et al. (1997). "Direct regulation of the Akt proto-oncogene product by phosphatidylinositol-3,4-bisphosphate." Science **275**(5300): 665-668.
- Freeman, D. J., A. G. Li, et al. (2003). "PTEN tumor suppressor regulates p53 protein levels and activity through phosphatase-dependent and -independent mechanisms." Cancer Cell **3**(2): 117-130.
- Friedman, J. M. (1999). "Epidemiology of neurofibromatosis type 1." American Journal of Medical Genetics **89**(1): 1-6.

- Friesner, R. A., J. L. Banks, et al. (2004). "Glide: A new approach for rapid, accurate docking and scoring. 1. method and assessment of docking accuracy." Journal of Medicinal Chemistry **47**(7): 1739-1749.
- Friesner, R. A., R. B. Murphy, et al. (2006). "Extra precision glide: docking and scoring incorporating a model of hydrophobic enclosure for protein-ligand complexes." Journal of medicinal chemistry **49**(21): 6177-6196.
- Friesner, R. A., R. B. Murphy, et al. (2006). "Extra precision Glide: docking and scoring incorporating a model of hydrophobic enclosure for protein-ligand complexes." Journal of Medicinal Chemistry **49**(21): 6177-6196.
- Fruman, D. A., R. E. Meyers, et al. (1998). "Phosphoinositide kinases." Annual Review of Biochemistry **67**(1): 481-507.
- Fruman, D. A. and C. Rommel (2014). "PI3K and cancer: lessons, challenges and opportunities." Nature reviews. Drug discovery **13**(2): 140-156.
- Fuhler, G. M., R. Brooks, et al. (2012). "Therapeutic potential of SH2 domain-containing inositol-5'-phosphatase 1 (SHIP1) and SHIP2 inhibition in cancer." Molecular medicine **18**: 65-75.
- Gallego, O., M. J. Betts, et al. (2010). "A systematic screen for protein-lipid interactions in *Saccharomyces cerevisiae*." Molecular Systems Biology **6**(1).
- Gallop, J. L. and H. T. McMahon (2005). "BAR domains and membrane curvature: bringing your curves to the BAR." Biochemical Society symposium(72): 223-231.
- Garcia-Bustos, J. F., F. Marini, et al. (1994). "PIK1, an essential phosphatidylinositol 4-kinase associated with the yeast nucleus." The EMBO journal **13**(10): 2352-2361.
- García-Mata, R. and K. Burrige (2007). "Catching a GEF by its tail." Trends in Cell Biology **17**(1): 36-43.
- Garcia, P., R. Gupta, et al. (1995). "The pleckstrin homology domain of phospholipase C- δ .1 binds with high affinity to phosphatidylinositol 4,5-bisphosphate in bilayer membranes." Biochemistry **34**(49): 16228-16234.
- Gaullier, J. M., A. Simonsen, et al. (1998). "FYVE fingers bind PtdIns(3)P." Nature **394**(6692): 432-433.
- Gauthier, S. and A. Sniderman (1983). "Action tremor as a manifestation of chylomicron retention disease." Ann. Neurol **14**(5): 591.

- Gee, N. S., C. I. Ragan, et al. (1988). "The purification and properties of myo-inositol monophosphatase from bovine brain." The Biochemical journal **249**(3): 883-889.
- Gericke, A., M. Munson, et al. (2006). "Regulation of the PTEN phosphatase." Gene **374**(0): 1-9.
- Gietz, R. D. and A. Sugino (1988). "New yeast-Escherichia coli shuttle vectors constructed with in vitro mutagenized yeast genes lacking six-base pair restriction sites." Gene **74**(2): 527-534.
- Gillaspy, G. E., J. S. Keddie, et al. (1995). "Plant inositol monophosphatase is a lithium-sensitive enzyme encoded by a multigene family." The Plant cell **7**(12): 2175-2185.
- Gloyna, W., F. Schmitz, et al. (2005). "Inhibition of phospholipase C-independent exocytotic responses in rat peritoneal mast cells by U73122." Regulatory Peptides **125**(1-3): 179-184.
- Goclik, E., G. M. König, et al. (2000). "Pelorol from the tropical marine sponge *Dactylospongia elegans*." Journal of Natural Products **63**(8): 1150-1152.
- Goldstein, A. and J. O. Lampen (1975). "Beta-D-fructofuranoside fructohydrolase from yeast." Methods in enzymology **42**: 504-511.
- Golebiewska, U., M. Nyako, et al. (2008). "Diffusion coefficient of fluorescent phosphatidylinositol 4,5-bisphosphate in the plasma membrane of cells." Molecular biology of the cell **19**(4): 1663-1669.
- Golovleva, I., S. Bhattacharya, et al. (2003). "Disease-causing mutations in the cellular retinaldehyde binding protein tighten and abolish ligand interactions." Journal of Biological Chemistry **278**(14): 12397-12402.
- Golovleva, I., L. Köhn, et al. (2010). Mutation spectra in autosomal dominant and recessive retinitis pigmentosa in Northern Sweden: 255-262.
- Gottfried, O. N., D. H. Viskochil, et al. (2010). "Neurofibromatosis type 1 and tumorigenesis: molecular mechanisms and therapeutic implications." Neurosurgical FOCUS **28**(1): E8.
- Gow, N. A., A. J. Brown, et al. (2002). "Fungal morphogenesis and host invasion." Curr Opin Microbiol **5**(4): 366-371.
- Grelle, G., S. Kostka, et al. (2006). "Identification of VCP/p97, Carboxyl Terminus of Hsp70-interacting Protein (CHIP), and Amphiphysin II Interaction Partners

- Using Membrane-based Human Proteome Arrays." Molecular & Cellular Proteomics **5**(2): 234-244.
- Guillou, H., L. R. Stephens, et al. (2007). Quantitative measurement of phosphatidylinositol 3,4,5-trisphosphate. Methods in enzymology. H. A. Brown, Academic Press. **Volume 434**: 117-130.
- Guo, S., L. E. Stolz, et al. (1999). "SAC1-like domains of yeast SAC1, INP52, and INP53 and of human synaptojanin encode polyphosphoinositide phosphatases." The Journal of biological chemistry **274**(19): 12990-12995.
- Haffner, C., K. Takei, et al. (1997). "Synaptojanin 1: localization on coated endocytic intermediates in nerve terminals and interaction of its 170 kDa isoform with Eps15." FEBS letters **419**(2-3): 175-180.
- Halgren, T. A., R. B. Murphy, et al. (2004). "Glide: a new approach for rapid, accurate docking and scoring. 2. enrichment factors in database screening." Journal of Medicinal Chemistry **47**(7): 1750-1759.
- Hallcher, L. M. and W. R. Sherman (1980). "The effects of lithium ion and other agents on the activity of myo-inositol-1-phosphatase from bovine brain." The Journal of biological chemistry **255**(22): 10896-10901.
- Hama, H., E. A. Schnieders, et al. (1999). "Direct involvement of phosphatidylinositol 4-phosphate in secretion in the yeast *Saccharomyces cerevisiae*." The Journal of biological chemistry **274**(48): 34294-34300.
- Hamada, K., T. Shimizu, et al. (2000). "Structural basis of the membrane-targeting and unmasking mechanisms of the radixin FERM domain." The EMBO journal **19**(17): 4449-4462.
- Hamilton, B. A., D. J. Smith, et al. (1997). "The vibrator mutation causes neurodegeneration via reduced expression of PITP α : positional complementation cloning and extragenic suppression." Neuron **18**(5): 711-722.
- Hamilton, M. J., V. W. Ho, et al. (2011). "Role of SHIP in cancer." Experimental hematology **39**(1): 2-13.
- Hammond, S. M., Y. M. Altshuller, et al. (1995). "Human ADP-ribosylation factor-activated phosphatidylcholine-specific phospholipase D defines a new and highly conserved gene family." Journal of Biological Chemistry **270**(50): 29640-29643.
- Hampton, A., L. W. Brox, et al. (1969). "Analogues of inosine 5'-phosphate with phosphorus-nitrogen and phosphorus-sulfur bonds. binding and kinetic studies with inosine-5'-phosphate dehydrogenase." Biochemistry **8**(6): 2303-2311.

- Han, G.-S., A. Audhya, et al. (2002). "The *Saccharomyces cerevisiae* LSB6 gene encodes phosphatidylinositol 4-kinase activity." Journal of Biological Chemistry **277**(49): 47709-47718.
- Harlan, J. E., P. J. Hajduk, et al. (1994). "Pleckstrin homology domains bind to phosphatidylinositol-4,5-bisphosphate." Nature **371**(6493): 168-170.
- Harris, S. D. and J. R. Pringle (1991). "Genetic analysis of *Saccharomyces cerevisiae* chromosome I: on the role of mutagen specificity in delimiting the set of genes identifiable using temperature-sensitive-lethal mutations." Genetics **127**(2): 279-285.
- Hartman, J. L. t., B. Garvik, et al. (2001). "Principles for the buffering of genetic variation." Science **291**(5506): 1001-1004.
- Hartwell, L. H. (1974). "*Saccharomyces cerevisiae* cell cycle." Bacteriological reviews **38**(2): 164-198.
- Hasegawa, J., E. Tokuda, et al. (2011). "SH3YL1 regulates dorsal ruffle formation by a novel phosphoinositide-binding domain." The Journal of cell biology **193**(5): 901-916.
- Haslam, R. J., H. B. Koide, et al. (1993). "Pleckstrin domain homology." Nature **363**(6427): 309-310.
- Hatjiharissi, E., H. Ngo, et al. (2007). "Proteomic analysis of waldenstrom macroglobulinemia." Cancer Res **67**(8): 3777-3784.
- Hay, J. C. and T. F. Martin (1995). "Phosphatidylinositol transfer protein required for ATP-dependent priming of Ca²⁺-activated secretion." Nature **374**(6518): 173-177
- Hayakawa, A., S. Hayes, et al. (2007). "Evolutionarily conserved structural and functional roles of the FYVE domain." Biochemical Society symposium(74): 95-105.
- Hayakawa, Y., M. Itoh, et al. (2007). "Expression and localization of Cayman ataxia-related protein, Caytaxin, is regulated in a developmental- and spatial-dependent manner." Brain Research **1129**: 100-109.
- Hayashi-Takagi, A., M. Takaki, et al. (2010). "Disrupted-in-schizophrenia 1 (DISC1) regulates spines of the glutamate synapse via Rac1." Nat Neurosci **13**(3): 327-332.

- Hayashi, E., T. Maeda, et al. (1974). "The effect of myo-inositol deficiency on lipid metabolism in rats. II. The mechanism of triacylglycerol accumulation in the liver of myo-inositol-deficient rats." Biochimica et biophysica acta **360**(2): 146-155.
- He, J., J. Gajewiak, et al. (2011). "Metabolically stabilized derivatives of phosphatidylinositol 4-phosphate: synthesis and applications." Chemistry & Biology **18**(10): 1312-1319.
- He, X., J. Lobsiger, et al. (2009). "Bothnia dystrophy is caused by domino-like rearrangements in cellular retinaldehyde-binding protein mutant R234W." Proceedings of the National Academy of Sciences **106**(44): 18545-18550.
- Hendricks, K. B., B. Qing Wang, et al. (1999). "Yeast homologue of neuronal frequenin is a regulator of phosphatidylinositol-4-OH kinase." Nature cell biology **1**(4): 234-241.
- Henry, S. A., S. D. Kohlwein, et al. (2012). "Metabolism and regulation of glycerolipids in the yeast *Saccharomyces cerevisiae*." Genetics **190**(2): 317-349.
- Herman, P. K. and S. D. Emr (1990). "Characterization of VPS34, a gene required for vacuolar protein sorting and vacuole segregation in *Saccharomyces cerevisiae*." Molecular and cellular biology **10**(12): 6742-6754.
- Herman, P. K., J. H. Stack, et al. (1991). "A genetic and structural analysis of the yeast Vps15 protein kinase: evidence for a direct role of Vps15p in vacuolar protein delivery." The EMBO journal **10**(13): 4049-4060.
- Hiroaki, H., T. Ago, et al. (2001). "Solution structure of the PX domain, a target of the SH3 domain." Nature structural biology **8**(6): 526-530.
- Hirono, M., C. S. Denis, et al. (2004). "Hair cells require phosphatidylinositol 4,5-bisphosphate for mechanical transduction and adaptation." Neuron **44**(2): 309-320.
- Hirsch, E., M. Pozzato, et al. (2002). "Defective Dendrite Elongation but Normal Fertility in Mice Lacking the Rho-Like GTPase Activator *Dbl*." Mol. Cell. Biol. **22**(9): 3140-3148.
- Hollander, M. C., G. M. Blumenthal, et al. (2011). "PTEN loss in the continuum of common cancers, rare syndromes and mouse models." Nature reviews. Cancer **11**(4): 289-301.
- Holthuis, J. C. M. and T. P. Levine (2005). "Lipid traffic: floppy drives and a superhighway." Nat Rev Mol Cell Biol **6**(3): 209-220.

- Hong, S.-K., C. Levin, et al. (2010). "Pre-gastrula expression of zebrafish extraembryonic genes." BMC Developmental Biology **10**(1): 42.
- Honigberg, S. M., C. Conicella, et al. (1992). "Commitment to meiosis in *Saccharomyces cerevisiae*: involvement of the SPO14 gene." Genetics **130**(4): 703-716.
- Hoon, S., A. M. Smith, et al. (2008). "An integrated platform of genomic assays reveals small-molecule bioactivities." Nature chemical biology **4**(8): 498-506.
- Hopkins, B. D., C. Hodakoski, et al. (2014). "PTEN function: the long and the short of it." Trends in biochemical sciences **39**(4): 183-190.
- Horiguchi, M., M. Arita, et al. (2003). "pH-dependent translocation of α -tocopherol transfer protein between hepatic cytosol and late endosomes." Genes to Cells **8**(10): 789-800.
- Howell, A. S. and D. J. Lew (2012). "Morphogenesis and the Cell Cycle." Genetics **190**(1): 51-77.
- Hu, L., C. Zaloudek, et al. (2000). "In Vivo and in Vitro Ovarian Carcinoma Growth Inhibition by a Phosphatidylinositol 3-Kinase Inhibitor (LY294002)." Clinical Cancer Research **6**(3): 880-886.
- Huang, W., M. Barrett, et al. (2013). "Small molecule inhibitors of phospholipase C from a novel high-throughput screen." The Journal of biological chemistry **288**(8): 5840-5848.
- Huang, W., H. Zhang, et al. (2007). "Stabilized phosphatidylinositol-5-phosphate analogues as ligands for the nuclear protein ING2: Chemistry, Biology, and Molecular Modeling." Journal of the American Chemical Society **129**(20): 6498-6506.
- Hughes, S.-A. C. F., W. J. Gibson, et al. (2000). "The interaction of U-73122 with the histamine H1 receptor: implications for the use of U-73122 in defining H1 receptor-coupled signalling pathways." Naunyn-Schmiedeberg's Archives of Pharmacology **362**(6): 555-558.
- Hughes, T. (2002). "Yeast and drug discovery." Functional & Integrative Genomics **2**(4-5): 199-211.
- Huynh, H., N. Bottini, et al. (2004). "Control of vesicle fusion by a tyrosine phosphatase." Nat Cell Biol **6**(9): 831-839.
- Huynh, H., X. Wang, et al. (2003). "Homotypic secretory vesicle fusion induced by the protein tyrosine phosphatase MEG2 depends on polyphosphoinositides in T cells." J Immunol **171**(12): 6661-6671.

- Ichihara, Y., R. Fujimura, et al. (2013). "Rational design and synthesis of 4-substituted 2-pyridin-2-ylamides with inhibitory effects on SH2 domain-containing inositol 5'-phosphatase 2 (SHIP2)." European Journal of Medicinal Chemistry **62**(0): 649-660.
- Ile, K. E., S. Kassen, et al. (2010). "Zebrafish Class 1 Phosphatidylinositol Transfer Proteins: PITPB and Double Cone Cell Outer Segment Integrity in Retina." Traffic.
- Im, Y. J. and J. H. Hurley (2008). "Integrated structural model and membrane targeting mechanism of the human ESCRT-II complex." Developmental cell **14**(6): 902-913.
- Imai, H., S. Tanaka, et al. (1997). "Differential distribution of mRNAs encoding phosphatidylinositol transfer proteins alpha and beta in the central nervous system of the rat." Mol. Brain Res. **46**(1-2): 256-264
- Irino, Y., E. Tokuda, et al. (2012). "Quantification and visualization of phosphoinositides by quantum dot-labeled specific binding-domain probes." Journal of lipid research **53**(4): 810-819.
- Irvine, R. F. (2003). "Nuclear lipid signalling." Nature reviews. Molecular cell biology **4**(5): 349-360.
- Irvine, R. F. (2005). "Inositide evolution-towards turtle domination?" The Journal of physiology **566**(Pt 2): 295-300.
- Isakoff, S. J., T. Cardozo, et al. (1998). "Identification and analysis of PH domain-containing targets of phosphatidylinositol 3-kinase using a novel in vivo assay in yeast." The EMBO journal **17**(18): 5374-5387.
- Itoh, T. and T. Takenawa (2009). "Mechanisms of membrane deformation by lipid-binding domains." Progress in lipid research **48**(5): 298-305.
- Ivanova, P. T., S. B. Milne, et al. (2009). "Lipidomics: a mass spectrometry based systems level analysis of cellular lipids." Current Opinion in Chemical Biology **13**(5-6): 526-531.
- Janmey, P. A. and U. Lindberg (2004). "Cytoskeletal regulation: rich in lipids." Nature reviews. Molecular cell biology **5**(8): 658-666.
- Jeffries, T. R., S. K. Dove, et al. (2004). "PtdIns-specific MPR Pathway Association of a novel WD40 repeat protein, WIPI49." Molecular biology of the cell **15**(6): 2652-2663.

- Jin, L., G. Liu, et al. (2009). "Nm23-H1 regulates the proliferation and differentiation of the human chronic myeloid leukemia K562 cell line: A functional proteomics study." Life Sciences **84**(13-14): 458-467.
- Johnson, R. C., P. Penzes, et al. (2000). "Isoforms of kalirin, a neuronal Dbl family member, generated through use of different 5'- and 3'-ends along with an internal translational initiation site." Journal of Biological Chemistry **275**(25): 19324-19333.
- Johnstone, C. N., S. Castellví-Bel, et al. (2004). "ARHGAP8 is a novel member of the RHOGAP family related to ARHGAP1/CDC42GAP/p50RHOGAP: mutation and expression analyses in colorectal and breast cancers." Gene **336**(1): 59-71.
- Johnykutty, S., P. Tang, et al. (2009). "Dual expression of [alpha]-tocopherol-associated protein and estrogen receptor in normal/benign human breast luminal cells and the downregulation of α -tocopherol-associated protein in estrogen-receptor-positive breast carcinomas." Mod Pathol **22**(6): 770-775.
- Jones, B., E. L. Jones, et al. (2003). "Mutations in a Sar1 GTPase of COPII vesicles are associated with lipid absorption disorders." Nature Genetics **34**(1): 29-31.
- Jones, G., P. Willett, et al. (1995). "Molecular recognition of receptor sites using a genetic algorithm with a description of desolvation." Journal of Molecular Biology **245**(1): 43-53.
- Jones, G., P. Willett, et al. (1997). "Development and validation of a genetic algorithm for flexible docking." Journal of molecular biology **267**(3): 727-748.
- Jones, S. M. and A. Kazlauskas (2001). "Growth factor-dependent signaling and cell cycle progression." Chemical Reviews **101**(8): 2413-2424.
- Jović, M., F. Kieken, et al. (2009). "Eps15 Homology Domain 1-associated Tubules Contain Phosphatidylinositol-4-Phosphate and Phosphatidylinositol-(4,5)-Bisphosphate and Are Required for Efficient Recycling." Molecular biology of the cell **20**(11): 2731-2743.
- Kadamur, G. and E. M. Ross (2013). "Mammalian phospholipase C." Annual Review of Physiology **75**(1): 127-154.
- Kanai, F., H. Liu, et al. (2001). "The PX domains of p47phox and p40phox bind to lipid products of PI(3)K." Nature cell biology **3**(7): 675-678.
- Katoh, Y., B. Ritter, et al. (2009). "The Clavesin Family, Neuron-specific Lipid- and Clathrin-binding Sec14 Proteins Regulating Lysosomal Morphology." Journal of Biological Chemistry **284**(40): 27646-27654.

- Kauffmann-Zeh, A., G. Thomas, et al. (1995). "Requirement for phosphatidylinositol transfer protein in epidermal growth factor signaling." Science **268**(5214): 1188-1190
- Kempná, P., J.-M. Zingg, et al. (2003). "Cloning of novel human SEC14p-like proteins: ligand binding and functional properties." Free Radical Biology and Medicine **34**(11): 1458-1472.
- Kennedy, M. A., N. Kabbani, et al. (2011). "Srf1 is a novel regulator of phospholipase D activity and is essential to buffer the toxic effects of C16:0 platelet activating factor." PLoS genetics **7**(2): e1001299.
- Kerr, W. G. (2011). "Inhibitor and activator: dual functions for SHIP in immunity and cancer." Annals of the New York Academy of Sciences **1217**: 1-17.
- Kielkowska, A., I. Niewczas, et al. (2014). "A new approach to measuring phosphoinositides in cells by mass spectrometry." Advances in biological regulation **54C**: 131-141.
- Kihara, A., T. Noda, et al. (2001). "Two distinct Vps34 phosphatidylinositol 3-kinase complexes function in autophagy and carboxypeptidase Y sorting in *Saccharomyces cerevisiae*." The Journal of cell biology **152**(3): 519-530.
- Kim, J. W., S. H. Ryu, et al. (1989). "Cyclic and noncyclic inositol phosphates are formed at different ratios by phospholipase C isozymes." Biochemical and biophysical research communications **163**(1): 177-182.
- Kim, S., D. N. Cullis, et al. (2001). "Solution Structure of the Repl1 EH Domain and Characterization of Its Binding to NPF Target Sequences." Biochemistry **40**(23): 6776-6785.
- Kim, Y., S. R. Shanta, et al. (2010). "Mass spectrometry based cellular phosphoinositides profiling and phospholipid analysis: a brief review." Experimental & molecular medicine **42**(1): 1-11.
- Kitahara, N., A. Endo, et al. (1981). "Thielavin A and B, new inhibitors of prostaglandin biosynthesis produced by *Thielavia terricola*." The Journal of antibiotics **34**(12): 1562-1568.
- Klein, R. R., D. M. Bourdon, et al. (2011). "Direct activation of human phospholipase C by its well known inhibitor U73122." Journal of Biological Chemistry **286**(14): 12407-12416.
- Kleyn, P. W., W. Fan, et al. (1996). "Identification and characterization of the mouse obesity gene *tubby*: a member of a novel gene family." Cell **85**(2): 281-290.

- Klose, A., T. Huth, et al. (2008). "1-[6-[[[(17 β)-3-Methoxyestra-1,3,5(10)-trien-17-yl]amino]hexyl]-1H-pyrrole-2,5-dione (U73122) Selectively Inhibits Kir3 and BK Channels in a Phospholipase C-Independent Fashion." Molecular Pharmacology **74**(5): 1203-1214.
- Kobayashi, K., T. M. Forte, et al. (2000). "The db/db mouse, a model for diabetic dyslipidemia: Molecular characterization and effects of western diet feeding." Metabolism **49**(1): 22-31.
- Kofman, O. and R. H. Belmaker (1990). "Intracerebroventricular myo-inositol antagonizes lithium-induced suppression of rearing behaviour in rats." Brain Research **534**(1-2): 345-347.
- Komai, K., N. Mukae-Sakairi, et al. (2003). "Characterization of novel splicing variants of the mouse MCF-2 (DBL) proto-oncogene." Biochemical and Biophysical Research Communications **309**(4): 906-909.
- Komander, D., A. Fairservice, et al. (2004). "Structural insights into the regulation of PDK1 by phosphoinositides and inositol phosphates." The EMBO journal **23**(20): 3918-3928.
- Kong, D. and T. Yamori (2008). "Phosphatidylinositol 3-kinase inhibitors: promising drug candidates for cancer therapy." Cancer Science **99**(9): 1734-1740.
- Kong, Y.-H., G.-M. Ye, et al. (2006). "Cloning and Characterization of a Novel, Human Cellular Retinaldehyde-binding Protein CRALBP-like (CRALBPL) Gene." Biotechnology Letters **28**(17): 1327-1333.
- Kono, N., U. Ohto, et al. (2013). "Impaired α -TTP-PIPs Interaction Underlies Familial Vitamin E Deficiency." Science **340**(6136): 1106-1110.
- Koshihara, S., T. Kigawa, et al. (1999). "Solution structure of the Eps15 homology domain of a human POB1 (partner of RalBP1)." FEBS letters **442**(2-3): 138-142.
- Kostenko, E. V., G. M. Mahon, et al. (2005). "The Sec14 homology domain regulates the cellular distribution and transforming activity of the Rho-specific guanine nucleotide exchange factor Dbs." Journal of Biological Chemistry **280**(4): 2807-2817.
- Kroes, J. F., D. M. Hegsted, et al. (1973). "Inositol deficiency in gerbils: dietary effects on the intestinal lipodystrophy." The Journal of nutrition **103**(10): 1448-1453.
- Krug, T., H. Manso, et al. (2010). "Kalirin: a novel genetic risk factor for ischemic stroke." Human Genetics **127**(5): 513-523.

- Kulagowski, J. J., R. Baker, et al. (1991). "Inhibitors of myo-inositol monophosphatase containing methylenebisphosphonic acid as a replacement for a phosphate group." Journal of the Chemical Society, Chemical Communications(22): 1649-1650.
- Kurtz, J.-E. and I. Ray-Coquard (2012). "PI3 kinase inhibitors in the clinic: an update." Anticancer Research **32**(7): 2463-2470.
- Kutateladze, T. and M. Overduin (2001). "Structural Mechanism of Endosome Docking by the FYVE Domain." Science **291**(5509): 1793-1796.
- Kutateladze, T. G. (2006). "Phosphatidylinositol 3-phosphate recognition and membrane docking by the FYVE domain." Biochimica et Biophysica Acta (BBA) - Molecular and Cell Biology of Lipids **1761**(8): 868-877.
- Kutateladze, T. G. (2007). "Mechanistic similarities in docking of the FYVE and PX domains to phosphatidylinositol 3-phosphate containing membranes." Progress in Lipid Research **46**(6): 315-327.
- Kutateladze, T. G. (2010). "Translation of the phosphoinositide code by PI effectors." Nature chemical biology **6**(7): 507-513.
- Labute, P. (2001). "Probabilistic Receptor Potentials." Journal of the Chemical Computing Group Retrieved 2013, from <http://www.chemcomp.com/journal/cstat.htm>.
- LaMarche, M. J., J. Borawski, et al. (2012). "Anti-hepatitis C virus activity and toxicity of type III phosphatidylinositol-4-kinase beta inhibitors." Antimicrobial Agents and Chemotherapy **56**(10): 5149-5156.
- Lampe, D., C. Liu, et al. (1994). "Synthesis of Selective Non-Ca²⁺ Mobilizing inhibitors of D-myo-Inositol 1,4,5-trisphosphate 5-phosphatase." Journal of medicinal chemistry **37**(7): 907-912.
- Langcake, P. and R. J. Pryce (1977). "A new class of phytoalexins from grapevines." Experientia **33**(2): 151-152.
- Larkin, M. A., G. Blackshields, et al. (2007). "Clustal W and clustal X version 2.0." Bioinformatics **23**(21): 2947-2948.
- Lazar, D. F. and A. R. Saltiel (2006). "Lipid phosphatases as drug discovery targets for type 2 diabetes." Nature reviews. Drug discovery **5**(4): 333-342.
- LeDoux, M. S. and J. F. Lorden (2002). "Abnormal spontaneous and harmaline-stimulated Purkinje cell activity in the awake genetically dystonic rat." Exp Brain Res **145**(4): 457-467.

- LeDoux, M. S., J. F. Lorden, et al. (1993). "Cerebellectomy eliminates the motor syndrome of the genetically dystonic rat." Experimental Neurology **120**(2): 302-310.
- LeDoux, M. S., J. F. Lorden, et al. (1995). "Selective elimination of cerebellar output in the genetically dystonic rat." Brain Research **697**(1-2): 91-103.
- Lee, D. W., X. Zhao, et al. (2005). "ATP binding regulates oligomerization and endosome association of RME-1 family proteins." The Journal of biological chemistry **280**(17): 17213-17220.
- Lee, E., M. Marcucci, et al. (2002). "Amphiphysin 2 (Bin1) and T-Tubule Biogenesis in Muscle." Science **297**(5584): 1193-1196.
- Lee, J.-O., H. Yang, et al. (1999). "Crystal structure of the PTEN tumor suppressor: implications for its phosphoinositide phosphatase activity and membrane association." Cell **99**(3): 323-334.
- Leivers, A. L., M. Tallant, et al. (2013). "Discovery of selective small molecule type III phosphatidylinositol 4-kinase alpha (PI4KIII α) inhibitors as anti hepatitis C (HCV) agents." Journal of medicinal chemistry.
- Leloup, L., H. Shao, et al. (2010). "m-calpain activation is regulated by Its membrane localization and by its binding to phosphatidylinositol 4,5-bisphosphate." Journal of Biological Chemistry **285**(43): 33549-33566.
- Lemmon, M. (2003). "Phosphoinositide recognition domains." Traffic **4**(4): 201 - 213.
- Lemmon, M. A. (2007). "Pleckstrin homology (PH) domains and phosphoinositides." Biochemical Society symposium(74): 81-93.
- Lemmon, M. A. (2008). "Membrane recognition by phospholipid-binding domains." Nat Rev Mol Cell Biol **9**(2): 99-111.
- Lemmon, M. A. and K. M. Ferguson (2000). "Signal-dependent membrane targeting by pleckstrin homology (PH) domains." The Biochemical journal **350 Pt 1**: 1-18.
- Lemmon, M. A., K. M. Ferguson, et al. (1995). "Specific and high-affinity binding of inositol phosphates to an isolated pleckstrin homology domain." Proceedings of the National Academy of Sciences **92**(23): 10472-10476.
- Leonard, S. W., Y. Terasawa, et al. (2002). "Incorporation of deuterated RRR- or all-rac- α -tocopherol in plasma and tissues of α -tocopherol transfer protein-null mice." Am J Clin Nutr **75**(3): 555-560.

- Leslie, N. R., H. Maccario, et al. (2009). "The significance of PTEN's protein phosphatase activity." Advances in enzyme regulation **49**(1): 190-196.
- Levine, T. P. and S. Munro (2002). "Targeting of Golgi-specific pleckstrin homology domains involves both PtdIns 4-kinase-dependent and -independent Components." Current Biology **12**(9): 695-704.
- Li, D., G. Carr, et al. (2011). "Turnagainolides A and B, cyclic depsipeptides produced in culture by a bacillus sp.: isolation, structure elucidation, and synthesis." Journal of Natural Products **74**(5): 1093-1099.
- Li, J., C. Yen, et al. (1997). "PTEN, a putative protein tyrosine phosphatase gene mutated in human brain, breast, and prostate cancer." Science **275**(5308): 1943-1947.
- Li, M., S. M. D. Shandilya, et al. (2011). "First-in-class small molecule inhibitors of the single-strand DNA cytosine deaminase APOBEC3G." ACS Chemical Biology **7**(3): 506-517.
- Li, R. (1997). "Bee1, a yeast protein with homology to Wiscott-Aldrich syndrome protein, is critical for the assembly of cortical actin cytoskeleton." The Journal of cell biology **136**(3): 649-658.
- Li, X., M. P. Rivas, et al. (2002). "Analysis of oxysterol binding protein homologue Kes1p function in regulation of Sec14p-dependent protein transport from the yeast Golgi complex." J Cell Biol **157**(1): 63-77.
- Li, X., S. M. Routt, et al. (2000). "Identification of a Novel Family of Nonclassic Yeast Phosphatidylinositol Transfer Proteins Whose Function Modulates Phospholipase D Activity and Sec14p-independent Cell Growth." Mol. Biol. Cell **11**(6): 1989-2005.
- Lindsley, C. W. (2010). "The Akt/PKB family of protein kinases: a review of small molecule inhibitors and progress towards target validation: a 2009 update." Current Topics In Medicinal Chemistry **10**(4): 458-477.
- Lipp, P. and G. Reither (2011). "Protein kinase C: the "masters" of calcium and lipid." Cold Spring Harbor perspectives in biology **3**(7).
- Liu, Y. and V. A. Bankaitis (2010). "Phosphoinositide phosphatases in cell biology and disease." Prog Lipid Res **49**(3): 201-217.
- Liu, Y., M. Boukhelifa, et al. (2009). "Functional studies of the mammalian Sac1 phosphoinositide phosphatase." Advances in enzyme regulation **49**(1): 75-86.

- Liu, Z., H. C. Adams, et al. (2009). "The Rho-specific guanine nucleotide exchange factor Dbs regulates breast cancer cell migration." Journal of Biological Chemistry **284**(23): 15771-15780.
- Loewith, R. and M. N. Hall (2011). "Target of Rapamycin (TOR) in Nutrient Signaling and Growth Control." Genetics **189**(4): 1177-1201.
- Lopez, M. C., J. M. Nicaud, et al. (1994). "A phosphatidylinositol/phosphatidylcholine transfer protein is required for differentiation of the dimorphic yeast *Yarrowia lipolytica* from the yeast to the mycelial form." J Cell Biol **125**(1): 113-127.
- Lu, Y., Y. Wang, et al. (2009). "C-X...H contacts in biomolecular systems: how they contribute to protein-ligand binding affinity." The journal of physical chemistry. B **113**(37): 12615-12621.
- Lua, B. L. and B. C. Low (2004). "BPGAP1 Interacts with Cortactin and Facilitates Its Translocation to Cell Periphery for Enhanced Cell Migration." Mol. Biol. Cell **15**(6): 2873-2883.
- Lua, B. L. and B. C. Low (2005). "Activation of EGF receptor endocytosis and ERK1/2 signaling by BPGAP1 requires direct interaction with EEN/endophilin II and a functional RhoGAP domain." J Cell Sci **118**(12): 2707-2721.
- Lueteteke, N. C., H. K. Phillips, et al. (1994). "The mouse waved-2 phenotype results from a point mutation in the EGF receptor tyrosine kinase." Genes & Development **8**(4): 399-413.
- Lutter, L. C. and C. G. Kurland (1975). "Chemical determination of protein neighbourhoods in a cellular organelle." Molecular and cellular biochemistry **7**(2): 105-116.
- Machida, T., T. Fujita, et al. (2005). "Increased expression of proapoptotic BMCC1, a novel gene with the BNIP2 and Cdc42GAP homology (BCH) domain, is associated with favorable prognosis in human neuroblastomas." Oncogene **25**(13): 1931-1942.
- MacMillan, D. and J. G. McCarron (2010). "The phospholipase C inhibitor U-73122 inhibits Ca²⁺ release from the intracellular sarcoplasmic reticulum Ca²⁺ store by inhibiting Ca²⁺ pumps in smooth muscle." British Journal of Pharmacology **160**(6): 1295-1301.
- Madania, A., P. Dumoulin, et al. (1999). "The *Saccharomyces cerevisiae* homologue of human wiskott-aldrich syndrome protein Las17p interacts with the Arp2/3 complex." Molecular biology of the cell **10**(10): 3521-3538.

- Madsen, K. L., V. K. Bhatia, et al. (2010). "BAR domains, amphipathic helices and membrane-anchored proteins use the same mechanism to sense membrane curvature." FEBS letters **584**(9): 1848-1855.
- Maehama, T. and J. E. Dixon (1998). "The tumor suppressor, PTEN/MMAC1, dephosphorylates the lipid second messenger, phosphatidylinositol 3,4,5-Trisphosphate." Journal of Biological Chemistry **273**(22): 13375-13378.
- Mahajan, K. and N. P. Mahajan (2012). "PI3K-independent AKT activation in cancers: a treasure trove for novel therapeutics." Journal of Cellular Physiology **227**(9): 3178-3184.
- Majerus, P. W., T. M. Connolly, et al. (1988). "Inositol phosphates: synthesis and degradation." Journal of Biological Chemistry **263**(7): 3051-3054.
- Majerus, P. W. and J. D. York (2009). "Phosphoinositide phosphatases and disease." J. Lipid Res. **50**(Supplement): S249-254.
- Mak, L., R. Vilar, et al. (2010). "Characterisation of the PTEN inhibitor VO-OHpic." Journal of Chemical Biology **3**(4): 157-163.
- Mani, N., P. Sancheti, et al. (1998). "Screening systems for detecting inhibitors of cell wall transglycosylation in Enterococcus. cell wall transglycosylation inhibitors in Enterococcus." The Journal of antibiotics **51**(5): 471-479.
- Mao, Y., A. Nickitenko, et al. (2000). "Crystal structure of the VHS and FYVE tandem domains of Hrs, a protein involved in membrane trafficking and signal transduction." Cell **100**(4): 447-456.
- Margolin, W. (2000). "Green Fluorescent Protein as a Reporter for Macromolecular Localization in Bacterial Cells." Methods **20**(1): 62-72.
- Mariotti, C., C. Gellera, et al. (2004). "Ataxia with isolated vitamin E deficiency: neurological phenotype, clinical follow-up and novel mutations in TTPA gene in Italian families." Neurological Sciences **25**(3): 130-137.
- Martin, T. F. J. (1998). "Phosphoinositide lipids as signaling molecules: common themes for signal transduction, cytoskeletal regulation, and membrane trafficking." Annual Review of Cell and Developmental Biology **14**(1): 231-264.
- Martins-de-Souza, D., W. Gattaz, et al. (2009). "Prefrontal cortex shotgun proteome analysis reveals altered calcium homeostasis and immune system imbalance in schizophrenia." European Archives of Psychiatry and Clinical Neuroscience **259**(3): 151-163.

- Masuda, M. and N. Mochizuki (2010). "Structural characteristics of BAR domain superfamily to sculpt the membrane." Seminars in Cell & Developmental Biology **21**(4): 391-398.
- Maw, M. A., B. Kennedy, et al. (1997). "Mutation of the gene encoding cellular retinaldehyde-binding protein in autosomal recessive retinitis pigmentosa." Nat Genet **17**(2): 198-200.
- Mayer, B. J., R. Ren, et al. (1993). "A putative modular domain present in diverse signaling proteins." Cell **73**(4): 629-630.
- Mayr, G. W. (1988). "A novel metal-dye detection system permits picomolar-range HPLC analysis of inositol polyphosphates from non-radioactively labelled cell or tissue specimens." The Biochemical journal **254**(2): 585-591.
- McIntire, L. B. J., K.-I. Lee, et al. (2013). "Screening assay for small-molecule inhibitors of synaptojanin 1, a synaptic phosphoinositide phosphatase." Journal of Biomolecular Screening.
- McLaughlin, S. and D. Murray (2005). "Plasma membrane phosphoinositide organization by protein electrostatics." Nature **438**(7068): 605-611.
- McNamara, C. W., M. C. Lee, et al. (2013). "Targeting Plasmodium PI(4)K to eliminate malaria." Nature **504**(7479): 248-253.
- McPherson, C. E., B. A. Eipper, et al. (2002). "Genomic organization and differential expression of Kalirin isoforms." Gene **284**(1-2): 41-51.
- McPherson, P. S., E. P. Garcia, et al. (1996). "A presynaptic inositol-5-phosphatase." Nature **379**(6563): 353-357.
- McPherson, P. S., K. Takei, et al. (1994). "p145, a major Grb2-binding protein in brain, is co-localized with dynamin in nerve terminals where it undergoes activity-dependent dephosphorylation." Journal of Biological Chemistry **269**(48): 30132-30139.
- Mei, Y. and F. Zhang (2012). "Molecular tools and approaches for optogenetics." Biological psychiatry **71**(12): 1033-1038.
- Meimetis, L. G., M. Nodwell, et al. (2012). "Synthesis of SHIP1-Activating Analogs of the Sponge Meroterpenoid Pelorol." European Journal of Organic Chemistry **2012**(27): 5195-5207.
- Meng, E., I. Kuntz, et al. (1994). "Evaluating docked complexes with the HINT exponential function and empirical atomic hydrophobicities." Journal of Computer-Aided Molecular Design **8**(3): 299-306.

- Mentel, M., V. Laketa, et al. (2011). "Photoactivatable and cell-membrane-permeable phosphatidylinositol 3,4,5-trisphosphate." Angewandte Chemie **50**(16): 3811-3814.
- Metrangolo, P. and G. Resnati (2001). "Halogen bonding: a paradigm in supramolecular chemistry." Chemistry **7**(12): 2511-2519.
- Meyers, R. and L. C. Cantley (1997). "Cloning and characterization of a Wortmannin-sensitive Human Phosphatidylinositol 4-Kinase." Journal of Biological Chemistry **272**(7): 4384-4390.
- Michell, R. H. (2008). "Inositol derivatives: evolution and functions." Nature reviews. Molecular cell biology **9**(2): 151-161.
- Michell, R. H., V. L. Heath, et al. (2006). "Phosphatidylinositol 3,5-bisphosphate: metabolism and cellular functions." Trends in biochemical sciences **31**(1): 52-63.
- Miehe, S., A. Bieberstein, et al. (2010). "The phospholipid-binding protein SESTD1 is a novel regulator of the transient receptor potential channels TRPC4 and TRPC5." Journal of Biological Chemistry **285**(16): 12426-12434.
- Miettinen, P. J., J. E. Berger, et al. (1995). "Epithelial immaturity and multiorgan failure in mice lacking epidermal growth factor receptor." Nature **376**(6538): 337-341
- Milanovic, M., S. Radtke, et al. (2012). "Anomalous inhibition of c-Met by the kinesin inhibitor aurintricarboxylic acid." International Journal of Cancer **130**(5): 1060-1070.
- Miliaras, N. and B. Wendland (2004). "EH proteins." Cell Biochemistry and Biophysics **41**(2): 295-318.
- Miller, D. J. and R. K. Allemann (2007). "myo-Inositol monophosphatase: a challenging target for mood stabilising drugs." Mini Reviews In Medicinal Chemistry **7**(2): 107-113.
- Miller, E. A. and C. Barlowe (2001). "Regulation of coat assembly-sorting things out at the ER." Curr. Opin. Cell Biol.
- Miller, J. N. (2005). "Fluorescence energy transfer methods in bioanalysis." The Analyst **130**(3): 265-270.
- Miller, S., B. Tavshanjian, et al. (2010). "Shaping development of autophagy inhibitors with the structure of the lipid kinase Vps34." Science **327**(5973): 1638-1642.

- Milligan, S. C., J. G. Alb, et al. (1997). "The phosphatidylinositol transfer protein domain of drosophila retinal degeneration B protein is essential for photoreceptor cell survival and recovery from light stimulation." The Journal of Cell Biology **139**(2): 351-363.
- Mills, S. J., C. Persson, et al. (2012). "A synthetic polyphosphoinositide headgroup surrogate in complex with SHIP2 provides a rationale for drug discovery." ACS Chemical Biology **7**(5): 822-828.
- Misra, S. and J. H. Hurley (1999). "Crystal structure of a phosphatidylinositol 3-phosphate-specific membrane-targeting motif, the FYVE domain of Vps27p." Cell **97**(5): 657-666.
- Miyawaki, A., J. Llopis, et al. (1997). "Fluorescent indicators for Ca²⁺ based on green fluorescent proteins and calmodulin." Nature **388**(6645): 882-887.
- Moleirinho, S., A. Tilston-Lunel, et al. (2013). "The expanding family of FERM proteins." The Biochemical journal **452**(2): 183-193.
- Mollinedo, F., C. Gajate, et al. (2004). "ET-18-OCH₃ (edelfosine): a selective antitumour lipid targeting apoptosis through intracellular activation of Fas/CD95 death receptor." Current Medicinal Chemistry **11**(24): 3163-3184.
- Monaco, M. E., J. Kim, et al. (2004). "Lipid metabolism in phosphatidylinositol transfer protein α -deficient vibrator mice." Biochemical and Biophysical Research Communications **317**(2): 444-450.
- Monteoliva, L., M. Sanchez, et al. (1996). "Cloning of *Candida albicans* SEC14 gene homologue coding for a putative essential function." Yeast **12**(11): 1097-1105.
- Montero, E., L. M. Gonzalez, et al. (2007). "Taenia solium: Identification and preliminary characterization of a lipid binding protein with homology to the SEC14 catalytic domain." Experimental Parasitology **116**(3): 191-200.
- Montesinos, M. L., M. Castellano-Muñoz, et al. (2005). "Recycling and EH domain proteins at the synapse." Brain Research Reviews **49**(2): 416-428.
- Moravcevic, K., Camilla L. Oxley, et al. (2012). "conditional peripheral membrane proteins: facing up to limited specificity." Structure **20**(1): 15-27.
- Morgan, C. P., V. Allen-baume, et al. (2006). "Differential expression of a C-terminal splice variant of phosphatidylinositol transfer protein β lacking the constitutive-phosphorylated Ser262 that localizes to the Golgi compartment." Biochem J **398**(3): 411-421.

- Morley, S., M. Cecchini, et al. (2008). "Mechanisms of Ligand Transfer by the Hepatic Tocopherol Transfer Protein." Journal of Biological Chemistry **283**(26): 17797-17804.
- Morley, S., C. Panagabko, et al. (2004). "Molecular Determinants of Heritable Vitamin E Deficiency†." Biochemistry **43**(14): 4143-4149.
- Morohaku, K., Y. Hoshino, et al. (2013). "Incorporation of phosphatase inhibitor in culture prompts growth initiation of isolated non-growing oocytes." PLoS ONE **8**(11): e77533.
- Moskwa, P., M.-H. Paclet, et al. (2005). "Autoinhibition of p50 Rho GTPase-activating Protein (GAP) Is Released by Prenylated Small GTPases." Journal of Biological Chemistry **280**(8): 6716-6720.
- Mousley, C. J., K. Tyeryar, et al. (2008). "Trans-Golgi network and endosome dynamics connect ceramide homeostasis with regulation of the unfolded protein response and TOR signaling in yeast." Mol. Biol. Cell **19**(11): 4785-4803.
- Mousley, C. J., P. Yuan, et al. (2012). "A sterol-binding protein integrates endosomal lipid metabolism with TOR signaling and nitrogen sensing." Cell **148**(4): 702-715.
- Mu, F.-T., J. M. Callaghan, et al. (1995). "EEA1, an early endosome-associated protein.: EEA1 is a conserved α -helical peripheral membrane protein flanked by cysteineE "fingers" and contains a calmodulin binding IQ motif." Journal of Biological Chemistry **270**(22): 13503-13511.
- Mukhopadhyay, S. and P. K. Jackson (2011). "The tubby family proteins." Genome biology **12**(6): 225.
- Murias, M., N. Handler, et al. (2004). "Resveratrol analogues as selective cyclooxygenase-2 inhibitors: synthesis and structure–activity relationship." Bioorganic & medicinal chemistry **12**(21): 5571-5578.
- Murray, A. W. and M. R. Atkinson (1968). "Adenosine 5'-phosphorothioate. A nucleotide analog that is a substrate, competitive inhibitor, or regulator of some enzymes that interact with adenosine 5'-phosphate." Biochemistry **7**(11): 4023-4029.
- Murray, J. T. and J. M. Backer (2005). Analysis of hVps34/hVps15 Interactions with Rab5 In Vivo and In Vitro. Methods in enzymology. C. J. D. William E. Balch and H. Alan, Academic Press. **403**: 789-799.
- Myers, M. P., J. P. Stolarov, et al. (1997). "P-TEN, the tumor suppressor from human chromosome 10q23, is a dual-specificity phosphatase." Proceedings of the National Academy of Sciences **94**(17): 9052-9057.

- Nadler, A., G. Reither, et al. (2013). "The fatty acid composition of diacylglycerols determines local signaling patterns." Angewandte Chemie International Edition **52**(24): 6330-6334.
- Nahorski, S. R., C. I. Ragan, et al. (1991). "Lithium and the phosphoinositide cycle: an example of uncompetitive inhibition and its pharmacological consequences." Trends in pharmacological sciences **12**(8): 297-303.
- Nakanishi, S., K. J. Catt, et al. (1995). "A wortmannin-sensitive phosphatidylinositol 4-kinase that regulates hormone-sensitive pools of inositolphospholipids." Proceedings of the National Academy of Sciences **92**(12): 5317-5321.
- Naslavsky, N. and S. Caplan (2011). "EHD proteins: key conductors of endocytic transport." Trends in cell biology **21**(2): 122-131.
- Naslavsky, N., J. Rahajeng, et al. (2007). "EHD1 and Eps15 interact with phosphatidylinositols via their Eps15 homology domains." The Journal of biological chemistry **282**(22): 16612-16622.
- Nasuhoglu, C., S. Feng, et al. (2002). "Nonradioactive analysis of phosphatidylinositides and other anionic phospholipids by anion-exchange high-performance liquid chromatography with suppressed conductivity detection." Analytical Biochemistry **301**(2): 243-254.
- Nawrot, M., K. West, et al. (2004). "Cellular retinaldehyde-binding protein interacts with ERM-binding phosphoprotein 50 in retinal pigment epithelium." Invest. Ophthalmol. Vis. Sci. **45**(2): 393-401.
- Nelson, C. P., S. R. Nahorski, et al. (2008). "Temporal profiling of changes in phosphatidylinositol 4,5-bisphosphate, inositol 1,4,5-trisphosphate and diacylglycerol allows comprehensive analysis of phospholipase C-initiated signalling in single neurons." Journal of neurochemistry **107**(3): 602-615.
- Nemoto, Y., M. R. Wenk, et al. (2001). "Identification and characterization of a synaptojanin 2 splice isoform predominantly expressed in nerve terminals." Journal of Biological Chemistry **276**(44): 41133-41142.
- Ni, J., X. Wen, et al. (2005). "Tocopherol-associated protein suppresses prostate cancer cell growth by inhibition of the phosphoinositide 3-kinase pathway." Cancer Res **65**(21): 9807-9816.
- Nile, A. H., V. A. Bankaitis, et al. (2010). "Mammalian diseases of phosphatidylinositol transfer proteins and their homologs." Clinical lipidology **5**(6): 867-897.
- Nile, A. H., A. Tripathi, et al. (2014). "PITPs as targets for selectively interfering with phosphoinositide signaling in cells." Nature chemical biology **10**(1): 76-84.

- Nishida, K., Y. Kaziro, et al. (1999). "Association of the proto-oncogene product Dbl with G protein [beta][gamma] subunits." FEBS Letters **459**(2): 186-190.
- Nishioka, T., K. Aoki, et al. (2008). "Rapid Turnover Rate of phosphoinositides at the front of migrating MDCK cells." Molecular biology of the cell **19**(10): 4213-4223.
- Noben-Trauth, K., J. K. Naggert, et al. (1996). "A candidate gene for the mouse mutation tubby." Nature **380**(6574): 534-538.
- Nobukuni, T., M. Joaquin, et al. (2005). "Amino acids mediate mTOR/raptor signaling through activation of class 3 phosphatidylinositol 3OH-kinase." Proceedings of the National Academy of Sciences of the United States of America **102**(40): 14238-14243.
- Notredame, C., D. G. Higgins, et al. (2000). "T-Coffee: A novel method for fast and accurate multiple sequence alignment." Journal of molecular biology **302**(1): 205-217.
- Nurse, P., P. Thuriaux, et al. (1976). "Genetic control of the cell division cycle in the fission yeast *Schizosaccharomyces pombe*." Molecular and General Genetics MGG **146**(2): 167-178.
- Nyquist, D. A. and G. M. J. Helmkamp (1989). "Developmental patterns in rat brain of phosphatidylinositol synthetic enzymes and phosphatidylinositol transfer protein." Biochim Biophys Acta. **987**(2): 165-170
- Nystuen, A., P. J. Benke, et al. (1996). "A cerebellar ataxia locus identified by DNA pooling to search for linkage disequilibrium in an isolated population from the Cayman Islands." Hum Mol Genet **5**(4): 525-531.
- O'Brien, S. P., K. Seipel, et al. (2000). "Skeletal muscle deformity and neuronal disorder in Trio exchange factor-deficient mouse embryos." Proceedings of the National Academy of Sciences of the United States of America **97**(22): 12074-12078.
- O'Brien, W. T. and P. S. Klein (2009). "Validating GSK3 as an in vivo target of lithium action." Biochemical Society transactions **37**(Pt 5): 1133-1138.
- Ohashi, M., K. Jan de Vries, et al. (1995). "A role for phosphatidylinositol transfer protein in secretory vesicle formation." Nature **377**(6549): 544-547.
- Ohlemiller, K. K., R. M. Hughes, et al. (1995). "Cochlear and retinal degeneration in the tubby mouse." Neuroreport **6**(6): 845-849.
- Okonechnikov, K., O. Golosova, et al. (2012). "Unipro UGENE: a unified bioinformatics toolkit." Bioinformatics **28**(8): 1166-1167.

- Ong, C. J., A. Ming-Lum, et al. (2007). "Small-molecule agonists of SHIP1 inhibit the phosphoinositide 3-kinase pathway in hematopoietic cells." Blood **110**(6): 1942-1949.
- Ozaki, S., D. B. DeWald, et al. (2000). "Intracellular delivery of phosphoinositides and inositol phosphates using polyamine carriers." Proceedings of the National Academy of Sciences **97**(21): 11286-11291.
- Padilla-Parra, S. and M. Tramier (2012). "FRET microscopy in the living cell: Different approaches, strengths and weaknesses." BioEssays **34**(5): 369-376.
- Palmieri, M., C. J. Nowell, et al. (2010). "Analysis of cellular phosphatidylinositol (3,4,5)-trisphosphate levels and distribution using confocal fluorescent microscopy." Analytical Biochemistry **406**(1): 41-50.
- Panagabko, C., S. Morley, et al. (2003). "Ligand Specificity in the CRAL-TRIO Protein Family." Biochemistry **42**(21): 6467-6474.
- Panaretou, C., J. Domin, et al. (1997). "Characterization of p150, an Adaptor Protein for the human phosphatidylinositol (PtdIns) 3-kinase: substrate presentation by phosphatidylinositol transfer protein to the p150;PtdIns 3-kinase complex." Journal of Biological Chemistry **272**(4): 2477-2485.
- Papakonstanti, E. A., A. J. Ridley, et al. (2007). "The p110 δ isoform of PI 3-kinase negatively controls RhoA and PTEN." The EMBO journal **26**(13): 3050-3061.
- Pathak, G. P., J. D. Vrana, et al. (2013). "Optogenetic control of cell function using engineered photoreceptors." Biology of the Cell **105**(2): 59-72.
- Patki, V., D. C. Lawe, et al. (1998). "A functional PtdIns(3)P-binding motif." Nature **394**(6692): 433-434.
- Patki, V., J. Virbasius, et al. (1997). "Identification of an early endosomal protein regulated by phosphatidylinositol 3-kinase." Proceedings of the National Academy of Sciences **94**(14): 7326-7330.
- Paulus, H. and E. P. Kennedy (1960). "The enzymatic synthesis of inositol monophosphate." The Journal of biological chemistry **235**: 1303-1311.
- Pearson, M. A., D. Reczek, et al. (2000). "Structure of the ERM protein moesin reveals the FERM domain fold masked by an extended actin binding tail domain." Cell **101**(3): 259-270.

- Penzes, P., R. C. Johnson, et al. (2001). "The Neuronal Rho-GEF Kalirin-7 Interacts with PDZ Domain Containing Proteins and Regulates Dendritic Morphogenesis." *29*(1): 229-242.
- Penzes, P. and K. A. Jones (2008). "Dendritic spine dynamics - a key role for kalirin-7." *Trends in Neurosciences* **31**(8): 419-427.
- Peter, B. J., H. M. Kent, et al. (2004). "BAR domains as sensors of membrane curvature: the amphiphysin BAR structure." *Science* **303**(5657): 495-499.
- Pettersen, E. F., T. D. Goddard, et al. (2004). "UCSF Chimera--a visualization system for exploratory research and analysis." *Journal of computational chemistry* **25**(13): 1605-1612.
- Pfaller, M. A. and D. J. Diekema (2007). "Epidemiology of invasive candidiasis: a persistent public health problem." *Clin Microbiol Rev* **20**(1): 133-163.
- Phillips, S. E., K. E. Ile, et al. (2006). "Specific and nonspecific membrane-binding determinants cooperate in targeting phosphatidylinositol transfer protein β -Isoform to the mammalian trans-Golgi network." *Mol. Biol. Cell* **17**(6): 2498-2512.
- Phillips, S. E., B. Sha, et al. (1999). "Yeast Sec14p deficient in phosphatidylinositol transfer activity is functional in vivo." *Molecular cell* **4**(2): 187-197.
- Phillips, S. E., P. Vincent, et al. (2006). "The diverse biological functions of phosphatidylinositol transfer proteins in eukaryotes." *Critical Reviews in Biochemistry and Molecular Biology* **41**(1): 21-49.
- Pilarski, R., R. Burt, et al. (2013). "Cowden syndrome and the PTEN hamartoma tumor syndrome: systematic review and revised diagnostic criteria." *Journal of the National Cancer Institute* **105**(21): 1607-1616.
- Ponting, C. P. (1996). "Novel domains in NADPH oxidase subunits, sorting nexins, and PtdIns 3-kinases: binding partners of SH3 domains?" *Protein science : a publication of the Protein Society* **5**(11): 2353-2357.
- Portales-Casamar, E., A. Briançon-Marjollet, et al. (2006). "Identification of novel neuronal isoforms of the Rho-GEF Trio." *Biol. Cell* **98**(3): 183-193.
- Posner, B. I., R. Faure, et al. (1994). "Peroxo vanadium compounds. A new class of potent phosphotyrosine phosphatase inhibitors which are insulin mimetics." *Journal of Biological Chemistry* **269**(6): 4596-4604.
- Potts, B. C. M., D. J. Faulkner, et al. (1992). "Phospholipase A2 inhibitors from marine organisms." *Journal of Natural Products* **55**(12): 1701-1717.

- Powis, G., M. J. Seewald, et al. (1992). "Selective inhibition of phosphatidylinositol phospholipase C by cytotoxic ether lipid analogues." Cancer Research **52**(10): 2835-2840.
- Prasad, N. K. and S. J. Decker (2005). "SH2-containing 5'-inositol phosphatase, SHIP2, regulates cytoskeleton organization and ligand-dependent down-regulation of the epidermal growth factor receptor." Journal of Biological Chemistry **280**(13): 13129-13136.
- Premkumar, L., A. A. Bobkov, et al. (2010). "Structural basis of membrane targeting by the Dock180 family of Rho family guanine exchange factors (Rho-GEFs)." The Journal of biological chemistry **285**(17): 13211-13222.
- Pulcinelli, F. M., P. Gresele, et al. (1998). "Evidence for separate effects of U73122 on phospholipase C and calcium channels in human platelets." Biochemical Pharmacology **56**(11): 1481-1484.
- Qian, J., J. Atkinson, et al. (2006). "Biochemical consequences of heritable mutations in the α -tocopherol transfer protein." Biochemistry **45**(27): 8236-8242.
- Qian, J., S. Morley, et al. (2005). "Intracellular trafficking of vitamin E in hepatocytes: the role of tocopherol transfer protein." J. Lipid Res. **46**(10): 2072-2082.
- Qin, W., J. Hu, et al. (2003). "BNIPL-2, a novel homologue of BNIP-2, interacts with Bcl-2 and Cdc42GAP in apoptosis." Biochemical and Biophysical Research Communications **308**(2): 379-385.
- Quadri, M., M. Fang, et al. (2013). "Mutation in the SYNJ1 gene associated with autosomal recessive, early-onset parkinsonism." Human Mutation **34**(9): 1208-1215.
- Quinn, K. V., P. Behe, et al. (2008). "Monitoring changes in membrane phosphatidylinositol 4,5-bisphosphate in living cells using a domain from the transcription factor tubby." The Journal of physiology **586**(Pt 12): 2855-2871.
- Rabiner, C. A., R. E. Mains, et al. (2005). "Kalirin: A dual Rho guanine nucleotide exchange factor that is so much more than the sum of its many parts." Neuroscientist **11**(2): 148-160.
- Raike, R. S., H. A. Jinnah, et al. (2005). "Animal models of generalized dystonia." NeuroRx **2**(3): 504-512.
- Rameh, L. E. and L. C. Cantley (1999). "The role of phosphoinositide 3-kinase lipid products in cell function." Journal of Biological Chemistry **274**(13): 8347-8350.

- Ramjaun, A. R. and P. S. McPherson (1996). "Tissue-specific alternative splicing generates two synaptojanin isoforms with differential membrane binding properties." Journal of Biological Chemistry **271**(40): 24856-24861.
- Razzaq, A., I. M. Robinson, et al. (2001). "Amphiphysin is necessary for organization of the excitation-contraction coupling machinery of muscles, but not for synaptic vesicle endocytosis in *Drosophila*." Genes & Development **15**(22): 2967-2979.
- Reagan-Shaw, S. and N. Ahmad (2006). "RNA interference-mediated depletion of phosphoinositide 3-kinase activates forkhead box class O transcription factors and induces cell cycle arrest and apoptosis in breast carcinoma cells." Cancer Research **66**(2): 1062-1069.
- Rebecchi, M. J. and S. N. Pentylala (2000). "Structure, function, and control of phosphoinositide-specific phospholipase C." Physiological Reviews **80**(4): 1291-1335.
- Ren, J., G. Schaaf, et al. (2011). "Crystallization and preliminary X-ray diffraction analysis of Sfh3, a member of the Sec14 protein superfamily." Acta Crystallogr Sect F Struct Biol Cryst Commun **67**(Pt 10): 1239-1243.
- Rentsch, D., M. Laloi, et al. (1995). "NTR1 encodes a high affinity oligopeptide transporter in *Arabidopsis*." FEBS Letters **370**(3): 264-268.
- Rhee, S. G. and K. D. Choi (1992). "Regulation of inositol phospholipid-specific phospholipase C isozymes." The Journal of biological chemistry **267**(18): 12393-12396.
- Ribeiro, F. M., L. T. Ferreira, et al. (2007). "SEC14-like protein 1 interacts with cholinergic transporters." Neurochemistry International **50**(2): 356-364.
- Rivas, M. P., B. G. Kearns, et al. (1999). "Pleiotropic alterations in lipid metabolism in yeast *sac1* mutants: relationship to "bypass Sec14p" and inositol auxotrophy." Mol Biol Cell **10**(7): 2235-2250.
- Robinson, J. S., D. J. Klionsky, et al. (1988). "Protein sorting in *Saccharomyces cerevisiae*: isolation of mutants defective in the delivery and processing of multiple vacuolar hydrolases." Molecular and cellular biology **8**(11): 4936-4948.
- Roscoe, D. H., H. Robinson, et al. (1973). "DNA synthesis and mitosis in a temperature sensitive Chinese hamster cell line." Journal of Cellular Physiology **82**(3): 333-338.
- Rose, K., S. A. Rudge, et al. (1995). "Phospholipase D signaling is essential for meiosis." Proceedings of the National Academy of Sciences **92**(26): 12151-12155.

- Rosivatz, E., J. G. Matthews, et al. (2006). "A small-molecule inhibitor for phosphatase and tensin homologue deleted on chromosome 10 (PTEN)." ACS Chemical Biology **1**(12): 780-790.
- Rossman, K. L., C. J. Der, et al. (2005). "GEF means go: turning on RHO GTPases with guanine nucleotide-exchange factors." Nat Rev Mol Cell Biol **6**(2): 167-180.
- Routt, S. M., M. M. Ryan, et al. (2005). "Nonclassical PITPs activate PLD via the Stt4p PtdIns-4-kinase and modulate function of late stages of exocytosis in vegetative yeast." Traffic **6**(12): 1157-1172.
- Rowe, T., C. Hale, et al. (2006). "A high-throughput microfluidic assay for SH2 domain-containing inositol 5-phosphatase 2." Assay and drug development technologies **4**(2): 175-183.
- Roy, A. and T. P. Levine (2004). "Multiple pools of phosphatidylinositol 4-phosphate detected using the pleckstrin homology domain of Osh2p." The Journal of biological chemistry **279**(43): 44683-44689.
- Ryan, M. M., B. R. Temple, et al. (2007). "Conformational dynamics of the major yeast phosphatidylinositol transfer protein sec14p: insight into the mechanisms of phospholipid exchange and diseases of sec14p-like protein deficiencies." Molecular biology of the cell **18**(5): 1928-1942.
- Ryu, S. H., P. G. Suh, et al. (1987). "Bovine brain cytosol contains three immunologically distinct forms of inositolphospholipid-specific phospholipase C." Proceedings of the National Academy of Sciences **84**(19): 6649-6653.
- Saari, J. C., D. L. Bredberg, et al. (1994). "Control of substrate flow at a branch in the visual cycle." Biochemistry **33**(10): 3106-3112.
- Saari, J. C. and J. W. Crabb (2005). "Focus on molecules: cellular retinaldehyde-binding protein (CRALBP)." Experimental Eye Research **81**(3): 245-246.
- Saari, J. C., M. Nawrot, et al. (2001). "Visual cycle impairment in cellular retinaldehyde binding protein (CRALBP) knockout mice results in delayed dark adaptation." **29**(3): 739-748.
- Saari, J. C., M. Nawrot, et al. (2009). "Release of 11-cis-retinal from cellular retinaldehyde-binding protein by acidic lipids." Mol Vis **15**: 844-854.
- Saito, K., L. Tautz, et al. (2007). "The lipid-binding SEC14 domain." Biochim Biophys Acta **1771**(6): 719-726.

- Saito, K., S. Williams, et al. (2007). "Association of Protein-tyrosine Phosphatase MEG2 via Its Sec14p Homology Domain with Vesicle-trafficking Proteins." Journal of Biological Chemistry **282**(20): 15170-15178.
- Sakemi, S., H. Hirai, et al. (2002). "Thielavins as glucose-6-phosphatase (G6Pase) inhibitors: producing strain, fermentation, isolation, structural elucidation and biological activities." The Journal of antibiotics **55**(11): 941-951.
- Salama, S. R., A. E. Cleves, et al. (1990). "Cloning and characterization of *Kluyveromyces lactis* SEC14, a gene whose product stimulates Golgi secretory function in *Saccharomyces cerevisiae*." J Bacteriol **172**(8): 4510-4521.
- Salazar, G., B. Craige, et al. (2005). "Phosphatidylinositol-4-Kinase Type II α Is a component of adaptor protein-3-derived vesicles." Molecular biology of the cell **16**(8): 3692-3704.
- Šali, A. and T. L. Blundell (1993). "Comparative protein modelling by satisfaction of spatial restraints." Journal of Molecular Biology **234**(3): 779-815.
- Sall, A., H. M. Zhang, et al. (2010). "Pro-apoptotic activity of mBNIP-21 depends on its BNIP-2 and Cdc42GAP homology (BCH) domain and is enhanced by coxsackievirus B3 infection." Cellular Microbiology **12**(5): 599-614.
- Saneyoshi, T., D. A. Fortin, et al. (2010). "Regulation of spine and synapse formation by activity-dependent intracellular signaling pathways." Current Opinion in Neurobiology **20**(1): 108-115.
- Santagata, S., T. J. Boggon, et al. (2001). "G-Protein signaling through tubby proteins." Science **292**(5524): 2041-2050.
- Santiago-Tirado, F. H. and A. Bretscher (2011). "Membrane-trafficking sorting hubs: cooperation between PI(4)P and small GTPases at the *trans*-Golgi network." Trends in cell biology **21**(9): 515-525.
- Sasaki, T., A. Suzuki, et al. (2002). "Phosphoinositide 3-kinases in inunimity: lessons from knockout mice." Journal of Biochemistry **131**(4): 495-501.
- Sato, M. (2006). "Imaging molecular events in single living cells." Analytical and Bioanalytical Chemistry **386**(3): 435-443.
- Sato, M., Y. Ueda, et al. (2003). "Production of PtdInsP₃ at endomembranes is triggered by receptor endocytosis." Nature cell biology **5**(11): 1016-1022.
- Schaaf, G., M. Dynowski, et al. (2011). "Resurrection of a functional phosphatidylinositol transfer protein from a pseudo-Sec14 scaffold by directed evolution." Molecular biology of the cell **22**(6): 892-905.

- Schaaf, G., E. A. Ortlund, et al. (2008). "Functional anatomy of phospholipid binding and regulation of phosphoinositide homeostasis by proteins of the sec14 superfamily." Molecular cell **29**(2): 191-206.
- Schaefer, T., C. Wiedemann, et al. (1994). "Effects of arsenicals on the secretory process in chromaffin cells." Annals of the New York Academy of Sciences **710**: 356-367.
- Schiller, M. R., F. Ferraro, et al. (2008). "Autonomous functions for the Sec14p/spectrin-repeat region of Kalirin." Experimental Cell Research **314**(14): 2674-2691.
- Schloesser, R. J., J. Huang, et al. (2008). "Cellular plasticity cascades in the pathophysiology and treatment of bipolar disorder." Neuropsychopharmacology : official publication of the American College of Neuropsychopharmacology **33**(1): 110-133.
- Schmid, A. C., R. D. Byrne, et al. (2004). "Bispermoxovanadium compounds are potent PTEN inhibitors." FEBS letters **566**(1-3): 35-38.
- Schneider, C. A., W. S. Rasband, et al. (2012). "NIH Image to ImageJ: 25 years of image analysis." Nat Methods **9**(7): 671-675.
- Schouten, A., B. Agianian, et al. (2002). "Structure of apo-phosphatidylinositol transfer protein [alpha] provides insight into membrane association." EMBO J **21**(9): 2117-2121.
- Schu, P., K. Takegawa, et al. (1993). "Phosphatidylinositol 3-kinase encoded by yeast VPS34 gene essential for protein sorting." Science **260**(5104): 88-91.
- Schultz, C. (2003). "Prodrugs of biologically active phosphate esters." Bioorganic & medicinal chemistry **11**(6): 885-898.
- Schwab, C. and P. L. McGeer (2008). "Inflammatory aspects of alzheimer disease and other neurodegenerative disorders." Journal of Alzheimer's Disease **13**(4): 359-369.
- Seet, L. F. and W. Hong (2006). "The Phox (PX) domain proteins and membrane traffic." Biochimica et biophysica acta **1761**(8): 878-896.
- Serafini, T., S. A. Colamarino, et al. (1996). "Netrin-1 Is required for commissural axon guidance in the developing vertebrate nervous system." Cell **87**(6): 1001-1014.
- Sha, B., S. E. Phillips, et al. (1998). "Crystal structure of the Saccharomyces cerevisiae phosphatidylinositol- transfer protein." Nature **391**(6666): 506-510.

- Shang, X., Y. T. Zhou, et al. (2003). "Concerted regulation of cell dynamics by BNIP-2 and Cdc42GAP homology/Sec14p-like, proline-rich, and GTPase-activating protein domains of a novel Rho GTPase-activating protein, BPGAP1." Journal of Biological Chemistry **278**(46): 45903-45914.
- Shen, W. H., A. S. Balajee, et al. (2007). "Essential role for nuclear PTEN in maintaining chromosomal integrity." Cell **128**(1): 157-170.
- Sherman, F., Fink, G.R., Hink, J.B. (1983). Methods in Yeast Genetics: A Laboratory Manual, Cold Spring Harbor.
- Sherman, W. R., B. G. Gish, et al. (1986). "Effects of lithium on phosphoinositide metabolism in vivo." Federation proceedings **45**(11): 2639-2646.
- Shibata, N., K.-i. Jishage, et al. (2006). "Regulation of hepatic cholesterol synthesis by a novel protein (SPF) that accelerates cholesterol biosynthesis." FASEB J. **20**(14): 2642-2644.
- Shin, H.-W., M. Hayashi, et al. (2005). "An enzymatic cascade of Rab5 effectors regulates phosphoinositide turnover in the endocytic pathway." The Journal of cell biology **170**(4): 607-618.
- Shtein, L., L. Toker, et al. (2013). "The inositol monophosphatase inhibitor L-690,330 affects pilocarpine-behavior and the forced swim test." Psychopharmacology **227**(3): 503-508.
- Sibilia, M. and E. F. Wagner (1995). "Strain-dependent epithelial defects in mice lacking the EGF receptor." Science **269**(5221): 234-238.
- Sikorski, R. S. and P. Hieter (1989). "A system of shuttle vectors and yeast host strains designed for efficient manipulation of DNA in *Saccharomyces cerevisiae*." Genetics **122**(1): 19-27.
- Simonsen, A. and S. A. Tooze (2009). "Coordination of membrane events during autophagy by multiple class III PI3-kinase complexes." The Journal of cell biology **186**(6): 773-782.
- Singh, N., A. C. Halliday, et al. (2013). "A safe lithium mimetic for bipolar disorder." Nature communications **4**: 1332.
- Sinha, S. and B. S. Sharma (2009). "Neurocysticercosis: A review of current status and management." Journal of Clinical Neuroscience **16**(7): 867-876.
- Sirokmány, G., L. Szidonya, et al. (2006). "Sec14 homology domain targets p50RhoGAP to endosomes and provides a link between Rab and Rho GTPases." Journal of Biological Chemistry **281**(9): 6096-6105.

- Skinner, H. B., J. G. Alb, Jr., et al. (1993). "Phospholipid transfer activity is relevant to but not sufficient for the essential function of the yeast SEC14 gene product." EMBO J **12**(12): 4775-4784.
- Skinner, K. (1993). "The hazards of chemical dependency among nurses." J Pract Nurs **43**(4): 8-11.
- Slagsvold, T., R. Aasland, et al. (2005). "Eap45 in mammalian ESCRT-II binds ubiquitin via a phosphoinositide-interacting GLUE domain." Journal of Biological Chemistry **280**(20): 19600-19606.
- Slater, S. J., J. L. Seiz, et al. (2003). "Inhibition of protein kinase C by resveratrol." Biochimica et biophysica acta **1637**(1): 59-69.
- Slessareva, J. E., S. M. Routt, et al. (2006). "Activation of the phosphatidylinositol 3-kinase Vps34 by a G protein α subunit at the endosome." Cell **126**(1): 191-203.
- Smirnova, T. I., T. G. Chadwick, et al. (2007). "Local polarity and hydrogen bonding inside the Sec14p phospholipid-binding cavity: high-field multi-frequency electron paramagnetic resonance studies." Biophysical Journal **92**(10): 3686-3695.
- Smith, R. J., L. M. Sam, et al. (1990). "Receptor-coupled signal transduction in human polymorphonuclear neutrophils: effects of a novel inhibitor of phospholipase C-dependent processes on cell responsiveness." Journal of Pharmacology and Experimental Therapeutics **253**(2): 688-697.
- Smith, W. J., N. Nassar, et al. (2003). "Structure of the active N-terminal domain of ezrin: conformational and mobility changes identify keystone interactions." Journal of Biological Chemistry **278**(7): 4949-4956.
- Sobel, J. D. (2008). Diagnosis and treatment of human Mycoses. Totowa, N.J., Humana Press.
- Soh, U. J. K. and B. C. Low (2008). "BNIP2 extra long inhibits RhoA and cellular transformation by Lbc RhoGEF via its BCH domain." J Cell Sci **121**(10): 1739-1749.
- Song, J. Y., J. K. Lee, et al. (2008). "Microarray analysis of normal cervix, carcinoma *in situ*, and invasive cervical cancer: identification of candidate genes in pathogenesis of invasion in cervical cancer." International Journal of Gynecological Cancer **18**(5): 1051-1059.
- Song, X., W. Xu, et al. (2001). "Phox homology domains specifically bind phosphatidylinositol phosphates†." Biochemistry **40**(30): 8940-8944.

- Sorensen, S. D., D. A. Linseman, et al. (1998). "A role for a Wortmannin-sensitive phosphatidylinositol-4-Kinase in the endocytosis of muscarinic cholinergic receptors." Molecular Pharmacology **53**(5): 827-836.
- Sparvero, L. J., A. A. Amoscato, et al. (2012). "Mapping of phospholipids by MALDI imaging (MALDI-MSI): realities and expectations." Chemistry and Physics of Lipids **165**(5): 545-562.
- Sreenivas, A., J. L. Patton-Vogt, et al. (1998). "A Role for phospholipase D (Pld1p) in growth, secretion, and regulation of membrane lipid synthesis in Yeast." Journal of Biological Chemistry **273**(27): 16635-16638.
- Srivastava, R., A. Ratheesh, et al. (2005). "Resveratrol inhibits type II phosphatidylinositol 4-kinase: A key component in pathways of phosphoinositide turn over." Biochemical Pharmacology **70**(7): 1048-1055.
- Stack, J. H., D. B. DeWald, et al. (1995). "Vesicle-mediated protein transport: regulatory interactions between the Vps15 protein kinase and the Vps34 PtdIns 3-kinase essential for protein sorting to the vacuole in yeast." The Journal of cell biology **129**(2): 321-334.
- Stack, J. H. and S. D. Emr (1994). "Vps34p required for yeast vacuolar protein sorting is a multiple specificity kinase that exhibits both protein kinase and phosphatidylinositol-specific PI 3-kinase activities." Journal of Biological Chemistry **269**(50): 31552-31562.
- Stack, J. H., P. K. Herman, et al. (1993). "A membrane-associated complex containing the Vps15 protein kinase and the Vps34 PI 3-kinase is essential for protein sorting to the yeast lysosome-like vacuole." The EMBO journal **12**(5): 2195-2204.
- Stahelin, R. V., J. L. Scott, et al. "Cellular and molecular interactions of phosphoinositides and peripheral proteins." Chemistry and Physics of Lipids(0).
- Stecher, H., M. H. Gelb, et al. (1999). "Preferential Release of 11-cis-retinol from Retinal Pigment Epithelial Cells in the Presence of Cellular Retinaldehyde-binding Protein." Journal of Biological Chemistry **274**(13): 8577-8585.
- Steck, P. A., M. A. Pershouse, et al. (1997). "Identification of a candidate tumour suppressor gene, MMAC1, at chromosome 10q23.3 that is mutated in multiple advanced cancers." Nature genetics **15**(4): 356-362.
- Stefan, C. J., A. Audhya, et al. (2002). "The Yeast Synaptojanin-like Proteins Control the Cellular Distribution of Phosphatidylinositol (4,5)-Bisphosphate." Molecular Biology of the Cell **13**(2): 542-557.

- Stenmark, H., R. Aasland, et al. (1996). "Endosomal Localization of the Autoantigen EEA1 Is Mediated by a Zinc-binding FYVE Finger." Journal of Biological Chemistry **271**(39): 24048-24054.
- Stenton, G. R., L. F. Mackenzie, et al. (2013). "Characterization of AQX-1125, a small-molecule SHIP1 activator: Part 2. Efficacy studies in allergic and pulmonary inflammation models in vivo." British Journal of Pharmacology **168**(6): 1519-1529.
- Stephens, L., K. Anderson, et al. (1998). "Protein kinase B kinases that mediate phosphatidylinositol 3,4,5-trisphosphate-dependent activation of protein kinase B." Science **279**(5351): 710-714.
- Stevens, T., B. Esmon, et al. (1982). "Early stages in the yeast secretory pathway are required for transport of carboxypeptidase Y to the vacuole." Cell **30**(2): 439-448.
- Stokoe, D., L. R. Stephens, et al. (1997). "Dual role of phosphatidylinositol-3,4,5-trisphosphate in the activation of protein kinase B." Science **277**(5325): 567-570.
- Stolt, P. C., H. Jeon, et al. (2003). "Origins of peptide selectivity and phosphoinositide binding revealed by structures of disabled-1 PTB domain complexes." Structure **11**(5): 569-579.
- Stolz, L. E., W. J. Kuo, et al. (1998). "INP51, a yeast inositol polyphosphate 5-phosphatase required for phosphatidylinositol 4,5-bisphosphate homeostasis and whose absence confers a cold-resistant phenotype." The Journal of biological chemistry **273**(19): 11852-11861.
- Stoyanova, S., G. Bulgarelli-Leva, et al. (1997). "Lipid kinase and protein kinase activities of G-protein-coupled phosphoinositide 3-kinase gamma: structure-activity analysis and interactions with wortmannin." Biochem. J. **324**(2): 489-495.
- Strahl, T., H. Hama, et al. (2005). "Yeast phosphatidylinositol 4-kinase, Pik1, has essential roles at the Golgi and in the nucleus." The Journal of cell biology **171**(6): 967-979.
- Strahl, T. and J. Thorner (2007). "Synthesis and function of membrane phosphoinositides in budding yeast, *Saccharomyces cerevisiae*." Biochimica et Biophysica Acta (BBA) - Molecular and Cell Biology of Lipids **1771**(3): 353-404.
- Strømhaug, P. E., F. Reggiori, et al. (2004). "Atg21 Is a Phosphoinositide Binding Protein Required for Efficient Lipidation and Localization of Atg8 during Uptake of Aminopeptidase I by Selective Autophagy." Molecular biology of the cell **15**(8): 3553-3566.

- Stryer, L. and R. P. Haugland (1967). "Energy transfer: a spectroscopic ruler." Proceedings of the National Academy of Sciences **58**(2): 719-726.
- Stubdal, H., C. A. Lynch, et al. (2000). "Targeted deletion of the tub mouse obesity gene reveals that tubby is a loss-of-function mutation." Molecular and cellular biology **20**(3): 878-882.
- Subramanian, D., V. Laketa, et al. (2010). "Activation of membrane-permeant caged PtdIns(3)P induces endosomal fusion in cells." Nature chemical biology **6**(5): 324-326.
- Suh, B. C., T. Inoue, et al. (2006). "Rapid chemically induced changes of PtdIns(4,5)P₂ gate KCNQ ion channels." Science **314**(5804): 1454-1457.
- Sun, Y.-J., K. Nishikawa, et al. (2006). "Solo/Trio8, a membrane-associated short isoform of Trio, modulates endosome dynamics and neurite elongation." Mol. Cell. Biol. **26**(18): 6923-6935.
- Suwa, A., T. Kurama, et al. (2010). "Glucose metabolism activation by SHIP2 inhibitors via up-regulation of GLUT1 gene in L6 myotubes." European journal of pharmacology **642**(1-3): 177-182.
- Suwa, A., T. Yamamoto, et al. (2009). "Discovery and functional characterization of a novel small molecule inhibitor of the intracellular phosphatase, SHIP2." British Journal of Pharmacology **158**(3): 879-887.
- Swigart, P., R. Insall, et al. (2000). "Purification and cloning of phosphatidylinositol transfer proteins from Dictyostelium discoideum: homologues of both mammalian PITPs and Saccharomyces cerevisiae sec14p are found in the same cell." Biochem. J. **347**(3): 837-843.
- Sykes, P. (1986). A guidebook to mechanism in organic chemistry, Pearson.
- Szentpetery, Z., A. Balla, et al. (2009). "Live cell imaging with protein domains capable of recognizing phosphatidylinositol 4,5-bisphosphate; a comparative study." BMC cell biology **10**: 67.
- Tabuchi, M., A. Audhya, et al. (2006). "The Phosphatidylinositol 4,5-bisphosphate and TORC2 binding proteins Slm1 and Slm2 function in sphingolipid regulation." Molecular and cellular biology **26**(15): 5861-5875.
- Tanaka, S. and K. Hosaka (1994). "Cloning of a cDNA Encoding a Second Phosphatidylinositol Transfer Protein of Rat brain by complementation of the yeast sec14 mutation." J Biochem **115**(5): 981-984.

- Taylor, C. W., A. A. Genazzani, et al. (1999). "Expression of inositol trisphosphate receptors." Cell calcium **26**(6): 237-251.
- Tcherkezian, J. and N. Lamarche-vane (2007). "Current knowledge of the large RhoGAP family of proteins." Biology of the Cell **099**(2): 67-86.
- Teo, H., D. J. Gill, et al. (2006). "ESCRT-I core and ESCRT-II GLUE domain structures reveal role for GLUE in linking to ESCRT-I and membranes." Cell **125**(1): 99-111.
- Terasawa, Y., Z. Ladha, et al. (2000). "Increased atherosclerosis in hyperlipidemic mice deficient in α -tocopherol transfer protein and vitamin E." Proceedings of the National Academy of Sciences of the United States of America **97**(25): 13830-13834.
- Thomas, G. M. H., E. Cunningham, et al. (1993). "An essential role for phosphatidylinositol transfer protein in phospholipase C-Mediated inositol lipid signaling." Cell **74**(5): 919-928.
- Thompson, D. A. and A. Gal (2003). "Vitamin A metabolism in the retinal pigment epithelium: genes, mutations, and diseases." Progress in Retinal and Eye Research **22**(5): 683-703.
- Tibarewal, P., G. Zilidis, et al. (2012). "PTEN protein phosphatase activity correlates with control of gene expression and invasion, a tumor-suppressing phenotype, but not with AKT activity." Sci. Signal. **5**(213): ra18-.
- Tibbetts, M. D., E. N. Shiozaki, et al. (2004). "Crystal structure of a FYVE-Type zinc finger domain from the caspase regulator CARP2." Structure **12**(12): 2257-2263.
- Tilley, S. J., A. Skippen, et al. (2004). "Structure-function analysis of phosphatidylinositol transfer protein alpha bound to human phosphatidylinositol." Structure **12**(2): 317-326.
- Titorenko, V. I., D. M. Ogrydziak, et al. (1997). "Four distinct secretory pathways serve protein secretion, cell surface growth, and peroxisome biogenesis in the yeast *Yarrowia lipolytica*." Mol Cell Biol **17**(9): 5210-5226.
- Togashi, K., H. R. Ko, et al. (2001). "Inhibition of telomerase activity by fungus metabolites, CRM646-A and thielavin B." Bioscience, biotechnology, and biochemistry **65**(3): 651-653.
- Touchberry, C. D., I. K. Bales, et al. (2010). "Phosphatidylinositol 3,5-bisphosphate (PI(3,5)P₂) potentiates cardiac contractility via activation of the ryanodine receptor." The Journal of biological chemistry **285**(51): 40312-40321.

- Traber, M. G. (2007). "Vitamin E regulatory mechanisms." Annual Review of Nutrition **27**(1): 347-362.
- Trapp, B. D. and K.-A. Nave (2008). "Multiple sclerosis: an immune or neurodegenerative disorder?" Annual Review of Neuroscience **31**(1): 247-269.
- Travis, G. H., M. Golczak, et al. (2007). "Diseases caused by defects in the visual cycle: retinoids as potential therapeutic agents." Annual Review of Pharmacology and Toxicology **47**(1): 469-512.
- Treadwell, J. A., K. B. Pagniello, et al. (2004). "Genetic segregation of brain gene expression identifies retinaldehyde binding protein 1 and syntaxin 12 as potential contributors to ethanol preference in mice." Behavior Genetics **34**(4): 425-439.
- Tsui, M. M. and J. D. York (2010). "Roles of inositol phosphates and inositol pyrophosphates in development, cell signaling and nuclear processes." Advances in enzyme regulation **50**(1): 324-337.
- Tyers, M., R. J. Haslam, et al. (1989). "Molecular analysis of pleckstrin: the major protein kinase C substrate of platelets." Journal of cellular biochemistry **40**(2): 133-145.
- Ueda, S., T. Kataoka, et al. (2004). "Role of the Sec14-like domain of Dbl family exchange factors in the regulation of Rho family GTPases in different subcellular sites." Cellular Signalling **16**(8): 899-906.
- Ueda, Y. and Y. Hayashi (2013). "PIP(3) regulates spinule formation in dendritic spines during structural long-term potentiation." The Journal of neuroscience : the official journal of the Society for Neuroscience **33**(27): 11040-11047.
- Ueda, Y., S. Kwok, et al. (2013). "Application of FRET probes in the analysis of neuronal plasticity." Frontiers in Neural Circuits **7**.
- Upadhyaya, M., J. Maynard, et al. (1995). "Characterisation of germline mutations in the neurofibromatosis type 1 (NF1) gene." J Med Genet **32**(9): 706-710.
- Utsunomiya, A., Y. Owada, et al. (1997). "Localization of gene expression for phosphatidylinositol transfer protein in the brain of developing and mature rats." Molecular Brain Research **45**(2): 349-352.
- Vaillancourt, F. H., M. Brault, et al. (2012). "Evaluation of phosphatidylinositol-4-kinase III α as a hepatitis C virus drug target." Journal of virology **86**(21): 11595-11607.
- Valencia, C. A., S. W. Cotten, et al. (2007). "Cleavage of BNIP-2 and BNIP-XL by caspases." Biochemical and Biophysical Research Communications **364**(3): 495-501.

- van der Schaar, H. M., P. Leyssen, et al. (2013). "A Novel, Broad-Spectrum Inhibitor of Enterovirus Replication That Targets Host Cell Factor Phosphatidylinositol 4-Kinase III β ." *Antimicrobial Agents and Chemotherapy* **57**(10): 4971-4981.
- van Dongen, C. J., H. Zwiers, et al. (1985). "Microdetermination of phosphoinositides in a single extract." *Analytical Biochemistry* **144**(1): 104-109.
- van Meer, G. (2005). "Cellular lipidomics." *The EMBO journal* **24**(18): 3159-3165.
- van Rheenen, J., E. Mulugeta Achame, et al. (2005). "PIP₂ signaling in lipid domains: a critical re-evaluation." *The EMBO journal* **24**(9): 1664-1673.
- van Weering, J. R. T., P. Verkade, et al. (2012). "SNX-BAR-mediated endosome tubulation is co-ordinated with endosome maturation." *Traffic* **13**(1): 94-107.
- Vandeput, F., L. Combettes, et al. (2007). "Biphenyl 2,3',4,5',6-pentakisphosphate, a novel inositol polyphosphate surrogate, modulates Ca²⁺ responses in rat hepatocytes." *The FASEB Journal* **21**(7): 1481-1491.
- Vanhaesebroeck, B., L. Stephens, et al. (2012). "PI3K signalling: the path to discovery and understanding." *Nature reviews. Molecular cell biology* **13**(3): 195-203.
- Vanni, C., P. Mancini, et al. (2002). "Regulation of Proto-Dbl by Intracellular Membrane Targeting and Protein Stability." *Journal of Biological Chemistry* **277**(22): 19745-19753.
- Varnai, P., B. Thyagarajan, et al. (2006). "Rapidly inducible changes in phosphatidylinositol 4,5-bisphosphate levels influence multiple regulatory functions of the lipid in intact living cells." *The Journal of cell biology* **175**(3): 377-382.
- Vergne, I. and V. Deretic (2010). "The role of PI3P phosphatases in the regulation of autophagy." *FEBS letters* **584**(7): 1313-1318.
- Vida, T. A. and S. D. Emr (1995). "A new vital stain for visualizing vacuolar membrane dynamics and endocytosis in yeast." *The Journal of Cell Biology* **128**(5): 779-792.
- Viernes, D. R., L. B. Choi, et al. (2013). "Discovery and development of small molecule SHIP phosphatase modulators." *Medicinal Research Reviews*.
- Vincent, P., M. Chua, et al. (2005). "A Sec14p-nodulin domain phosphatidylinositol transfer protein polarizes membrane growth of *Arabidopsis thaliana* root hairs." *The Journal of cell biology* **168**(5): 801-812.
- Vines, C. M. (2012). "Phospholipase C." *Advances in experimental medicine and biology* **740**: 235-254.

- Vlahos, C. J., W. F. Matter, et al. (1994). "A specific inhibitor of phosphatidylinositol 3-kinase, 2-(4-morpholinyl)-8-phenyl-4H-1-benzopyran-4-one (LY294002)." Journal of Biological Chemistry **269**(7): 5241-5248.
- Volinia, S., R. Dhand, et al. (1995). "A human phosphatidylinositol 3-kinase complex related to the yeast Vps34p-Vps15p protein sorting system." The EMBO journal **14**(14): 3339-3348.
- Wakelam, M. J. and J. Clark (2011). "Methods for analyzing phosphoinositides using mass spectrometry." Biochimica et biophysica acta **1811**(11): 758-762.
- Wakelam, M. J. O., T. R. Pettitt, et al. (2007). Lipidomic analysis of signaling pathways. Methods in enzymology. H. A. Brown, Academic Press. **432**: 233-246.
- Walch-Solimena, C. and P. Novick (1999). "The yeast phosphatidylinositol-4-OH kinase pik1 regulates secretion at the Golgi." Nature cell biology **1**(8): 523-525.
- Walker, E. H., M. E. Pacold, et al. (2000). "Structural determinants of phosphoinositide 3-Kinase inhibition by wortmannin, LY294002, quercetin, myricetin, and staurosporine." Molecular cell **6**(4): 909-919.
- Wang, J., H.-Q. Sun, et al. (2007). "PI4P Promotes the Recruitment of the GGA Adaptor Proteins to the Trans-Golgi Network and Regulates Their Recognition of the Ubiquitin Sorting Signal." Molecular biology of the cell **18**(7): 2646-2655.
- Wang, K., Z. Yang, et al. (2012). "Phosphatidylinositol 4-Kinases Are Required for Autophagic Membrane Trafficking." Journal of Biological Chemistry **287**(45): 37964-37972.
- Wang, L., E. R. Hauser, et al. (2007). "Peakwide mapping on chromosome 3q13 identifies the kalirin gene as a novel candidate gene for coronary artery disease." **80**(4): 650-663.
- Wang, L., L. Yang, et al. (2005). "Cdc42GAP regulates c-Jun N-terminal kinase (JNK)-mediated apoptosis and cell number during mammalian perinatal growth." Proceedings of the National Academy of Sciences of the United States of America **102**(38): 13484-13489.
- Wang, L., L. Yang, et al. (2007). "Cdc42 GTPase-activating protein deficiency promotes genomic instability and premature aging-like phenotypes." Proceedings of the National Academy of Sciences **104**(4): 1248-1253.
- Wang, P., L. Zhang, et al. (2011). "Developments in selective small molecule ATP-targeting the serine/threonine kinase Akt/PKB." Mini Reviews In Medicinal Chemistry **11**(13): 1093-1107.

- Wang, X., J. Ni, et al. (2009). "Reduced expression of tocopherol-associated protein (TAP/Sec14L2) in human breast cancer." Cancer Investigation **27**(10): 971-977.
- Wang, Y. J., J. Wang, et al. (2003). "Phosphatidylinositol 4 phosphate regulates targeting of clathrin adaptor AP-1 complexes to the Golgi." Cell **114**(3): 299-310.
- Ward, S. and J. Miwa (1978). "Characterization of temperature-sensitive, fertilization-defective mutants of the nematode *Caenorhabditis elegans*." Genetics **88**(2): 285-303.
- Waring, M. J., D. M. Andrews, et al. (2014). "Potent, selective small molecule inhibitors of type III phosphatidylinositol-4-kinase α - but not β -inhibit the phosphatidylinositol signaling cascade and cancer cell proliferation." Chemical Communications.
- Warnick, G. R. (1986). "Enzymatic methods for quantification of lipoprotein lipids." Methods Enzymol **129**: 101-123.
- Waugh, M. G. (2012). "Phosphatidylinositol 4-kinases, phosphatidylinositol 4-phosphate and cancer." Cancer letters **325**(2): 125-131.
- Weber, S. S., C. Ragaz, et al. (2006). "Legionella pneumophila exploits PI(4)P to anchor secreted effector proteins to the replicative vacuole." PLoS Pathog **2**(5): e46.
- Weimar, W. R., P. W. Lane, et al. (1982). "Vibrator (vb): a spinocerebellar system degeneration with autosomal recessive inheritance in mice." Brain Research **251**(2): 357-364.
- Weiner, O. D., P. O. Neilsen, et al. (2002). "A PtdInsP(3)- and Rho GTPase-mediated positive feedback loop regulates neutrophil polarity." Nature cell biology **4**(7): 509-513.
- Welker, M. E. and G. Kulik (2013). "Recent syntheses of PI3K/Akt/mTOR signaling pathway inhibitors." Bioorganic & medicinal chemistry **21**(14): 4063-4091.
- Welti, S., S. Fraterman, et al. (2007). "The Sec14 Homology Module of Neurofibromin Binds Cellular Glycerophospholipids: Mass Spectrometry and Structure of a Lipid Complex." Journal of Molecular Biology **366**(2): 551-562.
- Wen, X.-Q., X.-J. Li, et al. (2007). "Reduced expression of α -tocopherol-associated protein is associated with tumor cell proliferation and the increased risk of prostate cancer recurrence." Asian J Androl **9**(2): 206-212.
- Wenk, M. R. (2005). "The emerging field of lipidomics." Nature reviews. Drug discovery **4**(7): 594-610.

- Wenk, M. R. (2010). "Lipidomics: New Tools and Applications." Cell **143**(6): 888-895.
- Wenk, M. R. and P. De Camilli (2004). "Protein-lipid interactions and phosphoinositide metabolism in membrane traffic: insights from vesicle recycling in nerve terminals." Proceedings of the National Academy of Sciences of the United States of America **101**(22): 8262-8269.
- Wenk, M. R., L. Lucast, et al. (2003). "Phosphoinositide profiling in complex lipid mixtures using electrospray ionization mass spectrometry." Nature biotechnology **21**(7): 813-817.
- Wheeler, L. A., G. Sachs, et al. (1987). "Manoalide, a natural sesterterpenoid that inhibits calcium channels." Journal of Biological Chemistry **262**(14): 6531-6538.
- Whitehead, B., M. Tessari, et al. (1999). "The EH1 domain of Eps15 is structurally classified as a member of the S100 subclass of EF-hand-containing proteins." Biochemistry **38**(35): 11271-11277.
- Whitman, M., C. P. Downes, et al. (1988). "Type I phosphatidylinositol kinase makes a novel inositol phospholipid, phosphatidylinositol-3-phosphate." Nature **332**(6165): 644-646.
- Wiedemann, C., T. Schafer, et al. (1996). "Chromaffin granule-associated phosphatidylinositol 4-kinase activity is required for stimulated secretion." The EMBO journal **15**(9): 2094-2101.
- Williams, D. E., A. Amlani, et al. (2010). "Australin E Isolated from the Soft Coral *Cladiella* sp. Collected in Pohnpei Activates the Inositol 5-Phosphatase SHIP1." Australian Journal of Chemistry **63**(6): 895-900.
- Wirtz, K. W. A. (1991). "Phospholipid transfer proteins." Annual Review of Biochemistry **60**(1): 73-99.
- Wood, C. S., K. R. Schmitz, et al. (2009). "PtdIns4P recognition by Vps74/GOLPH3 links PtdIns 4-kinase signaling to retrograde Golgi trafficking." The Journal of Cell Biology **187**(7): 967-975.
- Woods, M. N. and D. M. Hegsted (1979). "Quantitative and qualitative changes in phospholipid in the intestine of the gerbil and the development of lipodystrophy." The Journal of nutrition **109**(12): 2146-2151.
- Workman, P., P. A. Clarke, et al. (2010). "Drugging the PI3 Kinome: From Chemical Tools to Drugs in the Clinic." Cancer Research **70**(6): 2146-2157.

- Wu, W.-I. and D. R. Voelker (2002). "Biochemistry and genetics of interorganelle aminoglycerophospholipid transport." Seminars in Cell and Developmental Biology **13**(3): 185-195.
- Wu, W. I., S. Routt, et al. (2000). "A new gene involved in the transport-dependent metabolism of phosphatidylserine, PSTB2/PDR17, shares sequence similarity with the gene encoding the phosphatidylinositol/phosphatidylcholine transfer protein, SEC14." The Journal of biological chemistry **275**(19): 14446-14456.
- Wymann, M. and A. Arcaro (1994). "Platelet-derived growth factor-induced phosphatidylinositol 3-kinase activation mediates actin rearrangements in fibroblasts." The Biochemical journal **298 Pt 3**: 517-520.
- Wymann, M. P., G. Bulgarelli-Leva, et al. (1996). "Wortmannin inactivates phosphoinositide 3-kinase by covalent modification of Lys-802, a residue involved in the phosphate transfer reaction." Molecular and cellular biology **16**(4): 1722-1733.
- Wymann, M. P. and R. Schreiner (2008). "Lipid signalling in disease." Nat Rev Mol Cell Biol **9**(2): 162-176.
- Wymann, M. P. and C. Schultz (2012). "The Chemical Biology of Phosphoinositide 3-Kinases." ChemBioChem **13**(14): 2022-2035.
- Xiao, J., S. Gong, et al. (2007). "Caytaxin deficiency disrupts signaling pathways in cerebellar cortex." Neuroscience **144**(2): 439-461.
- Xiao, J. and M. S. LeDoux (2005). "Caytaxin deficiency causes generalized dystonia in rats." Molecular Brain Research **141**(2): 181-192.
- Xie, L., W. Qin, et al. (2007). "BNIPL-2 promotes the invasion and metastasis of human hepatocellular carcinoma cells." Oncol Rep **17**(3): 605-610.
- Xie, Y., Y.-Q. Ding, et al. (2005). "Phosphatidylinositol transfer protein- α in netrin-1-induced PLC signalling and neurite outgrowth." Nature Cell Biology **7**(11): 1124-1132.
- Xie, Z., M. E. Cahill, et al. (2010). "Kalirin loss results in cortical morphological alterations." Molecular and Cellular Neuroscience **43**(1): 81-89.
- Xie, Z., M. Fang, et al. (1998). "Phospholipase D activity is required for suppression of yeast phosphatidylinositol transfer protein defects." Proceedings of the National Academy of Sciences of the United States of America **95**(21): 12346-12351.
- Xie, Z., D. P. Srivastava, et al. (2007). "Kalirin-7 controls activity-dependent structural and functional plasticity of dendritic spines." **56**(4): 640-656.

- Xu, G., P. O'Connell, et al. (1990). "The neurofibromatosis type 1 gene encodes a protein related to GAP." **62**(3): 599-608.
- Xu, Y., S. A. Lee, et al. (2006). "Chemical synthesis and molecular recognition of phosphatase-resistant analogues of phosphatidylinositol-3-phosphate." Journal of the American Chemical Society **128**(3): 885-897.
- Yang, L., L. Wang, et al. (2006). "Gene Targeting of Cdc42 and Cdc42GAP affirms the critical involvement of Cdc42 in filopodia induction, directed migration, and proliferation in primary mouse embryonic fibroblasts." Mol. Biol. Cell **17**(11): 4675-4685.
- Yang, L., D. E. Williams, et al. (2005). "Synthesis of pelorol and analogues: activators of the inositol 5-phosphatase SHIP." Organic Letters **7**(6): 1073-1076.
- Yang, X. and B. N. R. Cheyette (2013). "SEC14 and spectrin domains 1 (Sestd1) and dapper antagonist of catenin 1 (Dact1) scaffold proteins cooperatively regulate the van gogh-like 2 (Vangl2) four-pass transmembrane protein and planar cell polarity (PCP) pathway during embryonic development in mice." Journal of Biological Chemistry **288**(28): 20111-20120.
- Yizhar, O., L. E. Fenno, et al. (2011). "Optogenetics in neural systems." Neuron **71**(1): 9-34.
- Yoder, M. D., L. M. Thomas, et al. (2001). "Structure of a multifunctional Protein: mammalian phosphatidylinositol transfer protein complexed with phosphatidylcholine." J. Biol. Chem. **276**(12): 9246-9252.
- Yoko-o, T., Y. Matsui, et al. (1993). "The putative phosphoinositide-specific phospholipase C gene, PLC1, of the yeast *Saccharomyces cerevisiae* is important for cell growth." Proceedings of the National Academy of Sciences of the United States of America **90**(5): 1804-1808.
- Yokota, T., K. Igarashi, et al. (2001). "Delayed-onset ataxia in mice lacking α -tocopherol transfer protein: Model for neuronal degeneration caused by chronic oxidative stress." Proceedings of the National Academy of Sciences of the United States of America **98**(26): 15185-15190.
- York, J. D. (2006). "Regulation of nuclear processes by inositol polyphosphates." Biochimica et biophysica acta **1761**(5-6): 552-559.
- Yoshida, S., Y. Ohya, et al. (1994). "A novel gene, STT4, encodes a phosphatidylinositol 4-kinase in the PKC1 protein kinase pathway of *Saccharomyces cerevisiae*." Journal of Biological Chemistry **269**(2): 1166-1172.

- Youn, H., I. Ji, et al. (2007). "Under-expression of Kalirin-7 Increases iNOS activity in cultured cells and correlates to elevated iNOS activity in alzheimer's disease hippocampus." Journal of Alzheimer's Disease **12**(3): 271-281.
- Young, B. P., R. A. Craven, et al. (2001). "Sec63p and Kar2p are required for the translocation of SRP-dependent precursors into the yeast endoplasmic reticulum in vivo." EMBO J **20**(1-2): 262-271.
- Young, R. W. (1974). "Biogenesis and renewal of visual cell outer segment membranes." Exp. Eye Res. **18**(3): 215-223.
- Yue, J., J. Liu, et al. (2001). "Inhibition of phosphatidylinositol 4-kinase results in a significant reduced respiratory burst in formyl-methionyl-leucyl-phenylalanine-stimulated human neutrophils." The Journal of biological chemistry **276**(52): 49093-49099.
- Zadran, S., S. Standley, et al. (2012). "Fluorescence resonance energy transfer (FRET)-based biosensors: visualizing cellular dynamics and bioenergetics." Applied Microbiology and Biotechnology **96**(4): 895-902.
- Zhang, F., L. P. Wang, et al. (2007). "Multimodal fast optical interrogation of neural circuitry." Nature **446**(7136): 633-639.
- Zhang, H., J. He, et al. (2010). "5-stabilized phosphatidylinositol 3,4,5-trisphosphate analogues bind Grp1 PH, inhibit phosphoinositide phosphatases, and block neutrophil migration." ChemBioChem **11**(3): 388-395.
- Zhang, H., N. Markadieu, et al. (2006). "Synthesis and biological activity of PTEN-resistant analogues of phosphatidylinositol 3,4,5-trisphosphate." Journal of the American Chemical Society **128**(51): 16464-16465.
- Zhang, H., N. Markadieu, et al. (2006). "Synthesis and Biological Activity of PTEN-Resistant Analogues of Phosphatidylinositol 3,4,5-Trisphosphate." Journal of the American Chemical Society **128**(51): 16464-16465.
- Zhang, H., Y. Xu, et al. (2008). "Synthesis and biological activity of phosphatidylinositol-3,4,5-trisphosphorothioate." Bioorganic & Medicinal Chemistry Letters **18**(2): 762-766.
- Zhang, H., Y. Xu, et al. (2006). "Synthesis and biological activity of phospholipase C-resistant analogues of phosphatidylinositol 4,5-bisphosphate." Journal of the American Chemical Society **128**(17): 5642-5643.
- Zhang, H. M., P. Cheung, et al. (2003). "BNips: A group of pro-apoptotic proteins in the Bcl-2 family." Apoptosis **8**(3): 229-236.

- Zhang, W., G. Frahm, et al. (2009). "Effect of bilayer phospholipid composition and curvature on ligand transfer by the α -tocopherol transfer protein." Lipids **44**(7): 631-641.
- Zhao, R., X. Fu, et al. (2003). "Specific interaction of protein tyrosine phosphatase-MEG2 with phosphatidylserine." Journal of Biological Chemistry **278**(25): 22609-22614.
- Zhao, S., C. Xu, et al. (2008). "Cellular retinaldehyde-binding protein-like (CRALBPL), a novel human Sec14p-like gene that is upregulated in human hepatocellular carcinomas, may be used as a marker for human hepatocellular carcinomas." DNA and Cell Biology **27**(3): 159-163.
- Zheng, M., R. Simon, et al. (2004). "TRIO amplification and abundant mRNA expression is associated with invasive tumor growth and rapid tumor cell proliferation in urinary bladder cancer." American Journal of Pathology **165**(1): 63-69.
- Zhou, Y. T., G. R. Guy, et al. (2005). "BNIP-2 induces cell elongation and membrane protrusions by interacting with Cdc42 via a unique Cdc42-binding motif within its BNIP-2 and Cdc42GAP homology domain." Experimental Cell Research **303**(2): 263-274.
- Zornetta, I., L. Brandi, et al. (2010). "Imaging the cell entry of the anthrax oedema and lethal toxins with fluorescent protein chimeras." Cellular Microbiology **12**(10): 1435-1445.
- Zu, L., Z. Shen, et al. (2011). "PTEN inhibitors cause a negative inotropic and chronotropic effect in mice." European journal of pharmacology **650**(1): 298-302.
- Zykova, T. A., F. Zhu, et al. (2008). "Resveratrol directly targets COX-2 to inhibit carcinogenesis." Molecular Carcinogenesis **47**(10): 797-805.